The Passive Display Case

Climate control for the conservation of cultural heritage

Carlos A. Chang Lara

September 2015

TU Delft Delft University of Technology

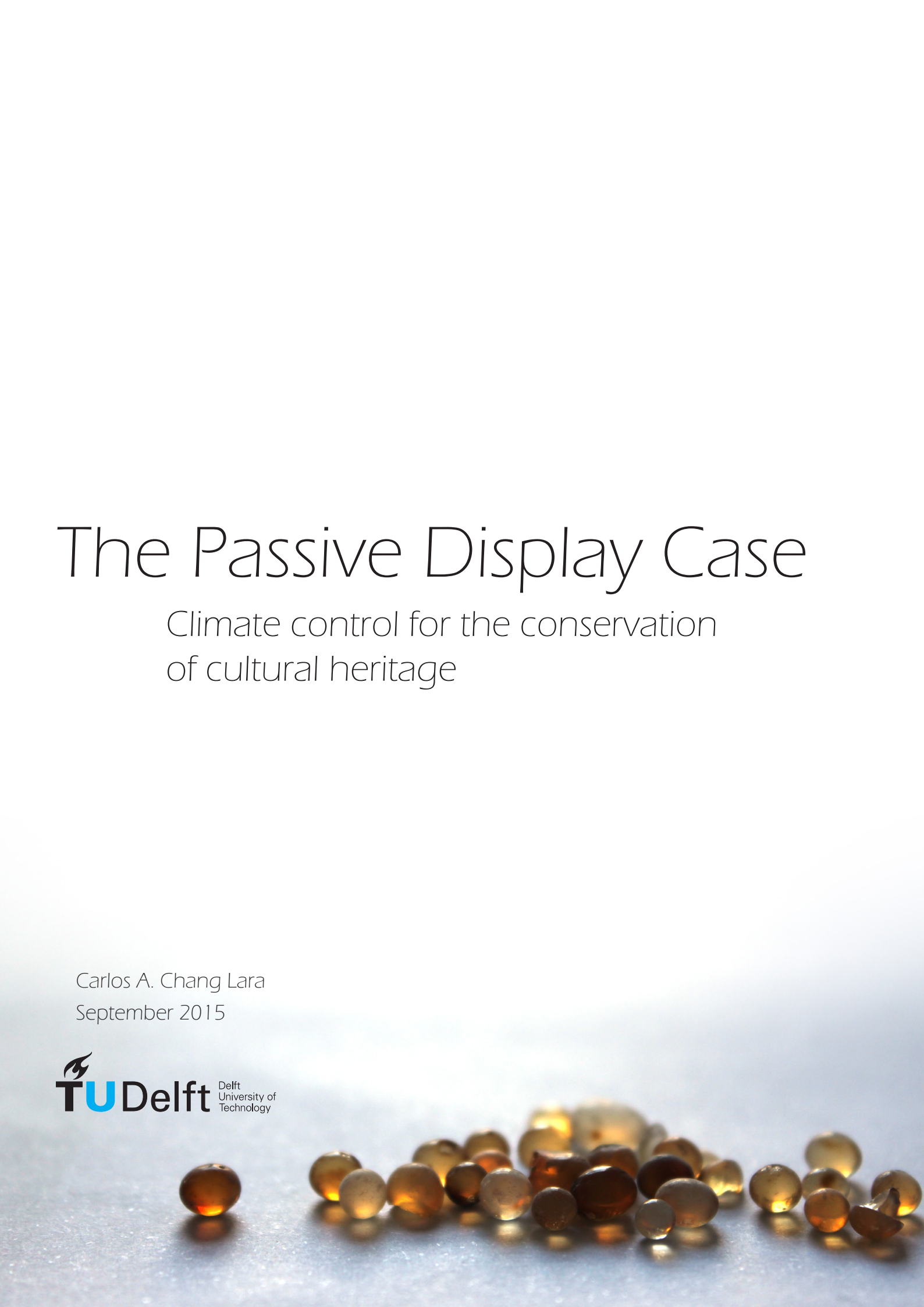

The Passive Display Case

Climate control for the conservation of cultural heritage

Faculty of Civil Engineering and Geosciences
Track: Building Engineering
Specialization: Building Technology & Physics

Graduation Committee:

Prof. Ir. P. G. Luscuere
Delft University of Technology
Faculty of Architecture and the Built Environment
B8 - 01WEST130
+31 (0)15 27 89752
P.G.Luscuere@tudelft.nl

Dr. Ir. Willem van der Spoel
Delft University of Technology
Faculty of Architecture and the Built Environment
B8 - 01WEST240
W.H.vanderSpoel@tudelft.nl

Dr. Ir. H.R. Schipper
Delft University of Technology
Faculty of Civil Engineering and Geosciences
Stevin II-Zuid 1.55
+31 (0)15 278 99 33
h.r.schipper@tudelft.nl

Ir. J.A. Pleysier
Deerns Nederland B.V.
088 374 03 72
arjan.pleysier@deerns.com

By:

Carlos A. Chang Lara
+31 (0)6 26792399
cchanglara@gmail.com
TU Delft ID: 4330773

Summary

Display cases around the world contain some of the most precious objects of our cultural heritage, from Leonardo Da Vinci's La Gioconda to the Gutenberg Bible. We trust that these display cases will protect our objects of cultural heritage from vandalism, light, pollution and most importantly, moisture. Nevertheless, museums sometimes find that although their objects of art are in display cases, these are not providing the ideal protective microclimate (Watts et. al., 2007). Hygroscopic materials can help restore this protective microclimate, but there are situations where the use of moisture-buffering materials is ineffective (Shiner, 2007). This project aims to find when these situations occur. In order to do this, a computational model was developed and validated, and the results are evaluated in this report.

In Chapter 2, the museum climate is introduced. The museum climate is the environment inside the building and outside of the display case. To understand the optimum state of conservation of an object of art, it is necessary to study its response to the surrounding environment. For this reason, the mechanical response of paintings on canvas were further explored. Mechanical failure is not the only form of failure due to unstable climate conditions inside of a display case. Biological and chemical failure are also explored to characterize the qualities of the ideal microclimate for conservation. Display cases have been developed as a response to these forms of failure, and we can recognize two different types, the active and the passive. Today, the development of active display cases has resulted in a very promising performance, however, these display cases present some disadvantages, such as high costs and required maintenance. Passive display cases, on the other hand, have the potential to guarantee a controlled environment with lower costs and, ideally, minimal maintenance. To further understand how passive display cases can do this, the hygroscopic material characteristics are explored.

In Chapter 3, the model is described. The mechanisms of moisture transfer are separated in two parts: the moisture transfer taking place inside the hygroscopic material package and the one taking place in the display case. The governing principles in each part are explained and the numerical approach used to solve the model is presented. Finally, the implementation of the model is provided.

In Chapter 4, the model validation is described. The conclusions were based on two sets of physical experiments: the air exchange rate (AER), and the environment control experiments. The AER experiment monitored how fast dry air inside of the display case reached the same level of humidity as the outside. The environment control experiments monitored the response of the climate inside of the display case when exposed to daily environmental loads. The validation of the developed model was based first on obtaining the AER value for the display case from the AER experiment results. Then, the environment control experiments were used in order to estimate the moisture transfer coefficient in the display case, using the computational model. This validation allowed us to simulate several different scenarios with full control of the multiple parameters that affected the model.

The parameters that influence the performance of the passive display case are explored in Chapter 5. A sensitivity analysis was done using five independent variables. These were, changes in relative humidity outside of the display case, in the temperature, in the air exchange rate, in the time domain, and in the moisture transfer coefficient. The change in relative humidity inside of the display case was the dependent parameter. Assessment of these results was divided in two parts: the evaluation of trends and observations of the buffering effect. From these results, we can observe that certain combinations of parameters provide no protection at all, and some other combinations provide considerable protection from the environmental loads.

Chapter 6 concludes this project, providing a thoroughly summary of the work presented with the concluding statements that define each section. Then, the research questions raised in Chapter 1 are assessed, concluding that no one single parameter can be used to fully determine the performance of a passive display case. It rather is the combination of parameters that define the display case performance. The relevance of this project can be found on the potential the numerical model has. The display case situation matrix developed in Chapter 5 not only to characterizes the effect of each parameter but it could also be used as a design tool for museum staff members and designers. The potential of this numerical model for the field of conservation is significant and this can be illustrated by the display case situaton matrix. Finally, recommendations for further research are presented based on the limitations the numerical model has with respect to the air exchange rate and the moisture transfer coefficient.

Preface

What can an engineer do to improve the field of art conservation? Why is the conservation of art important to us?

Over the years, we have tried to look for ways to conserve our objects of cultural heritage. But why? Some argue that these objects have a documental value; these pieces have become part and proof of the narrative we have inherited from past generations. Others find value in their aesthetic composition. And many others believe that our objects of cultural heritage have rather a combination of both, documental and aesthetic value. Regardless of the reasons, it is not hard to see the importance of cultural heritage in society. This leads us to the questions raised above. After all, what can an engineer really contribute to this field? In order to answer these questions we need to have a closer look into the field of conservation.

In February 2015, we saw how Islamic State militants destroyed many objects of art in Mosul, Iraq. Just last month, in August 2015, the Baalshamin temple in Palmyra, Syria was demolished. We find ourselves in despair when the loss of cultural heritage takes such a powerful form. However, there is a less dramatic threat that is compromising all of our objects of cultural heritage; no object has ever been exempt from natural decay. The effect of the environment is the most patient and perseverant of all threats that objects of art have ever faced. Over the years we have tried to face this threat with our most advanced technology. However, the patina of time seems to be always a step ahead. This challenge provides a great opportunity for engineers. The effects of the environment are not new to us. We have been faced with challenges such as stopping corrosion in a reinforcing steel bar one meter inside of a concrete deck bridge, and mitigating the risk of efflorescence in the facades of our buildings. To develop the most appropriate solutions, we as engineers, have learned how to contextualize and deliver creative and practical answers to those challenges. These, I believe, are our most valuable skills. These are skills that can find great use in many conservation challenges. Giovanni Urbani, (1981) one of the former directors of the Istituto Centrale del Restauro, perfectly describes this:

> "The demonstrated scientific imagination would be no less impressive than the creativity stamped on the art of the past. Finally then the work of art will be preserved in the only way that matters: as the matrix of renewed experience of the creative act, and no longer as a mere object of study or of aesthetic contemplation." (Urbani, 1981)

Today, I proudly present you with the results of my final thesis, required for the completion of the MSc degree at TU Delft. Over the past nine months I have immersed myself in the field of art conservation with great enthusiasm. The lessons I have learned have changed the way I see my profession, and most certainly the way I see art today. This project would not be possible without the support of our generous collaborators. Your contributions not only made this project possible but they also made it an unforgettable experience. Thank you for all the patience and enthusiasm transmitted over these past months.

Thank you, graduation committee. You have been an invaluable source of motivation and support during this project.

Thank you, Dr. W. van der Spoel for all the assistance, especially for the long afternoons taken for the development of the model.

Thank you, Dr. R. Schipper for all your assistance, especially when defining my research topic and the experimental setup.

Thank you, A. Pleysier for all your help and for bringing your unique perspective of this industry into this project.

Thank you, Dr. P. Luscuere for sharing and supporting my vision. Your encouragement has been a great source of inspiration throughout these months.

Thank you, GLASSOLUTIONS Glascom Museum Presentations for providing the invaluable display case. Thanks especially to Martin Weerheim and Harold Kool for the wonderful company tour and for sharing how the display case industry works in the Netherlands.

Thank you, Jewish Historical Museum in Amsterdam for providing the hygroscopic material. I am grateful especially to Netty Wendrich, who shared her perspective as museum conservator and provided me with an incredible tour of the Jewish Historical Museum.

Thank you, Maiko van Leeuwen from Stevin Laboratory in the TU Delft Faculty of Civil Engineering and Geoscience for all your help and patience during the performance of the AER experiments.

Table of Contents

Chapter 1 : Introduction

Introduction

Display cases are some of the most common items that we can see in a museum today. They provide protection to the objects they enclose from vandalism, light, pollution and most importantly, moisture. In this project we will explore the protection provided by a display case in terms of its capacity to buffer a certain environmental load, such as temperature and moisture fluctuations, with the main focus on passive display cases. A passive display case is one that relies on hygroscopic materials in order to stabilize the microclimate it encloses. In this chapter we will explore why further knowledge about the passive display case is required, focusing on defining a central research problem. This research problem is complemented by a set of research questions that define the trajectory of this research. Finally, some restrictions and limitations are provided followed by the outline of the entire project.

Background

The purpose of a display case is to provide protection to the object of art. This protection can take many forms, from providing protection from vandalism to allowing buffering of climate agents (i.e., moisture and temperature fluctuations). However, it is known that museums usually have their objects of art in display cases that do not provide the ideal protective microclimate (Watts et. al., 2007). Hygroscopic materials can help restore this protective microclimate, as it has been proven before (Martens, 2012). However, there are still important scenarios where the use of moisture-buffering materials proves to be ineffective (Shiner, 2007). The main purpose of this project is to find those scenarios where moisture-buffering materials prove to be ineffective. In the following paragraphs the main challenges of museum and display conditioning are presented.

Museums and art galleries have a unique set of climate characteristics that set them apart from other buildings. This is based on the fact that one of their main purposes is to ensure the conservation of the art while human comfort is adapted to the art conservation requirements. It can be said that the main clients and users of a museum are its own objects of art. These objects are particularly different from humans, as the objects require constant conditioning of their space. While in an office, the climate conditioning (i.e., air conditioning or heat) can be switched off during nonworking hours; the conditioning equipment of a museum must be functioning at all times. Additionally, wider fluctuations could be allowed based on human comfort, but similar fluctuations would surely result in the failure of the object, as shown in chapter two. These challenges are increased when museum buildings happen to be historic buildings where restoration/transformations are limited by their historical heritage. Martens, in 2012, carried out an extensive study of the risk assessment of museum buildings and among his conclusions was that the quality of the historic envelope was less important than its integration to the conditioning equipment; that is to say that a poor selection of the conditioning system causes more damage than the quality of the actual envelope (Martens, 2012).

One of the main challenges of museum conditioning is the humidity control. A high level of humidity below a certain temperature (the dew point) might lead to condensation, which would further deteriorate the building fabric, such as by increasing mold growth. However, a sufficiently high level of humidity at temperatures even below the dew point can compromise the safety of different objects of art, for example, by causing wood rot (Westfield, 1996). The risks of preserving an object of art are much higher than the risks of ensuring that no condensation will occur. In order to confront the challenges of museum conditioning, the concept of zoning has been proposed, where special attention is given to those spaces

that share the climate requirements of visitors and objects of art (Dexter Lord & Lord, 1999). Apart from the conditioning challenges, the current desire for more sustainable approaches adds to the complexity of the situation; here, passive conditioning methods have great potential. However, little research has been done on the passive conditioning of museums and there is a general lack of consistent data (Toledo, 2007).

As a result of the above-mentioned challenges, museums have needed to learn how to condition the microclimate inside a display case. It may seem that there are fewer variables in the conditioning of a display case than in the conditioning of a museum gallery. However, the challenges presented in the conditioning of a display case are not any easier to solve. Among the main challenges of the conditioning of a display case is the air exchange rate situation. It is well known that a smaller air exchange rate is better for the conservation of the object of art. This is due to the fact that through the air exchange, external moisture variations are introduced inside of the display case. Additionally, more external pollutants are allowed inside of the display case when the air exchange rate is high. For this reason, there is great enthusiasm from manufacturing companies for reducing the air exchange rate of the display case to as little as possible, yet letting the air exchange rate be driven by atmospheric pressure variations only. Display cases with rates of as little as 0.1 air exchanges per day are currently available.

However, it has been observed that low air exchange rate display cases have another important problem to be solved. Thicket et al. (2007) noticed that the concentrations of pollutants inherent to the object of art increases as the air exchange rate decreases. Interestingly, the concentrations of ethanoic acids behave in a non-linear way, which allowed Thicket et al. to conclude that if this behavior (object emission of pollutants) can be generalized in most display cases, then there is a serious implication on the display case air exchange requirements and the mitigation of deterioration risks.

Another challenge which is associated with the introduction of a hygroscopic material in a closely controlled environment, is the effect of certain materials with different adsorption/desorption rates. This challenge was particularly studied by Richards (2007) for microclimate packages developed in the National Gallery for panel paintings. Microclimate packages are engineered, air-tight envelopes that contain the object of art and sufficient hygroscopic material inside. Conceptually, the hygroscopic material is meant to stabilize the microclimate surrounding the object of art. These microclimate packages are particularly used for travelling collections or for objects of art for which a stable environment cannot be ensured at all locations. Richards points out the concern of some scientists, in which different responses to environmental variation by an induced hygroscopic material (i.e. silica gel) and any other hygroscopic material present (e.i., the object of art) could result in the object of art gaining or losing unacceptable amounts of moisture. It is important to highlight the concerns of the National Gallery when developing these packages. Their purpose was to control the microclimate surrounding the painting; this is especially demanded for loaned objects of art. While the package is perfectly sealed and the introduced hygroscopic material behavior is known, there is no way to control the environmental loads on the package (especially when on loan), specifically the temperature variations. It is known that the moisture response of objects depends on temperature. Therefore, a variation in temperature could offset the isothermal equilibrium moisture content of the hygroscopic material and the object of art. In order to find out how detrimental these environmental variations can be for the stability of the packages, Richards carried out a set of experiments where the sorption isotherm of microclimate packages with hygroscopic material was compared with those without hygroscopic material. This research concluded that any adverse effect of adding a hygroscopic material in close contact with an object of art under varying environmental loads is highly unlikely considering the amount of hygroscopic material that is being introduced. While this is an important issue for passively conditioned display cases, it is important to remark that these microclimate packages have a minimum amount of air and the air exchange rate is very small in comparison to an actual display case.

The effect of infrared radiation in the display case has also been considered an important challenge. Camuffo (2000) stated that most commonly used transparent glass panes are not fully infrared

transparent; this may potentially turn the display case into a greenhouse. By inducing infrared radiation inside of a display case, the temperature and relative humidity stability would be disturbed, which would not only endanger the conservation of the object of art, but it would increase internal air movement which allows a higher rate of suspended particle deposition. However, this infrared overheating is mostly attributed to the light sources in museums, since there is no other obvious infrared source present in a gallery display. Therefore, the effect of infrared radiation on the display case can be easily mitigated by making sure that the required illumination is obtained by cold lights, which cut off the unsafe infrared section of the light spectrum. Additionally, Camuffo recommends keeping all light sources outside of the display case.

Problem description

With the previous literature background, it has been recognized that there is a general gap in the understanding of the performance of hygroscopic materials when used as a passive method to condition a display case. Today, packages of hygroscopic material (e.g. regular silica gel, ProSorb and ArtSorb) are being widely used in museums and art galleries. However, their usage is mostly based on the recommendations made by the manufacturer and general rules of thumb. This might be attributed to the fact that the museum staff in charge of the maintenance of such packages has little to no experience with the performance of this material. While these recommendations and rules of thumb are helpful and applicable to a lot of scenarios, it happens rather often that a deeper knowledge of the use of these passive conditioning materials is needed, e.g., with special display cases or displays under limited conditioning. Understanding the performance of these hygroscopic materials will not only allow us to optimize their current use but also allow us to discover where their limitations lie.

Research questions

The above problem can be described with the following questions:

1. What are the mechanisms that allow hygroscopic materials to maintain a specific level of humidity, and how do they differ from other materials?

   We understand that the capacity of hygroscopic materials to buffer moisture is very large in comparison to any other regular material. Understanding the mechanisms that allow these materials to buffer such amounts of moisture can give us insight on the general use and limitations of their performance

2. How does a passive conditioned display case work and what boundary conditions for the internal and external environment are assumed in order to ensure their performance?

   Passive conditioned display cases are being used all around the world today. They have proven to effectively condition the microclimate surrounding a piece of art (Martens, 2012). It is important to understand how conceptually these display cases work and what steps have been taken on the optimization process of the current design. This will allow us to compare their actual use with their requirements.

3. What is the effect of the air exchange rate of the display case on the performance of the passive conditioned display case?

   As shown in the background section, the effect of the air exchange rate in the display case is very important when referring to a passive conditioned display case. Understanding the effect of the air exchange rate will allow us to mitigate the dynamic effect of the exterior climate.

Moreover, recognizing where the main leakage points might be located may serve useful for further optimization of the display case design.

4. What is the effect of the exterior climate on the performance of the passive conditioned display case?

   This is the main goal of this research project, understanding the response of the passive conditioned display case to a varying external load. The main purpose is to map under what environmental museum conditions the best performance of the display case is ensured. With this, the limitations of the passive conditioned display case can be located and useful information for its optimization can be gathered.

5. Can the original design of the passive conditioned display case be optimized?

   Once we have understood the performance and limitations of the passive conditioned display case, we will be able to evaluate the current design. Finding out the situations where the current display case design has its best performance or no performance at all, will not only open the opportunity for design recommendations for the industry, but also for recommendation in its range of use for the museum staff.

Focus and restrictions

While the purpose of this research is to evaluate the performance of the passive conditioned display case, the object of display must be defined first. It is important to state that this project places priority on the climate around the object and not on the response of the object to the climate. However, it is well known that the response of the object affects the microclimate of the surroundings. For that reason, acrylic paintings on canvas have been chosen for this project as they have a minimal effect on the microclimate, which is only influenced by the textile and the wooden frame. Nevertheless, the object selection was quite arbitrary.

The object definition also allowed us to specify the climate requirements, which are unique to the physical composition of the object (e.g., the climate required for the conservation of metals is very different from that of the paper fibers). Note that irrespective of the desired state of conservation of the object, the climate requirements are based on ensuring the minimum amount of decay of the object. This will be further explained in chapter two.

In order to characterize the climate inside of the display case, moisture and temperature are the primary parameters. However, moisture has been given priority based on the state of decay of the object being displayed. Differentials in relative humidity have a higher negative effect on the object than that of temperature differentials (Richards, 2007). Throughout this entire project, temperature will be considered an independent parameter, while the amount of moisture in the form of relative humidity, moisture content and partial vapor pressure will be used to characterize the microclimate inside the display case.

Outline

In order to solve the above mentioned questions, a computational model will be created. The parameterization of different elements playing a role in the conditioning of a passive display case will help us understand what has the greatest influence and how. Simulations will be run in order to understand the performance of the display case and this will be validated with measurements taken from a shadow box (particularly made for paintings) display case, conditioned with a package of ProSorb.

Chapter 2 introduces the environment of cultural heritage objects. This is the main literature study performed during this project and it concerns the risks and challenges associated with the stabilization

of the climate of objects of cultural heritage. The object response is given much significance in this chapter and finally the hygroscopic materials are introduced. Chapter 3 describes the computational model developed during this project. The moisture transport is separated on the forms of moisture transport inside of the packed bed of hygroscopic material and the forms of moisture transport in and out of the display case. Chapter 4 introduces how the previous model was validated through physical experiments. These experiments were separated into air exchange rate (AER), and the environment control experiments. The methodology and results of these experiments are described and the results and fitting of the model is explained. Chapter 5 presents the performance of a passive display case and the effect of certain parameters on its buffering capacity. Such parameters are the AER, temperature, relative humidity outside of the display case, time domain, and moisture transfer coefficient. Chapter 6 presents the conclusions and attempts to solve the above mentioned research questions offering recommendations for further research. This is shown in Figure 1.

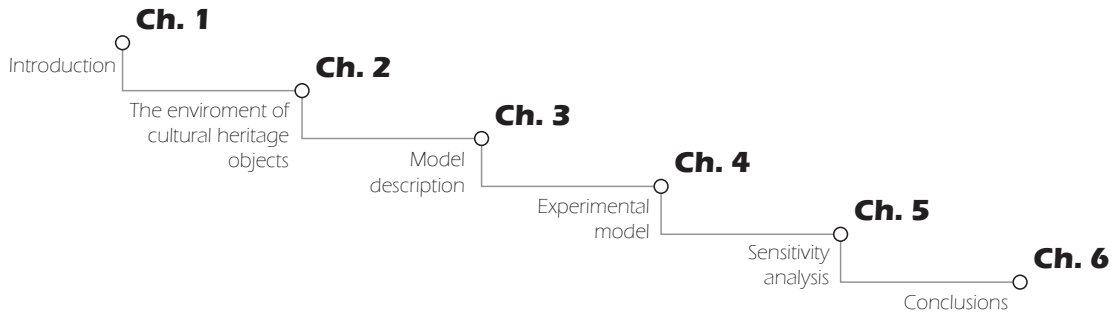

Figure 1: MSc. Report Structure

Chapter 2: The Environment of Cultural Heritage Objects

The main purpose of a museum is to protect its collection from any dangerous agents, such as vandalism, thieves, fire, pollution, pests, radiation and indoor climate among many others. Here, we will focus on the risks associated with the indoor climate. This chapter presents the theoretical background of this project. First, an overview of the museum environment is given, placing special emphasis on the ASHRAE guidelines for museums. Objects of art will have a particular response under a particular environmental load. We will continue with an overview of the mechanical response of paintings on canvas. However, mechanical deterioration is not the only form of degradation of objects of art; a short description of biological and chemical deterioration is given next. Once the main forms of deterioration have been considered, we can then look at the purpose of a display case and its current design, where an overview of the active and passive form is given. Finally, we will study the passive type of display case describing how the system is currently used and the challenges of using it today.

The museum environment

Museums are not any different from other buildings in terms of their structure and composition. However, it is the function of the museum, the reason for setting up such high requirements for the indoor climate that is different from a regular building. It is important to state that there is no one perfect environment for a museum (Martens, 2012). The optimum environment desired by museums is one that minimizes the indoor climate risks to the collections and ensures satisfactory human comfort within an integrated sustainable approach. The complexity of achieving this goal is further increased when the museum building has a historical background. Due to the historical heritage requirements, indoor climates might fall out of acceptable ranges and/or the efficiency of the building might jeopardize the sustainability approach. Furthermore, restorations/renovations/transformations are limited by the historical character of the building, which may not be based on a pragmatic approach, but are solely based on a heritage conservation approach.

The first step when evaluating the mitigation of indoor climate risks is to look into the original climate design. Indoor climate engineers use a set of guidelines when designing a particular climate in a building. For museums, the ASHRAE climate guidelines have often been used. In the following section, a detailed explanation of the ASHRAE climate classes will be presented.

The ASHRAE climate classes

The 2007 ASHRAE handbook gives a set of guidelines for the conditioning of museums, galleries, archives and libraries. However, these are design guidelines only. Nevertheless, it classifies the conditioning of a museum with respect to the quality and acceptable level of risks of the object of art. For this reason, it could also be used for non-designers in order to characterize a particular gallery and the requirements of the collection. The characteristics of the ASHRAE climate classes are shown in Table 1.

Table 1: *ASHRAE 2007 Museum Guidelines, Specifications for Collections (ASHRAE, 2007)*

Type	Set Point or Annual Average	Maximum Fluctuations and Gradients in Controlled Spaces			Collection Risks and Benefits
		Class of Control	Short Fluctuations plus Space Gradients	Seasonal Adjustments in System Set Point	
General Museums, Art Galleries, Libraries, and Archives All reading and retrieval rooms, rooms for storing chemically stable collections, especially if mechanically medium to high vulnerability.	50% rh (or historic annual average for permanent collections) Temperature set between 59 [15°C] and 77°F [25°C] Note: Rooms intended for loan exhibitions must handle set point specified in loan agreement, typically 50% rh, 70°F [21°C], but sometimes 55% or 60% rh.	**AA** Precision control, no seasonal changes	±5% rh, ±4°F [2°C]	Relative humidity no change Up 9°F [5°C]; down 9°F [5°C]	No risk of mechanical damage to most artifacts and paintings. Some metals and minerals may degrade if 50% rh exceeds a critical relative humidity. Chemically unstable objects unusable within decades.
		A Precision control, some gradients or seasonal changes, not both	**As** ±5% rh, ±4°F [2°C]	Up 10% rh, down 10% rh Up 9°F [5°C]; down 18°F [10°C]	Small risk of mechanical damage to highvulnerability artifacts; no mechanical risk to most artifacts, paintings, photographs, and books. Chemically unstable objects unusable within decades.
			A ±10% rh, ±4°F [2°C]	RH no change Up 9°F [5°C]; down 18°F [10°C]	
		B Precision control, some gradients plus winter temperature setback	±10% rh, ±9°F [5°C]	Up 10%, down 10% rh Up 18°F [10°C], but not above 86°F [30°C]	Moderate risk of mechanical damage to high vulnerability artifacts; tiny risk to most paintings, most photographs, some artifacts, some books; no risk to many artifacts and most books. Chemically unstable objects unusable within decades, less if routinely at 86°F [30°C], but cold winter periods double life.
		C Prevent all highrisk extremes	Within 25 to 75% rh year-round Temperature rarely over 86°F [30°C], usually below 77°F [25°C]		High risk of mechanical damage to high vulnerability artifacts; moderate risk to most paintings, most photographs, some artifacts, some books; tiny risk to many artifacts and most books. Chemically unstable objects unusable within decades, less if routinely at 86°F [30°C], but cold winter periods double life.
		D Prevent dampness	Reliably below 75% rh		High risk of sudden or cumulative mechanical damage to most artifacts and paintings because of low-humidity fracture; but avoids high-humidity delamination and deformations, especially in veneers, paintings, paper, and photographs. Mold growth and rapid corrosion avoided. Chemically unstable objects unusable within decades, less if routinely at 86°F [30°C], but cold winter periods double life
Archives, Libraries Storing chemically unstable collections.	Cold Store: –4°F [-20°C], 40% rh	±10% rh, ±4°F [2°C]			Chemically unstable objects usable for millennia. Relative humidity fluctuations under one month do not affect most properly packaged records at these temperatures (time out of storage becomes lifetime determinant).
	Cool Store: 50°F [10°C], 30 to 50% rh	(Even if achieved only during winter setback, this is a net advantage to such collections, as long as damp is not incurred)			Chemically unstable objects usable for a century or more. Such books and papers tend to have low mechanical vulnerability to fluctuations.
Special Metal Collections	Dry room: 0 to 30% rh	Relative humidity not to exceed some critical value, typically 30% rh			

In class AA, small short fluctuations are allowed, such as ±5% relative humidity and ±2°C. Additionally, no seasonal humidity changes are allowed and the temperature is limited by a ±5°C range. Class A is divided in As and A. Class As allows a small seasonal fluctuation (±10% and up 5°C, down 10°C) while keeping the short fluctuations low (±5% and 2°C). Class A however, gives a little bit more room in the short fluctuations (±10% and ±2°C) but limits the seasonal changes to 0% and up 5°C, down 10°C. Class B allows a short fluctuation of ±10% and ±5°C and the seasonal changes to ±10% and up to 10°C, as long as it does not exceed 30°C. Class C allows the relative humidity to stay within 25 – 75% year round and the temperature rarely above 30°C. Finally, the only requirement of class D is to prevent dampness, in other words, to keep the relative humidity below 75% (ASHRAE, 2007).

Class AA guarantees no risk of mechanical damage for most objects, while classes As and A guarantee a small risk. However, most objects in these classes are safe unless the object itself is chemically unstable. Class B has a moderate risk of mechanical damage to most materials, but a tiny risk for paintings. Class C poses moderate risks for mechanical damage for paintings and class D offers a high risk of mechanical damage to most objects (ASHRAE, 2007).

Using the ASHRAE museum climate classes as a useful guideline for early stage design is helpful because it represents, in an uncomplicated way, the risks that are associated with a particular class. However, Martens (2012) states that it can also be dangerous to use these guidelines as a form of risk assessment. This is because damage to a collection usually occurs in the periods that the climate does not comply with a particular class. In other words, in order to guarantee the mitigation of the risks associated to a particular class, it is customary that the environment complies with the requirements of that class for 100% of the time. Martens (2012) studied 21 museums in the Netherlands and found this to be a characteristic flaw, since for multiple reasons, complying 100% of the time to the requirements of a class is particularly difficult, and might not even be necessary. In order to understand why this may not be necessary, it is important to change the indoor climate approach to an object-specific approach. Understanding the response of a particular object of art will not only help us define the associated risks but also give information on the allowable periods of exposure, amplitude of indoor climate fluctuations and the behavior of the failure of the object. Therefore, the following section will introduce the response of canvas paintings to the indoor climate.

Another challenge to the overall museum environment is the current state of the art of the measurement technique. While guidelines such as the above mentioned ASHRAE environment classes provide recommendations in the range of ±5% relative humidity (e.g. short fluctuations in class AA) the current equipment museums use to monitor relative humidity is based on thermo hygrographs, in which accuracy is limited to ±5%, and electronic hygrometers, in which accuracy is limited to ±3%. Clearly, such specifications make no sense when the accuracy of the monitoring equipment is so high (Brown, 1994).

Mechanical response of paintings on canvas

Mecklenburg (2007) studied the effect of cycling relative humidity on canvas paintings, where the different components of a standard canvas painting were studied individually. The components studied were the canvas, the glue, the ground and the design layers (i.e., paint).

The canvas is the main component of paintings. It is a woven fabric (e.g. linen, cotton or hemp) that gives the base for the painting. Canvas fabric has two clearly defined directions; that is the warp and the weft. These are perpendicular to each other and are defined by its manufacturing process. The composition of the yarns and the manufacturing process (which, for example, define the amount of tension among the yarns) help define the quality of the textile, since these parameters are directly related to the degradation principle of the textile. However, the conservation of the material is not the only quality-defining property of canvas; also the texture and workability must be considered from the artist's perspective.

The glue is the principal ingredient used when sizing the canvas. Sizing is the process of applying hide glue or a polymer-based material in order to increase the support of the canvas and reduce the

absorbance of the textile. Hide glue is one of the oldest and most reliable materials for sizing the canvas (Saitzyk, 1987).

The ground is the surface that allows the attachment of the design layers and gives it a particular texture. Grounds allow a particular absorbance of the design layer with direct consequences on the final appearance. Gesso is the most broadly used ground. It was known as the product of combining rabbit skin glue (a hide glue as mentioned above) and calcium carbonate (chalk). Originally grounds were used for the preparation of flexible supports, however, the terms gesso and grounds have been used interchangeably over time. Acrylic polymer gesso is currently the most used ground; this is due to its versatility, simplicity of use, short drying time and flexibility.

The composition of the design layers varies depending on the type of painting. Oil paintings are composed mainly of a binder, a pigment and a solvent. The pigment is the color component of the design layer. The binder keeps the pigment attached to the surface, and the solvent allows the design layer to dry evenly (Clark).

Figure 2, Figure 3, and Figure 4 show the results from the Mecklenburg study. Force/width has been chosen over pressure, due to the fact that the cross sectional areas of the components are so small. It is important to note that for most of the relative humidity range, it is the glue that gives support to the painting, and not the textile. The textile gains considerable stress only at very high relative humidity. However, the magnitude of the stresses experienced in the design layer are considerably smaller than those of the glue and textile.

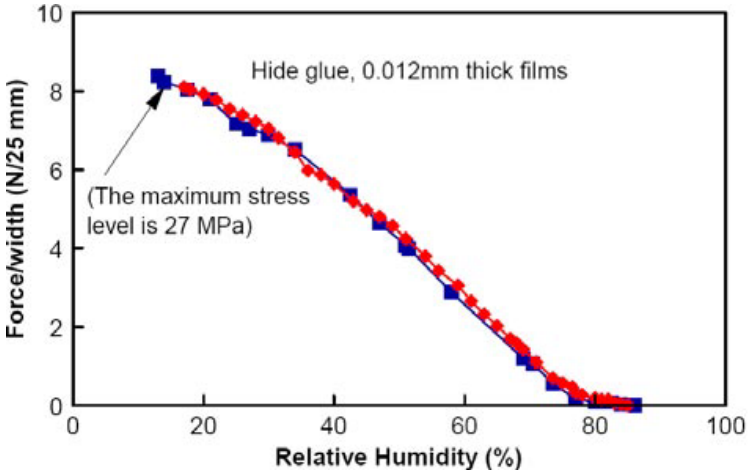

Figure 2: Mechanical response of hide glue to varying relative humidity (Mecklenburg, 2007)

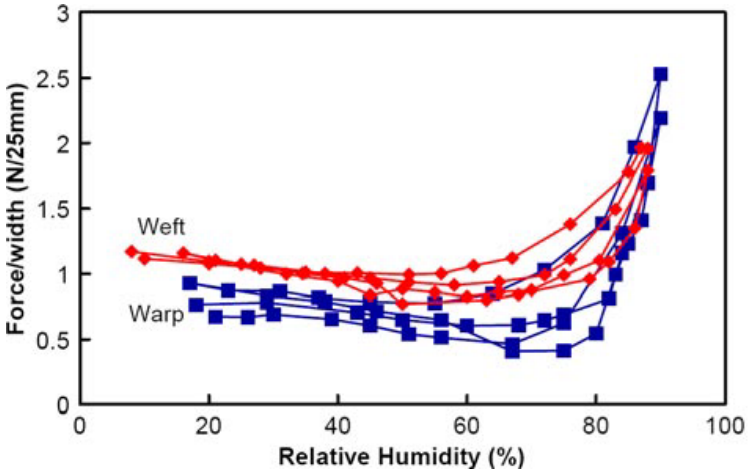

Figure 3: Mechanical response of canvas textile to varying relative humidity (Mecklenburg, 2007)

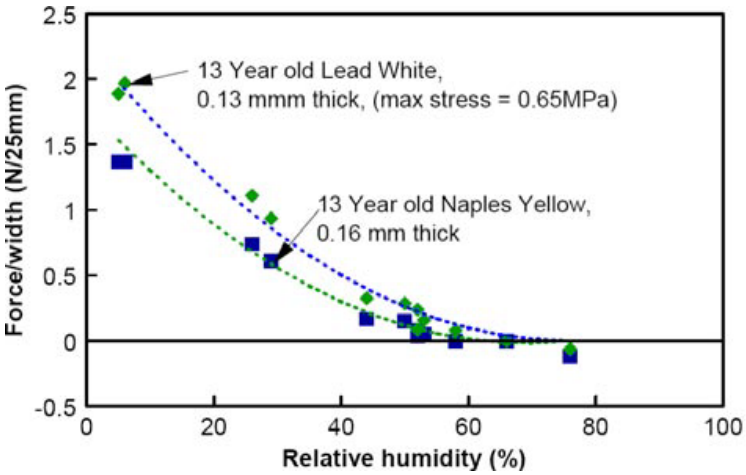

Figure 4: *Mechanical response of paints to varying relative humidity (Mecklenburg, 2007)*

Additionally, Mecklenburg superimposed these results and compared them with the behavior of an actual painting with the same components. This painting was an unknown portrait made by Duncan Smith in 1906. As it is shown in Figure 5 and Figure 6, the behavior of the superimposed results matches the actual behavior of the Duncan Smith painting.

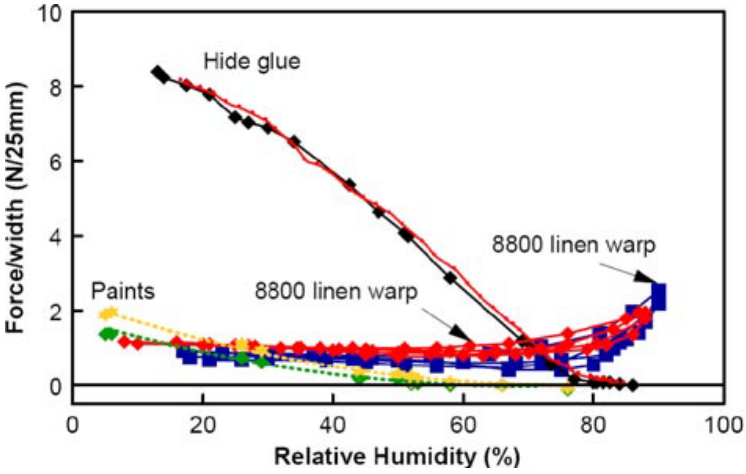

Figure 5: *Superimposed response of canvas painting materials (Mecklenburg, 2007)*

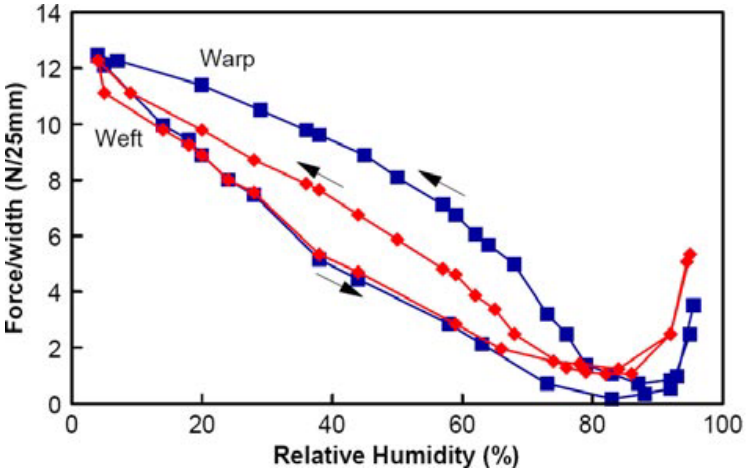

Figure 6: *Mechanical response of an actual painting by Duncan Smith (Mecklenburg, 2007)*

An agreement can be seen between the superimposition of the individual results and the response of the Duncan Smith painting. Basically, the hide glue dominates most of the relative humidity spectrum, which lowers as the relative humidity increases. The effect of the canvas, however is dominant over all the other components in the high relative humidities; note that the design layer never develops sufficiently high stresses, in comparison to the hide glue or the canvas. Additionally, Mecklenburg evaluated the mechanical failure characteristics of canvas paintings by letting a sample go through repetitive cycles of relative humidity. After each cycle, the canvas was inspected and each new crack was recorded. This is shown in Figure 7. Mecklenburg concluded that mechanical failure due to cyclic relative humidity appeared on the corners of the paintings and after the ninth cycle no newer cracks were formed. This might be attributed to the fact that after a certain number of cracks, (nine), enough room is available for the further strains produced by future cycles. Mecklenburg also concluded that the main responsible component for the mechanical failure is the desiccation of the glue component.

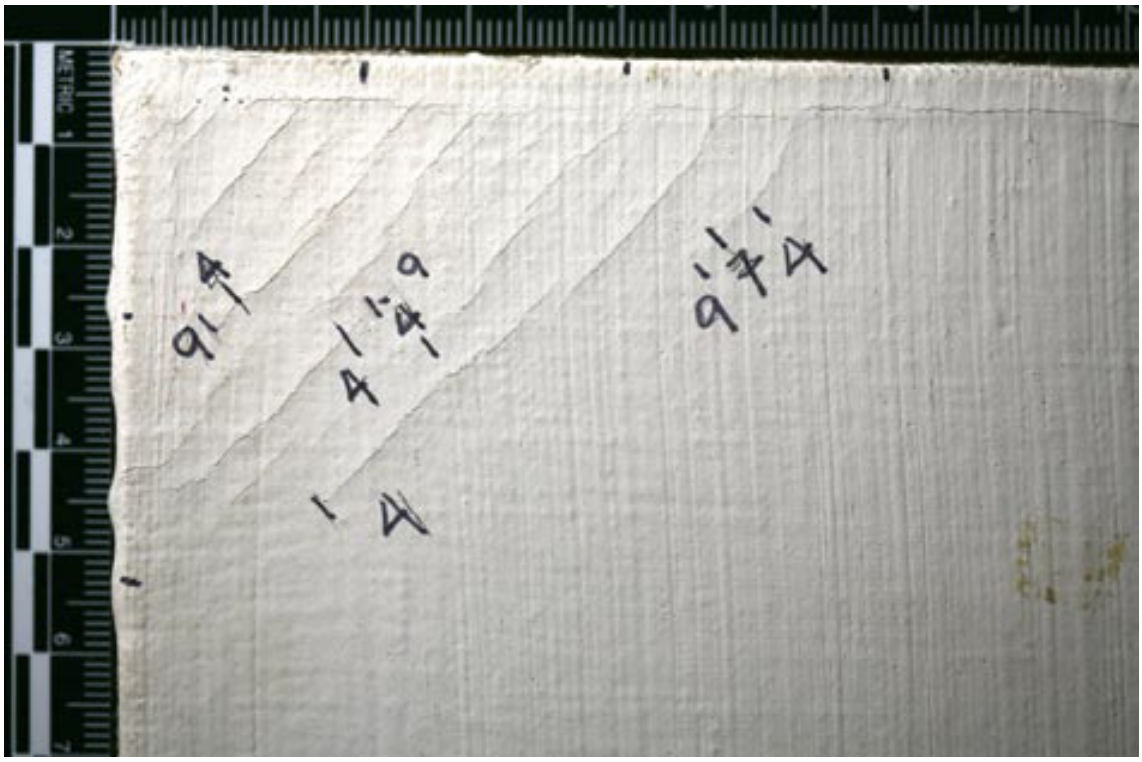

Figure 7: Cracks result from the mechanical failure due to varying relative humidity (Mecklenburg, 2007)

Deterioration mechanisms

In the previous section, the mechanical response of canvas paintings was presented. In this section, the main processes that define such mechanical response in objects of art are explained. However, mechanical deterioration is not the only form of deterioration influenced by the indoor climate. Biological and chemical deterioration can also endanger the quality of a collection; these deterioration forms will be introduced next.

Mechanical deterioration

Mechanical deterioration particularly occurs when the stresses induced by climatic variations (moisture variations, mainly) are much greater than the yield point/strength of specific layers in the object of art, as seen in the previous section. It is important to mention that deterioration only occurs when the material is constrained while subjected to such climatic variations.

The material can be constrained either by external elements (e.g. the frame) or by the composition of materials with varying stiffness (e.g. different paints and grounds). Mechanical failure produced by external elements is usually the product of slow variations in the moisture level; therefore these take longer time to be perceived and the failure is usually more severe. On the other hand, mechanical failure produced by materials of varying stiffness is the product of rapid changes in moisture content; where the failure is more immediate and perceived only on the outer layers of the material.

When referring to the conservation of cultural heritage, both fracture and deformation must be prevented. Among experts (Martens, 2012), strain has been chosen to better qualify the state of mechanical deterioration. This is because using stress must include the effect of creep and relaxation which are commonly seen among objects of art; the added complexity of creep and relaxation has been enough reason to discard stresses as the qualifying property of mechanical deterioration.

The mechanical response of a material under particular moisture content is closely related to its equilibrium moisture content, EMC. The EMC of a material is that particular moisture content where the moisture transfer with the environment is zero. Different materials at different moisture contents have their own particular EMCs. As mentioned before, EMC is also a function of temperature, however EMC is usually represented under constant temperature, as shown in Figure 8.

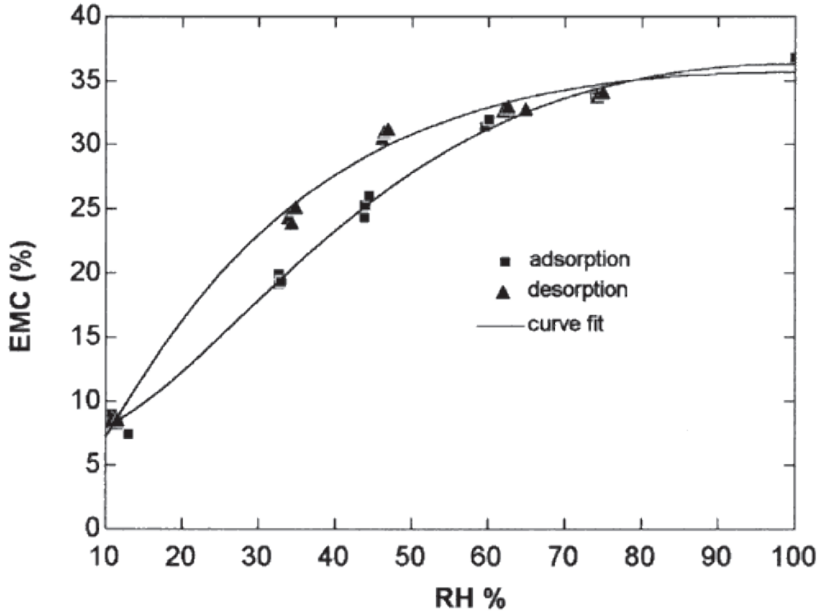

Figure 8: Sorption isotherm of regular silica gel (Yu et al. 2001)

The frequency of those fluctuations that result from mechanical failure must be higher than the object's response time. This is because the EMC of the object of art must be under a certain change in order to create the strain necessary for failure. In other words, if the EMC is constant, then no stresses are induced on the material.

Erhardt (1994) defined the parameters that have the most influence on the magnitude of moisture induced strains. These are shown below:

1. Moisture coefficient of expansion
2. Change of stiffness in the material
3. Degree of restraint of the material
4. Magnitude and rate of change in relative humidity

Similarly, Erhardt defined that the material response to such loads is based on:

1. The material strength
2. Ability to deform
3. Presence of defects
4. Fracture sensitivity

Therefore a very precise understanding of the material is required in order to evaluate the degree of mechanical deterioration an object experiences under a certain environmental load. However, considering the wide range of materials present in a collection, such understanding becomes very difficult. In order to assess this, more generalized methods have been developed that range from overall visual inspections to the detection of micro-cracks in wood by means of acoustical measurements (Kozlowski, 2007).

Biological deterioration

Biological deterioration occurs when the environment is optimum for living organisms to develop on the object of art. Fungus is the main biological agent responsible for most types of biological deterioration. Michalski (1993) concluded that environments with a relative humidity of 60% or lower have less risk of the development of mold growth; however environments with relative humidity of 75% or above are particularly susceptible. Mold growth depends mainly on three parameters: humidity, temperature and nutrients.

Condensation of water vapor is the main cause of mold growth. However, it has been shown that mold growth can develop at a relative humidity lower than 100%. In fact, the optimum relative humidity for mold growth is lower than 100% (Adan, 1994). In this case, temperature differentials have an important role with respect to biological deterioration; this is because at high relative humidity, any change in temperature may lead to condensation.

There is extensive research on the conditions for mold growth in museums, and they all conclude that controlling the peaks of relative humidity so that humidity does not exceed 75% should prevent the collection from biological deterioration. Particularly, Beuchat (1987) affirmed that at relative humidities lower than 55%, the DNA of fungus collapses.

Isopleth diagrams can be used to characterize the growth behavior of fungi. These are diagrams that map the growth rate of a fungus under specific relative humidity and temperature on a particular substrate, as shown in Figure 9. These isopleth diagrams are directly dependant on the type of substrate; this is true because the type of substrate determines the amount of nutrients available. Isopleth diagrams have been developed for a wide number of fungi species and at different substrates.

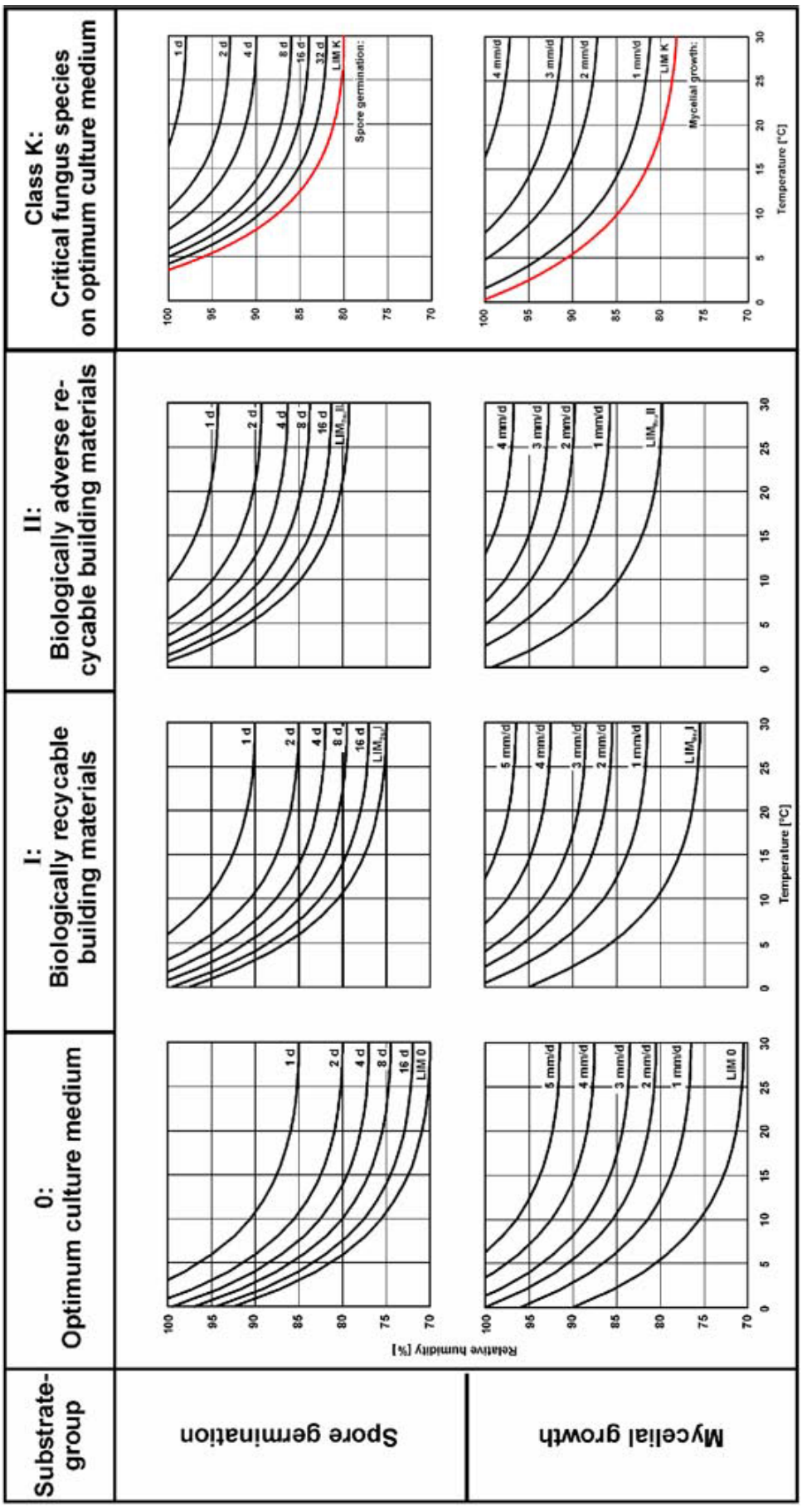

Figure 9: Isopleth diagrams (Krus et al. 2007)

Determining the mold growth characteristics solely from the isopleth diagrams has the disadvantage that the drying out of the spores cannot be taken into account when using transient boundary conditions. For this reason, Krus et. al. (2007) developed a biohygrothermal model, the main objective of which is to predict the moisture balance under realistic boundary conditions. This model assumes that growth starts above a particular moisture content, and no metabolic activities exist below that level. The model assumed isothermal conditions in order to lump liquid (i.e., capillary suction) and diffusion transport. This model proved its potential with the renovation of the Rijksmuseum. However, it has not been validated for cultural heritage materials yet.

Chemical deterioration

This form of deterioration is based on the chemical processes occurring on the object under particular relative humidity and temperature. Higher relative humidity increases the moisture content of the object which produces and/or increases chemical reactions. Similarly, higher temperatures increase the speed of chemical reactions. However, chemical deterioration is only a concern once mechanical and biological deterioration have been accounted for. This is because chemical deterioration usually takes more time and is less severe than the mechanical and biological form of deterioration. Take, for instance, newspaper fragments which become unrecognizable after 30 – 100 years have passed at 20°C and 50% relative humidity (Ankersmit, 2009).

In order to characterize the deterioration due to chemical processes a, parameter called lifetime multiplier has been developed. This is a measure of the number of life spans during which an object remains usable when compared to a standard condition of 20°C and 50% relative humidity, as shown in Figure 10.

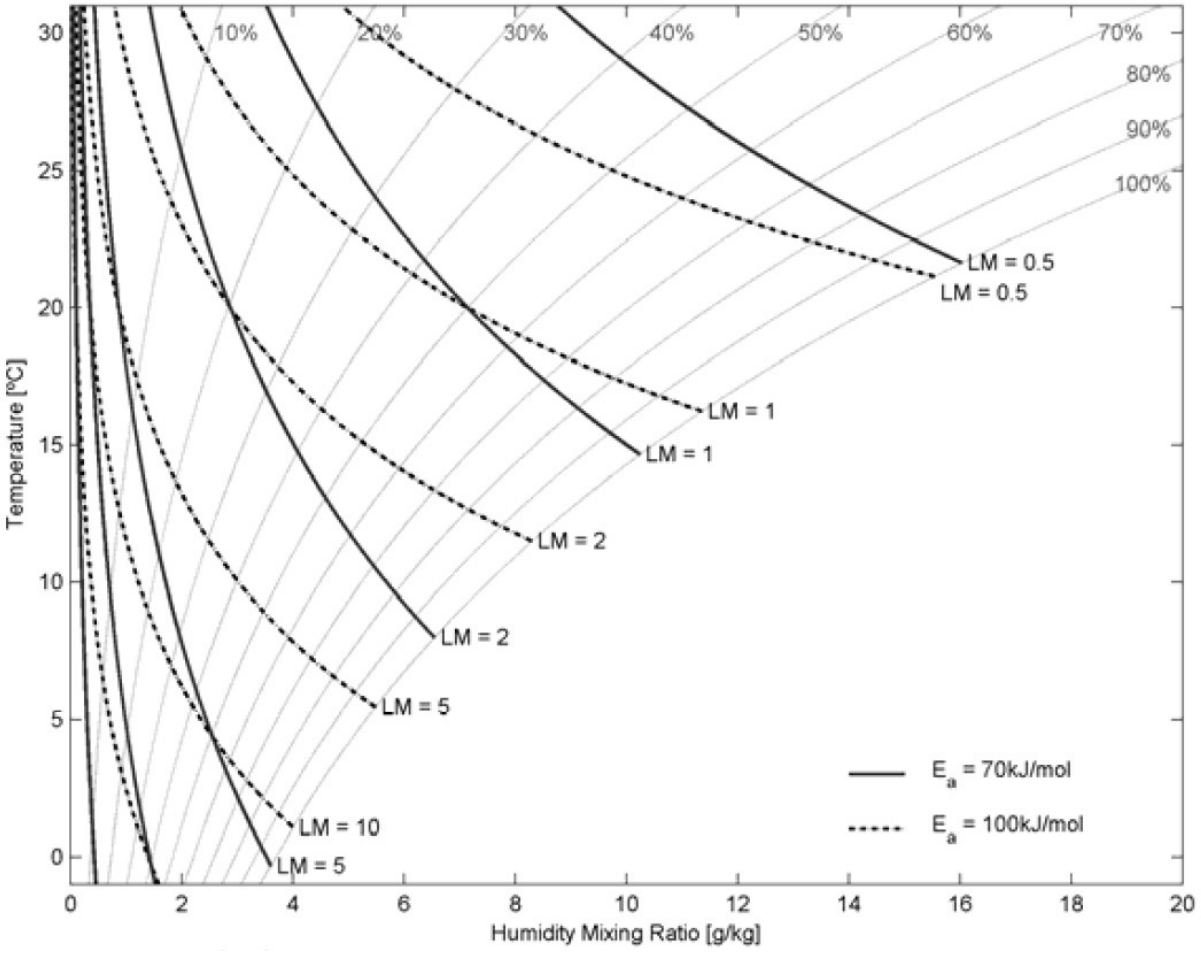

Figure 10: Psychrometric chart with lifetime multipliers (Martens, 2012)

The display case

Display cases have particularly been designed to mitigate the risks to which a highly valued object of art might be subjected. Mitigating the risks concerning the indoor climate has been proven to be rather difficult and the modes of deterioration quite severe. Sometimes the challenges of the museum environment outweigh the conservation requirements of the collection; it is in these scenarios that display cases have proven their benefits. Display cases enhance the microclimate surrounding the object of art by offering a buffer from the museum indoor environment. Display cases are object oriented products, so the behavior of the microclimate inside depends on each particular case (i.e., dimension, object composition, environmental loads...). Additionally, display cases must consider special requests from the clients which may or may not be related to the conservation of the piece, (e.g., special robbery-proof display cases.)

Specially designed spaces for the conditioning of objects of art have been discovered since ancient history. Take, for instance, the great conservation of different objects in burial chambers all around the world, such as, Egyptian pyramids. However, it was not until the 90th century that the modern display case was originated. This might be attributed to the necessity to protect objects of art from the newly found air pollution, and to the sudden availability of different materials. Consider, for instance, the harming effect of the burning of coal gas for lighting, upon the paintings in the National Gallery and the leather book bindings in the libraries in London (Shiner, 2007). As a response, the National Gallery started to glaze paintings and in 1892 patented a sealed enclosure to hold a painting by JMW Turner. This painting was recorded to be the most deteriorated painting of a group of several other paintings. This painting has remained undisturbed in that enclosure since then, and when compared with the other paintings in that group, a noticeable conservation can be seen (Shiner, 2007).

Today there are two main types of display cases, those conditioned actively, by means of an air conditioning unit; and those conditioned passively, by means of special hygroscopic materials. These types are explained below:

The passive display case

One of the earliest references of using a hygroscopic material to buffer moisture variations inside a sealed enclosure is from a patent from 1932 (British Patent 396.439), shown in Figure 11. In this case, a tray of saturated salts was added to the enclosure. Conceptually, saturated salts have a sensitive response to moisture content differentials in the environment, adding/extracting moisture when needed. This model has been used in several instances, including for objects in the National Gallery of Scotland.

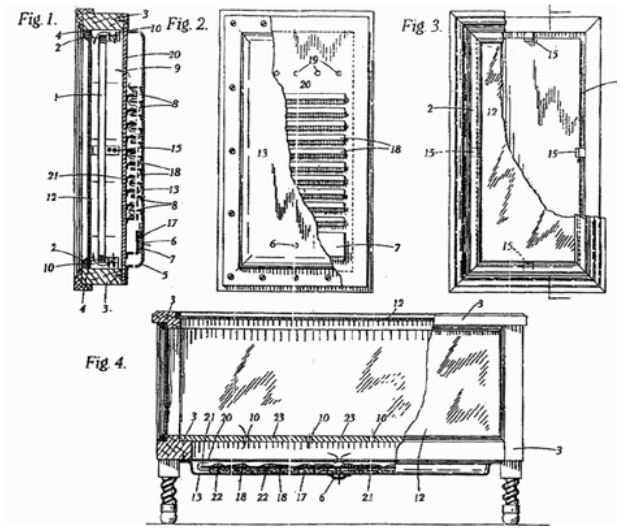

Figure 11: 1932 model of passive display case (British Patent 396.439)

Multiple materials have been used to condition the amount of moisture in air, including 1740 pounds of canvas hose for The Orangery of Hampton Court Palace in 1934 (Brown et al. 1997). However, it was not until the end of the World War I that silica gel was started to be used. Silica gel offered a property that the other organic materials failed to provide; this is, its infinite capacity for reuse. Over the years, the properties of silica gel have been designed in order to condition at a desired level of relative humidity.

Conceptually, once a perfectly sealed display case has been provided with the appropriately conditioned silica gel, there should be no maintenance required. However, this scenario is far from reality. There are significant practical challenges for creating a "perfectly-sealed" display case; some of these challenges were discussed in chapter one. Additionally, if the average long term relative humidity (e.i., yearly, seasonally) is not close to the desired relative humidity, there will be a need for reconditioning the silica gel. An important challenge for passively conditioned display cases is that with an inadequate transfer of moisture through the display case, leaks may result in an inadequate stratification of moisture (Buttler, 2007).

In chapter one, the challenges of a well-sealed and loosely-sealed display case were presented. These challenges are still under discussion among academics, which has presented the opportunity for the development of another form of conditioning; that is, active conditioning.

The active display case

Active display cases are based on the mechanical conditioning of the air in the museum environment. Clearly, the concerns about air quality seen in the passive display case are not an issue anymore. This is because by insuring that a well designed flow of air passes through the object, any pollutants and any residual leakage are displaced out of the microclimate of the object.

The development of the active display case goes hand in hand with the development of the HVAC system. However, creating an HVAC system of the appropriate size for a display case was the main challenge. A simple but difficult challenge, fitting an entire HVAC system in the subtle base of a display case, had to wait until the twentieth century. As early as 1938 we can see the attempts of creating this active display case. Young (1938) designed an elegant system for humidity control for an Egyptian bust in the Boston Museum of Fine Arts. This system was based on moving the museum air, by means of an electrical pump, through a bed of calcium chloride, removing a significant amount of the air moisture content.

The idea of fitting a full size HVAC unit in the base of a display case continuously intrigued conservation engineers since it had a lot of promise. However, it is important to note, that HVAC units condition the level of humidity by adding, at certain periods, a load of moist or dry air to the conditioned space and then allowing the relative humidity to reach a uniform level. This conditioning process resulted in spikes in the relative humidity which was, in turn, inappropriate for the conservation requirements of the collection. The challenge was to condition the air in the display case continuously and not by continuously adding a designed load. The Micro Climate Generator from 1984 successfully evaluated this issue. First, they replaced compressors with Peltier cells, which reduced significantly the size challenge and used a proprietary humidity modification system that allowed a delivery of constant, steadily conditioned air (Shiner, 2007).

Since then, a variety of active conditioning systems have been developed. An important addition is the computational monitoring of the condition system, which allowed, for the first time, a greater level of quality control. Shiner affirms that the state-of-the art active microclimate control system has to be capable of "supplying a dust, oxygen-free, humidity and temperature controlled environment" (Shiner, 2007). Currently, the technology to achieve this system is available; however, the costs of making such a system would be prohibitive. Shiner also mentions that such high control of all these factors might be rather unnecessary; in most cases conservation may be ensured by controlling only one factor.

For these reasons, the value of passive conditioning still proves significant; the relative low maintenance and low overall costs give a market opportunity for passive display cases. Furthermore, a passive system provides conditioning with zero energy input. This is a great advantage, especially now that integrated sustainable approaches are becoming more significant. Arguably, active systems are becoming more and more energy efficient; however, during the literature research of this project no active system was found to be able to function using zero energy.

The hygroscopic material

The key active ingredient of the passive display case is the hygroscopic material. While all materials are to a certain degree hygroscopic, we refer here to the hygroscopic material as one that has a particularly high moisture buffering capacity and is used solely for that purpose. In chapter 1, the passive display case was introduced and different hygroscopic materials were shown to be used, (i.e., saturated salts.) However, this project is limited in using only silica gel as a buffering mechanism. For this reason, when referring to the hygroscopic material it is meant to refer to the silica gel added for buffering purposes.

This chapter introduces silica gel as the hygroscopic material. Initially, defining its composition and manufacturing process will lead us to understand the physical properties of this material. As a consequence of the manufacturing process, there are multiple types of silica gel, which have been engineered to adsorb and desorb under certain relative humidities. The most common types of silica gel will be described next. Then, a theoretical background on the relevant diffusion process that takes place in the moisture transfer through the silica gel will be explained. Finally, the moisture transfer scheme is presented based on the mass balance law for this particular case.

Manufacturing process of silica gel

Silica gel is a form of precipitated silicon dioxide gel, a granular/porous form of silica made from sodium silicates. The process of manufacturing silica gel involves the acidification of a solution of sodium silicates, which in turn produces a gelatinous precipitate. This precipitate is the basic colorless silica gel after being washed and dehydrated (Primary Information Services). While silica gel can be produced from many different raw materials, it is the synthesis from the mineral acids that is the only relevant industrial process today (Primary Information Services). The acidification process primarily uses sulfuric acid. The idealized chemical balance of this process is shown below:

$$Na_2Si_3O_7 + H_2SO_4 \rightarrow 3\,SiO_2 + Na_2SO_4 + H_2O \qquad \text{(Eqn. 1)}$$

The porous nature of silica gel is the key property of this material. As a result, the adsorption of moisture occurs due to solely physical processes instead of chemical reactions. This makes the silica gel performance life nearly infinite. Additionally, silica gel is an inert and non-flammable material (GeeJay Chemicals Ltd.).

The colorless silica gel maintains its same appearance under a wide range of relative humidity; for this reason it is also commonly known as non-indicating silica gel. On the other hand, there is indicating silica gel in which a color indicator shows the moisture content of the gel. There are multiple types of indicators available, however, the most common are blue and orange silica gels. Blue silica gel turns blue when dry and turns pink when humid. It uses cobalt chloride as an indicator, however, this has been classified by the IARC to be possibly carcinogenic to humans (National Park Service). Orange silica gel was developed as a response to the high risk of using cobalt chloride. It uses a safe organic indicator that shows orange when dry and dark green when in humid environments. Figure 12 shows the gradation colors of blue and orange silica gel.

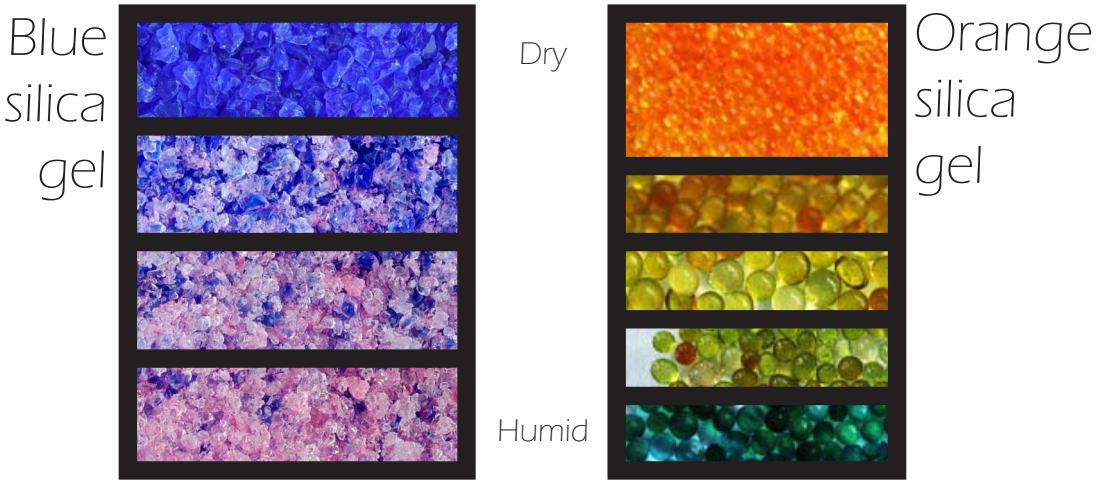

Figure 12: Blue and orange silica gel with gradation colors (International Silica Gel Co.,Ltd) (Silicagel Dessicants).

The modern manufacturing of silica gel allows the production of nearly 100% pure silicon dioxide with engineered pores and surface properties (Primary Information Service). This is how there is silica gel currently available to protect objects that require a specific level of humidity, such as art objects. The following section introduces some of the commercially available silica gel products for the conditioning of art.

Types of silica gel

Commercially available silica gel can be classified in multiple ways. Among these ways are manufacturing process, form, use, and physical properties (chemical composition, purity and pore structure). By the manufacturing process you can find the following classifications; silicone gel, silica-sol, aerogel, and fine silica. By the form of the silica gel you can find liquid, powder, lump, spherical and other specifications. By their use you can find silica gel for industrial, civil, preparation, chromatography analysis, and packing. From the classifications due to physical properties special attention is given to the pore structure, since this one parameter has a great effect on the sorption properties of the silica gel.

Due to the pore structure, standard silica gel has the following classifications. Fine pore silica gel [Type A] has an average pore diameter of 2nm -3nm, and a surface area ratio of 650 – 800 m^2/g. Medium pore silica gel [Type B] has an average pore diameter of 4.5nm -7nm, and a surface area ratio of 450 – 650 m^2/g. Macro pore silica gel [Type C] has an average pore diameter of 80nm -125nm, and a surface area ratio of 300 – 400 m^2/g (China Silica Gel Co., Ltd). The behavior of these types of silica gel can be better shown with isotherm adsorption curves for each type, Figure 13:

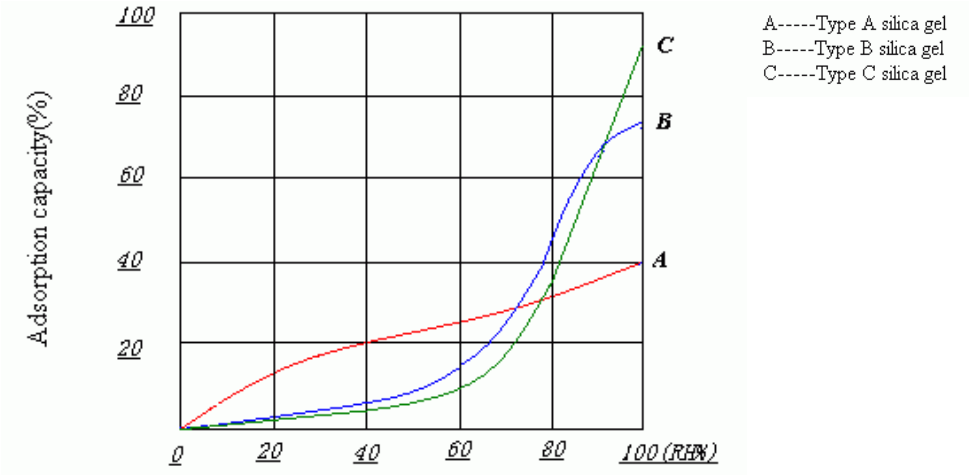

Figure 13: Adsorption curves of silica gel types A, B and C (China Silica Gel Co., Ltd)

We can see that type A has the best adsorption capacity at the lowest humidities. At 70% relative humidity, type B shows dominant performance, and beyond 90% relative humidity it is type C that displays the best adsorption. It is important to note, however, that these specific types of silica gel have been developed for particular uses. For example, fine pore silica gel [Type A] is developed for its desiccant properties used in packaging for such things as electronic equipment, mechanical equipment, textiles, food and medicines. Type B silica gel is usually used for liquid absorbent while type C is commonly used for dehydrated purification of industrial gasses and in the crystal cat litter, among other uses.

For the field of conservation of cultural heritage, regular density silica gel, such as types E and M, has been used.

Silica gel type E is a micro-porous silica with a surface area of 800 m^2/g. The diameter of the beads of this type of silica gel are between 2mm to 5mm. It has a globular shape which allows the air to pass through more easily; for this reason it is recommended to be used in thick layers. However, its optimum range of performance is between 15% and 35% relative humidity. It is because of its low humidity performance that this type of silica gel is commonly used for drying purposes.

Silica gel type M, as opposed to type E, is a macro-porous silica, with a much higher adsorption capacity. However, this capacity is limited to really high relative humidities; above 90%. This type of silica gel is commonly used to prevent condensation. The diameter of the beads of this type of silica gel are between 6mm and 10mm.

However, with the engineered properties necessary for conservation, better performing buffers have been developed under their commercial names, such as ArtSorb and ProSorb. Find in Figure 14 the comparison of the different types of buffering used for the conservation of art.

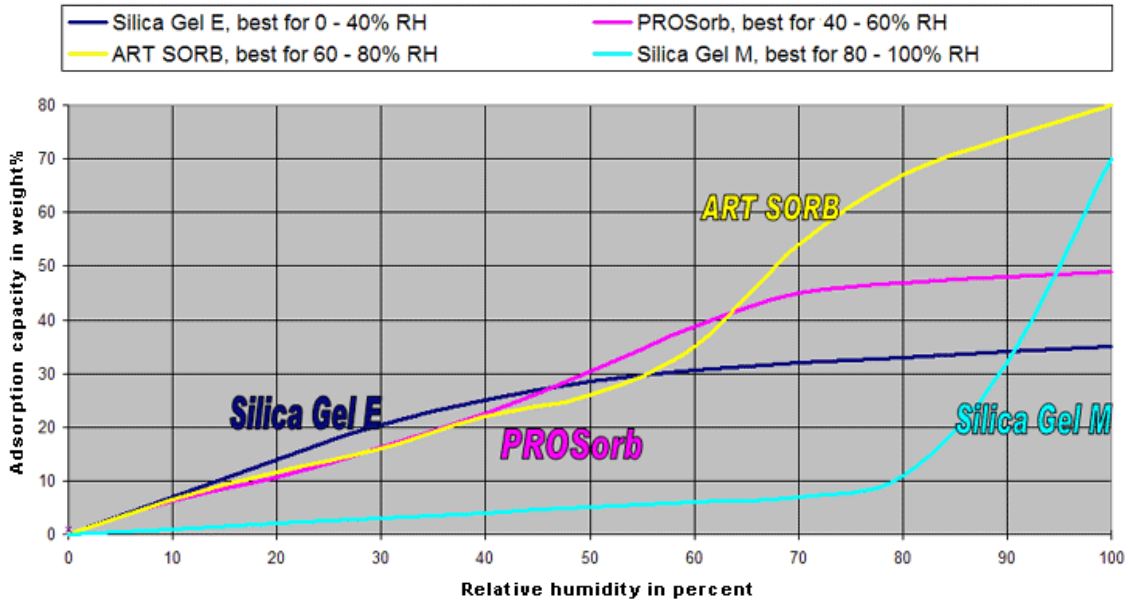

Figure 14: Sorption isotherm of different hygroscopic materials used for the conservation of cultural heritage (Waller).

ArtSorb is made by combining silica gel and lithium chloride and has a range of performance between 60% to 75% relative humidity. The diameter of the beads of this type of silica gel is between 1.5mm to 4mm and it has a very high M-value when compared to regular density silica gel. Additionally, ArtSorb is capable of adsorbing small amounts of organic volatiles. However, one of the key features of ArtSorb is its very small hysteresis, where both adsorption and desorption curves have a considerable high slope over the range of use of this material (Waller). Nevertheless, due to its lithium chloride component, this material can be potentially harmful to many metals; as this is a salt that may induce corrosion. Figure 15 shows the appereance of the ArtSorb beads.

Figure 15: ArtSorb beads

ProSorb has a range of high performance between 40% and 60% relative humidity. Its centered range at 50% relative humidity allows ProSorb to be used for a wide variety of objects of art, due to the fact that it fits the standard of climate conditioning requirement at 50% relative humidity. ProSorb is made of 97% silicon oxide (SiO_2) and 3% by aluminum oxide (Al_2O_3), which is much safer than lithium chloride. It has a surface area of 750 m^2/g, and a bead diameter of approximately 2 mm. Additionally, ProSorb reacts in the same way organic materials do, since it is conditioned by temperature only. In other words, the moisture transfer between organic materials and ProSorb is minimized when there is a temperature differential. Finally, ProSorb also has a higher bulk density, which allows a higher amount of buffer in less volume of contained silica gel. For the above reasons, ProSorb has been used in the physical measurements carried out in this project. Figure 16 shows the appereance of the ProSorb beads.

Figure 16: ProSorb beads

Conclusion

In Chapter 2, the museum climate was introduced. The ASHRAE conditioning guidelines for museums and art galleries gave us an idea of the characteristics of the climate that may surround a passive display case. Additionally, the challenges of conditioning a museum were presented, and in many cases passive display cases seem to be the most suitable solution to guarantee the conservation of the art pieces. However, to truly understand the optimum "state of conservation" of an object of art, it is necessary to study the response of that object to its surrounding environment. The response of objects of art cannot be generalized; it depends on the structure and composition of each material, and therefore the response must be assessed in a case-by-case manner. For this reason, this project presented the mechanical response of paintings on canvas only. Throughout the Mecklenburg study, we were able to discover that the moisture-induced stresses in some painting materials are quite high. For example, the hide glue was found to achieve a maximum stress of 27 MPa when the relative humidity was lower than 20%. This is the most significant form of failure for painted objects, so their conservation is really dependent on their surrounding climate. However, there are two more environment-related forms of failure: biological and chemical failure. Biological failure of an object of art occurs when the moisture content in the material is optimum for the growth of biological organisms, such as mold. Chemical failure depends on the speed of the chemical reactions taking place between the materials of the object of art; this failure form is the least severe of the three failure forms because the speed of these chemical reactions is usually very low.

Understanding the museum environment and the forms of failure that environment can produce on an object of art lead us to the display case; a possible solution to this challenge. A short historical summary of both the passive and the active display case was provided. This is important because the historical trajectory and development of the display case may provide insight into the way our ancestors approached these indoor environmental challenges. Today, the development of active display cases has resulted in a very promising state of conservation, however, the disadvantages of these display cases cannot be overlooked, such as high costs and maintenance needs. Passive display cases, on the other hand, have the potential to guarantee a controlled buffered environment with lower costs and minimal maintenance. To further understand how passive display cases can do this, we first need to look at the hygroscopic material itself. Silica gel is the most commonly used hygroscopic material in the conservation of art today. Its composition and manufacture allow for a wide range of silica gel to be developed resulting in many types used not only in the art conservation industry, but also in medical and electronics packaging. Understanding the performance of the passive display case requires us to study in further detail the mechanisms in which moisture can enter or exit the display case. In this project we chose to develop a computational model with the aim of predicting this behavior. Not only did building the model give us insight into the mechanisms of moisture transport but it also served as a tool for simulating the performance of the display case under any possible environment.

Chapter 3 : Model Description

The following chapter describes the model developed during this project. This chapter is organized in four basic sections; the moisture transport in packed beds of hygroscopic materials, the moisture balance of the display case, the numerical approach and the model implementation. The first section provides the ruling principles that determined the moisture transfer process inside of a packed bed of hygroscopic material. The following sections extend this principle to a display case setup, where the moisture transfer is determined by differentials in temperature and pressure. The numerical approach describes the discretization of the model. The way that these equations are solved is explained in the last section; the model implementation.

Moisture transport in packed beds of hygroscopic materials

Hygroscopic material is commonly found in packages. These packages contain many beads of hygroscopic material and allow, through their permeable composition, the flow of moisture in and out of the package. This package has been assumed to behave like a packed bed of hygroscopic material. One of the greatest challenges in this project is on modelling the moisture transfer through a packed bed, considering that not only diffusion but also advection in the pores space between the beads can be a significant mechanism of moisture transfer. In the following section the principles that allow us to model the moisture transfer in a packed bed are explained.

Mechanisms of adsorption and desorption

As previously mentioned, the mechanism of adsorption and desorption of hygroscopic materials such as silica gel, is strongly related to the properties of its nanopores and its internal surface. It is important, however, to further understand how these mechanisms occur, in order to simulate its behavior. For this, it is necessary to look at how the moisture molecules are adsorbed by the silica gel. Particularly, this will lead to increase the understanding of the diffusion behavior of moisture through silica gel, and bring insight on the reason and potential of its properties.

Pesaran and Mills (1986) elaborated on a theoretical study of the moisture transport through silica gel, and affirmed that for silica gel at atmospheric pressure, the Fick's law diffusion mechanism has a negligible contribution. Fick's law diffusion is commonly used in the field of building physics to estimate the moisture transfer through different porous building materials. However, common building materials have very different porous structures. In silica gel, the moisture transfer is governed by surface and Knudsen diffusion. These mechanisms will be discussed in the following sections.

Knudsen diffusion

Knudsen diffusion occurs in a porous solid when the pore is small. Knudsen diffusion is based on the fact that when the mean free path of a gas particle is sufficiently large in comparison with the pore diameter, collisions with the wall of the pore are more common than collisions among the gas particles. The reflections from the walls of the pore are essentially diffuse, as opposed to specular; that is to say that the particles rebound in almost all random directions. So the diffusion resistance is very much attributed to the pore wall, and not to the gas properties as is in the case of ordinary diffusion (Sherwood et al. 1975).

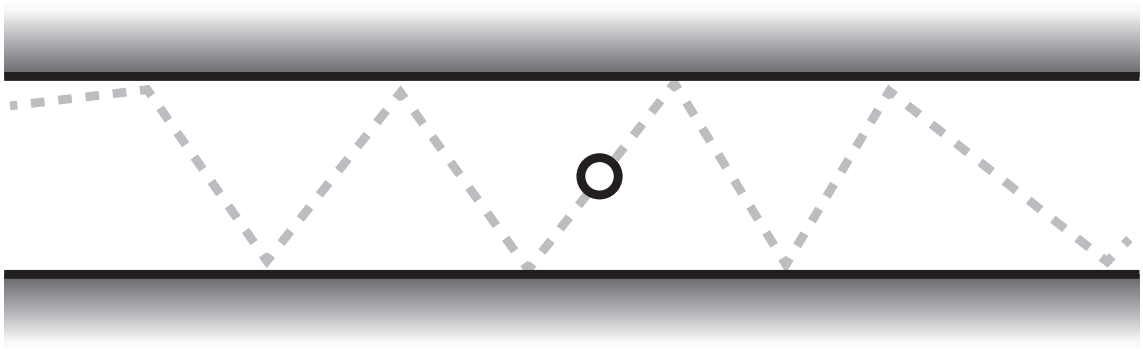

Figure 17: Knudsen diffusion: Trajectory of a water vapor molecule inside a silica gel pore

Pesaran and Mills (1986) provide a Fick's law-type of equation for Knudsen diffusion, based on a Knudsen diffusion coefficient, D_K. In the case of moisture transport in a straight, cylindrical pore of radius a, the Knudsen diffusion coefficient is defined as:

$$\mathrm{D}_K = 22.86 \times T^{\frac{1}{2}} \times a \qquad \text{(Eqn. 2)}$$

A modified Knudsen diffusion coefficient, $\mathrm{D}_{K,eff}$, is introduced for real porous media.

$$\mathrm{D}_{K,eff} = \frac{\varepsilon_p}{\tau_g}\mathrm{D}_K = \frac{\varepsilon_p}{\tau_g} \times 22.86 \times T^{\frac{1}{2}} \times a \qquad \text{(Eqn. 3)}$$

Where ε_p is the particle porosity and τ_g is the gas tortuosity factor.

Pesaran and Mills concluded as part of their research that Knudsen diffusion is dominant when the pore size is smaller than 200 Å. For silica gel the pore size is well in this 200 Å range.

Surface diffusion

Surface diffusion occurs when the equilibrium surface concentration of the gas particles increases when the concentration of particles in the gas increases. In other words, the equilibrium surface concentration of the gas particles develop a gradient of the same direction of the concentration gradient of the gas. When developing the surface diffusion mechanism, it is commonly assumed that the adsorbed layer is sufficiently thin so that the effective pore size remains unchanged. Under certain types of adsorption this adsorbed layer is mobile (Sherwood et al. 1975). Kruckel (1973) proposed that the mechanism of surface diffusion on regular density silica gel particles is one of activated hopping molecules in random walk process.

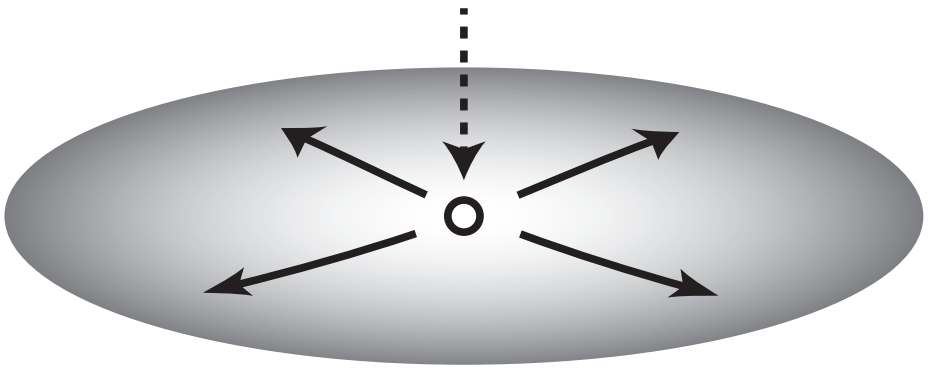

Figure 18: Surface diffusion: Trajectory of a water vapor molecule across a surface

Pesaran and Mills (1986) used in their research a modified version of the Sladek et al. (1974) definition of

surface diffusion coefficient, D_S. That is:

$$\mathrm{D}_{S,eff} = \frac{1}{\tau_s}\mathrm{D}_S = \frac{\varepsilon_p}{\tau_g}\mathrm{D}_o e^{\left[-0.947\times10^3\left(\frac{H_{ads}}{T}\right)\right]} \quad \text{(Eqn. 4)}$$

Where τ_s is the surface tortuosity factor, H_{ads} is the heat of adsorption (kJ/kg) and D_o is 1.6 x 10^{-6} m^2/s. The assumed value for D_o was further confirmed by Pesaran and Mills by matching their theoretical and experimental results of the transient response of packed beds of silica gel. The heat of adsorption represents the energy released during the adsorption process, and constitutes a good measure of the quality of a material to adsorb a particular substance, in this case water vapor. Pesaran and Mills used the following relationships based on the moisture content, w (kg/kg), for the heat of adsorption:

For regular density silica gel:

$$H_{ads} = -12400w + 3500w \le 0.05 \quad \text{(Eqn. 5)}$$

$$H_{ads} = -1400w + 2950w > 0.05 \quad \text{(Eqn. 6)}$$

For intermediate density silica gel:

$$H_{ads} = -300w + 2095w \le 0.15 \quad \text{(Eqn. 7)}$$

$$H_{ads} = -2050w > 0.15 \quad \text{(Eqn. 8)}$$

The moisture transfer process inside the silica gel

Hagentoft (2001) defined the mass transfer mechanism, starting from the principle of conservation of mass:

$$\nabla \cdot \vec{g} = \frac{\partial w}{\partial t} \qquad \text{(Eqn. 9)}$$

Which means that the rate of change of the moisture flow, $\vec{g}$, must be equal to the rate of change of the moisture content, w (kg/m^3), with respect to time. $\vec{g}$ can also be defined as:

$$\vec{g} = \vec{g}_v + \vec{g}_l \qquad \text{(Eqn. 10)}$$

Where $\vec{g}_v$ is attributed to the vapor transport, and $\vec{g}_l$ to the liquid transport. In this project, the liquid transport of moisture is neglected, therefore, when referring to the moisture flow rate, only the vapor transport is considered. This vapor diffusion flow can be defined as:

$$\vec{g}_v = -\delta_p \left(w, T\right) \nabla P \qquad \text{(Eqn. 11)}$$

Where δ_p (kg/mPas) is the moisture permeability, and P is the partial vapor pressure (Pa).

Andersson (1985) developed the moisture flow rate as a function of the moisture content and the temperature:

$$\vec{g}_v = \delta_p P_s \frac{1}{\xi} \nabla w - \delta_p P_s \left(\left. \frac{\partial \phi}{\partial T} \right|_{w,fix} + \phi \frac{M_w L_{lv}}{RT^2} \right) \nabla T \qquad \text{(Eqn. 12)}$$

Where P_s is the saturated pressure, ϕ is the relative humidity, M_w is the molar weight of water, L_{lv} is the latent heat of evaporation, and ξ is the moisture differential capacity (kg/m^3), also known as the specific hygroscopic moisture capacity, and it is defined as the slope of the sorption isotherm curve at a particular temperature and relative humidity.

In this work, ∇T is assumed to be negligible due to the fact that the gradients in temperature are much smaller than the gradients in moisture content, in other words, $\nabla T \ll \nabla w$. With this assumption, the moisture flux can be expressed as:

$$\vec{g}_v = \delta_p P_s \frac{1}{\xi} \nabla w \qquad \text{(Eqn. 13)}$$

And going back to (Eqn. 9):

$$\nabla \cdot \left(\delta_p P_s \frac{1}{\xi} \nabla w \right) = \frac{\partial w}{\partial t} \qquad \text{(Eqn. 14)}$$

It is important to note from this equation that the specific hygroscopic moisture capacity is not constant in the process of moisture transfer.

Additionally, due to the previously taken assumptions, this differential equation has been defined with a single, dependent variable; that is moisture content, w. This is due to the fact that conservation of mass is the physical principle on which the continuity equation is based. While vapor pressure is continuous across interfaces, the moisture content does not directly depend on temperature. However, some forms of moisture transfer are governed by vapor pressure differentials, such as the air-solid transfer. The pros and cons for using moisture content, and partial vapor pressure are shown in Table 2:

Table 2: Evaluation between moisture content and partial vapor pressure as possible dependant variables

	Pros	Cons
Moisture content [kg/m3]	• Independent of temperature	• Air-solid moisture transfer is governed by vapor pressure differentials • Discontinuities at interfaces
Partial vapor pressure [Pa]	• Air-solid moisture transfer is governed by vapor pressure differentials • No discontinuities at interfaces	• Dependent on temperature

Moisture transport in the packed bed

Once the mode of diffusion inside of the hygroscopic material has been determined, we will now focus on the moisture exchange between the pore air space and the silica gel surface . as shown in Figure 19.

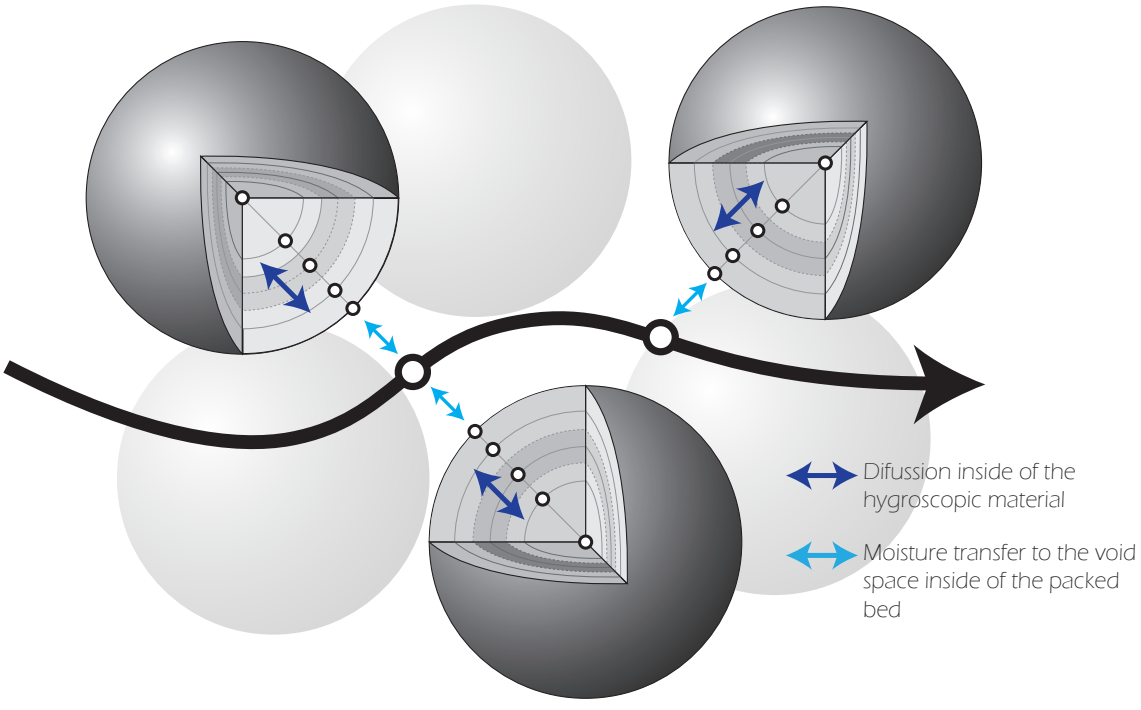

Figure 19: Moisture transfer mechanisms inside of the packed bed

The gel-air interaction

When there is moisture transfer between two different mediums, the interface between these mediums plays a crucial role. This interface controls the moisture transfer between the mediums, independently of the diffusion inside of each respective medium. Additionally, our dependent variable, moisture content, is defined as the ratio of the amount of water vapor over the unit volume of the medium. Therefore, when defining the interface interaction, particular attention must be paid so that in our model the change of medium in the moisture content is considered. For simplification purposes, the solid hygroscopic material medium here is called gel, and the moisture transfer mechanism at the interface has been defined as gel-air interaction.

The mass transfer rate between the gel and the air is described as following:

$$\beta_{c-g} A_r \left(w_a - w_{a-g} \right) \qquad \text{(Eqn. 15)}$$

Where β_{c-g} is the moisture transfer coefficient between the pore space and the gel surface, w_a is the moisture content in the pore space, w_{a-g} is the moisture content of the air right at the silica gel surface, and A_r is the surface area that interfaces the silica gel beads and the air. In order to define A_r the folowing assumptions were taken.

The total number of beads in the packed bed can be defined as:

$$\frac{\left(1-\varepsilon\right) AL}{\frac{4}{3}\pi R^3} = \frac{3\left(1-\varepsilon\right) AL}{4\pi R^3} \qquad \text{(Eqn. 16)}$$

Therefore:

$$\frac{\text{Number of beads}}{\text{m}^3} = \frac{\frac{3\left(1-\varepsilon\right) AL}{4\pi R^3}}{AL} = \frac{3\left(1-\varepsilon\right)}{4\pi R^3} \qquad \text{(Eqn. 17)}$$

And,

$$\frac{\text{solid-air surface}}{\text{m}^3} = \frac{3\left(1-\varepsilon\right)}{4\pi R^3} 4\pi R^2 = \frac{3\left(1-\varepsilon\right)}{R} \qquad \text{(Eqn. 18)}$$

Therefore, the solid-air surface in a layer of thickness d_z and surface area A is:

$$A_r = \frac{3\left(1-\varepsilon\right) A d_z}{R} \qquad \text{(Eqn. 19)}$$

Where R is the radius of the hygroscopic material bead, L is the thickness of the packed bed, A is the surface area of the hygroscopic material packed bed, and ε is the macroscopic porosity of the packed bed; assumed to be 0.36. This is based on a packed bed of rigid spheres.

In (Eqn. 15), the moisture transfer coefficient, β_{c-g}, is assumed to be 0.024 m/s. This assumption is based on the mass–heat transfer analogy. From the Lewis relationship, the moisture transfer coefficient can be defined in terms of the heat transfer coefficient, α:

$$\beta_{c-g} = \rho_a{}^{-1} 0.8^{(n-1)} 10^{-3} \alpha \qquad \text{(Eqn. 20)}$$

Where n is 0 for laminar and 1 for turbulent flows. Since the air flow that passes through the packed bed is so small, n has been assumed to be 0.

Therefore:

$$\beta_{c-g} \approx 10^{-3}\alpha \qquad \text{(Eqn. 21)}$$

On the other hand, the surface heat transfer coefficient, α can be obtained as following:

$$\alpha = \frac{Nu\lambda}{2R} \qquad \text{(Eqn. 22)}$$

Where λ is the thermal conduction coefficient of air and it has been assumed to be 0.024 W/mK. Nu is the Nusselt number which may be assumed to be 2, due to the assumption of no flow present (Achenbach, 1994). If we let R = 0.001 m, we find β_{c-g}= 0.024 m/s. The assumption of a gel bead radius of 1 mm, was held throughout this project.

w_{a-g} from (Eqn. 15), can be further defined as following:

$$w_{a-g} = aw_g + b \qquad \text{(Eqn. 23)}$$

(Eqn. 23) is illustrated in Figure 20.

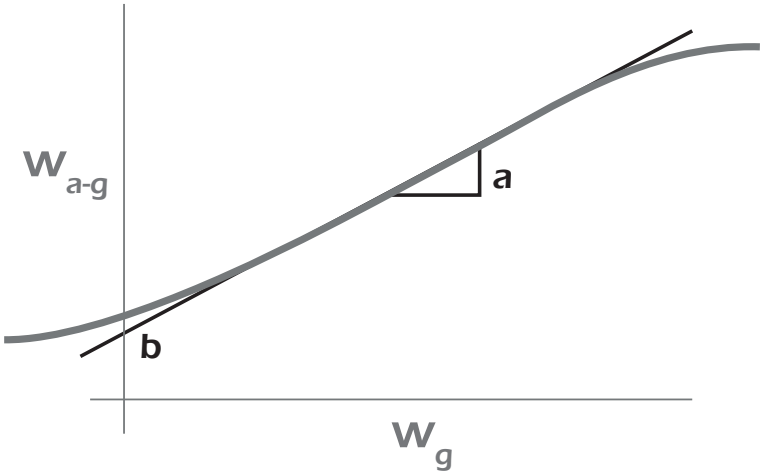

Figure 20: Moisture content of the air right at the silica gel surface vs. moisture content in the gel

Where w_g is the moisture content at the gel surface, and a, b are both constants. These constants are defined by the sorption isotherm of the silica gel. In this model, the sorption isotherm has been assumed to be linear; an assumption that holds true for many silica gel types in the range of 40% - 60% relative humidity. In order to be able to use the sorption isotherm of the material, it is necessary to define the moisture content of the gel in terms of the relative humidity; in this project this was done as following:

(Eqn. 24)

$$w_g = c_1\phi + c_2$$

(Eqn. 24) is illustrated in Figure 21.

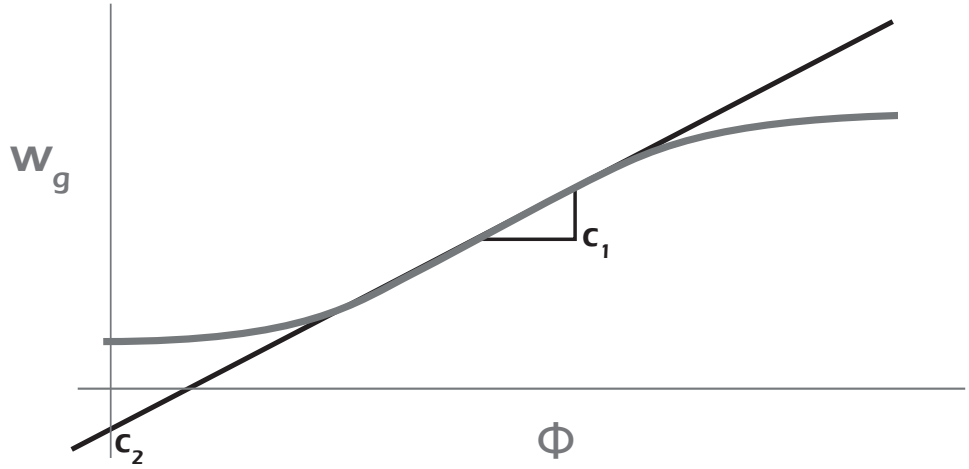

Figure 21: Sorption Isotherm

Where ϕ is the relative humidity, c_1 and c_2 are assumed to be constant. By means of the ideal gas law, the relative humidity can be further defined as:

$$\phi = \frac{R_v T}{P_{Sat}} w_{a-g} \qquad \text{(Eqn. 25)}$$

Where R_v is the specific gas constant [462 J/Kg K], T is the temperature, and P_{Sat} is the saturated vapor pressure. Therefore using (Eqn. 24) and (Eqn. 25), the moisture content in the silica gel can be further written as:

$$w_g = c_1 \frac{R_v T}{P_{Sat}} w_{a-g} + c_2 \qquad \text{(Eqn. 26)}$$

Using (Eqn. 23) we get:

$$w_{a-g} = a w_g + b = \frac{P_{Sat}}{R_v T c_1} w_g + \frac{P_{Sat}}{R_v T c_1} c_2 \qquad \text{(Eqn. 27)}$$

Where:

$$a = \frac{P_{Sat}}{R_v T c_1} \qquad b = \frac{P_{Sat}}{R_v T c_1} c_2 = a c_2$$

The constants c_1 and c_2 were derived from the sorption isotherm of the hygroscopic material as given by the manufacturer.

Moisture transport in the void space

From Hagentoft (2001) work we can characterize the moisture transfer due to diffusion in the air void space. (Eqn. 14) was derived from the mass balance equation shown in (Eqn. 9). This was done by assuming that gradients in temperature are negligible, in other words by having the moisture content be the only dependent variable. This situation is applicable to the moisture transfer due to diffusion in the void air space. From (Eqn. 14) we have:

$$\nabla \cdot \left(\delta_p P_s \frac{1}{\xi} \nabla w \right) = \frac{\partial w}{\partial t}$$

Therefore we can define the vapor diffusivity as:

$$D_a = \delta_p P_s \frac{1}{\xi} \quad \text{(Eqn. 28)}$$

It was assumed that the gradients of this vapor diffusivity with respect to the moisture content are negligible. The vapor diffusivity in standard conditions was used as a constant all throughout this project. D_a was assumed to be 2.4 x 10^{-5} m^2/s.

Additionally, moisture transfer due to advection was introduced in the air void space. This is based on the ventilation flow rate. In our model this flow rate was produced by temperature and pressure differentials in the environment which will be discussed in the following section. In order to solve the direction dependent flow through the air void space the first-order upwind numerical scheme for advection was used.

Moisture transport in the display case

Once we have defined the principles that govern the moisture transfer inside of the packed bed, the mechanism by which air flows in and out of a display case is described here. First, the moisture transfer between the packed bed and the air inside of the display case is explained as an extension from the last node in the void space of the packed bed. Finally, no display case is fully airtight; so the performance of the display case will depend on the air conditions outside, and so does the performance of the hygroscopic material as we will see soon.

Packed bed - display case inside air interaction

The coupling factor between packed bed and the air inside of the display case is shown below:

$$\beta_c A_z \Delta w \quad \text{(Eqn. 29)}$$

Where β_c is the moisture transfer coefficient. This moisture transfer coefficient is assumed to account for all forms of transfer, such as diffusion and convection. Δw is the difference in moisture content. A_z is the cross section area of all of the void space in the packed bed. A_z is defined as:

$$A_z = \varepsilon A \quad \text{(Eqn. 30)}$$

Advection

An air flow will occur into and out of the display case as a result of atmospheric pressure and temperature fluctuations. If this air flow passes through the packed bed, advection of water vapor will occur in the pore air space. The volumetric flow rate, Q, can be written as:

$$Q = V \frac{1}{\rho} \frac{\delta \rho}{\delta t} = V \frac{\rho'}{\rho} \quad \text{(Eqn. 31)}$$

Where V is the display case volume and ρ is the air density in the case.

Using the ideal gas law:

(Eqn. 32)

We have: $$\rho = \frac{P}{RT}$$

$$Q = V\frac{RT}{P}\frac{\delta\left(\frac{P}{RT}\right)}{\delta t} = V\frac{RT}{P}\frac{1}{R}\frac{\delta\left(\frac{P}{T}\right)}{\delta t} \quad \text{(Eqn. 33)}$$

And applying the quotient rule:

$$Q = V\frac{T}{P}\frac{T\frac{\delta(P)}{\delta t} - P\frac{\delta(T)}{\delta t}}{T^2} = V\left(\frac{P'}{P} - \frac{T'}{T}\right) \quad \text{(Eqn. 34)}$$

Note that a negative value of Q means flow out of the display case

Numerical approach

Model scheme

In order to develop the process of moisture transfer through a silica gel packed bed, a distinction is made between the solid (silica gel part, only diffusion in spherical beads) and the void space (air) where, besides diffusion, also air flow may occur (in and out of the display case).). Mathematically, the process is described using a so-called double- (or dual-) porosity model. This is shown in Figure 22:

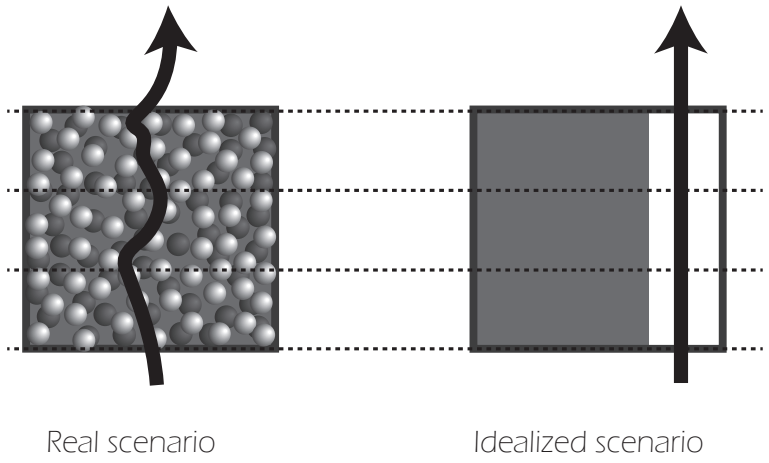

Figure 22: Real vs. idealized scenario

When numerically simulating the moisture transfer through a packed bed of silica gel, we are faced with a two-dimensional process; a transfer of moisture through the beads of the silica gel and through the air voids in the packed bed. For this reason, the packed bed is discretized in a number of layers across its thickness; in the illustration the number of layers is equal to 3. This serves to define the number of points where the silica gel transports moisture to the void space. In Figure 23, the problem domain has been roughly discretized in parts in order to clarify what each section represents.

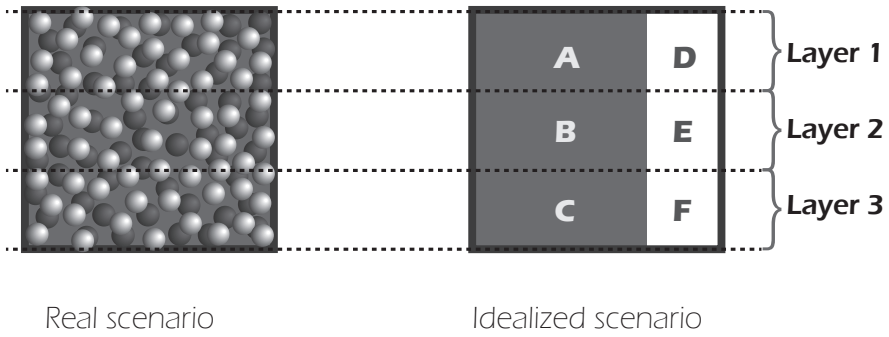

Figure 23: Discretization of the packed bed description: sections

Section A is the solid part that represents all the silica gel beads present in layer one of the packed bed of silica gel; while section D represents all the voids present in the same layer. Similarly, section B is the solid part that represents all the silica gel beads present in layer two; while section E represents all the voids present in that same layer. Finally, section C is the solid part that represents all the silica gel beads present in layer three; while section F represents all the voids present in that same layer.

In this model, nodes have been distributed per layer and across the solid. Figure 24 provides a closer look at what the representation of the nodes in the solid and void side mean.

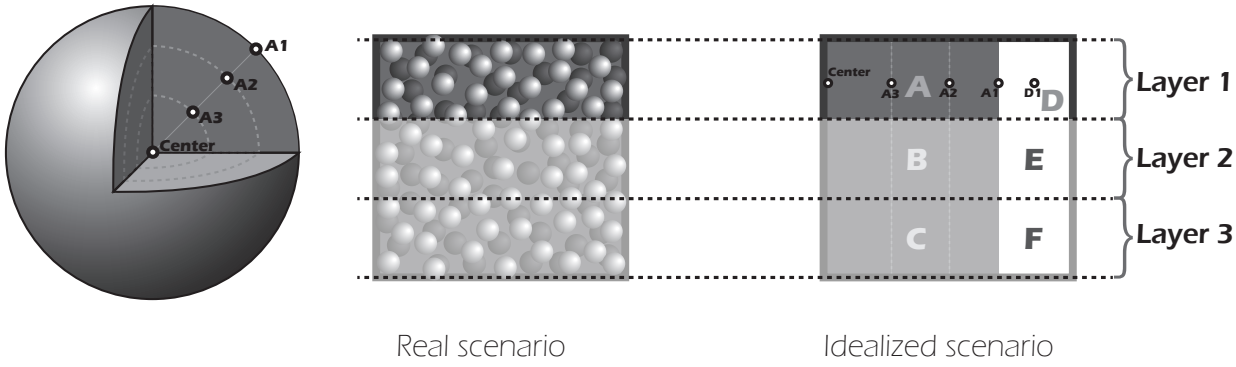

Figure 24: Discretization of the packed bed description: nodes

As it is shown, the void side of layer one, defined as section D, has a single node; D1, that represents all the water vapor molecules present in section D. As for the solid side of layer one, section A has been discretized in J nodes, J is equal to four in the above figure; that is A1, A2, A3, and Center. Node A1 represents the surface of all the beads in in layer 1, as shown in Figure 24. Similarly, node A2 represents the spherical section of all nodes in layer 1, below A1. Node A3 is the layer below A2, and so on, until the center node is reached. Center node represents the center of all beads in the packed bed at each respective layer.

This way of discretizing the packed bed permits the simple setup of the double-porosity model. This is because, on one hand, the moisture transfer across the voids, driven by air diffusion and advection, happens in the vertical direction between sections D, E and F. But the moisture transfer inside the silica gel beads occurs horizontally in within the nodes of each section A, B and C, separately.

Following the above principle, the model scheme for this project was developed. For all the simulations run, I and J were set up to be six and four layers, respectively. That is, the packed bed was divided in six layers across the thickness and the silica gel beads in each layer were divided in four layers. This is shown in Figure 25.

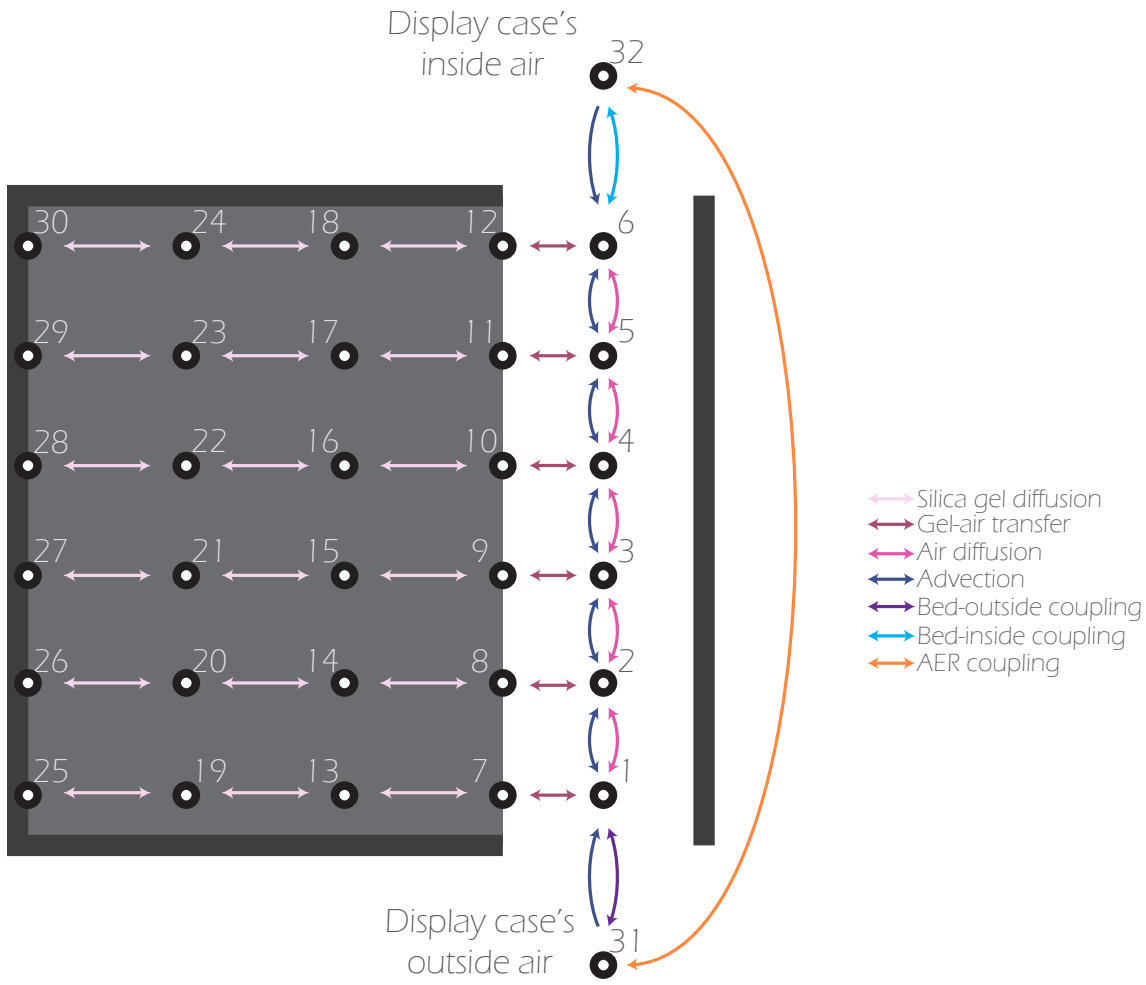

Figure 25: Discretization of the packed bed with the governing moisture transfer mechanisms

The moisture transfer in the model is based on the mass balance of each particular node. Take, for instance, the control volume of node one which is shown in Figure 26:

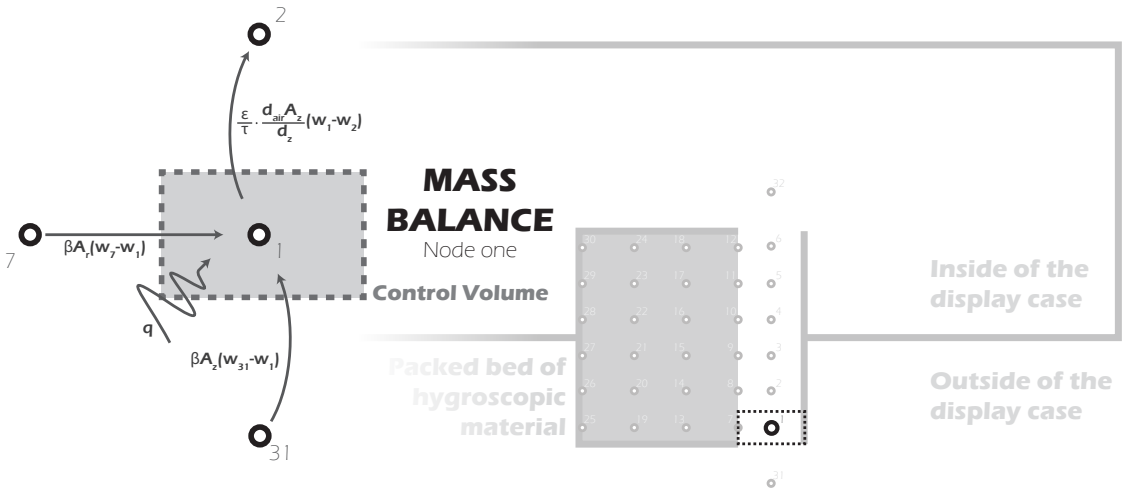

Figure 26: Control volume of node one

The mass balance starts from the conservation of mass law, shown in (Eqn. 9).

$$\nabla \cdot \vec{g} = \frac{\partial w}{\partial t}$$

Which for node one can be written as:

$$\mathrm{q} + \beta_{c-g} A_r \left(w_{a-g,7} - w_1 \right) + \beta_c A_z \left(w_{31} - w_1 \right) - \frac{\varepsilon}{\tau} \frac{D_{air} A_z}{d_z} \left(w_1 - w_2 \right) - V_1 \frac{\partial w}{\partial t} = 0 \qquad \text{(Eqn. 35)}$$

Where:

q is the load factor which in this case represent the advection effect. This follows the first-order upwind numerical scheme for advection. That means that:

$q = Q\left(w_{31} - w_1 \right)$ when the flow is going into the display case

$q = -Q\left(w_2 - w_1 \right)$ when the flow is going out of the display case

$\beta_{c-g} A_r \left(w_{a-g,7} - w_1 \right)$ represents the moisture transfer from the gel-air interaction with node seven.

$\beta_c A_z \left(w_{31} - w_1 \right)$ represents the moisture transfer between node one and the fixed node, the node outside of the display case.

$\frac{\varepsilon}{\tau} \frac{D_{air} A_z}{d_z} \left(w_1 - w_2 \right)$ represents the moisture transfer between the nodes one and two; in the void space of the packed bed.

$V_1 \frac{\partial w}{\partial t}$ is the volume of the display case times the rate of change of the moisture content. It is the rate of change of the moisture content what we are interested on finding out.

Similarly, if we write the mass balance equation for each free node in the system, we end up with as many equations and unknowns as free nodes. These equations can be organized in matrix form and solved as a set of differential equations with the respective boundary conditions. The following section, will further explain the implementation and solution method used in this model.

Model implementation

The first step is to organize the equations for all free nodes simultaneously in matrix form. For this, the load matrix, Q, the stiffness, $\mathbf{S}$, and mass matrix, M, are defined. Q is the load factor that each node has. $\mathbf{S}$ corresponds to the coupling factors between all the nodes. M represents the characteristics of the control volume with respect to moisture transfer. The mass balance requires that:

$$\mathbf{S}w + M\dot{w} - Q = 0 \qquad \text{(Eqn. 36)}$$

$$\begin{pmatrix} S_{1,1} & \dots & S_{1,n} \\ \vdots & \ddots & \vdots \\ S_{n,1} & \dots & S_{n,n} \end{pmatrix} \begin{pmatrix} w_1 \\ \vdots \\ w_n \end{pmatrix} + \begin{pmatrix} M_{1,1} & \dots & 0 \\ \vdots & \ddots & \vdots \\ 0 & \dots & M_{n,n} \end{pmatrix} \begin{pmatrix} \dot{w}_1 \\ \vdots \\ \dot{w}_n \end{pmatrix} - \begin{pmatrix} Q_1 \\ \vdots \\ Q_n \end{pmatrix} = 0 \qquad \text{(Eqn. 37)}$$

The stiffness matrix contains the coupling factor of both, free and bound (or fixed) nodes. In order to simplify the setup of the equations, the bound and free elements in the stiffness matrix have been extracted from the equation and defined as the S_{free} and S_{bound}, respectively.

$$S_{free} w_{free} + S_{bound} w_{bound} + M\dot{w} - Q = 0 \qquad \text{(Eqn. 38)}$$

In order to find out the solution, the following matrix equation was solved:

$$\dot{w} = \left(\mathrm{Q} - S_{free} w_{free} - S_{bound} w_{bound}\right) \frac{1}{M} \qquad \text{(Eqn. 39)}$$

$$w = \int \left(\mathrm{Q} - S_{free} w_{free} - S_{bound} w_{bound}\right) \frac{1}{M} \qquad \text{(Eqn. 40)}$$

The above mentioned set of equations was solved using Matlab/Simulink. A Matlab script was used in order to define all the nodes, parameters, variables and constants; with the main purpose of defining the matrices that will allow us to solve this set of differential equations. These equations are then solved in Simulink using the solver ode23tb. This solver is designed for stiff problems and it is an implementation of an implicit Runge-Kutta formula (Mathworks). The output times were set for each 15 minutes from the start to the end time set for the model.

In the Matlab script the following variables are defined:

Table 3: Variables defined in Matlab

Script variable	Description
`start_time`	Simulation start time
`end_time`	Simulation end time
`A_bed`	Surface area of packed bed
`R_v`	Gas constant of water
`V_v`	Volume of the packed bed

Script variable	Description
l_bed	Thickness of the packed bed
V_case	Volume of the display case
R_sp	Radius of the hygroscopic material sphere
d_sg	Assumed effective diffusion coefficient of hygroscopic material
e_bed	Porosity of the packed bed
A_z	Cross section area of idealized air void in bed
d_air	Assumed effecive diffusion coefficient of moisture on air
t_bed	Tortuosity of the packed bed
beta_c_g	Moisture transfer coefficient between the pore space and the gel surface
f_flow_gel	Fraction of ventilation flow that goes through the gel
beta_out	The moisture transfer coefficient between the bed and outside the display case
loss_coef	Diffusive exchange in and directly out of the display case
beta_in	The moisture transfer coefficient between the bed and the display case inside
c1_sorp	Slope of the sorption isotherm
c2_sorp	Constant in the sorption isotherm linear assumption
a_sorp	Constant number one, used to link the initial moisture content in the air with the hygroscopic material
b_sorp	Constant number two, used to link the initial moisture content in the air with the hygroscopic material
W_init_a	Initial moisture content in the air
W_init_g	Initial moisture content in the hygroscopic material

Once the structure and content of the model has been placed in the respective matrices, Simulink was used to solve the ordinary differential equations.

(Eqn. 40) was solved in Simulink in the following way, Figure 27:

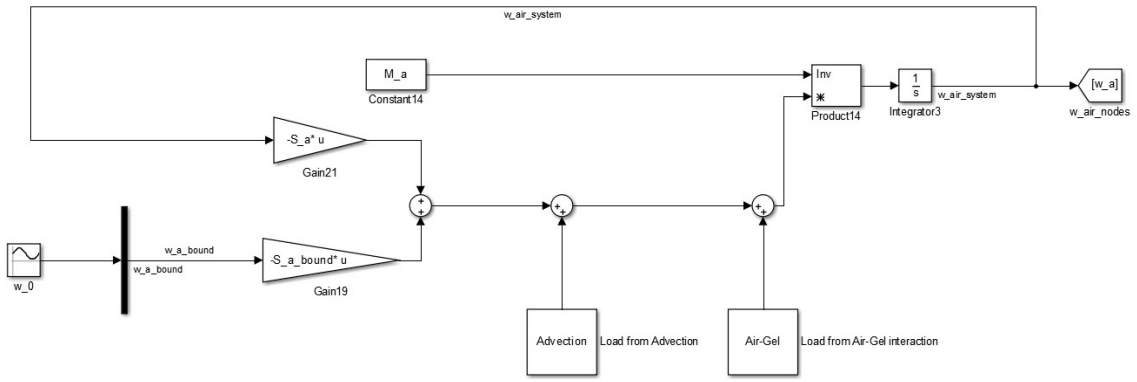

Figure 27: Simulink setup for the air nodes equations

Here, the Simulink scheme follows quite straightforward the structure of (Eqn. 40), for the air nodes. Similarly, the moisture content in the gel nodes were defined as shown in Figure 28:

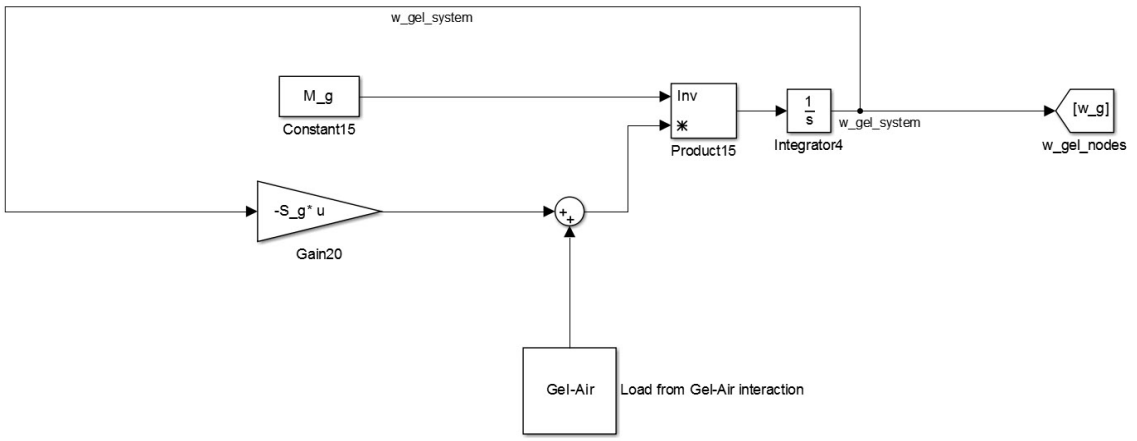

Figure 28: Simulink setup for the air nodes equations

The gel-air interaction parameters a and b, were computed in Simulink in the following way, Figure 29:

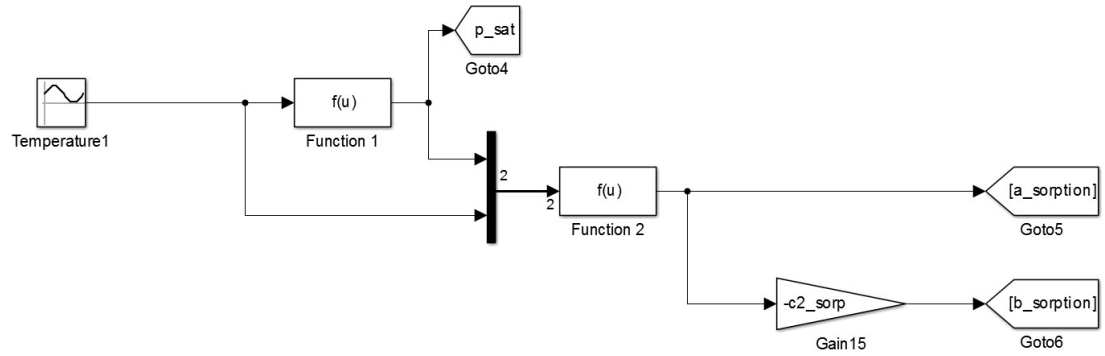

Figure 29: Simulink setup for the gel-air interaction

Where Function 1 in Figure 29, is the psychrometric equation that defines the saturated vapor pressure associated with a certain temperature, this equation is shown defined as:

$$P_{Sat} = e^{\frac{\left(77.3450+0.0057T-\frac{7235}{T}\right)}{T^{8.2}}} \quad \text{(Eqn. 41)}$$

For which T is the dry bulb temperature in degrees Kelvin.

Function 2 in Figure 29, is equivalent to the definition of a, as defined in (Eqn. 27).

The volumetric flow rate calculated in (Eqn. 34) was computed in Simulink as shown in Figure 30:

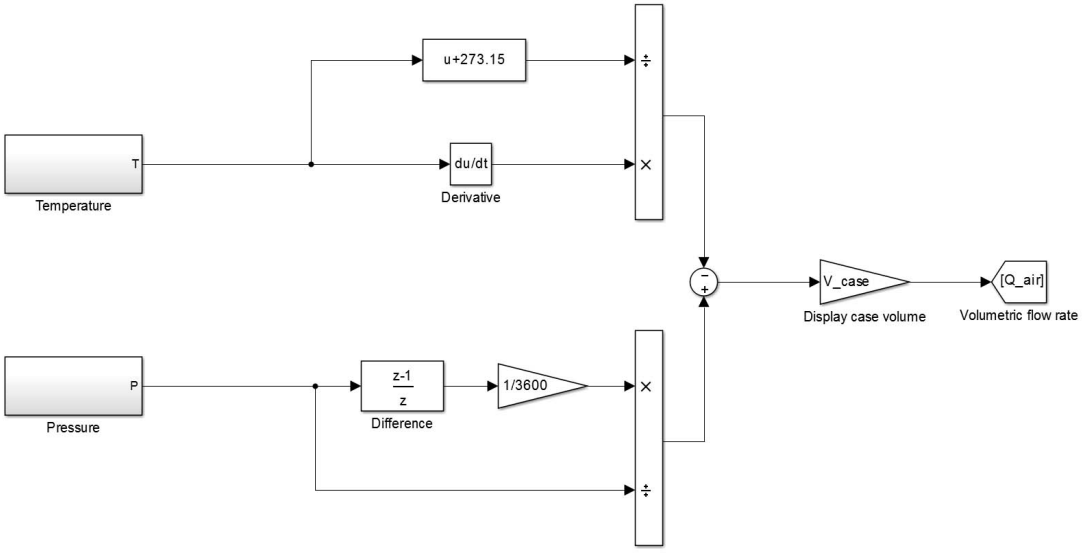

Figure 30: Simulink setup for the volumetric flow rate

The volumetric flow rate calculated above is used to calculate the advection load factor shown in figure.

Conclusion

In Chapter 3, this model is described based on the conservation of mass principle. The mechanisms of moisture transfer are separated in two parts; the hygroscopic material package and the display case. The hygroscopic material package is assumed as a packed bed of hygroscopic spherical beads. The diffusion of moisture inside of each bead is governed by surface and Knudsen diffusion. A particularly challenging part of this model was the connection between the beads and the air void inside of the packed bed, which was solved using the sorption isotherm of the hygroscopic material. The moisture transfer between the packed bed and the inside of the display case is based on a moisture transfer coefficient, assumed to take into account all possible forms of moisture transfer. The moisture transfer inside/outside of the display case is based on the air exchange rate (AER) of the display case. While the development and construction of this model gave us insight into the mechanisms of moisture transport, the model still needed some form of validation with the actual physical behavior of the display case in order to ensure the strength of our assumptions.

Chapter 4 : Experimental model

The purpose of this chapter is to describe the methodology of the experiments performed in this project. The experiments performed in this project can be categorized in two sections; environment control experiments and AER experiment. The purpose of the environment control experiments is to evaluate the performance of different setups of ProSorb in a passively conditioned display case. The purpose of the AER experiments is to find out the air exchange rate (AER) in the same display case. The environment control experiments were carried out in the TU Delft Faculty of Architecture and the Built Environment building. The AER experiments were carried out in the Faculty of Civil Engineering and Geoscience building. Both experiments were performed in the summer of 2015. The first section intends to provide the specifications of the equipment used while the following sections describe the setup and methodology of each experiment.

The materials and the methodology

The display case

The display case used is known as a shadow-box display case. It is designed to hold paintings and to be hung onto the wall. GLASSOLUTIONS Glascom Museum Presentations was in charge of the manufacturing of the display case; particularly, the glass work and assembly. The display case used is 656 x 727 x 93.5 mm, as shown in Figure 31. The Appendix 2 can be consulted for further information on the display case details and dimensional properties.

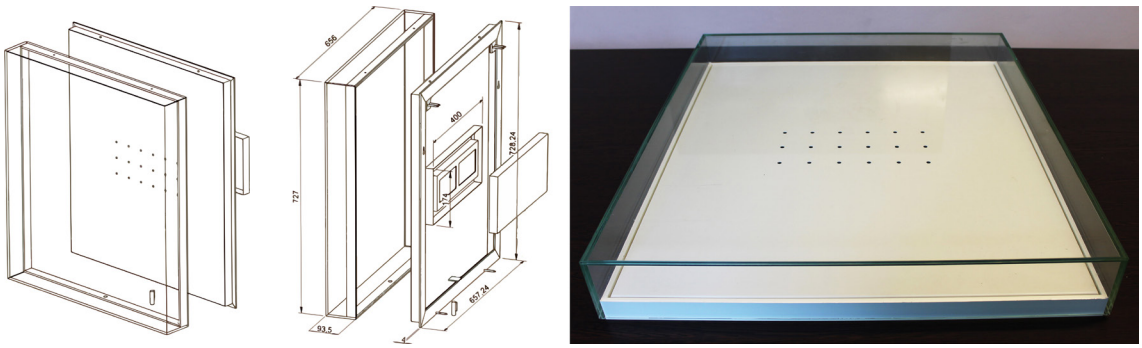

Figure 31: Shadow-box display case

This display case uses a double glass pane of Clear-Lite glass of 22.1 mm thickness. This particular type of glass is commonly used for museum display purposes for its low reflection and high transparency characteristics. The non-glass part of the display case is made of pure white, 90% matte, coated steel. This steel back panel not only provides a background for the piece of art but also provides support and stiffness to the display case. The mechanism for air exchange minimization is attributed to a shape memory polymer strip located at the junction between the glass case and the steel back panel support, shown in Figure 32.

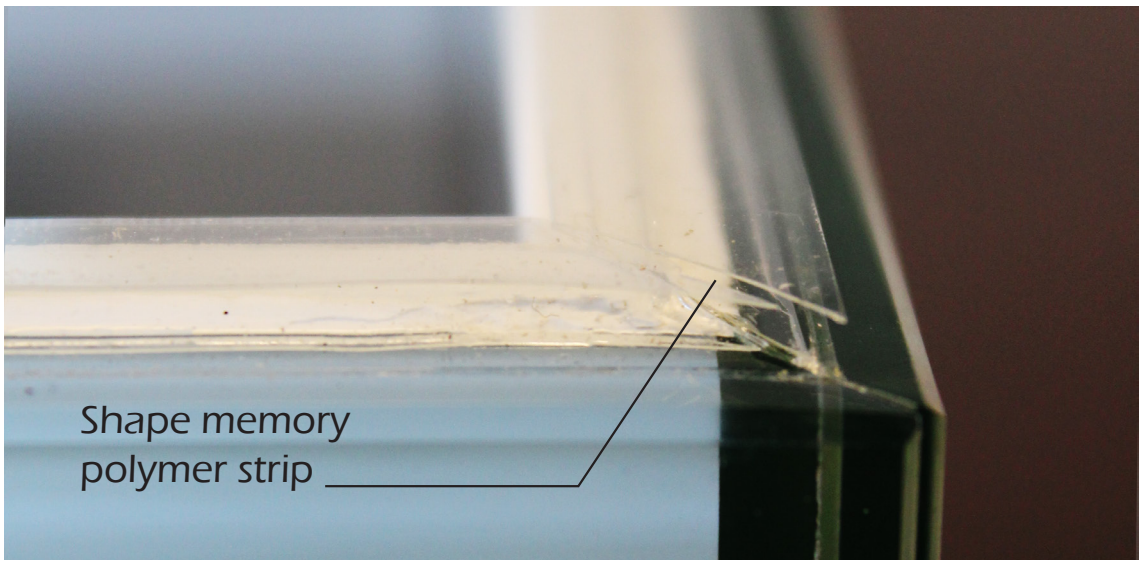

Figure 32: Shape memory polymer strip

The hygroscopic material

The hygroscopic material used in this experiment is ProSorb in a 500 gram package conditioned at 50% relative humidity. The sachet is made of low density polyethylene, LDPE, film and TYVEK® 1073. The LDPE is a non-woven polyethylene, which is dustproof, sturdy and vapor permeable (Waller). The TYVEK® is a high density polyethylene with an outstanding moisture resistance (Dupont), commonly used for medical packaging. Packages containing ProSorb, Figure 33, are commonly used by museums and galleries because they can be used exactly like a cassette and can be re-conditioned in the exact same way. However, the packages are sturdier than the cassettes which makes them easier to handle. Also, the dustproof characteristics of the LDPE are an important advantage when compared with cassettes.

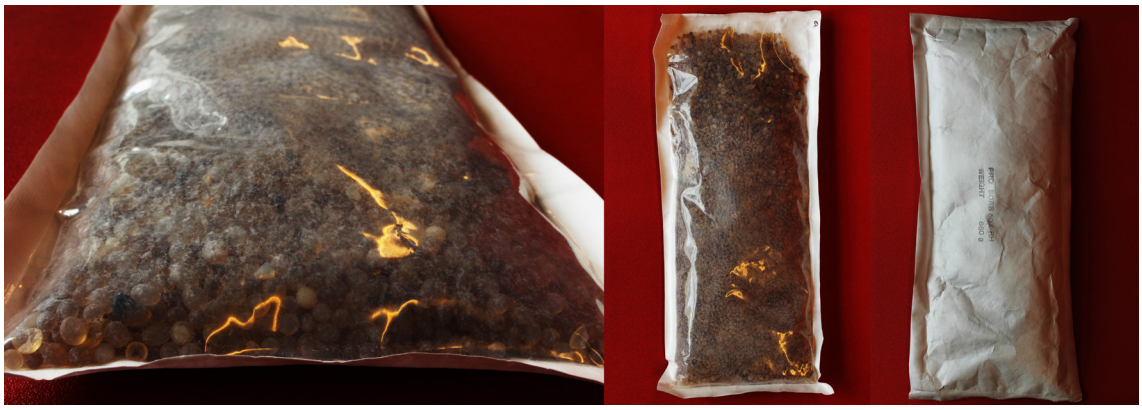

Figure 33: ProSorb package

AER EXPERIMENT METHOD

The purpose of this experiment was to evaluate the air exchange rate (AER) of the studied display case. It was found in the literature review that the AER can radically vary in a display case due to the quality of the closing mechanism. The importance of the AER in the design of a display case is based on its buffering quality; it has been found that AER is a significant parameter and its determination is much needed.

Measuring AER has been reviewed by multiple academics in this field. Calver et al. (2005) for example, studied and proposed simplified methods to calculate air exchange rates and detect leaks. Calculating AER usually involves the injection of a tracer gas inside of the display case and the measurement of decay of this gas as it is driven out of the display case through potential leakage points. However, in this project, a new approach to evaluating the measurement of AER has been performed.

The proposed innovative measurement of AER is based on the transfer of moisture instead of the decay of a tracer gas. This experiment is based on placing the display case containing dry air in a highly humid environment. The TU Delft faculty of Civil Engineering and Geoscience has several concrete curing chambers which are controlled at different temperature and relative humidity. A dry curing chamber (50%RH – 20C) and a wet chamber (95%RH – 20C) were used in this experiments.

Firstly, the display case was assembled in the dry chamber in order to make sure that the air inside was dry. Here, two HOBO – U12-012 sensors were placed (with an interval time of 15 minutes), one inside and one outside of the display case, respectively. Then, the display case was placed in the wet chamber. Finally, after one full week of logging, the sensors were collected and the data analyzed. This is shown in Figure 34:

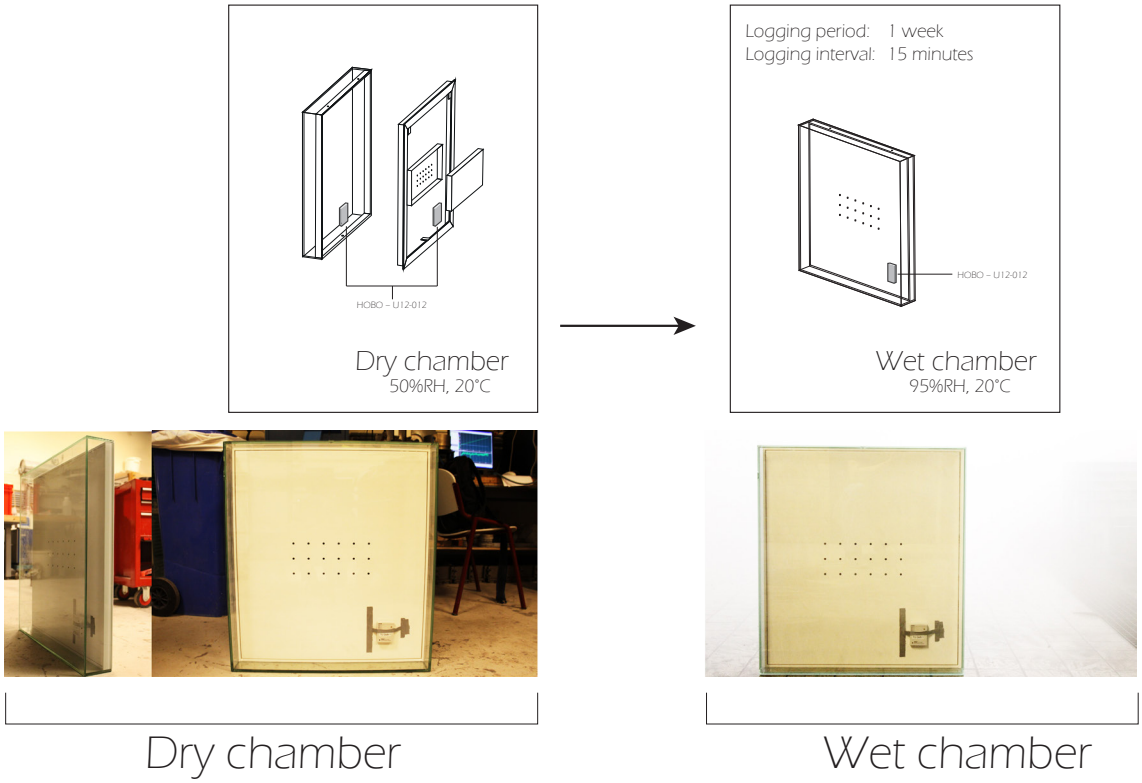

Figure 34: AER experiment setup

Environment control experiments method

The main purpose of this experiment is to compare the performance of the developed simulation with the actual behavior of the display case. For this, the microclimate inside of the display case was studied as an environmental load was applied. This environmental load is the same as the daily environmental load, as experienced at the location of the experiment. Due to the practicality of this project, only the short term fluctuations were evaluated, that is the daily change of temperature and relative humidity. In the following section the experimental setup is explained.

Here, three scenarios were studied. The first one was the display case with no hygroscopic material. The second was the display case with one package of ProSorb of 500 grams at 50% relative humidity in the built-in drawer. The third scenario studied was the display case with the same conditioning and amount of ProSorb as the previous case but distributed all over the bottom of the display case without any barrier between the ProSorb beads and the display case inside air. Finally, the fourth scenario studied was similar to the third case scenario, however, with a higher ProSorb exposed surface. These scenarios are illustrated in Figure 35.

a. No hygroscopic material – default scenario

b. 500 grams of ProSorb – set in the package container as recommended by manufacturer

c. 500 grams of ProSorb – set in the bottom of the display case without any barrier

d. 500 grams of ProSorb – set in the front of the display case without any barrier

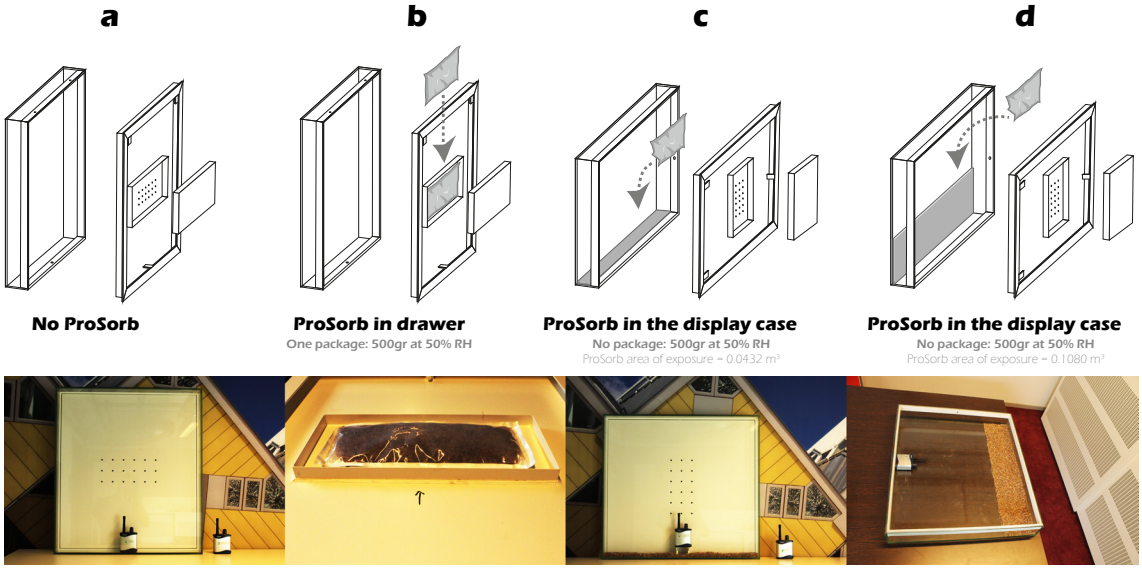

Figure 35: Case scenarios studied in the environment control experiements

These experiments were performed in room 01+.West.240 in the TU Delft Faculty of Architecture and the Built Environment. For each of the four scenarios, the temperature/relative humidity data was collected for seven continuous days, in which the time interval for data collection was set for 15 minutes. The setup was identical in each of the four scenarios, and was based on placing one GC10 transmitter inside of the display case and another GC10 transmitter outside of the display case. This is shown in Figure 36:

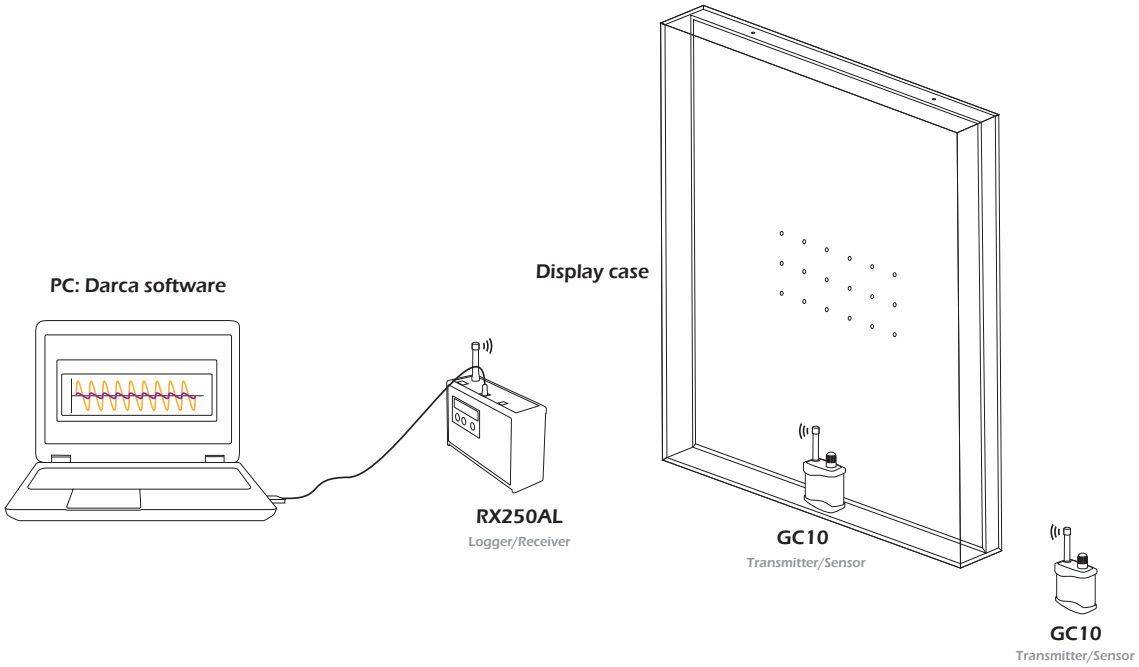

Figure 36: Environment control experiment setup

Once the log period (seven days) was completed, the data was downloaded using the Darca software and the new experimental setup was prepared. This preparation involved weighing, Figure 37, (before and after) the ProSorb, placing the ProSorb inside of the display case according to the scenario and closing/opening the case, making sure the airtight system (the shape memory polymer strip) was properly placed.

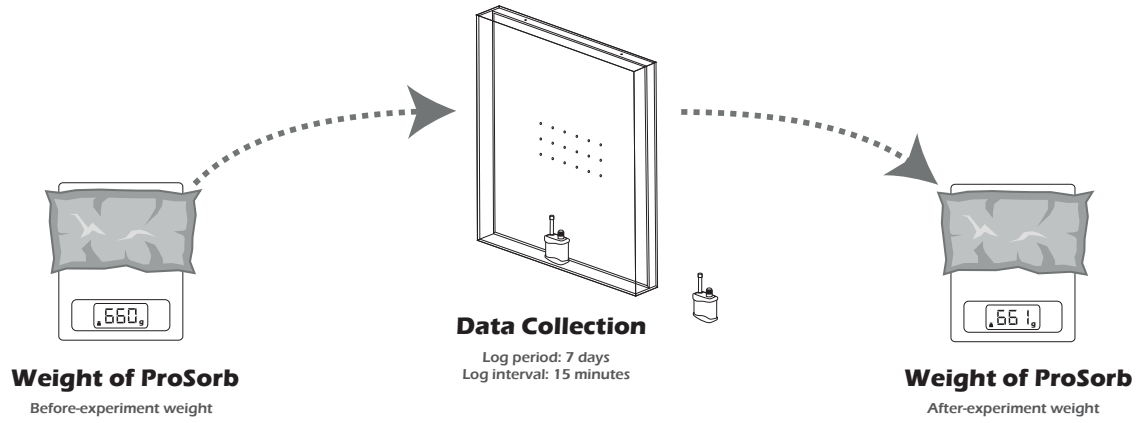

Figure 37: Weighing procedure of the environment control experiments

Experiment results

AER experiment results

After one week of logging the relative humidity and temperature inside the wet room, on the 27th of August 2015, the data was collected and analyzed. The results from the sensor placed outside of the display case were neglected due to inconsistencies on the measured data; this will be further discussed in the following chapter.

The results from the sensor placed inside of the display case are shown below in Figure 38 and Figure 39; for further information about these results see Appendix 3:

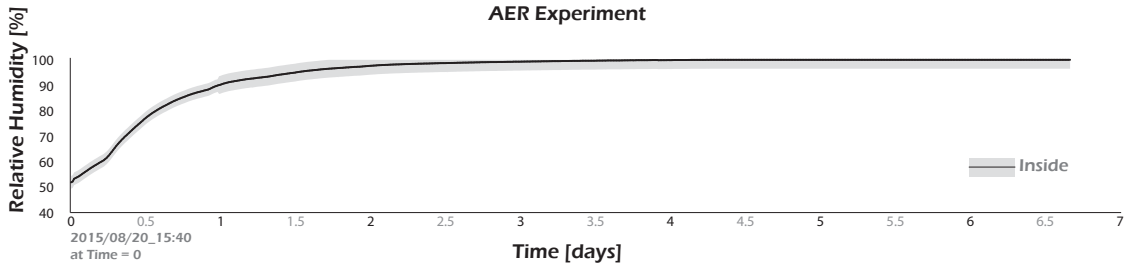

Figure 38: AER experiment results: Relative humidity inside of the display case

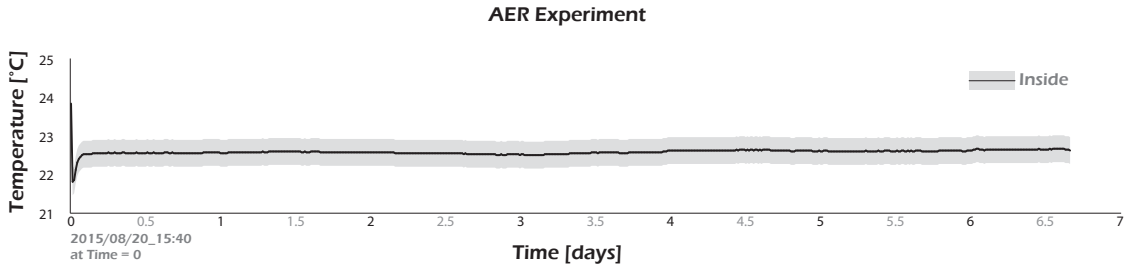

Figure 39: AER experiment results: Temperature inside of the display case

In order to calculate the AER, a temperature and relative humidity sensor was placed outside of the display case. However, this sensor showed inconsistent results; this will be further discussed in Chapter 6. Therefore, the outside conditions were assumed be 100% relative humidity and 22.6 °C; which is the recorded average temperature of the display. These conditions are equivalent to a moisture content of 0.02 Kg/m3. The AER was calculated using the respective moisture content on each time interval.

AER can be obtained from the following realtionship (Calver et al. 2005):

$$N = \frac{\left[\ln\left(C_{int}{}^{t_0} - C_{ext}\right) - \ln\left(C_{int}{}^{t_1} - C_{ext}\right)\right]}{t_1 - t_0} \qquad \text{(Eqn. 42)}$$

Where N is the air exchange rate, $C_{int}{}^{t_0}$ is the concentration of moisture inside of the display case at the begining, C_{ext} is the concentraition of moisture outside of the display case, $C_{int}{}^{t_1}$ is the concentration of moisture inside of the display case at the end, t_1 is the end time, t_0 and is the beginning time.

Therefore, the difference of moisture content (the moisture content outside minus the one inside; w_

outside – w_inside) was studied. The rate of change of the difference of moisture content was estimated to be the AER inside of the display case. This is shown below in Figure 40:

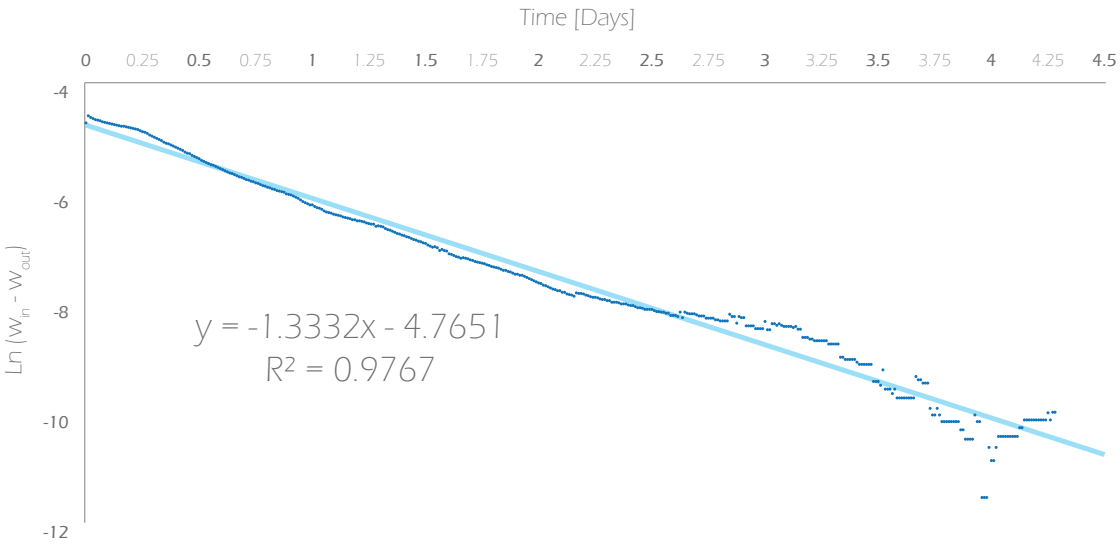

Figure 40: Calculation of air exchange rate per unit time

Therefore, the air exchange of the display case is 1.33 ac/d.

Environment control experiment results

The weight change of the ProSorb in scenario **b**, **c** and **d** is shown below in Table 4 and :

Table 4: Change in weight of ProSorb for each scenario

Scenarios	Before the experiment	After the experiment
b	661 g	662 g
c	651 g	652 g
d	652 g	653 g

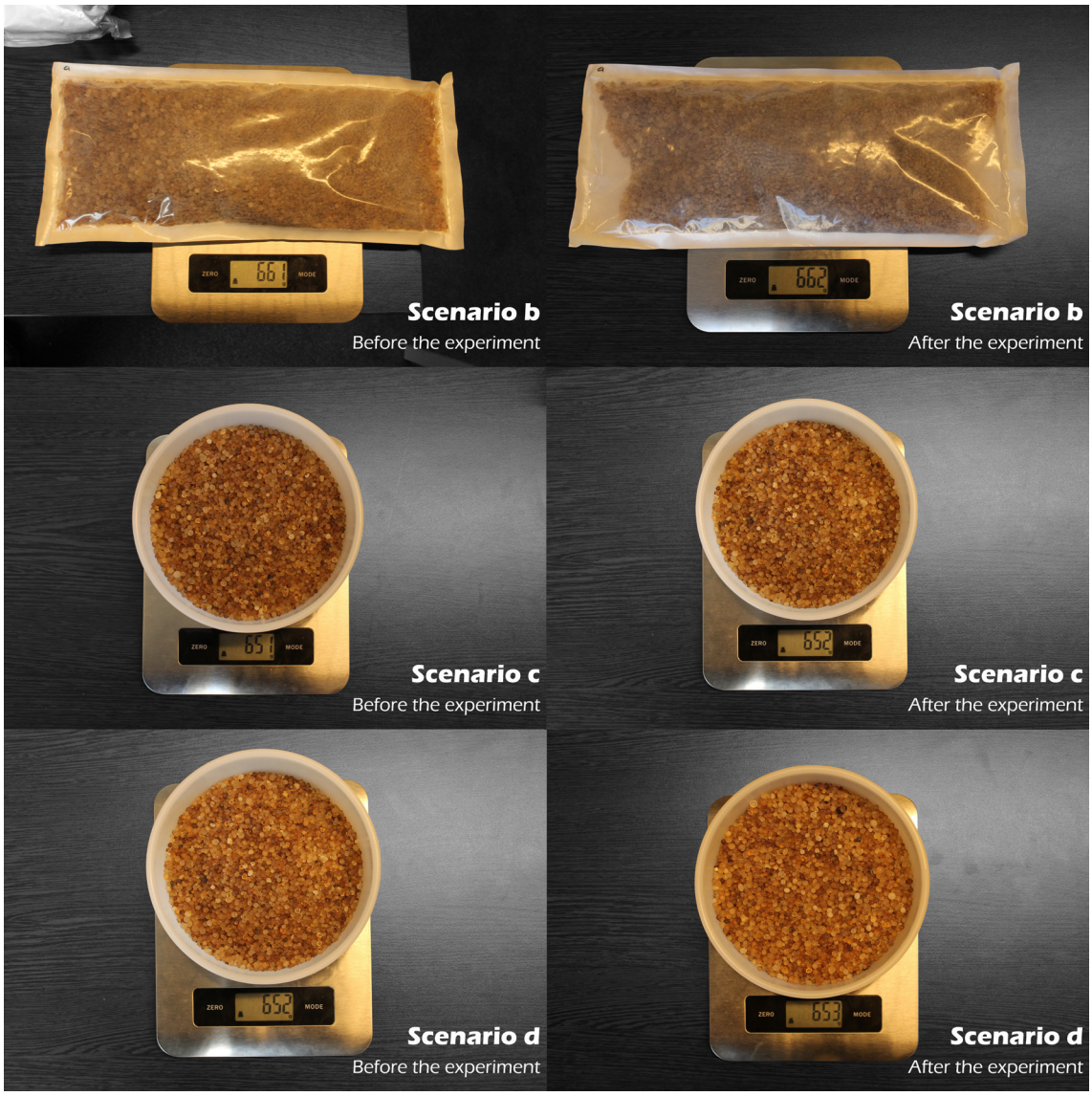

Figure 41: Change in weight of ProSorb for each scenario

The temperature results from the sensor placed inside and outside of the display case for each scenario are shown below in Figure 42, Figure 43, Figure 44 and Figure 45; for further information about these results see Appendix 4:

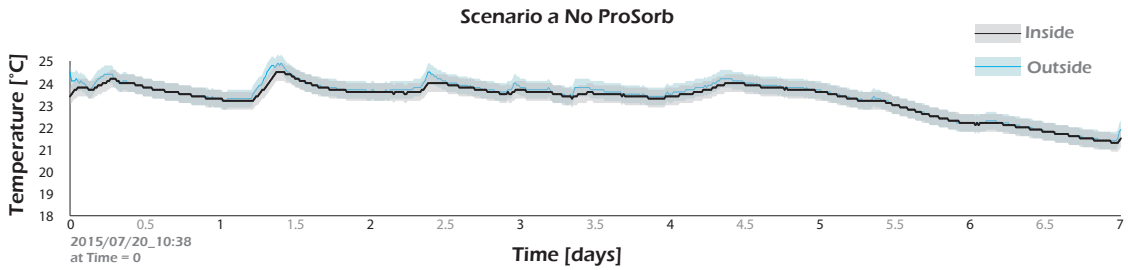

Figure 42: Environment control experiment: Temperature results - Scenario a

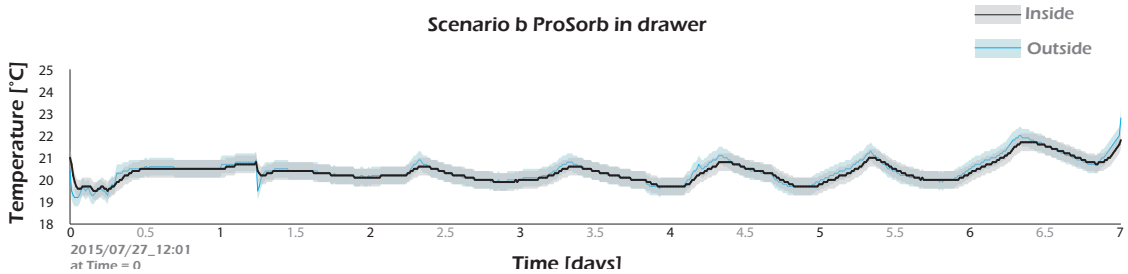

Figure 43: Environment control experiment: Temperature results - Scenario b

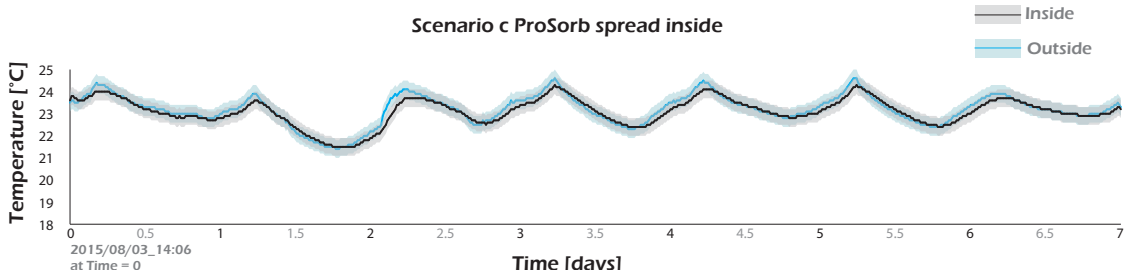

Figure 44: Environment control experiment: Temperature results - Scenario c

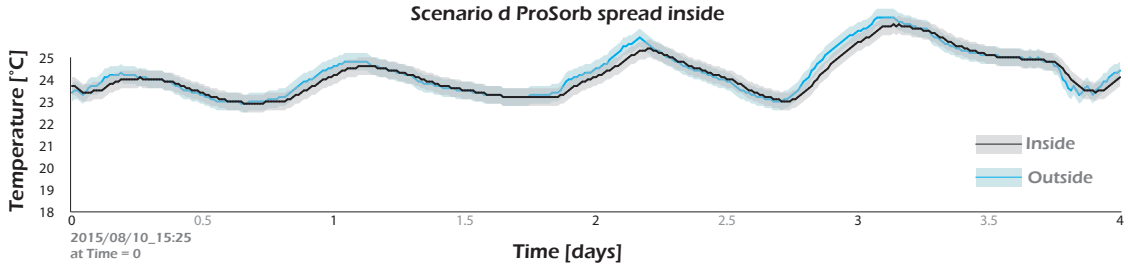

Figure 45: Environment control experiment: Temperature results - Scenario d

The relative humidity results from the sensor placed inside and outside of the display case for each scenario are shown below in Figure 46, Figure 47, Figure 48 and Figure 49; for further information about these results see Appendix 4:

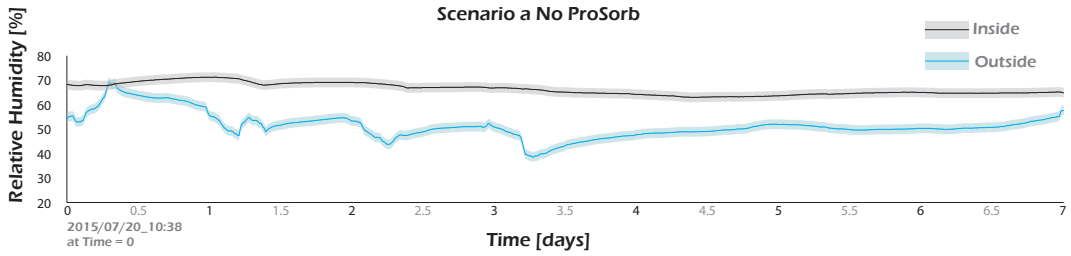

Figure 46: Environment control experiment: Relative humidity results - Scenario a

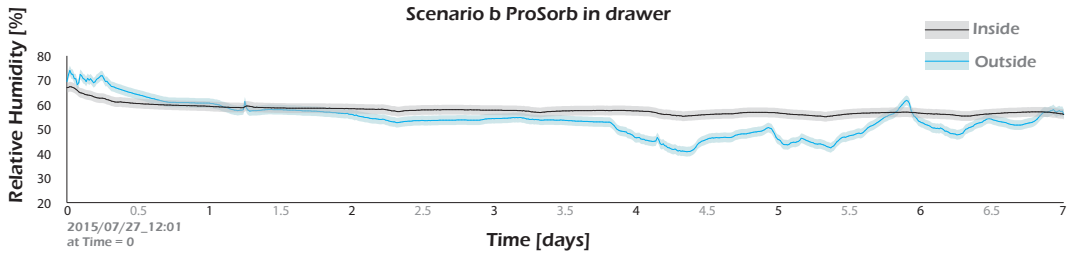

Figure 47: Environment control experiment: Relative humidity results - Scenario b

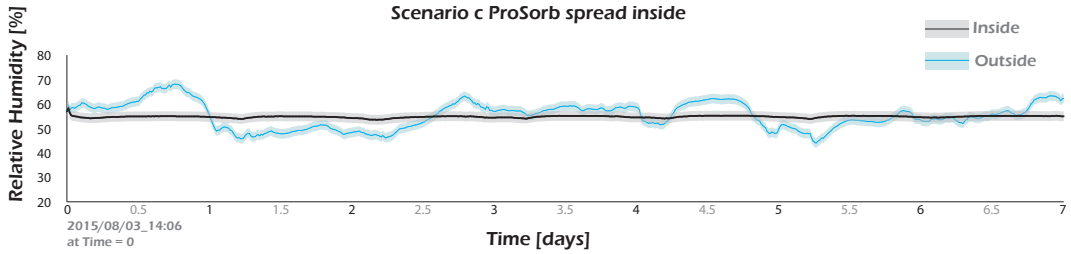

Figure 48: Environment control experiment: Relative humidity results - Scenario c

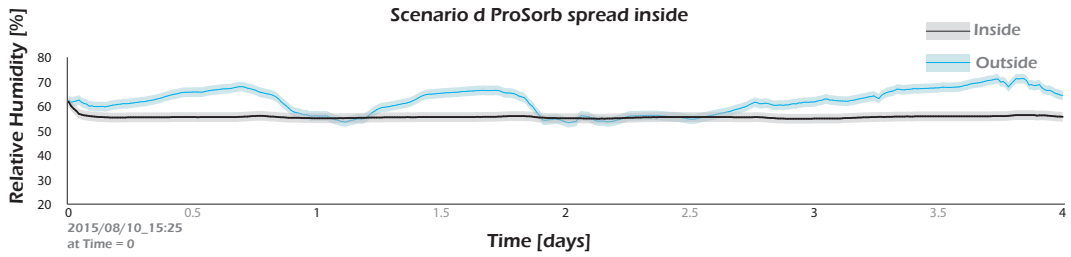

Figure 49: Environment control experiment: Relative humidity results - Scenario d

Parameters fit

The purpose of the environment control experiments was to evaluate the performance of different setups of ProSorb in a display case. However, it was the moisture transfer coefficient, $\beta_{c'}$ between the silica gel and the inside air, that was being studied during these experiments. By changing the exposure surface area of ProSorb inside of the display case and by changing the scenario of exposure (i.e., behind the steel support in the drawer, versus completely open inside) the moisture transport coefficient was being directly modified. This coefficient accounts for all forms of effective transfer (such as convective and diffusion). In fact, this transport coefficient proved to have a very significant role on the climatization of the display case. Within the environment control experiments, this moisture transfer coefficient could be estimated for each of the different studied scenarios.

In order to estimate the moisture transfer coefficient for each case scenario, a least square fit analysis was performed. This fit analysis was based on the results from the inside relative humidity from the experiments and the simulation results having two variables as the regression parameters; that is the moisture transfer coefficient, $\beta_{c'}$ and the initial moisture content of the ProSorb ($W_{g\_initial}$).

For this least square fit analysis, the data from the experiments was selected to be the most stable section of the overall experiments. For this, the first two days were neglected and only the rest of the days were used for the least square fit analysis. Furthermore, the previously found AER = 1.33 ac/d, was used.

The iterations for the least square fit analysis were carried out manually and the results can be found in Table 5, which is illustrated in Figure 50, Figure 51 and Figure 52:

Table 5: Moisture transfer coefficient least square fit analysis results: For AER = 1.33 ac/d

Moisture transfer coefficient, β_c [Kg/m²s]		
b	**c**	**d**
2.3×10^{-4} $\begin{vmatrix} +0.1 \times 10^{-4} \\ -0.1 \times 10^{-4} \end{vmatrix}$	9.0×10^{-4} $\begin{vmatrix} +0.5 \times 10^{-4} \\ -0.4 \times 10^{-4} \end{vmatrix}$	8.0×10^{-4} $\begin{vmatrix} +1.2 \times 10^{-4} \\ -0.9 \times 10^{-4} \end{vmatrix}$

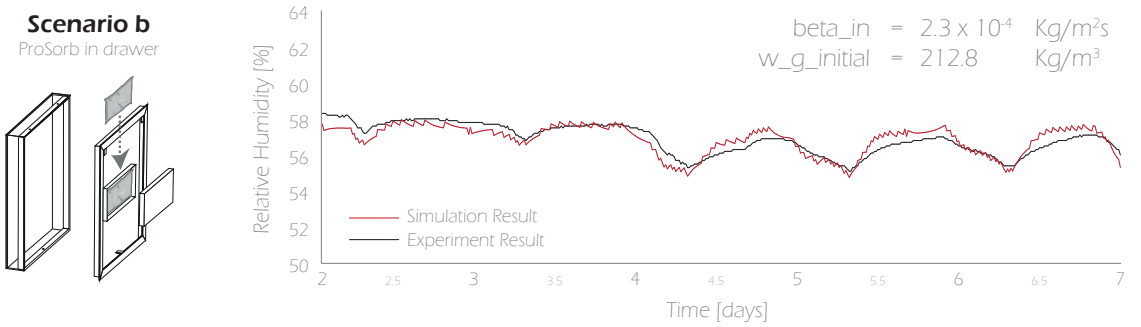

Figure 50: Least square fit analysis: Scenario **b** - With AER = 1.33 ac/d

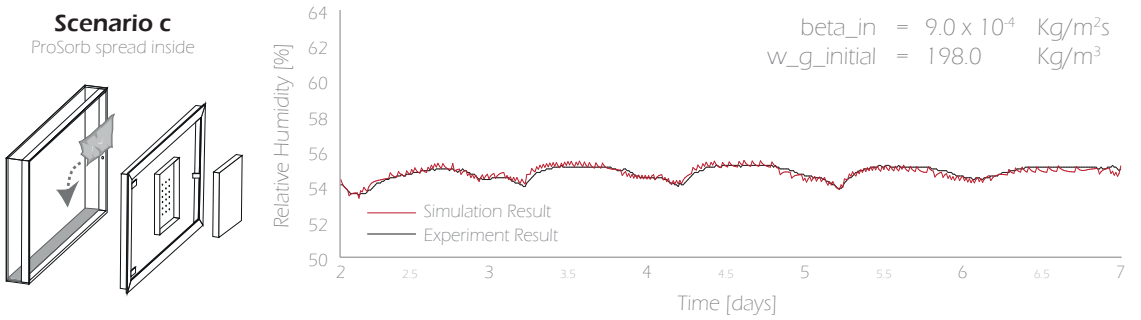

Figure 51: Least square fit analysis: Scenario **c** - With AER = 1.33 ac/d

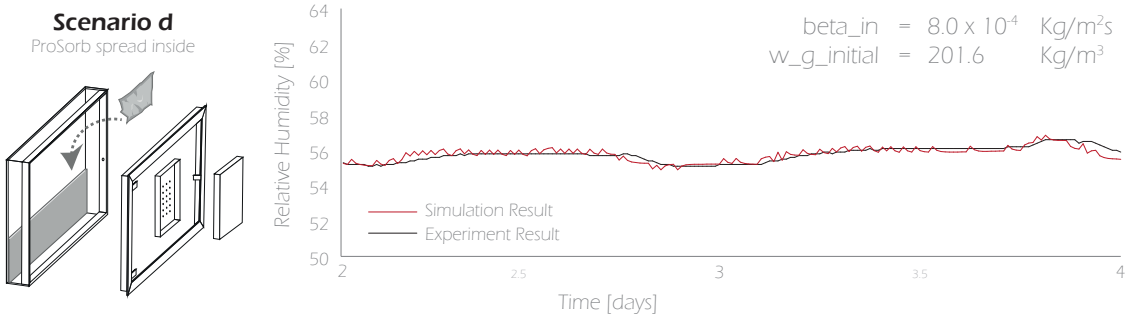

Figure 52: Least square fit analysis: Scenario **d** - With AER = 1.33 ac/d

Additionally, it was noticed that case scenario **a** of the display case with no ProSorb could be analyzed with our model using the same least square fit analysis as before, however, using different parameters as the independent variables; that is the the air exchange rate (AER), and the the initial moisture content of the air inside, ($W_{g\_initial}$).

Similarly, the least square fit analysis of the data from the experiments was sampled from the most stable section of the overall experiments. For this, the first two days were neglected and only the rest of the days were used for the least square fit analysis. The iterations for the least square fit analysis were carried out manually and the results can be found below in Table 6, which is illustrated in Figure 53.

Table 6: AER least square fit analysis results: Case scenario **a**

AER [ac/d]	
a	
0.12	$+0.29 \times 10^{-2}$ -0.05×10^{-2}

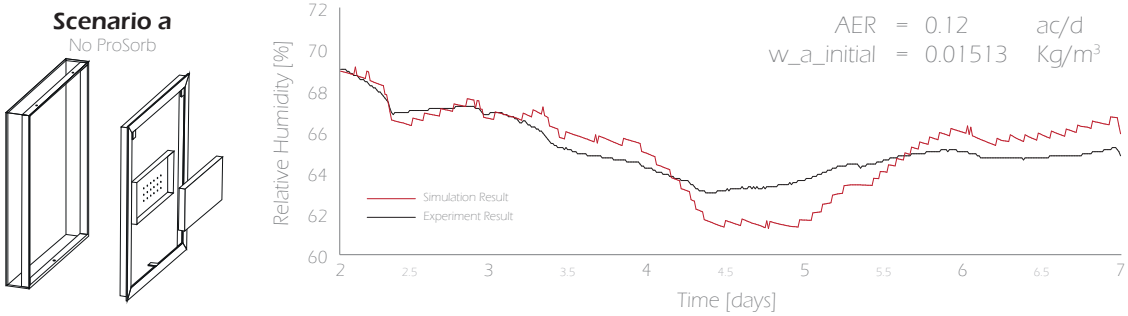

Figure 53: Least square fit analysis: Scenario a

We can observe, therefore, a difference in the AER parameter between the AER experiments and the fit analysis in the environment control experiment of case scenario **a**. The assesment of this difference will be further discussed in Chapter 6. Meanwhile, a new research question arose from these results; that is:

- On the experiments carried out during this work, how much influence does the AER have over the moisture transfer coefficient, β_c?

In order to answer this question, a new least square fit analysis was performed for each of the ProSorb-containing case scenarios; that is case **b**, case **c** and case **d**, with an assumed AER = 0.12 ac/d as previously found in the environment control experiment of case scenario **a**.

These iterations were carried out in the same way as the previous iterations, where the first two days were neglected and only the rest of the days were used. The results can be found in Table 7, which is illustrated in Figure 54, Figure 55 and Figure 56.

Table 7: Moisture transfer coefficient least square fit analysis results - With AER = 0.12 ac/d

Moisture transfer coefficient, β_c [Kg/m²s]		
b	**c**	**d**
2.0×10^{-4} $\begin{vmatrix} +0.4 \times 10^{-4} \\ -0.3 \times 10^{-4} \end{vmatrix}$	7.3×10^{-4} $\begin{vmatrix} +0.5 \times 10^{-4} \\ -0.5 \times 10^{-4} \end{vmatrix}$	7.9×10^{-4} $\begin{vmatrix} +1.9 \times 10^{-4} \\ -1.5 \times 10^{-4} \end{vmatrix}$

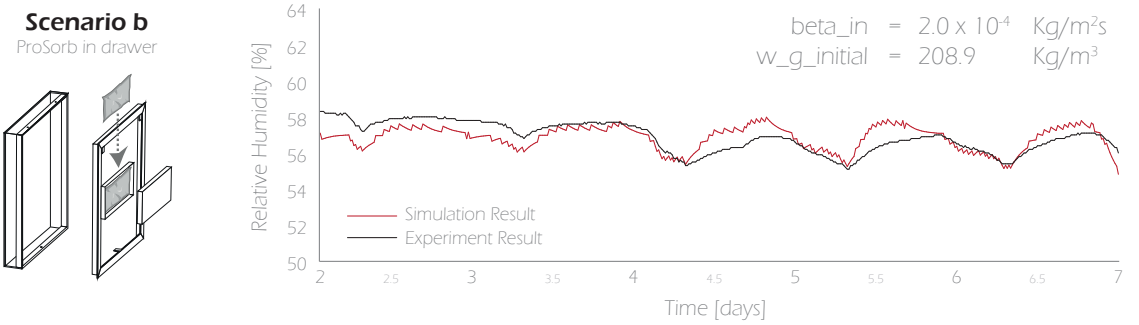

Figure 54: Least square fit analysis: Scenario **b** - With AER = 0.12 ac/d

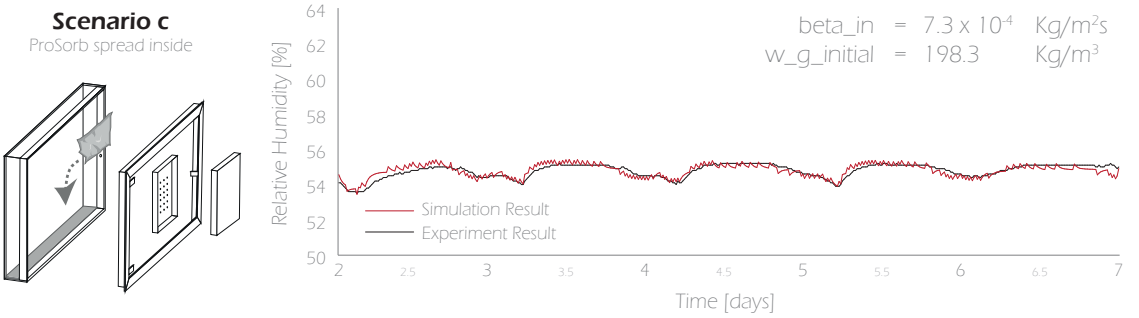

Figure 55: Least square fit analysis: Scenario **c** - With AER = 0.12 ac/d

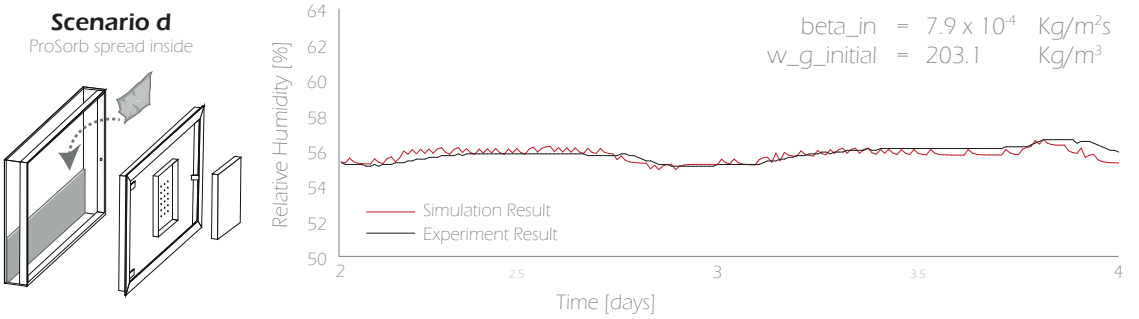

Figure 56: Least square fit analysis: Scenario **d** - With AER = 0.12 ac/d

The comparison between the moisture transfer coefficient calculated by assuming an AER = 0.12 ac/d and the moisture transfer coefficient calculated by assuming an AER = 1.33 ac/d with their respective uncertainty is shown in Figure 57, Figure 58 and Figure 59:

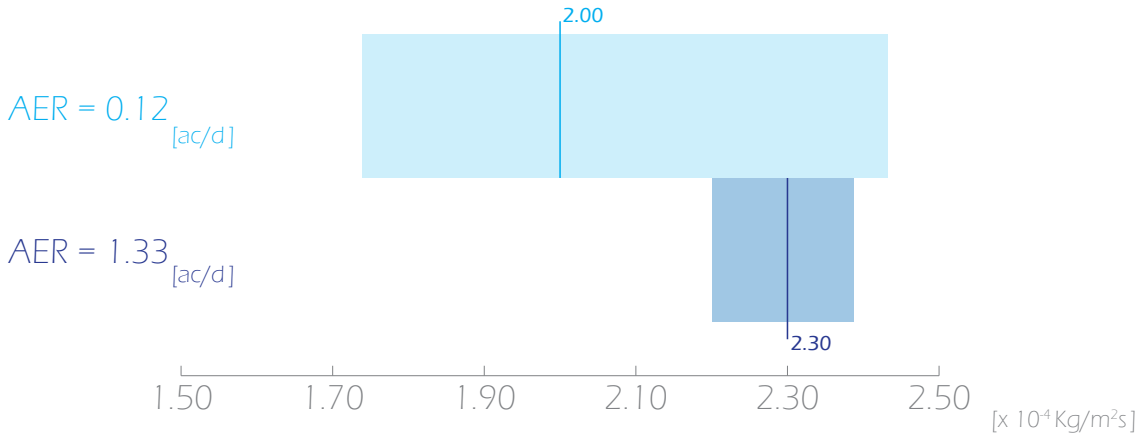

Figure 57: Moisture transfer coefficient comparison (AER = 0.12 ac/d vs.1.33 ac/d): Scenario b.

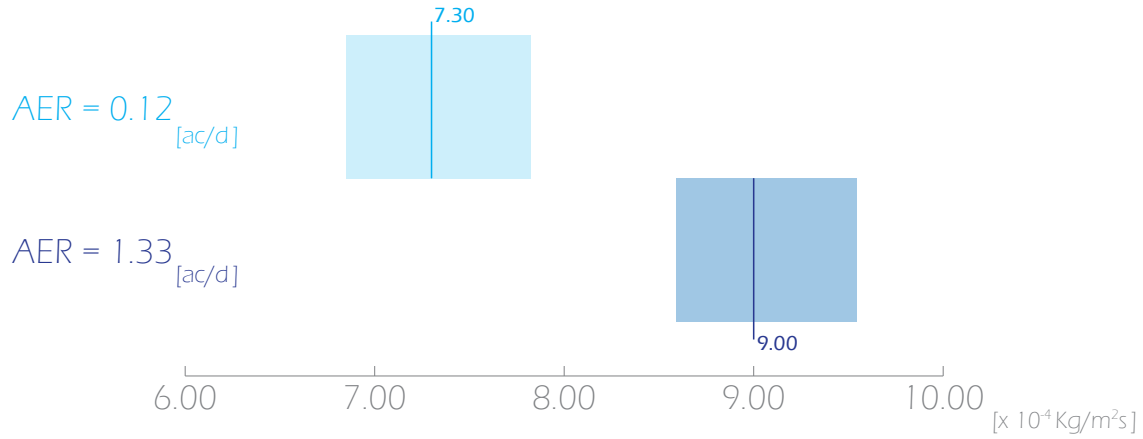

Figure 58: Moisture transfer coefficient comparison (AER = 0.12 ac/d vs.1.33 ac/d): Scenario c.

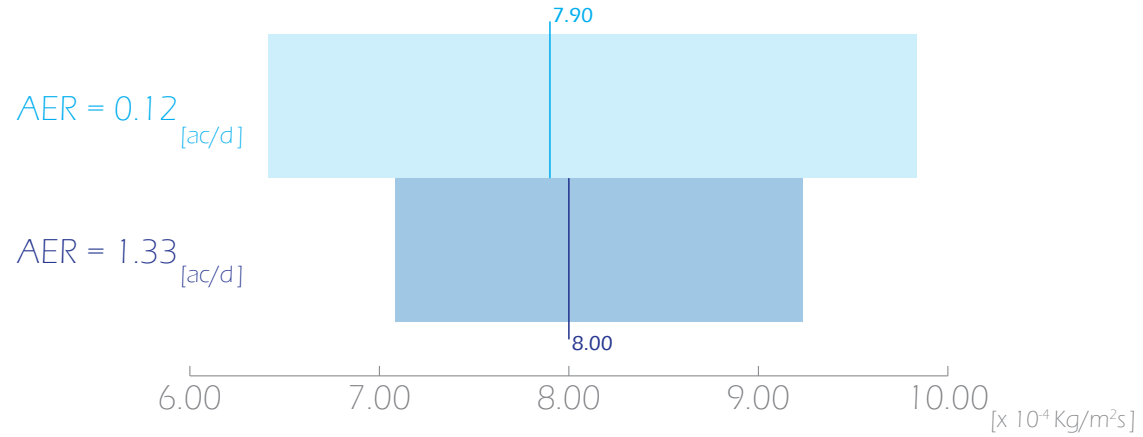

Figure 59: Moisture transfer coefficient comparison (AER = 0.12 ac/d vs.1.33 ac/d): Scenario d.

Discussion

The model developed in Chapter 3 served to estimate the value of the moisture transfer coefficient shown in Chapter 4. However, it is important to keep in mind that this is only valid under the circumstances experienced during the experiments. There are still multiple opportunities for further validation of the model.

In Chapter 4, we were presented with the paradigm of having two different air exchange rates for the same display case, as measured by different experiments. So, how can this be possible? And what is the meaning of such results? These are some of the questions that were raised here.

The air exchange rate quantifies the amount of air that leaks through the display case, and this depends on the temperature and pressure differentials, as shown in Chapter 3, and especially in the closing mechanism. With our model, we can see the contribution to the air exchange rate due to temperature and pressure differentials. For this, the simulation was set for one full year and different configurations of temperature were studied. The temperature variations correspond to the amplitude of the sinusoidal wave in which the temperature has been assumed with a frequency of one day. Yearly variations of temperature were not considered in this case due to simplicity. This is shown in Figure 60:

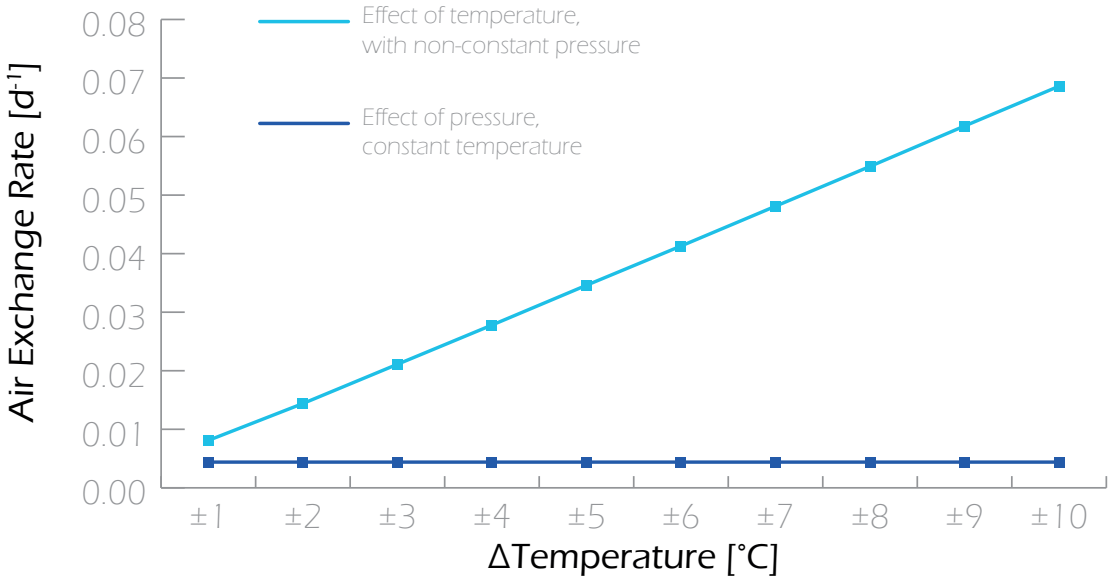

Figure 60: Effect of temperature and pressure change in the air exchange rate

The above graph presents in dark blue the effect of a pressure load in the AER. This shows the contribution of the pressure load to the AER, which is, as expected, constant throughout any temperature variation (Note, pressure has been assumed to be independent of temperature here.) This pressure load is the corresponding atmospheric pressure data for the year 1995 in the Netherlands. On the other hand, the light blue line in the above graph shows the effect of varying temperature in addition to the pressure load. It is clear from the above graph that temperature variations are dominant over pressure variations.

From the results above, it can be said that due to temperature and pressure variations, the AER is in the range of [0.0081 – 0.0686] ac/d. However, this is the minimum AER that this display case can present under these circumstances. In this project, we have assumed the AER based on the experiment results. So, we can attribute the missing part of the AER to the potential leakage points. This is shown in Figure 61.

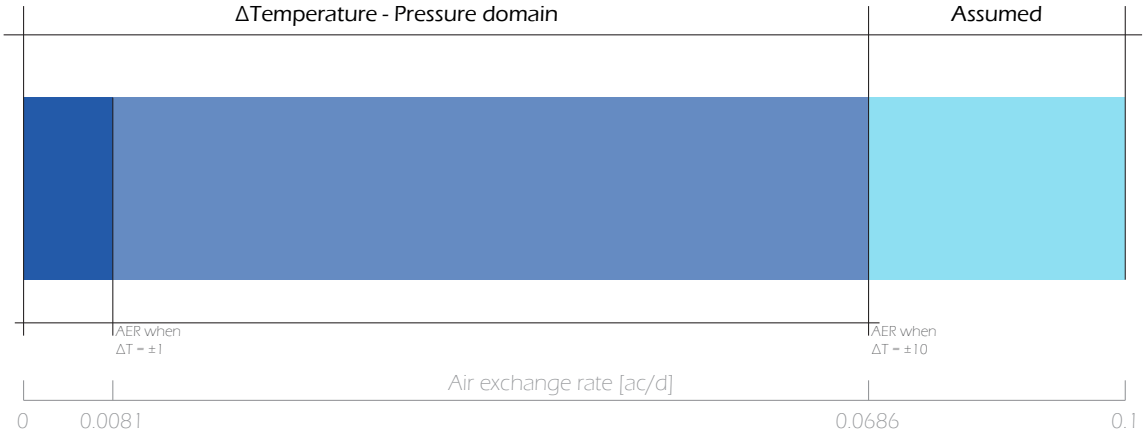

Figure 61: *Assumed section of the air exchange rate*

We can observe that the assumed portion of the air exchange rate can be considerable, since it is uncommon that temperature changes reach 10°C within one day. Therefore, the potential leakage points make up the most significant factor when considering air exchange rate. We can expect these potential leakage points to be mainly in the closing mechanism of the display case.

The display case used for the validation of the model has a particular high ratio of length of closing mechanism (glass to back support joint) to enclosed air volume when compared to other display cases used in museums. This ratio, shown in Figure 62, compares the amount of potential leakage over the amount of air enclosed and can be used to characterize the air exchange rate. Since our display case has a large amount of potential leakage points with respect to the amount of air inside, the air exchange rate of this display case becomes particularly susceptible to the way in which the display case is opened and closed every time. So in theory, we could expect a different air exchange rate every time the display case is opened. By increasing the air volume enclosed or reducing the length of the closing mechanism we could improve the reliability of the air exchange results.

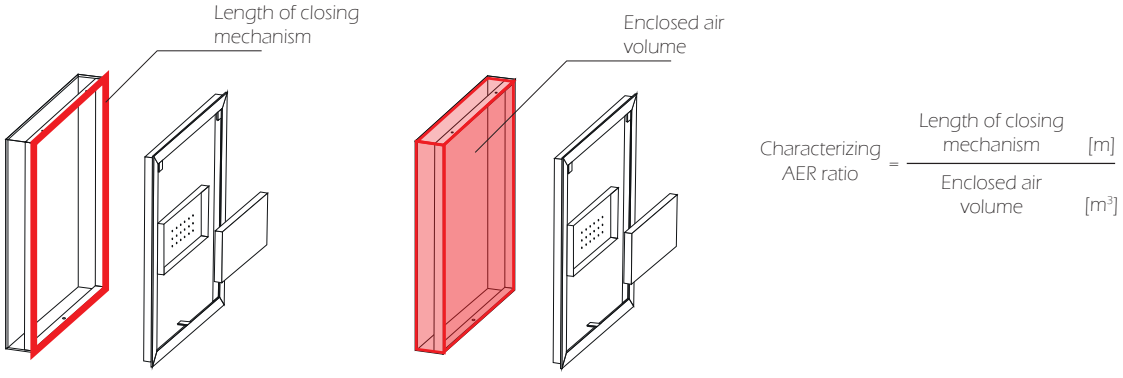

Figure 62: *Description of the length of closing mechanism to enclosed air volume ratio*

However, when calculating the moisture transfer coefficient we observe that the air exchange rate has no significant effect as shown in Table 58, Table 59 and Table 60. So, despite the controversy of the two different air exchange results, we were still able to estimate with significant accuracy the moisture transfer coefficient for each case scenario in a daily time base. The effect of the air exchange rate on the moisture transfer coefficient on a yearly time base is encouraged for further research.

It was mentioned during the AER results presentation in Chapter 3 that the sensor placed outside the display case collected inconsistent results. These results can be found in the Appendix 3. They are inconsistent because they record a relative humidity which is lower than the relative humidity inside of the display case. We know that the air inside of the display case is initially drier than the relative humidity outside which is at the condensation point. Two possible reasons were found to explain this inconsistency. The first is that the sensor was found on the ground, not taped to the display case at the end of the experiment; the impact of this fall could have influenced the logging system. The second is that due to the high relative humidity, condensation occurred inside which could have short-circuited the sensor. Due to these inconsistencies the results from this sensor were discarded.

Conclusion

In Chapter 4, the model validation is described. This was based on two sets of physical experiments: the AER, and the environment control experiments. The AER experiment was based on monitoring how dry air inside of the display case reached the same level of humidity as the outside. For this, a display case containing dry air was placed inside of a very wet chamber with 100% relative humidity. For the wet chamber, one of the concrete curing rooms at The TU Delft faculty of Civil Engineering and Geoscience was used. The environment control experiments were based on monitoring the response of climate inside of the display case when exposed to daily environmental loads. These experiments were repeated each time using the hygroscopic material in a different way. These experiments were performed in The TU Delft Faculty of Architecture and the Built Environment. One of the greatest challenges in the experimental part of this project was with respect to the equipment. Despite the apparent simplicity of the experimental setup, the high level of accuracy required by the equipment was the main concern. While the measuring equipment was borrowed from the TU Delft Faculty of Architecture and the Built Environment, the rest of the equipment was attained with the support from the generous collaborators of this project, particularly GLASSOLUTIONS Glascom Museum Presentations for the display case, and the Jewish Historical Museum in Amsterdam for the hygroscopic material.

The validation was based first on obtaining the AER value for the display case from the results of the AER experiments; that is AER = 1.33 ac/d. Then, the environment control experiments were used in order to estimate the moisture transfer coefficient in the display case; that is for case **b**, $\beta_c = 2.30 \times 10^{-4}$ Kg/m^{2}s, for case **c**, $\beta_c = 9.00 \times 10^{-4}$ Kg/m^{2}s, and for case **d**, $\beta_c = 8.00 \times 10^{-4}$ Kg/m^{2}s. On the other hand, case **a** of the environment control experiments contains no hygroscopic material, and therefore the AER could also be estimated from these experiments; that resulted in AER = 0.12 ac/d. There is one full order of magnitude difference between these two experiment results for AER. Since the moisture transfer coefficient was calculated assuming AER = 1.33 ac/d, these coefficients were calculated again now using AER = 0.12 ac/d. The results are nearly the same considering the uncertainty of the experiment. This means that the AER has no effect on the derivation of the moisture transfer coefficient, at least when evaluated over a daily time domain. Overall, we observed that with the newly found moisture content coefficients our model does replicate the experiment results with a significant level of accuracy. While the model has been built and validated, we still need a way to understand the performance of the passive display case under varying environmental loads. For this reason a study of the effect of the most significant parameters is taken in the form of a sensitivity analysis.

Chapter 5: Sensitivity analysis

In this chapter, we will use the model presented in Chapter 3, and validated in Chapter 4, to gain further insight into the performance of a passive display case. This computational model gives us the advantage of gathering a considerable amount of data in a relatively short period of time. Furthermore, it gives us full control over the parameters that comprise it. Therefore, to evaluate the performance of the passive display case, a study based on a sensitivity analysis was performed. Firstly, it is necessary to define the significant parameters that influence the performance of the display case. We have already seen most of them, as we had to manipulate them in the construction of the model in chapter 3. The relationship between these parameters will then be evaluated. This chapter aims to describe these parameters and present their influence.

Sensitivity analysis parameters

For the sensitivity analysis, five independent variables and one dependent variable were used. The independent variables are as follows:

1. The change in relative humidity outside of the display case; ΔRH_{out}
2. The temperature change; ΔT
3. The air exchange rate; AER
4. The time domain
5. The moisture transfer coefficient; β_c

The dependent variable is the change in relative humidity inside of the display case; ΔRH_{in}. This selection allows us to evaluate the effect of the outside conditions of a display case (through the ΔRH_{out}, and ΔT), the display case properties (through the AER, and β_c), and the exposure period (through the time domain).

The following section describes the parameters selected for the sensitivity analysis.

Temperature change, ΔT

This refers to the temperature surrounding the display case. As we saw in the previous chapter, the temperature inside of the display case follows quite closely the temperature outside of the display case; for this reason, no distinction has been made between them. This temperature does depend on multiple parameters; take, for instance, a museum gallery for which the outdoor temperature, the quality of the envelope, the quality of the conditioning unit and the number of visitors play a significant role in determining the temperature of the space. However, as an indoor space, museum galleries have consistently stable temperatures when compared to the outdoors. In this project it was assumed that the space temperature followed a sinusoidal behavior within some arbitrary range and period. Two periods were considered, daily and yearly; they depend on the time domain parameter, explained later in this section. Finally, the temperature change ΔT, is defined as the amplitude of the assumed space temperature wave, as shown in Figure 63:

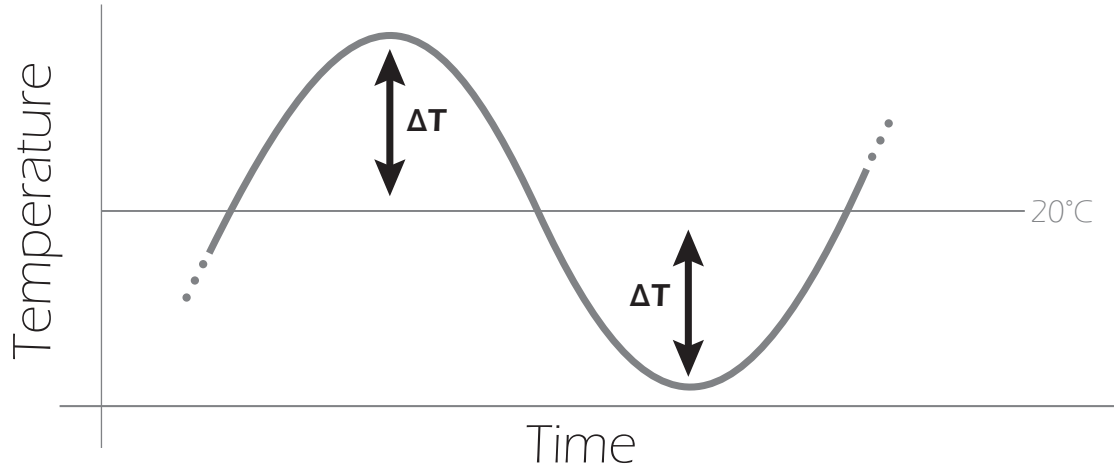

Figure 63: *Definition of the ΔT parameter*

0°C, 1°C, 2°C, 3°C were the selected values for ΔT, with an average of 20˚C.

Change in relative humidity outside of the display case, ΔRH_{OUT}

Relative humidity variations outside of a display case, such as in a museum gallery, are significantly difficult to simulate. This is because there can be multiple sources of moisture that must be considered and they all depend on a case-by-case situation, such as number of visitors, quality of the building envelope, quality of the conditioning unit and amount of moisture buffering material present in the space. Despite this challenge, the relative humidity outside of the display case was simplified within some arbitrary range with a sinusoidal behavior. It is important to note that the relative humidity has a great response to temperature change, and it is for this reason that the relative humidity outside of the display case is in anti-phase to the temperature change wave. Similarly to ΔT, the change in relative humidity outside of the display case has been defined as the amplitude of such relative humidity sinusoidal wave, shown in Figure 64:

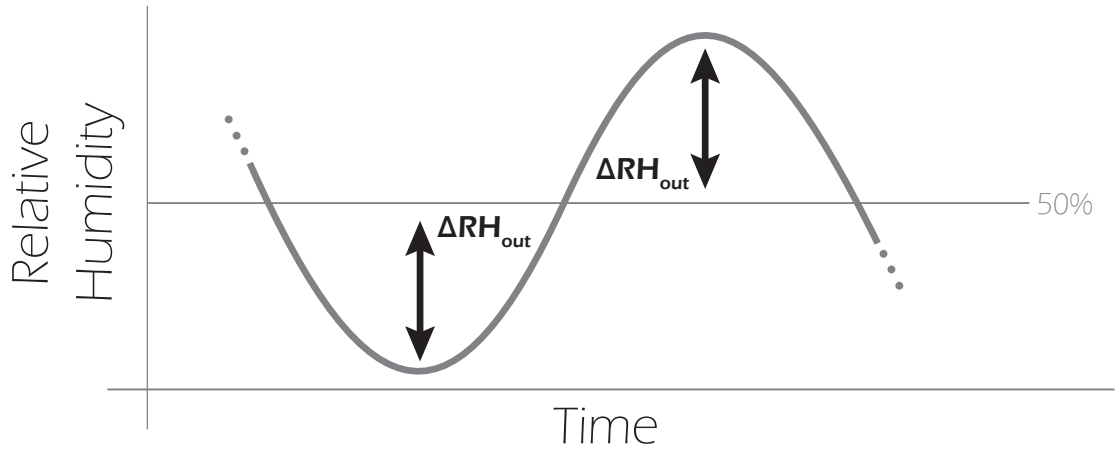

Figure 64: *Definition of the ΔRH_{out} parameter*

0%, 5%, 10%, 20% were the selected values for ΔRH_{out}, with an average of 50%.

Air exchange rate, AER:

The air exchange rate (AER), represents the amount of air transfer between the inside and the outside of the display case per unit time. In the previous chapters, we have seen how significant the air exchange is, particularly for the display case manufacturing industry, where the closing/opening mechanism of the display case plays a significant role. We have already seen that AER not only depends on the closing/opening mechanisms but also on the pressure and temperature variations in the space. Following the results presented in Chapter 3, air exchange rates of 0.00 ac/d, 0.12 ac/d, 1.33 ac/d were selected for the sensitivity analysis.

Time domain

It was noted in the literature review (Martens, 2012) that the period of exposure has a significant effect on the performance of the passive display case. So when evaluating the effect of the passive conditioning in a display case, the time period cannot be ignored. For this reason, two domains were selected: one day and one year. Note that when defining ΔT and ΔRH_{out} the respective time periods were selected for their assumed sinusoidal behavior. In other words, when simulating one year, no daily variations of ΔT and ΔRH_{out} were considered.

Moisture transfer coefficient, β_c

In Chapter 3, we saw that the values for the moisture transfer coefficient change considerably when the position and configuration of the ProSorb changes. For this reason, evaluating the effect of the moisture transfer coefficient in the display case becomes important. The values for the moisture transfer coefficient in case scenario **b** and case scenario **d**, when AER = 0.12 ac/d, were selected for this sensitivity analysis. These values are 2.00 x 10^{-4} Kg/m^{2}s and 7.90 x 10^{-4} Kg/m^{2}s.

Change in relative humidity inside of the display case, ΔRH_{IN}

The relative humidity inside of the display case is the dependent variable of the sensitivity analysis; that is, we are looking to find out the effect that the previously mentioned parameters have on the relative humidity inside of the display case. The change in relative humidity inside of the display case, ΔRH_{in} , is defined similarly to ΔRH_{out}, as shown in Figure 65:

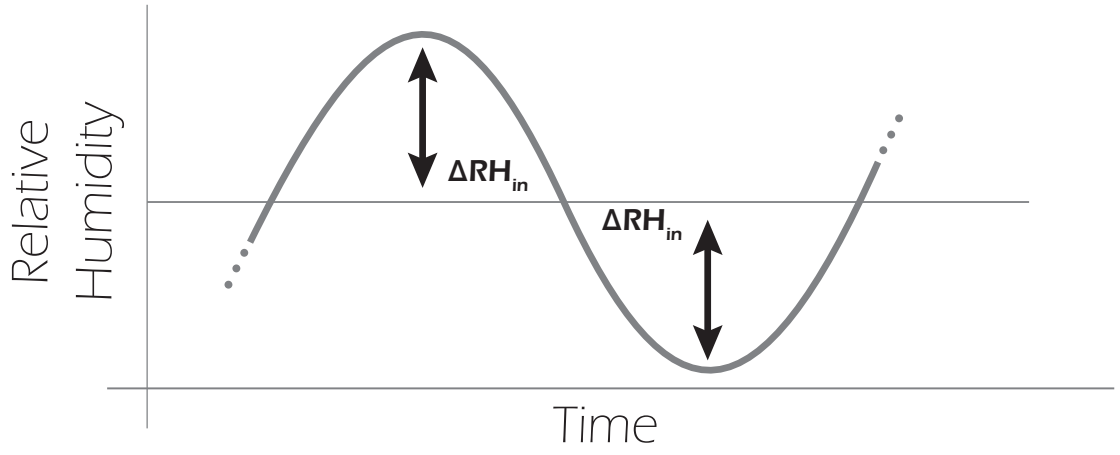

Figure 65: Definition of the ΔRH_{in} parameter

When the time domain is one day, the simulation is run for seven days and the amplitude of the last day was selected as ΔRH_{in}. Similarly, when the time domain is one year, the simulation is run for two years and the amplitude of the last year was selected as ΔRH_{in}. This allowed the simulation to stabilize, which could significantly affect the results throughout the entire sensitivity analysis.

Sensitivity analysis results

Find in the following tables and figures the results from the sensitivity analysis :

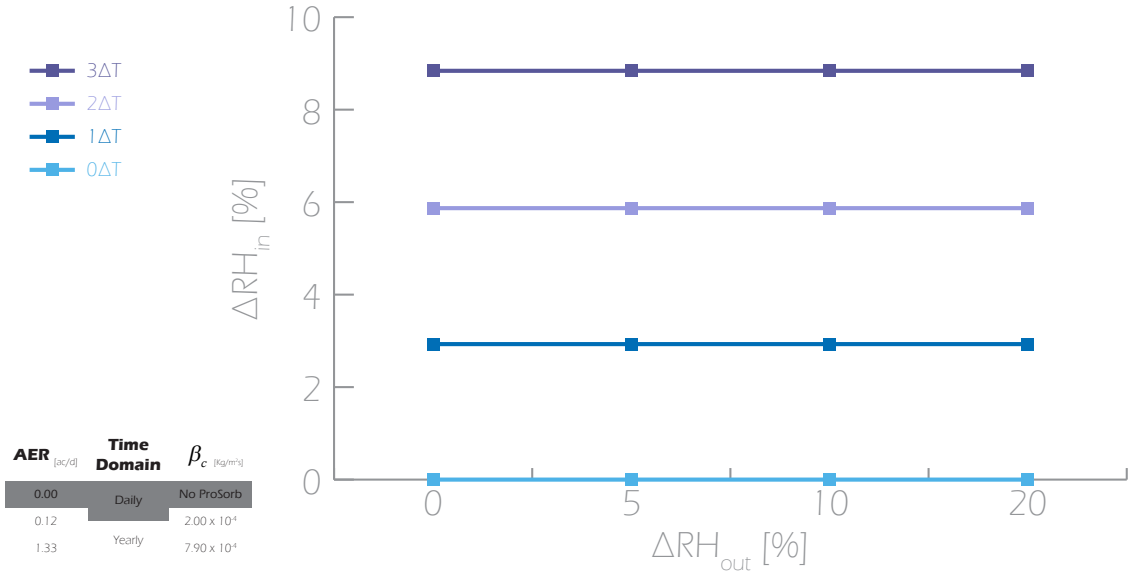

Figure 66: ΔRH_{in} when AER = 0.00, Time domain = daily, and no ProSorb is present

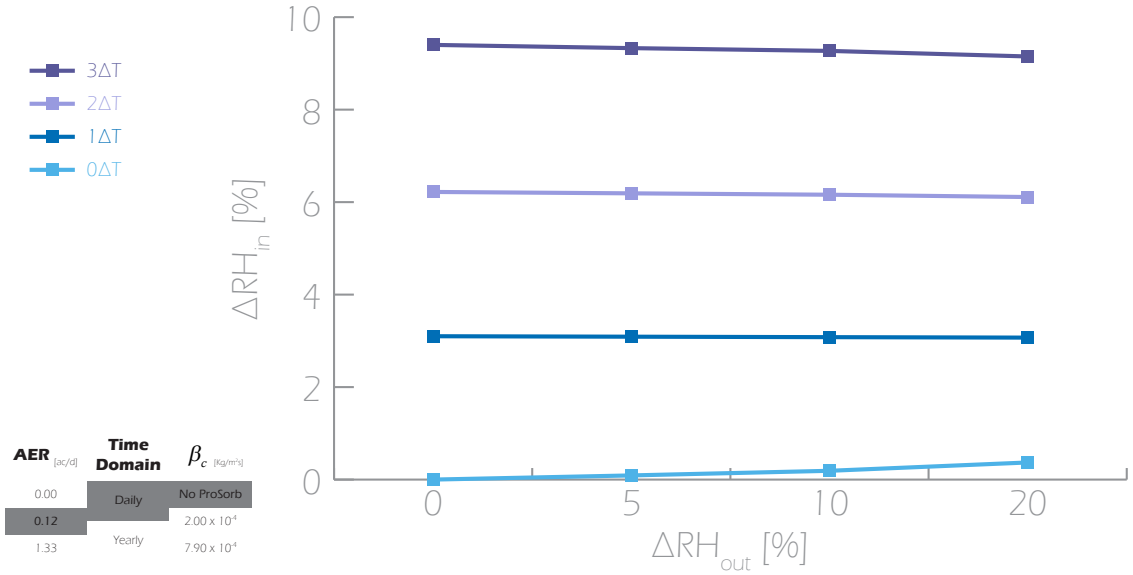

Figure 67: ΔRH_{in} when AER = 0.12, Time domain = daily, and no ProSorb is present

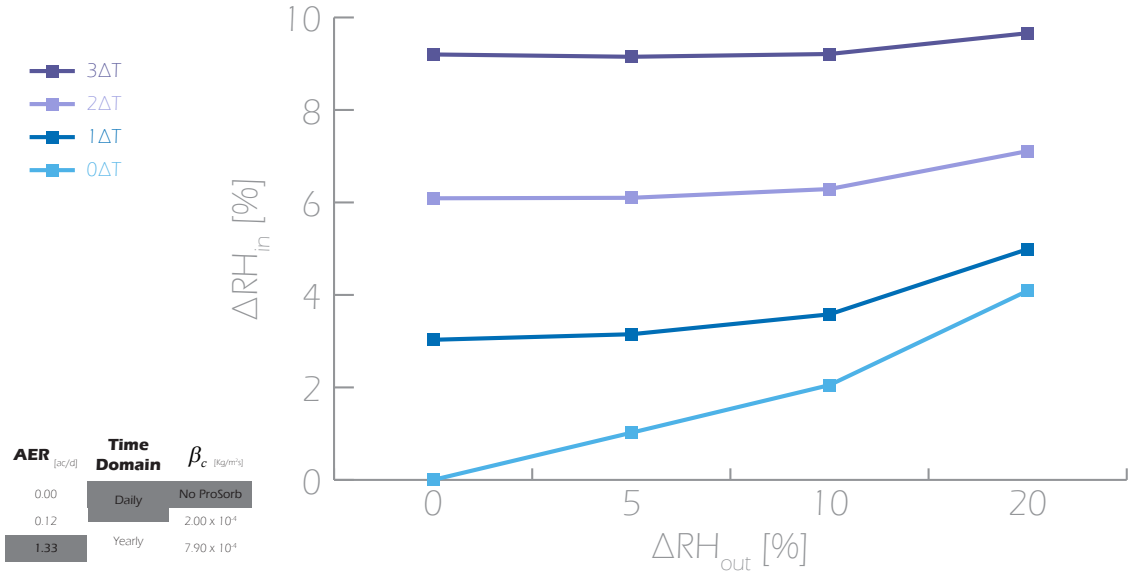

Figure 68: ΔRH_{in} when AER = 1.33, Time domain = daily, and no ProSorb is present

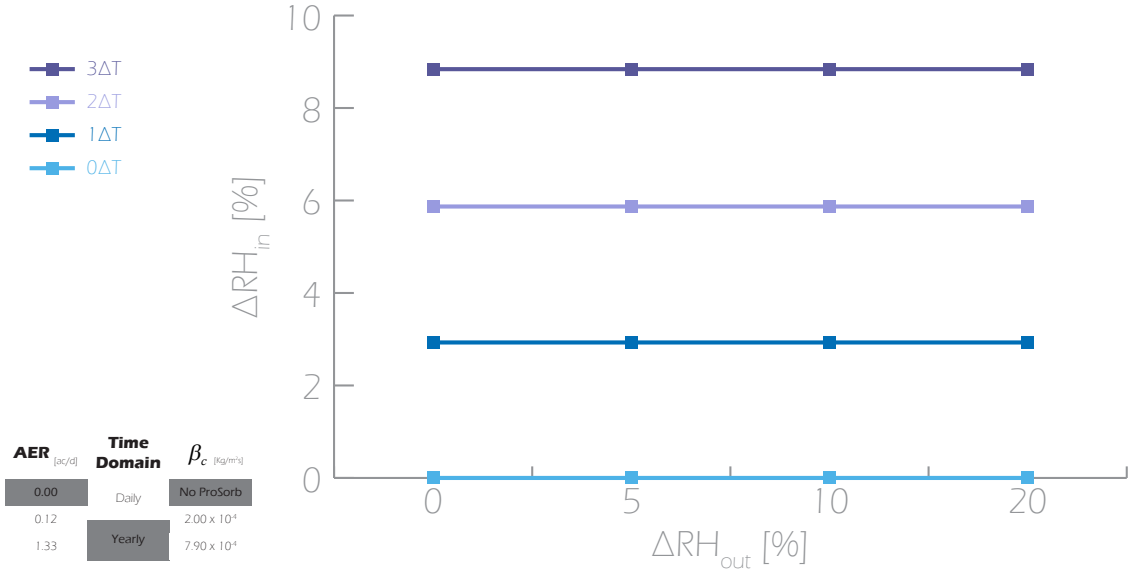

Figure 69: ΔRH_{in} when AER = 0.00, Time domain = yearly, and no ProSorb is present

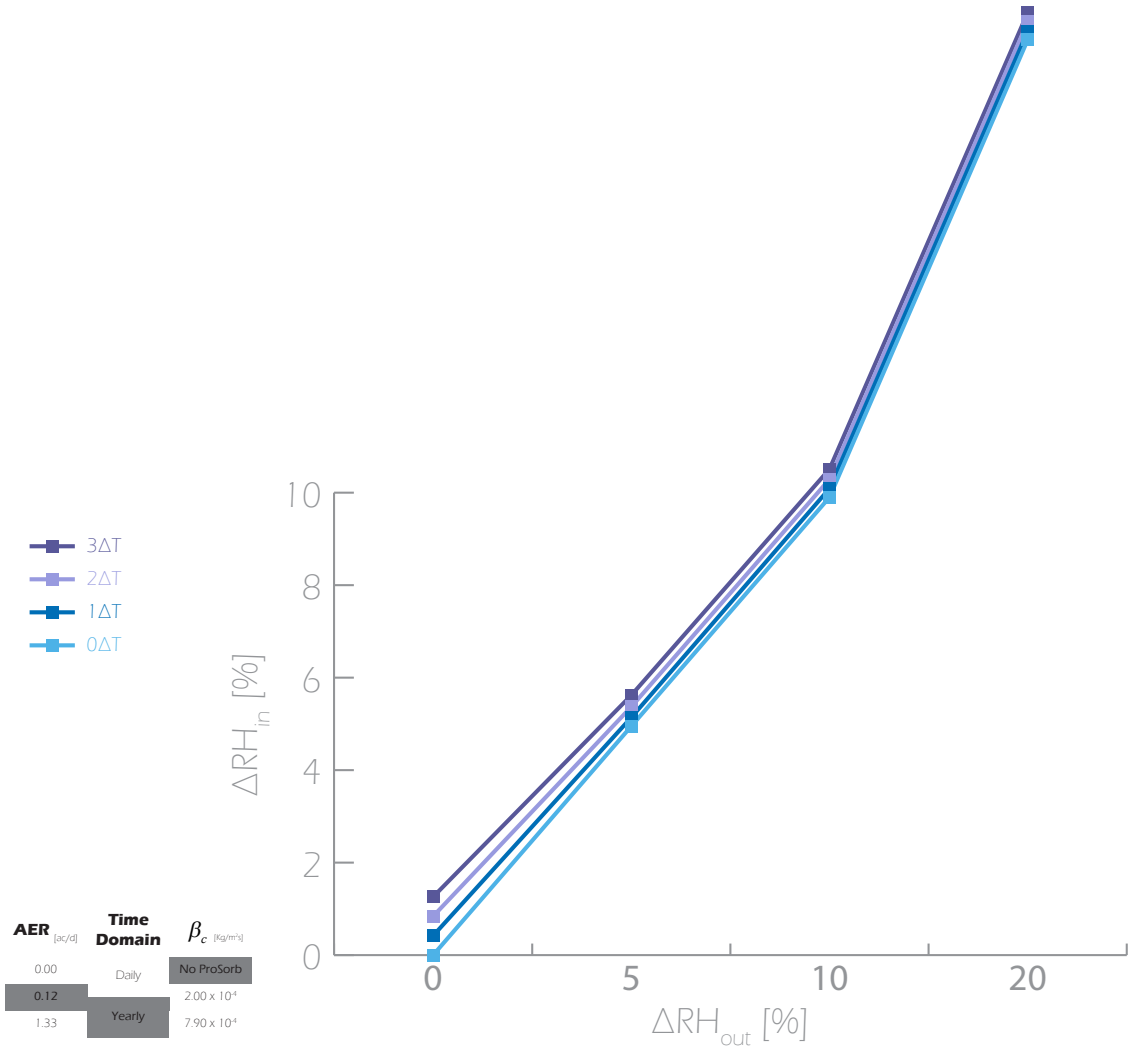

Figure 70: ΔRH_{in} when AER = 0.12, Time domain = yearly, and no ProSorb is present

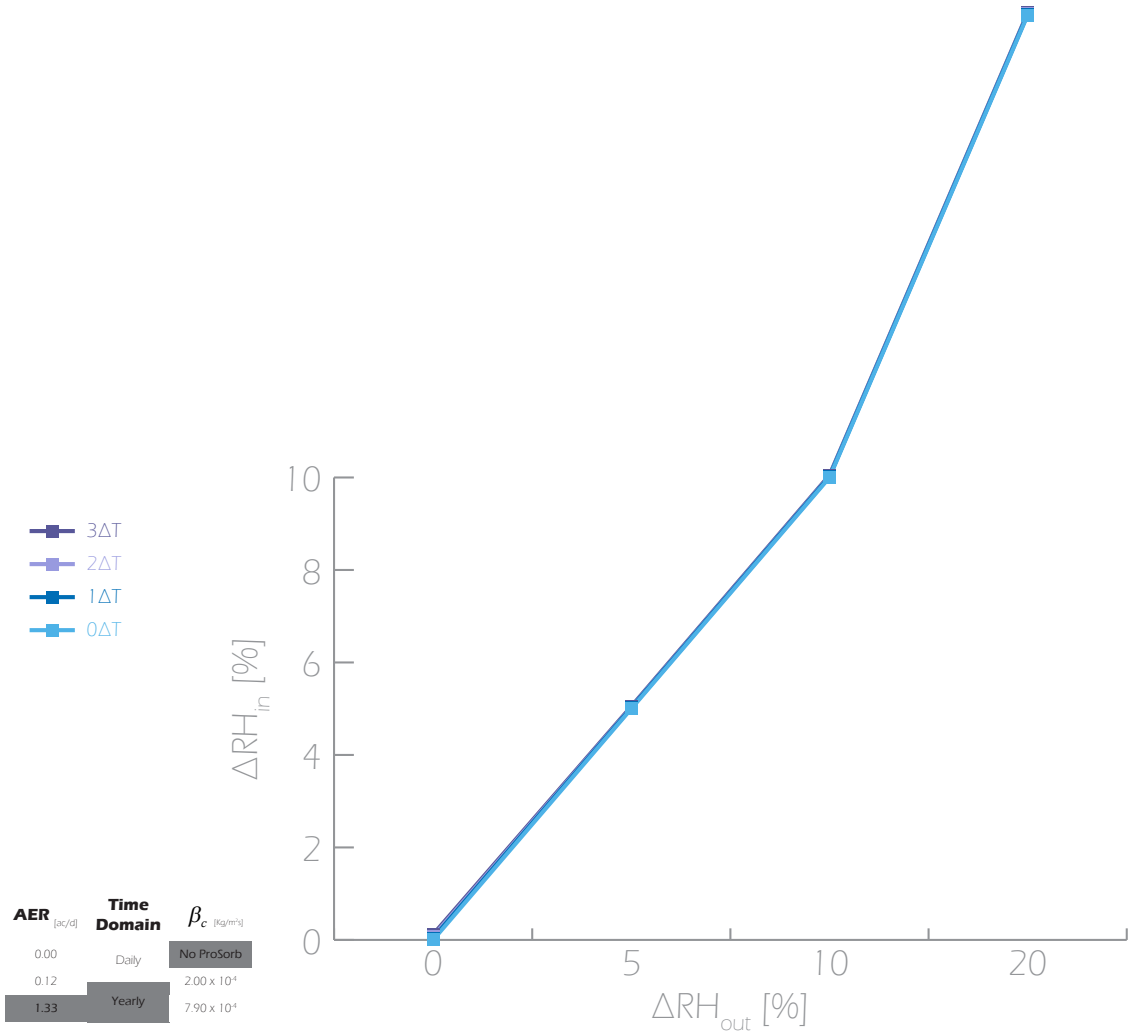

Figure 71: ΔRH_{in} when AER = 1.33, Time domain = yearly, and no ProSorb is present

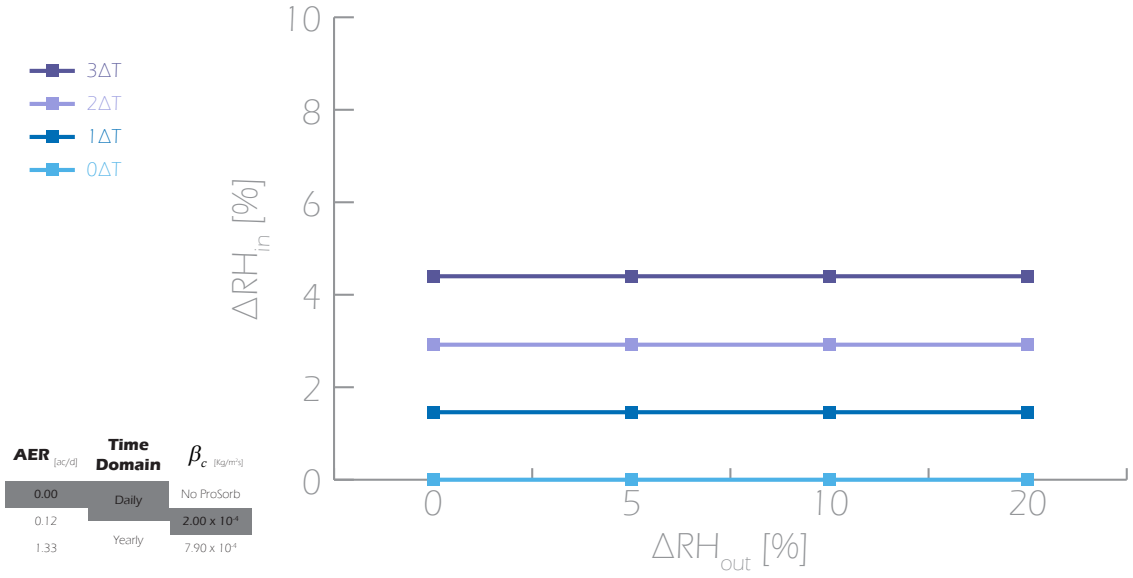

Figure 72: ΔRH_{in} when AER = 0.00, Time domain = daily, and β_c = 2.00 x 10^{-4} Kg/m^{2}s

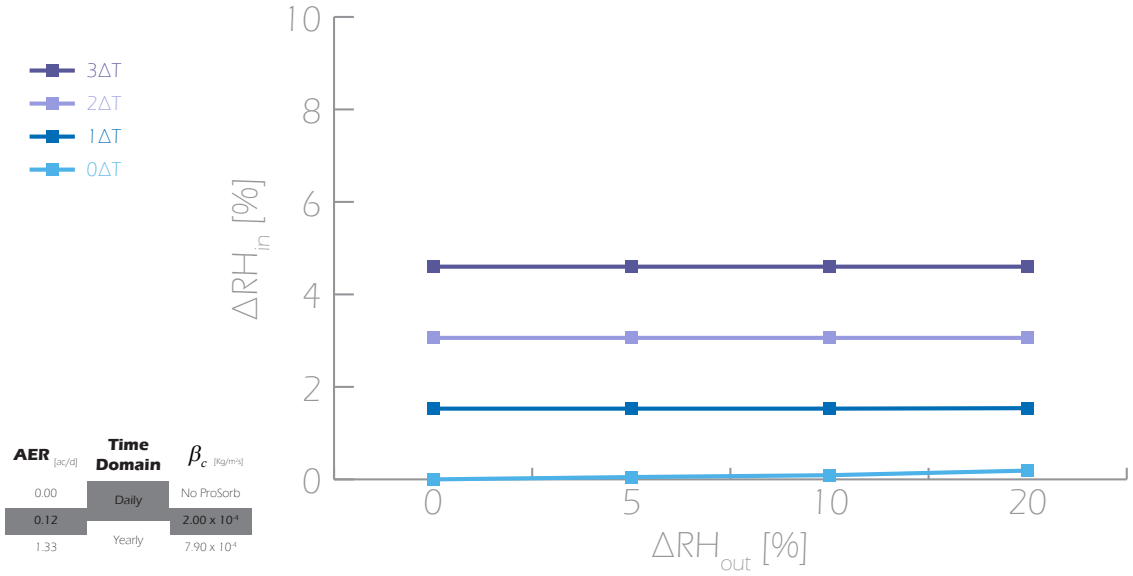

Figure 73: ΔRH_{in} when AER = 0.12, Time domain = daily, and β_c = 2.00 x 10^{-4} Kg/m^{2}s

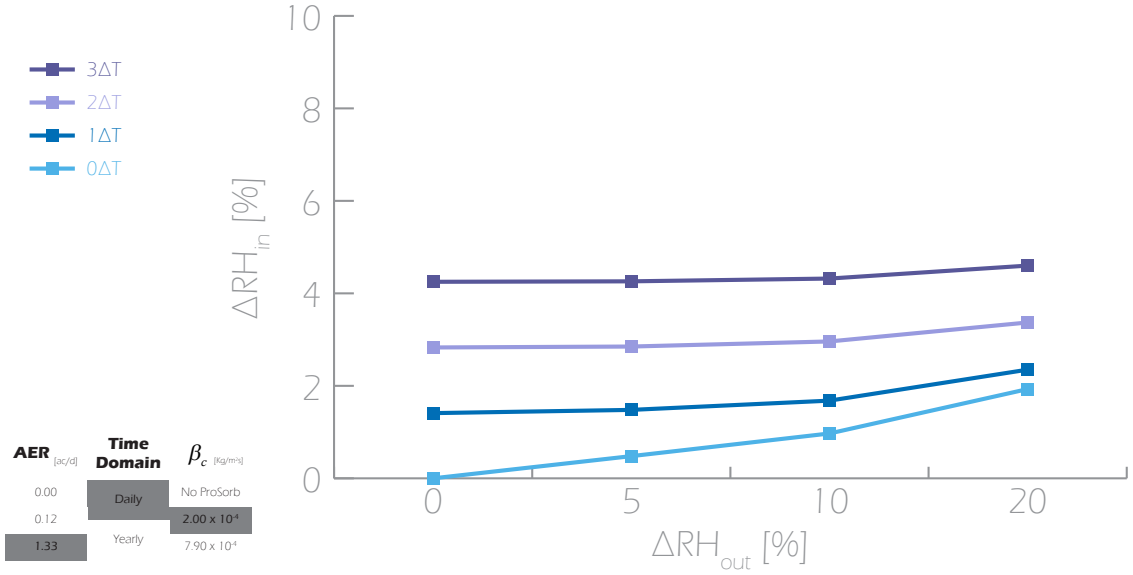

Figure 74: ΔRH_{in} when AER = 1.33, Time domain = daily, and β_c = 2.00 x 10^{-4} Kg/m^{2}s

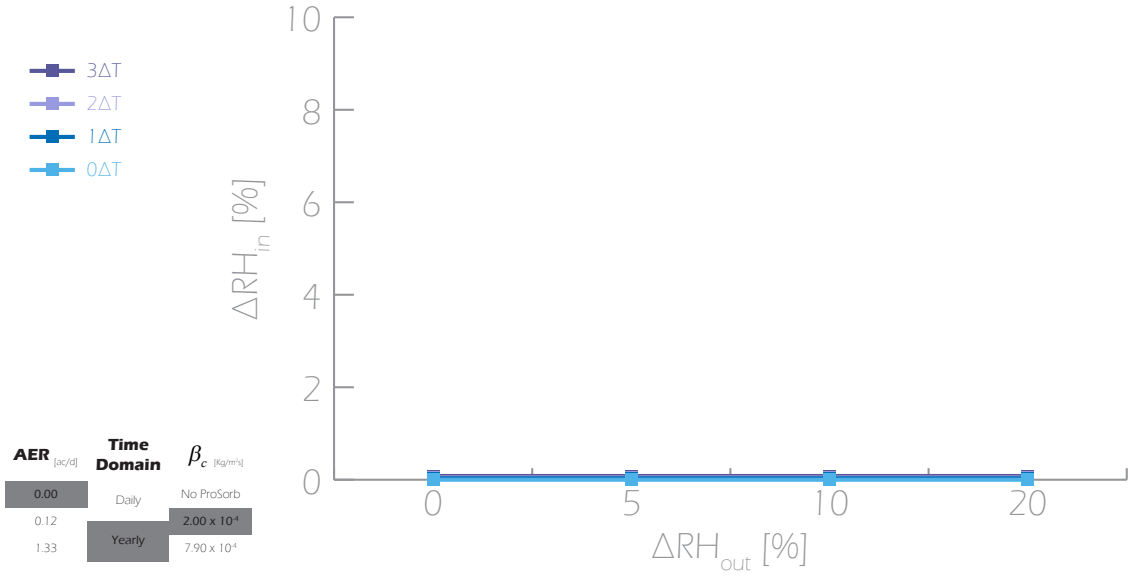

Figure 75: ΔRH_{in} when AER = 0.00, Time domain = yearly, and β_c = 2.00 x 10^{-4} Kg/m^{2}s

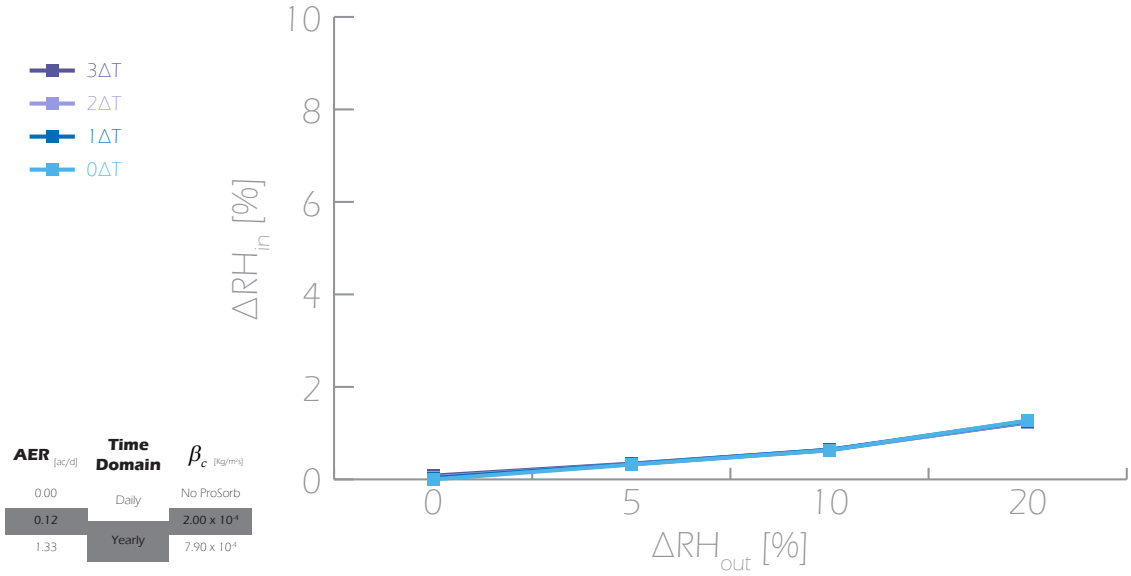

Figure 76: ΔRH_{in} when AER = 0.12, Time domain = yearly, and β_c = 2.00 x 10^{-4} Kg/m^{2}s

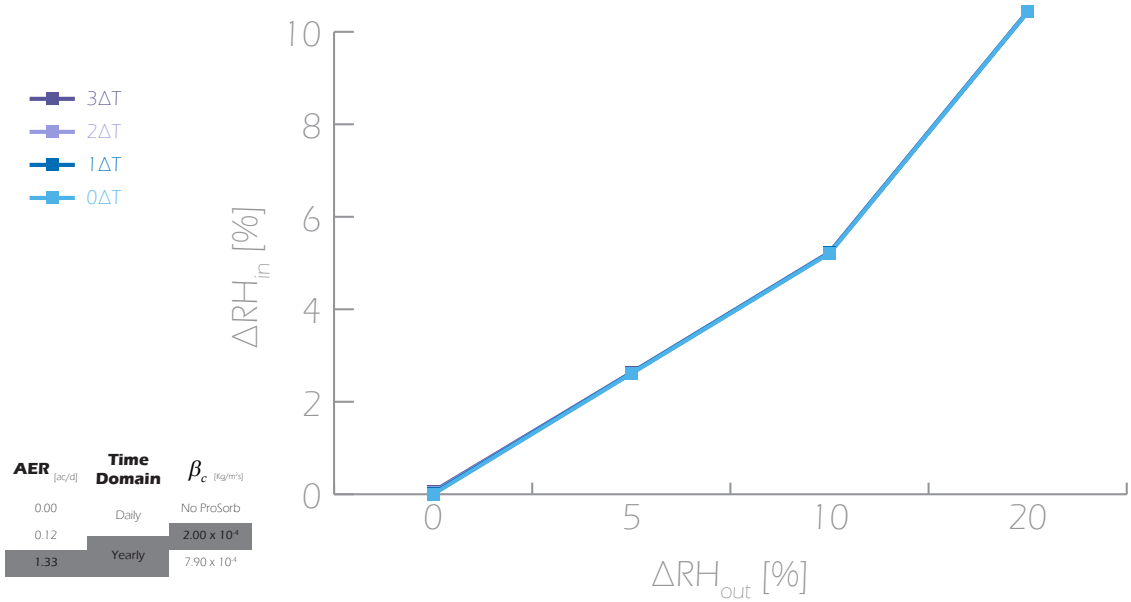

Figure 77: ΔRH_{in} when AER = 1.33, Time domain = yearly, and β_c = 2.00 x 10^{-4} Kg/m^{2}s

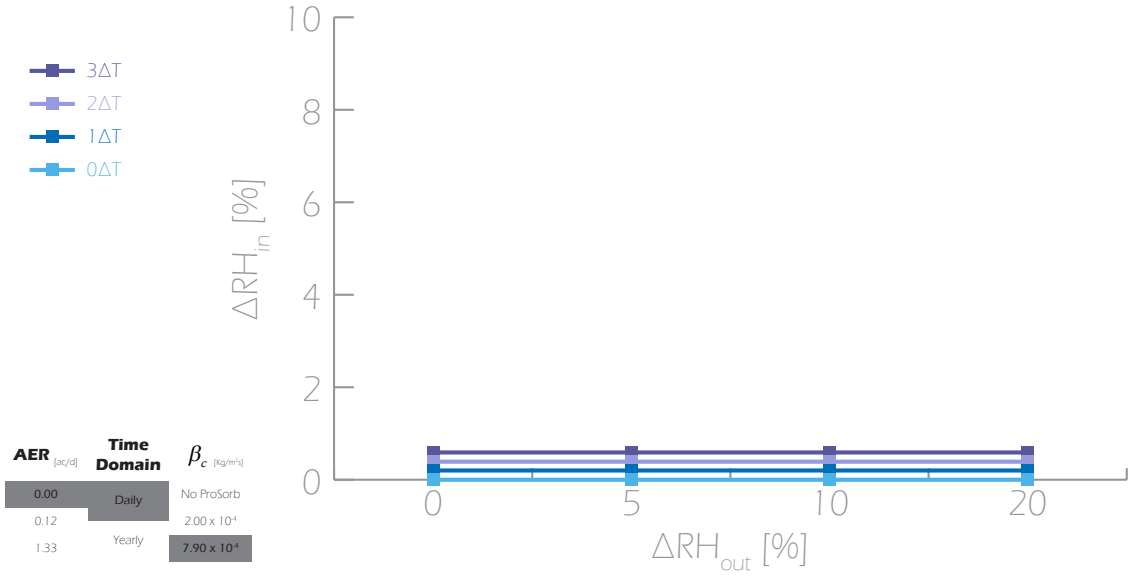

Figure 78: ΔRH_{in} when AER = 0.00, Time domain = daily, and β_c = 7.90 x 10^{-4} Kg/m^2s

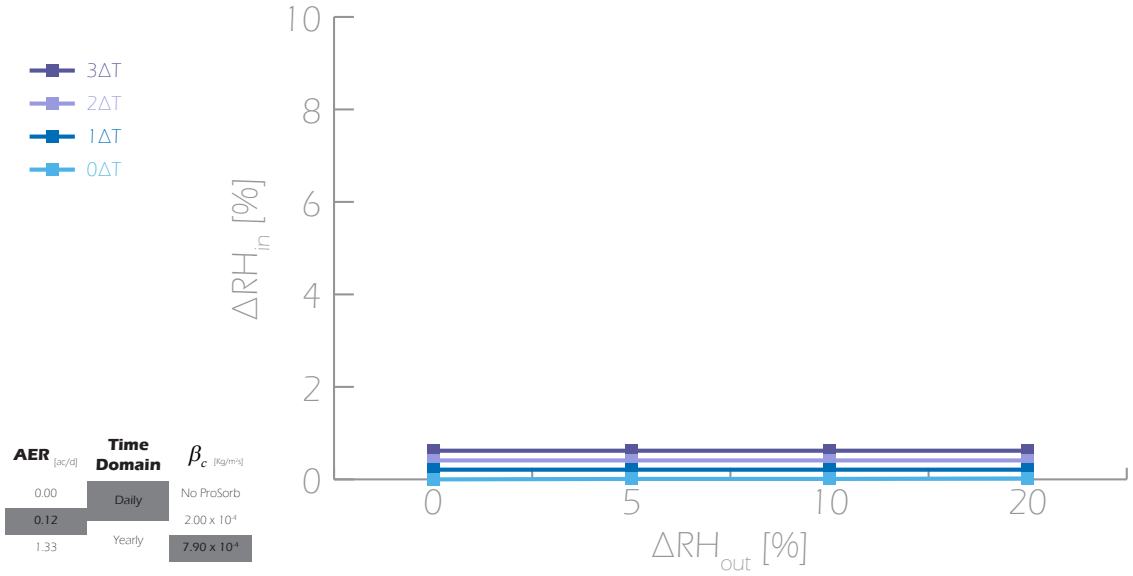

Figure 79: ΔRH_{in} when AER = 0.12, Time domain = daily, and β_c = 7.90x 10^{-4} Kg/m^2s

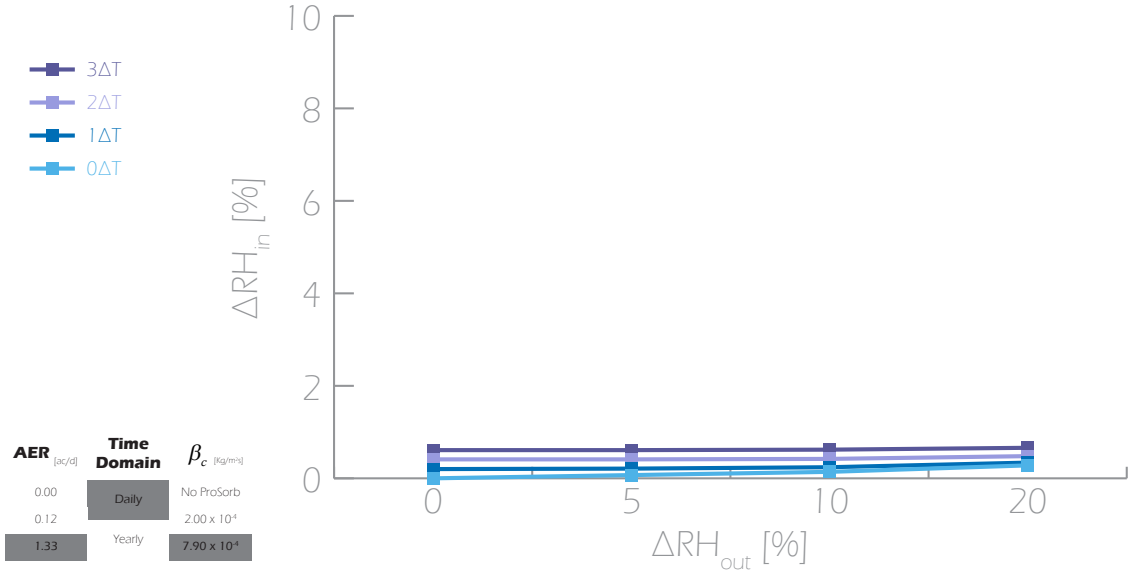

Figure 80: ΔRH_{in} when AER = 1.33, Time domain = daily, and β_c = 7.90 x 10^{-4} Kg/m^2s

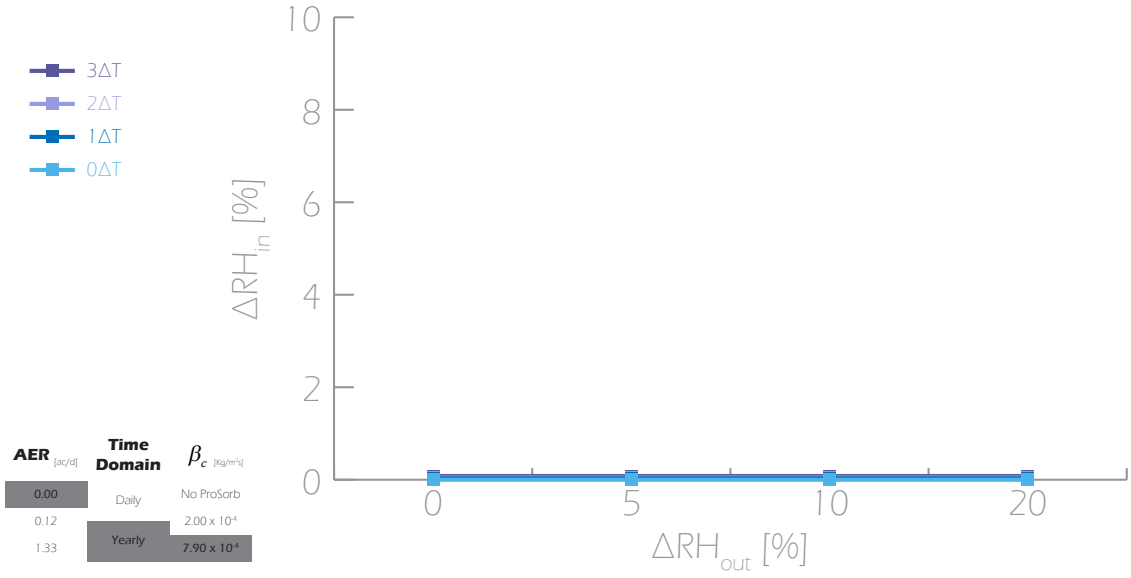

Figure 81: ΔRH_{in} when AER = 0.00, Time domain = yearly, and β_c = 7.90 x 10^{-4} Kg/m^2s

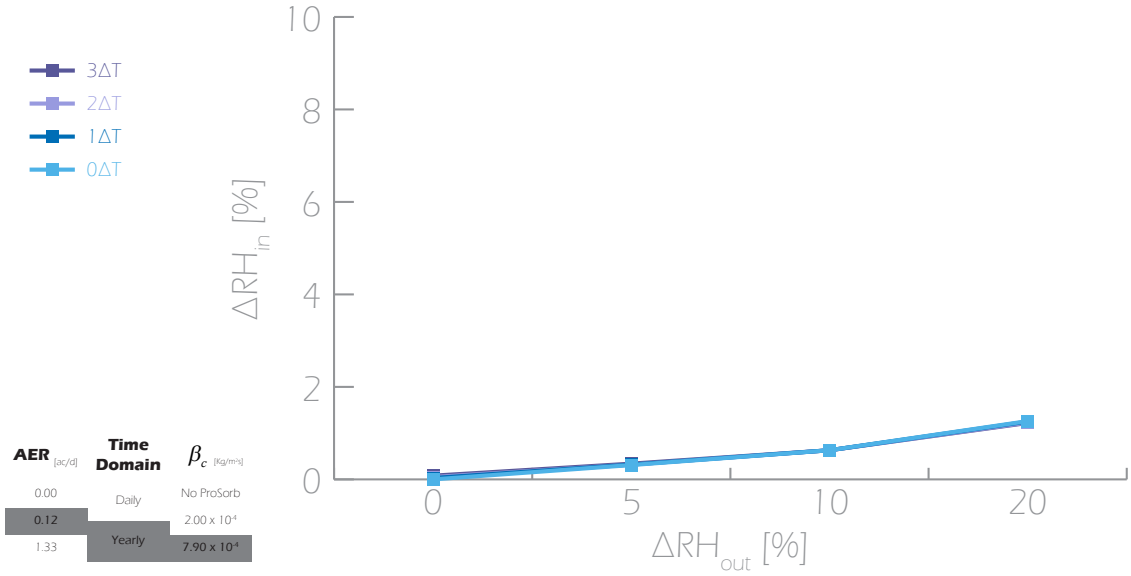

Figure 82: ΔRH_{in} when AER = 0.12, Time domain = yearly, and β_c = 7.90 x 10^{-4} Kg/m^2s

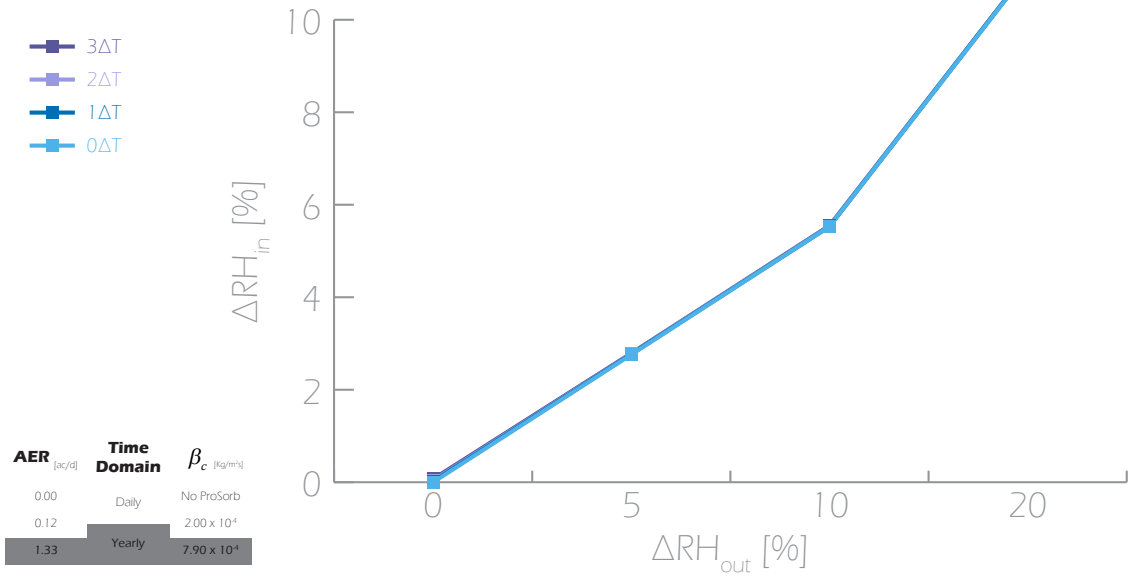

Figure 83: ΔRH_{in} when AER = 1.33, Time domain = yearly, and β_c = 7.90 x 10^{-4} Kg/m^2s

Analysis of the parameters

The data presented in the previous section came after running 288 different simulations; this is the result of combining the selected ranges for each one of the five different independent variables. This significant amount of data requires a systematic way for interpreting the results. In this section, the results presented from the sensitivity analysis will be analyzed and interpreted in two parts. First, the trends of the behavior of the parameters are considered with respect to each other, with no regards to the result values. The second part aims to evaluate the buffering effect, where the result vaues will be analyzed.

In order to analyze this data, all the ΔT range has been plotted in a graph defined by ΔRH_{out} and ΔRH_{in} for each case studied. Take, for instance, the situation when there is no AER, in a daily time domain, and β_c = 2.00 x 10^{-4} Kg/m^{2}s, shown in Figure 84. We will call these graphs ΔT-ΔRH_{out}-ΔRH_{in} graphs, which represent one display case situation.

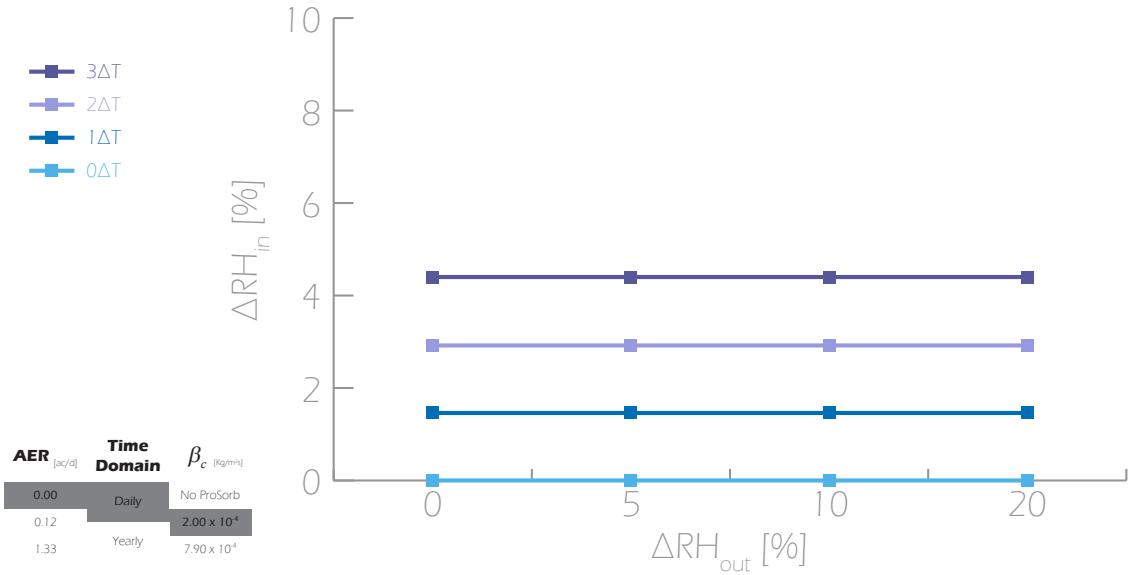

Figure 84: ΔRH_{in} when AER = 0.00, Time domain = daily, and β_c = 2.00 x 10^{-4} Kg/m^{2}s

In this way, all the simulations have been divided in display case situations. These display case situations depend only on the AER, the time domain and the β_c. Therefore, we have 18 different display case situations. In order to see the overall results from each of these 18 display case situations, a matrix containing each one of the 18 ΔT-ΔRH_{out}-ΔRH_{in} graphs has been developed. Figure 84 shows a simplified form of this matrix, where each colored rectangle represents the location of each ΔT-ΔRH_{out}-ΔRH_{in} graph. For more detail on the full matrix, see Appendix 7:

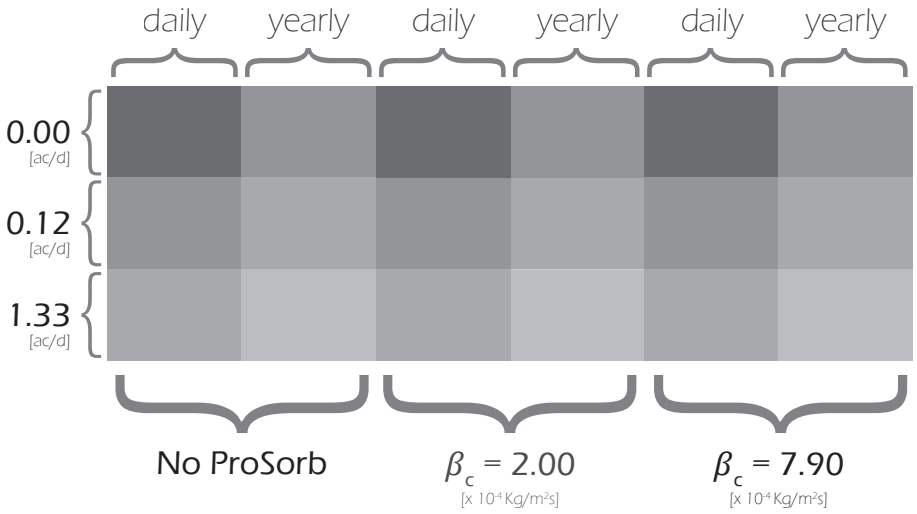

Figure 85: Display case situations matrix

Observed trends among the parameters

First we will consider the effect of ΔRH_{out}, ΔT and AER. The most important trends can be derived from these three parameters and we will call them the ΔT-ΔRH_{out}-ΔRH_{in} trends. However, it is necessary to first evaluate their effect on ΔRH_{in} individually.

Consider the outside conditions when the ΔT is fixed and the ΔRH_{out} is allowed to vary in the daily domain. The result of this situation depends on the AER value of the display case. We see that when AER = 0 then, ΔRH_{in} is insensitive to ΔRH_{out}. This is based on the fact that since there is no air exchange rate, no moisture transfer takes place between the inside and the outside of the display case. However, when AER ≠ 0 we can observe an increase in ΔRH_{in} as ΔRH_{out} increases. This is based on the fact that as ΔRH_{out} increases, while ΔT is fixed, there is an overall increase in the change of moisture content in the outside air. This is also evidenced by the fact that when AER increases, the effect of ΔRH_{out} on ΔRH_{in} is magnified. This is illustrated in Figure 86:

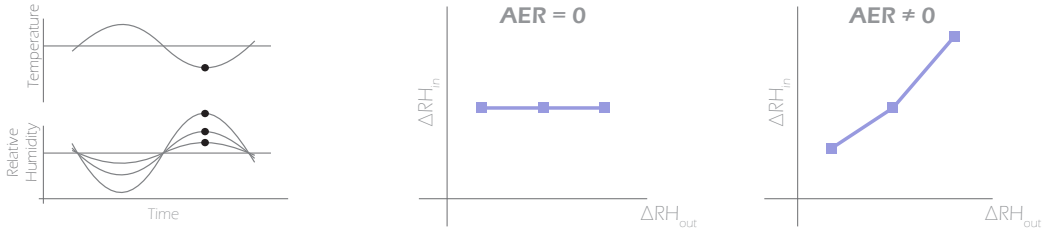

Figure 86: Analysis of the sensitivity trends when ΔT is fixed and the ΔRH_{out} is free

Now consider the outside conditions when the ΔRH_{out} is fixed and the ΔT is allowed to vary in the daily domain. Once again, this situation depends on the AER value of the display case. When AER =0 it is observed that as ΔT increases, ΔRH_{in} increases. Since there is no moisture transfer between the outside and the inside of the display case, this increment in ΔRH_{in} must come only from the effect of increasing temperature change. Since no gradients in temperature were assumed, each ΔT will produce a different unique ΔRH_{in}. When AER ≠ 0 then, the effect of the fixed ΔRH_{out} starts to play a significant role. As the moisture transfer between the inside and outside of the display case increases, we observe that the ΔRH_{in} for each particular ΔT seems to converge into a particular change in relative humidity, that is specifically ΔRH_{out}. This is based on the fact that as AER increases, the moisture transfer between the inside and outside of the display case is increased, and the change of moisture content inside of the display case starts influencing each different ΔT until the AER is so large that $\Delta RH_{in} = \Delta RH_{out}$. This converging effect of ΔRH_{in} into ΔRH_{out} makes ΔRH_{in} insensitive to ΔT . This is illustrated in Figure 87:

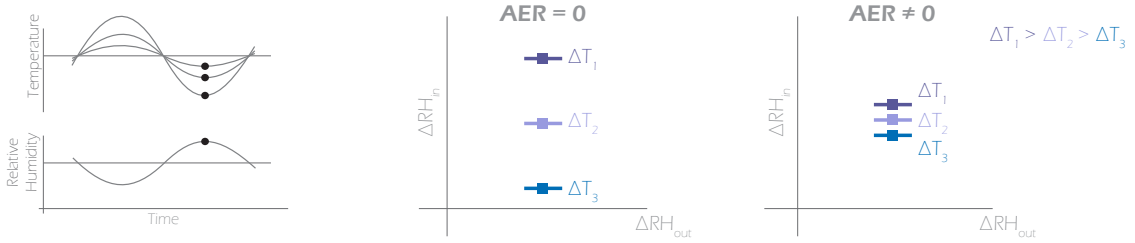

Figure 87: Analysis of the sensitivity trends when ΔRH_{out} is fixed and the ΔT is free

Therefore when considering ΔRH_{out}, ΔT, and AER we can recognize four main trends: **a**, **b**, **c**, and **d**. Trend **a** is when ΔRH_{in} shows to be insensitive to ΔRH_{out}. Trend **b** is when ΔRH_{out} controls the behavior of ΔRH_{in}. Trend **c** is when ΔT controls the behavior of ΔRH_{in}. Finally trend **d** is when ΔRH_{in} shows to be insensitive to ΔT; in other words, ΔRH_{in} seems to approach ΔRH_{out} irrespective of the value of ΔT. This is illustrated in Figure 88:

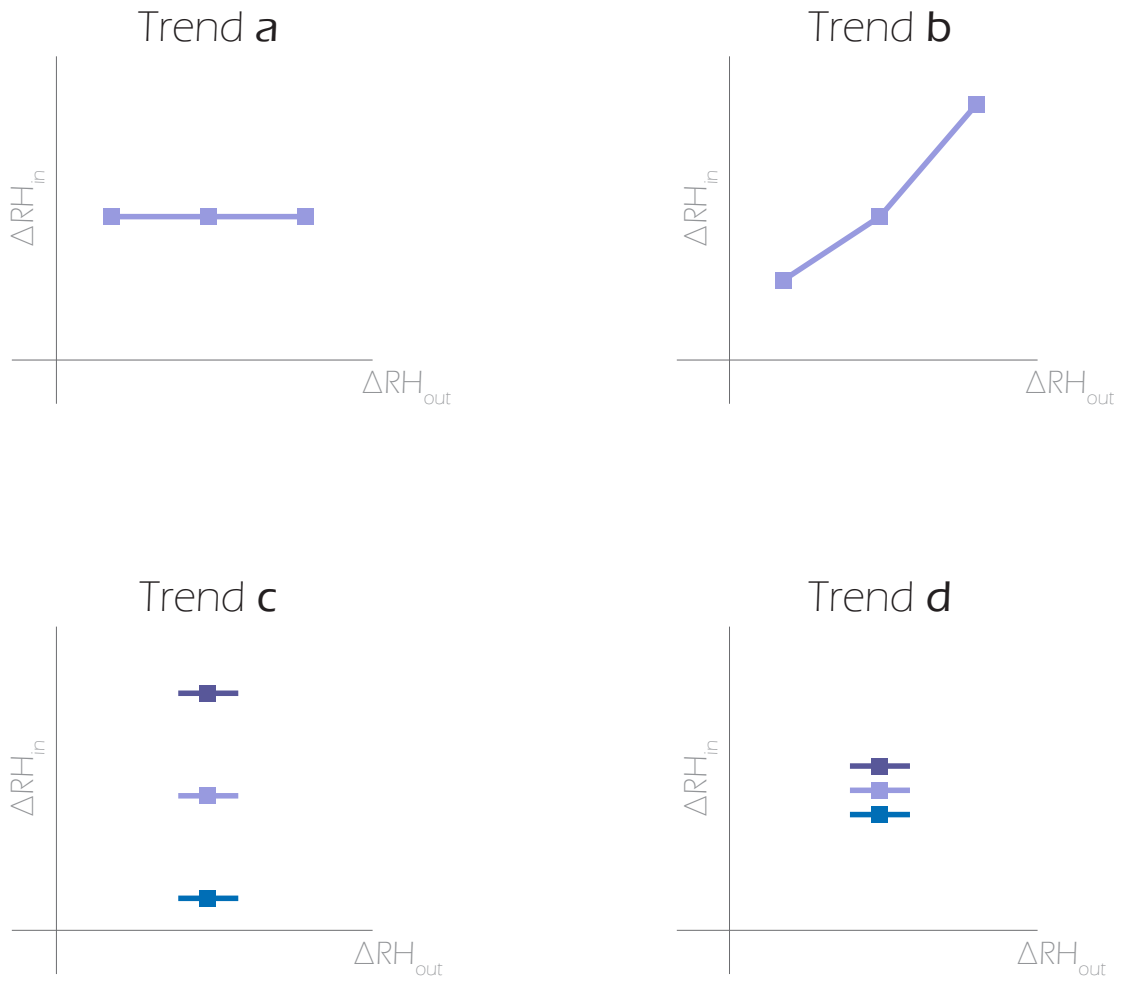

Figure 88: ΔT-ΔRH_{out}-ΔRH_{in} trends observed

These trends can be recognized for each display case condition studied in this sensitivity analysis. Take, for instance, the case when AER=0 is on the daily domain and no ProSorb is present, where trend **a** and **c** are dominant. Similarly, the dominant ΔRH_{out}, ΔT, and AER trends have been recognized throughout each display case condition studied in this sensitivity analysis. Find in Table 26 the dominant trends observed in each display case situation; also illustrated in a simplified form of the display case situation matrix in Figure 89.

Table 26: ΔT-ΔRH_{out}-ΔRH_{in} trends observed over all the display case situations studied

Display case situation			Observed Trends
β_c [x 10^{-4} Kg/m^{2}s]	Time domain	AER [ac/d]	
No ProSorb	Daily	0.00	**a, c**
		0.12	**a, c**
		1.33	**a, b, c**
	Yearly	0.00	**a, c**
		0.12	**b, d**
		1.33	**b, d**
2.00	Daily	0.00	**a, c**
		0.12	**a, c**
		1.33	**a, b, c**
	Yearly	0.00	**a, c**
		0.12	**b, d**
		1.33	**b, d**
7.90	Daily	0.00	**a, c**
		0.12	**a, c**
		1.33	**a, b, c**
	Yearly	0.00	**a, c**
		0.12	**b, d**
		1.33	**b, d**

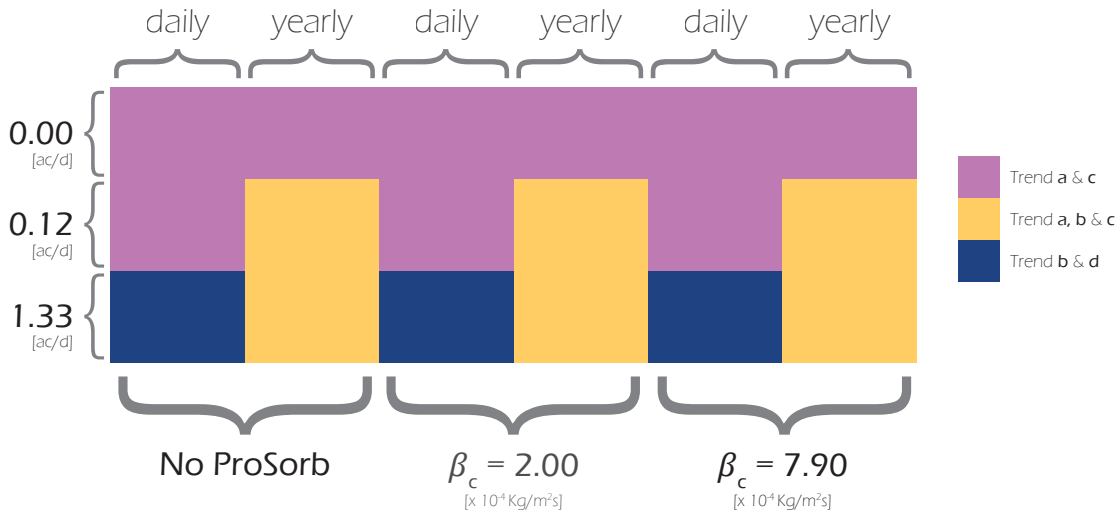

Figure 89: ΔT-ΔRH_{out}-ΔRH_{in} trends in the display case situation matrix

From Table 26, we can observe that the effects of the time domain parameter in the ΔRH_{out}, ΔT, and AER trends. On a daily time domain we see that trend **a** and **c** are dominant irrespectively of β_c. Note that we are evaluating only the trend behavior, not the actual buffering effect (observed as a reduction or increase in the values of ΔRH_{in}). The buffering effect will be studied in the following section. On the yearly time domain we see that trends **b** and **d** are the dominant ones, also irrespectively of β_c. Additionally it can be observed how trend **b** starts becoming dominant over trend **a** on a daily time domain and with AER = 1.33. This is attributed to the fact that when there is a high AER, ΔRH_{out} starts becoming more dominant over ΔRH_{in} which in turns reduces the effect of ΔT in ΔRH_{in}. On the other hand, a high β_c counteracts the ΔRH_{out} effect on ΔRH_{in}, reason for which we see that trend **b** is not as obvious as the other situations when β_c = 7.9x10^{-4} with AER=1.33 on a daily time domain.

One of the most important parameters in this work is the situation in which the hygroscopic material is placed inside of the display case; this is represented by the β_c parameter. In Chapter 4, we observed

that different situations of placing the same amount of ProSorb resulted in different β_c values. β_c parameter was studied here in order to gain insight about the effect of the moisture transfer coefficient in the performance of the display case. We can see from Table 26 that the ΔT-ΔRH_{out}-ΔRH_{in} trends are consistent across the two values for β_c studied and the situation without ProSorb. In other words, a display case with the studied amount of ProSorb will not influence the domain of control of the ΔT-ΔRH_{out}-ΔRH_{in} trends parameters.

Buffering effect

To evaluate the buffering effect of the display case with respect to the studied parameters, we will compare the ΔRH_{in} values within the display case conditions that only share the same trend. For this reason the 18 display case situations studied during this sensitivity analysis were divided into the three groups observed to share the same ΔT-ΔRH_{out}-ΔRH_{in} trend combination. This is shown in Table 27, Table 28, and Table 29:

Table 27: Display case situations observed to follow trend **a** and **c**

Observed Trend	Display case situation		
	β_c [x 10^{-4} Kg/m^{2}s]	Time domain	AER [ac/d]
a, c	No ProSorb	Daily	0.00
			0.12
		Yearly	0.00
	2.00	Daily	0.00
			0.12
		Yearly	0.00
	7.90	Daily	0.00
			0.12
		Yearly	0.00

Table 28: Display case situations observed to follow trend **a**, **b** and **c**

Observed Trend	Display case situation		
	β_c [x 10^{-4} Kg/m^{2}s]	Time domain	AER [ac/d]
a, b, c	No ProSorb	Daily	1.33
	2.00		
	7.90		

Table 29: Display case situations observed to follow trend **b** and **d**

Observed Trend	Display case situation		
	β_c [x 10^{-4} Kg/m^{2}s]	Time domain	AER [ac/d]
b, d	No ProSorb	Yearly	0.12
			1.33
	2.00		0.12
			1.33
	7.90		0.12
			1.33

It can be observed that within each of these ΔT-ΔRH_{out}-ΔRH_{in} trend combination groups there are display case situations that present the same performance of ΔRH_{in}. (There is no major difference between their ΔRH_{in} values.) Among these display case situations, there is no buffering effect taking place. These situations have been highlighted and sub-grouped inside of each ΔT-ΔRH_{out}-ΔRH_{in} trend group, as shown in Table 30, Table 31, and Table 32, and also illustrated in the display case situation matrix in Figure 90 on page 70. Ten of these sub-groups or equivalent buffering groups have been recognized.

Table 30: Equivalent buffering groups in trend **a** and **c**

Observed Trend	Display case situation		
	β_c [x 10^{-4} Kg/m²s]	Time domain	AER [ac/d]
a, c	No ProSorb	Daily	0.00
	No ProSorb	Daily	0.12
	No ProSorb	Yearly	0.00
	2.00	Daily	0.00
	2.00	Daily	0.12
	2.00	Yearly	0.00
	7.90	Daily	0.00
	7.90	Daily	0.12
	7.90	Yearly	0.00

Group 1
Group 2

Group 3
Group 4

Table 31: Equivalent buffering groups in trend **a**, **b** and **c**

Observed Trend	Display case situation		
	β_c [x 10^{-4} Kg/m²s]	Time domain	AER [ac/d]
a, b, c	No ProSorb	Daily	1.33
	2.00	Daily	1.33
	7.90	Daily	1.33

Group 5
Group 6
Group 7

Table 32: Equivalent buffering groups in trend **b** and **d**

Observed Trend	Display case situation		
	β_c [x 10^{-4} Kg/m^{2}s]	Time domain	AER [ac/d]
b, d	No ProSorb	Yearly	0.12
	No ProSorb	Yearly	1.33
	2.00	Yearly	0.12
	2.00	Yearly	1.33
	7.90	Yearly	0.12
	7.90	Yearly	1.33

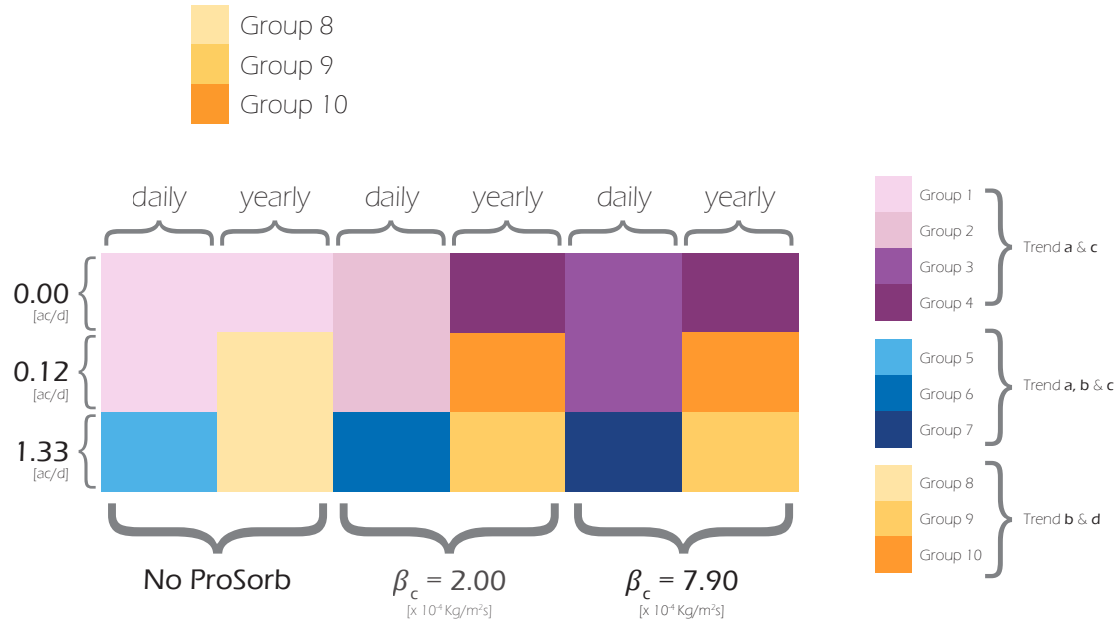

Figure 90: Equivalent buffering groups in the display case situation matrix

In other words, when β_c is the same on a daily time domain and between AER = 0.00 and AER = 0.12 ac/d, there is no buffering taking place, they are in the same equivalent buffering group. Note that the condition determining if buffering takes place is not tied to any individual parameter. For example, as opposed to group one where there is no difference in ΔRH_{in} between AER = 0.00 and AER = 0.12, when we compare groups 8 and 10, we observe that AER does have an influence and additionally, no difference can be observed in ΔRH_{in} between β_c = 2.00 and β_c = 7.90 in either of these groups.

For the situations that share trends, **a** and **c**, the most significant parameter for the buffering effect is the time domain and the β_c; AER seems to play no major role here. For the situations that share trends **a**, **b** and **c**; the most significant parameter for the buffering effect seems to only be β_c. However, keep in mind that this is an intermediate state, where due to AER, trend **b** starts becoming more influential over trend **a**. Finally, for the situations that share trend **b** and **d**, the most significant parameter for the buffering effect is AER, and ony β_c when comparing the situation with and without ProSorb.

We can observe from the ΔT-ΔRH_{out}-ΔRH_{in} graphs that between Group 1 and Group 2 there is some

buffering taking place (ΔRH_{in} in Group 1 is approximately twice the ΔRH_{in} in Group 2). However, between Group 4 and Group 3 there is a very significant amount of buffering taking place (where ΔRH_{in} in Group 3 is approximately 7.70 times bigger than ΔRH_{in} in Group 4). The factor by which ΔRH_{in} is increased or reduced when comparing two different groups will be defined as the buffering factor; for example, the buffering factor between Group 3 and Group 4 is 7.70. Note that the buffering factor depends on the direction of comparison, while the buffering factor between Group 3 and Group 4 is 7.70, the buffering factor between Group 4 and Group 3 is 0.13.

In order to calculate this buffering factor, the average ΔRH_{in} between each equivalent buffering group was calculated. Take, for instance, the results for Group 2, shown in Table 33. Note that the standard deviation in Table 33 can be interpreted as the degree in which the ΔRH_{in} in each display case situation are the equivalent for each group. For the results of the average ΔRH_{in} in each group, Appendix 6 can be consulted. The buffering factor is therefore the average value taken from dividing each ΔRH_{in} value between two different equivalent buffering groups.

Table 33: Trend ***a*** and **c**: Group 2 ΔRH_{in} average

ΔRH$_{out}$ [%] \ **ΔT** [°C]	0	1	2	3
0	0.00 ±0.00	1.49 ±0.05	2.99 ±0.10	4.50 ±0.14
5	0.02 ±0.03	1.49 ±0.05	2.99 ±0.10	4.50 ±0.14
10	0.05 ±0.07	1.49 ±0.05	2.99 ±0.10	4.50 ±0.14
20	0.09 ±0.13	1.50 ±0.05	2.99 ±0.10	4.50 ±0.14

In this way, we can define the amount of buffering taking place among all the groups in each ΔT-ΔRH_{out}-ΔRH_{in} trend; this is shown in Table 34. Note that the standard deviation of the buffering factor can be interpreted as a measure of the strength each of the ΔT-ΔRH_{out}-ΔRH_{in} trend groups has:

Table 34: Buffering factors

Trend group	Comparison between:	Buffering factor
a, c	Group 1 & Group 2	1.86 ±0.28
	Group 1 & Group 4	114.57 ±0.40
	Group 1 & Group 3	13.86 ±2.11
	Group 2 & Group 4	57.43 ±0.12
	Group 2 & Group 3	7.45 ±0.07
	Group 4 & Group 3	0.13 ±0.00
a, b, c	Group 5 & Group 6	2.13 ±0.02
	Group 5 & Group 7	14.83 ±0.11
	Group 6 & Group 7	6.96 ±0.01
b, d	Group 8 & Group 10	15.99 ±0.26
	Group 8 & Group 9	1.88 ±0.03
	Group 10 & Group 9	0.12 ±0.00

Discussion

The main idea behind developing the sensitivity analysis presented in this chapter was to make a tool where, under a particular scenario, the amount of buffering, if any, could be determined. For this reason, the display case situation matrix was developed and can be found in Appendix 7. There are multiple conclusions that can be derived from these results and they are presented below:

The situations where no buffering occurs are shown in Table 35:

Table 35: Display case situations that show minimal difference among their respective ΔRH_{in} values. All AER values are shown in [ac/d] and all β_c are shown in [x 10^{-4} Kg/m^2s]

1	the AER = 0.00	in a daily time domain	with no ProSorb	Is compared with	the AER = 0.12	in a daily time domain	with no ProSorb
2	the AER = 0.00	in a daily time domain	with no ProSorb		the AER = 0.00	in a yearly time domain	with no ProSorb
3	the AER = 0.00	in a daily time domain	with β_c = 2.00		the AER = 0.12	in a daily time domain	with β_c = 2.00
4	the AER = 0.00	in a yearly time domain	with β_c = 2.00		the AER = 0.00	in a yearly time domain	with β_c = 7.90
5	the AER = 0.00	in a daily time domain	with β_c = 7.90		the AER = 0.12	in a daily time domain	with β_c = 7.90
6	the AER = 0.12	in a yearly time domain	with no ProSorb		the AER = 1.33	in a yearly time domain	with no ProSorb
7	the AER = 0.12	in a yearly time domain	with β_c = 2.00		the AER = 0.12	in a yearly time domain	with β_c = 7.90
8	the AER = 1.33	in a yearly time domain	with β_c = 2.00		the AER = 1.33	in a yearly time domain	with β_c = 7.90

On the other hand, the amount of buffering that can be observed in ΔRH_{in} is described in Table 36:

Table 36: *Display case situations that show some buffering among their respective ΔRH_{in} values. All AER values are shown in [ac/d] and all β_c are shown in [x 10^{-4} Kg/m^2s]*

	The situation in which ...	... is ...	... larger than the situation in which ...
1	the AER = 0.00 in a daily time domain with no ProSorb	1.86 times	the AER = 0.00 in a daily time domain with β_c = 2.00
2			the AER = 0.12 in a daily time domain with β_c = 2.00
3		114.6 times	the AER = 0.00 in a yearly time domain with β_c = 2.00
4			the AER = 0.00 in a yearly time domain with β_c = 7.90
5		13.86 times	the AER = 0.00 in a daily time domain with β_c = 7.90
6			the AER = 0.12 in a daily time domain with β_c = 7.90
7	the AER = 0.00 in a yearly time domain with no ProSorb	1.86 times	the AER = 0.00 in a daily time domain with β_c = 2.00
8			the AER = 0.12 in a daily time domain with β_c = 2.00
9		114.6 times	the AER = 0.00 in a yearly time domain with β_c = 2.00
10			the AER = 0.00 in a yearly time domain with β_c = 7.90
11		13.86 times	the AER = 0.00 in a daily time domain with β_c = 7.90
12			the AER = 0.12 in a daily time domain with β_c = 7.90
13	the AER = 0.00 in a daily time domain with no ProSorb	1.86 times	the AER = 0.00 in a daily time domain with β_c = 2.00
14			the AER = 0.12 in a daily time domain with β_c = 2.00
15		114.6 times	the AER = 0.00 in a yearly time domain with β_c = 2.00
16			the AER = 0.00 in a yearly time domain with β_c = 7.90
17		13.86 times	the AER = 0.00 in a daily time domain with β_c = 7.90
18			the AER = 0.12 in a daily time domain with β_c = 7.90
19	the AER = 0.00 in a daily time domain with BETA = 2.00	57.43 times	the AER = 0.00 in a yearly time domain with β_c = 2.00
20			the AER = 0.00 in a yearly time domain with β_c = 7.90
21		7.45 times	the AER = 0.00 in a daily time domain with β_c = 7.90
22			the AER = 0.12 in a daily time domain with β_c = 7.90

	The situation in which ...			... is ...	... larger than the situation in which ...		
23	the AER = 0.12	in a daily time domain	with BETA = 2.00	57.43 times	the AER = 0.00	in a yearly time domain	with β_c = 2.00
24					the AER = 0.00	in a yearly time domain	with β_c = 7.90
25				7.45 times	the AER = 0.00	in a daily time domain	with β_c = 7.90
26					the AER = 0.12	in a daily time domain	with β_c = 7.90
27	the AER = 0.00	in a yearly time domain	with BETA = 2.00	0.13 times	the AER = 0.00	in a daily time domain	with β_c = 7.90
28					the AER = 0.12	in a daily time domain	with β_c = 7.90
29	the AER = 0.00	in a yearly time domain	with BETA = 7.90	0.13 times	the AER = 0.00	in a daily time domain	with β_c = 7.90
30					the AER = 0.12	in a daily time domain	with β_c = 7.90
31	the AER = 1.13	in a daily time domain	with no ProSorb	2.13 times	the AER = 1.13	in a daily time domain	with β_c = 2.00
32				14.83 times	the AER = 1.13	in a daily time domain	with β_c = 7.90
33	the AER = 1.13	in a daily time domain	with BETA = 2.00	6.96 times	the AER = 1.13	in a daily time domain	with β_c = 7.90
34	the AER = 0.12	in a yearly time domain	with no ProSorb	15.99 times	the AER = 0.12	in a yearly time domain	with β_c = 2.00
35					the AER = 0.12	in a yearly time domain	with β_c = 7.90
36				1.88 times	the AER = 1.33	in a yearly time domain	with β_c = 2.00
37					the AER = 1.33	in a yearly time domain	with β_c = 7.90
38	the AER = 1.33	in a yearly time domain	with no ProSorb	15.99 times	the AER = 0.12	in a yearly time domain	with β_c = 2.00
39					the AER = 0.12	in a yearly time domain	with β_c = 7.90
40				1.88 times	the AER = 1.33	in a yearly time domain	with β_c = 2.00
41					the AER = 1.33	in a yearly time domain	with β_c = 7.90
42	the AER = 1.33	in a yearly time domain	with BETA = 2.00	0.12 times	the AER = 0.12	in a yearly time domain	with β_c = 2.00
43					the AER = 0.12	in a yearly time domain	with β_c = 7.90
44	the AER = 1.33	in a yearly time domain	with BETA = 7.90		the AER = 0.12	in a yearly time domain	with β_c = 2.00
45					the AER = 0.12	in a yearly time domain	with β_c = 7.90

Recommendations for designers and consultants

The results provided in Chapter 5 can be applied in multiple situations, such as aiding the designing and curating process of a new collection in a museum. However due to the great amount of parameters studied these results are quite vast and interpreting them can be rather confusing. This section will focus on providing clear recommendations to designers and consultants involved in the display case field. All these recommendations are based in the display case situation matrix shown in Appendix 7. It is important to keep on mind, that all these recommendations are based on first, on the trends found in the results, as shown in chapter 5. Secondly, these recommendations are based on the buffering factor also shown in Chapter 5.

Investing in better conditioning system for the indoor museum environment sometimes is not the most feasible solution. Fortunately, the state of conservation of an art piece is not only based on the environment surrounding the display case. In this work it was found that there are more parameters that are easier to manipulate by the museum curator in order to stabilize the microclimate inside of a display case. Take for instance, how long does the art piece will be in display? This is the time domain studied in Chapter 5 and can only be assessed by the museum curator. Additionally, what type of display case will be used to display the art piece? This is based on the parameters inherent to the display case itself; the air exchange rate and the moisture transfer coefficient in particular, also studied in Chapter 5.

The first step when deciding how to display an object of art would be

What is the material composition of the object of art?

> As mentioned in Chapter 2, the material response of the object is of outmost importance when determining its state of conservation. Despite the fact, that in this project we chose to focus on the conditioning of the microclimate only, the object response should always be assessed thoughtfully. Due to the wide amount of materials that can be present in an object of art, the object can be simplified to its most elemental and moisture-active materials. In the literature review of this project it was found that there is an increasing effort in the academia on determining the response of different materials. Additionally, it is important to characterize the environment where the object has been present in the past. The historical average behaviour will have an impact on the material response to the environment.

Is it feasible to improve the conditioning system of the environment surrounding the display case?

> Museums all around the world have faced this question. This is based on finding the condition where all objects of art on display are sufficiently safe and the visitors comfortable at the same time. This, of course, is very difficult to find. In Chapter 3, we saw how conditioning guidelines have been developed to assess this issue, such as the ASHRAE guideline. However, guaranteeing such conditions may be unfeasible. Some museums may find that such investment is prohibitively expensive. Some other museums, may be located in historical buildings, and the restoration involved in the placement of the new conditioning unit may not be allowed. So, evaluating carefully how feasible is it to manipulate and control the environment surrounding the display case will help us in finding out the most appropriate way to display the object.

How long would this object be on display?

> The period of display of a collection may be one of the most important parameters in the conservation of an object being display, and also one of the easiest to find. The period of display of a collection is usually fixed and may depend on the lending time of certain travelling pieces. By allowing the manipulation of this parameter we could find what optimum time is the object of art under minimum risk.

What type of display case is feasible to use for this object?

> At this point, the conditioning system of the environment surrounding the display case has been found to be unfeasible. A display case is used in order to buffer the environmental load from the indoor museum environment. We saw in this project how we can characterize a display case based on the air exchange rate. Additionally, a passive display case can be further characterized by the way on how the hygroscopic material is placed inside of the display case by means of a moisture transfer coefficient. By knowing what is the material response of the object of art being display and the time of exhibition we could evaluate different display case options in order to guarantee the best display case buffering.

Once this questions have been assessed we could use the display case situation matrix to evaluate the necessary microclimate environment, based on the environment surrounding the display case, the time of exhibition and the display case characteristics. Furthermore, the necessary microclimate environment can be found in within a trend group. This means that there is going to be other combinations of parameters that will produce the same buffering (scenarios within an equivalent buffering group) which may provide a more feasible way to reach the previously determined microclimate environment. On the other hand you may also find that different levels of buffering occur within each trend group. This can serve you to find out if the improvement/investment can be justified.

Example

Take for instance, a museum located in a historical building where no possibilities of improving the indoor museum environment were possible. It was found that the indoor environment characteristics were $\Delta T = 3°C$ and $\Delta RH_{out} = 10\%$ over one day. The potential to borrow a new art piece from another museum is presented with the condition that the microclimate around such piece must be approximately ±5%RH or $\Delta RH_{in} = 5\%$ over one day. The lending period is set to be two weeks.

Since the museum indoor conditions are out of range from the requirements set by the owner of the piece, the museum is required to do something if they want to borrow and exhibit this piece. A passive display case may be used and we can use the display case situation matrix in order to evaluate its characteristics.

The options in the display case sitation matrix where at $\Delta T = 3°C$ and $\Delta RHout = 10\%$ produce a $\Delta RHin < 5\%$ are highlighted below:

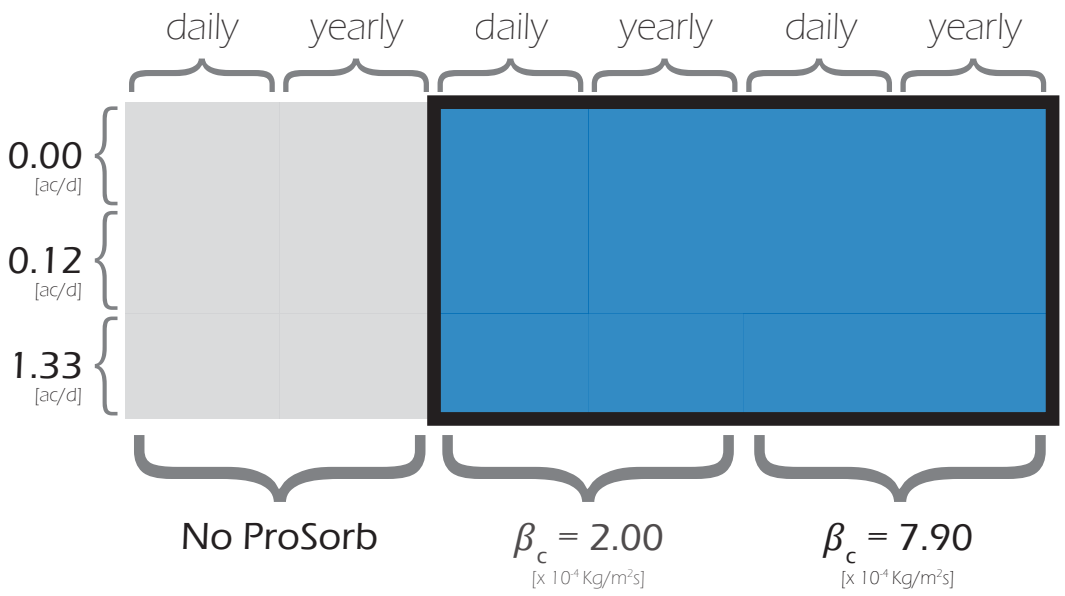

Figure 91: Places where $\Delta T = 3°C$, $\Delta RHout = 10\%$ produce a $\Delta RHin < 5\%$

This means that the display case must have hygroscopic material in order to insure the conditioning requirements. Since the borrowing time of the piece is only two weeks, we could assume the time domain would be in the daily range. This is based on the fact that in this example we are assuming that daily fluctuations are much higher than any possible fluctuation observed over one entire week. Additionally, a display case with no air exchange rate is unrealistic (its use in the display case situation matrix was solely for the purposes of comparing the other parameters without the influence of the air exchange rate. Now our options are reduced to the situations highlighted below:

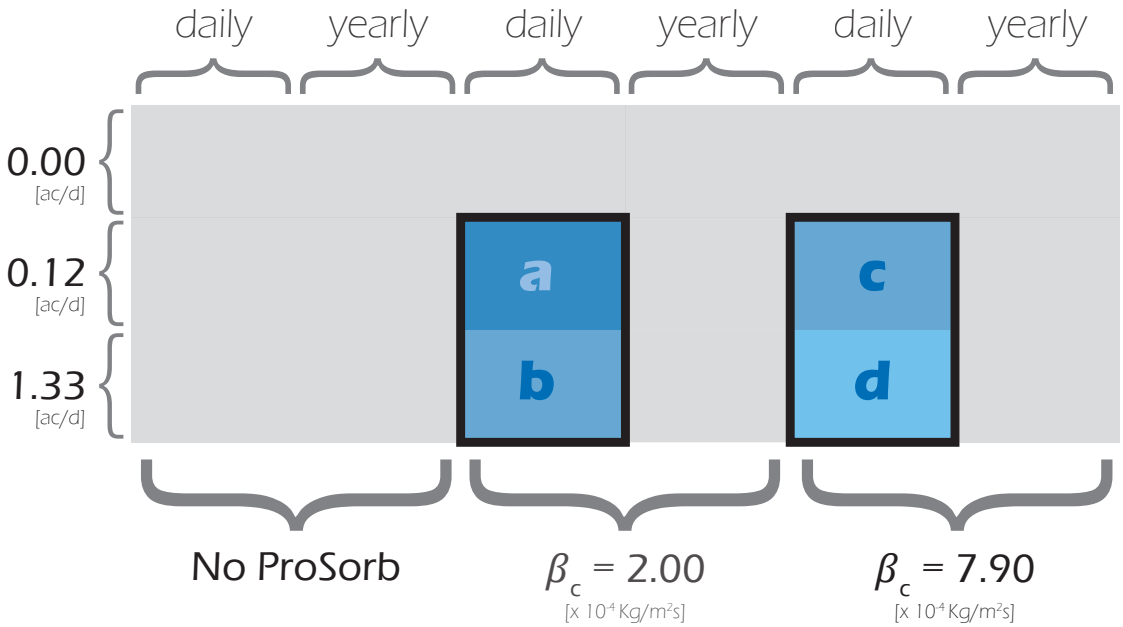

Figure 92: Options available for the museum to design their display case

Any of the four highlighted situations; options **a**, **b**, **c** and **d** would satisfied the requirements for borrowing the piece in question. Now the decision is based on what is the most appropriate investment for the museum, a display case with a lower air exchange rate or a display case with a different setup of hygroscopic material.

To define what parameter will control the characteristics of the display case we can see how much buffering occurs between each parameter. This will help us to justify the investment made for this display case. For example, let us say that we chose the museum to invest on a lower air exchange rate display case, AER = 0.12 ac/d. The question now is, what placement of hygroscopic material would we want to use? Which option, **a** or **c** should we use? By means of the buffering factor we can evaluate this. Option **a** is located in group 2 of the display case situation matrix. Option **c** is located in group 4 of the display case situation matrix. Therefore the buffering factor between these two options is 7.45. That is by using option **c** the climate inside of the display case is improved 7.45 times with respect to option **a**.

Similarly, let us say that instead of the improving the air exchange rate, the museum decided to let the air exchange be high, AER = 1.33 ac/d. The question now is, what type of display case would we want to use? One with an air exchange rate of 0.12 ac/d or 1.33 ac/d? Which option, **b** or **d** should we use? By means of the Option **b** is located in group 6 of the display case situation matrix. Option **d** is located in group 7 of the display case situation matrix. Therefore the buffering factor between these two options is 6.96. That is by using option **d** the climate inside of the display case is improved 6.96 times with respect to option **b**.

The purpose of this example is to guide the designers and museum curators on their process of deciding how to display an object. Here, it can be argued that making a new display case for the purposes of displaying an object for two weeks may seem unreasonably. However, museums usually own multiple display cases with different air exchange rates. The same process followed in this example could be used

to justify the decision between the display cases that the museum already owns.

The range of parameters may also arguably seem to be low and rather arbitrary. For example, what if the air exchange rate in my display case is neither 0.12 ac/d nor 1.33 ac/d? This is the reason for which the numerical model has been developed. Here, any value for each parameter could be studied. The main purpose of the display case situation matrix presented in Appendix 7 is to illustrate the potential the numerical model has.

Conclusion

Chapter 5 describes this sensitivity analysis. The following parameters were considered as independent.

The change in relative humidity outside of the display case

The temperature change

The air exchange rate

The time domain

The moisture transfer coefficient

The dependent parameter was the change in relative humidity inside of the display case. Numerous simulations were run in order to study the effect each parameter had on the change in relative humidity inside of the display case. The assessment of these results was divided in two parts: the evaluation of trends and the buffering effect. From all these results the change in relative humidity outside was plotted against change in relative humidity inside for all the temperature change values studied and grouped with respect to exchange rate, time domain, and moisture transfer coefficient. Within these groups we could recognize four trends: trend a when the change in relative humidity inside shows to be insensitive to the change in relative humidity outside, trend b when the behavior of the change in relative humidity inside is controlled by the change in relative humidity outside, trend c when the temperature change controls the behavior of the change in relative humidity inside, and finally trend d when the change in relative humidity inside shows to be insensitive to the temperature change.

The combination of these trends was observed across all simulation results, and only three combinations were found present; that is trend **a** and **c**, trend **a**, **b** and **c**; and finally trend **b** and **d**. Trends **a** and **c** occur when the air exchange rate is not significant for the change in relative humidity inside. Trend **a**, **b** and **c** occurs as an intermediate state where the air exchange rate starts making a significant effect on the change in relative humidity inside. The **b** trend is particularly obvious when there is no change in temperature. Trend **b** and **d** occurs when the air exchange rate is the most significant parameter and therefore, so it is the change in relative humidity outside. Here the change in temperature is quite insignificant as opposed to trend **a** and **c**.

Given the fact that the evaluations across trend groups are based on different controlling parameters, the buffering effect is only evaluated between each of the display case conditions inside the same trend group. For this, the buffering factor is defined for each display case combination. The buffering factor is a measure of how much the change in relative humidity inside of the display case is reduced (below zero) or increased (above zero) when compared to another display case situation. We can see that some display case situations present no difference at all, for example, the situation when there is no air exchange rate on a daily time domain, and the situation when the air exchange rate is 0.12 ac/d on a daily time domain with no ProSorb. This means that upgrading this display case design by reducing its air exchange rate brings no benefit when considered on a daily time base. On the other hand, we observe that certain parameters have a great influence in the buffering effect of the display case. One of these examples is in the situation when there is no air exchange rate on a daily time domain with no ProSorb and the situation when there is no air exchange rate on a yearly time domain with ProSorb with a moisture transfer coefficient of 7.90×10^{-4} Kg/m^{2}s. Here the addition of ProSorb in the yearly domain produces115 times more buffering than the daily behavior of the display case without any ProSorb. Due to these results, we can observe that the buffering mechanism of the display case does not depend on one single parameter. While controlling one parameter in a display case, we can see a decrease or a rise in performance depending on all the other assumed parameters. This set of results does provide a lot of insight and knowledge about the relationship between these parameters; this knowledge will be used to answer the research questions raised in Chapter 1.

Chapter 6: Conclusion

In Chapter 2, the museum climate was introduced. Throughout the Mecklenburg study, we were able to discover that the moisture-induced stresses in some painting materials are quite high. However, there are two more environment-related forms of failure: biological and chemical failure. Today, the development of active display cases has resulted in a very promising state of conservation, however, the disadvantages of these display cases cannot be overlooked, such as high costs and maintenance needs. Passive display cases, on the other hand, have the potential to guarantee a controlled buffered environment with lower costs and minimal maintenance. Silica gel is the most commonly used hygroscopic material in the conservation of art today.

In Chapter 3, this model is described based on the conservation of mass principle. The diffusion of moisture inside of each bead is governed by surface and Knudsen diffusion. The moisture transfer between the packed bed and the inside of the display case is based on a moisture transfer coefficient. The moisture transfer inside/outside of the display case is based on the air exchange rate (AER) of the display case.

In Chapter 4, the model validation is described. The AER experiment was based on monitoring how dry air inside of the display case reached the same level of humidity as the outside. The environment control experiments were based on monitoring the response of climate inside of the display case when exposed to daily environmental loads. The validation was based first on obtaining the AER value for the display case from the results of the AER experiments; that is AER = 1.33 ac/d. Then, the environment control experiments were used in order to estimate the moisture transfer coefficient in the display case; that is for case **b**, β_c = 2.30 x 10^{-4} Kg/m^2s, for case **c**, β_c = 9.00 x 10^{-4} Kg/m^2s, and for case **d**, β_c = 8.00 x 10^{-4} Kg/m^2s. On the other hand, case **a** of the environment control experiments contains no hygroscopic material, and therefore the AER could also be estimated from these experiments; that resulted in AER = 0.12 ac/d. There is one full order of magnitude difference between these two experiment results for AER. Since the moisture transfer coefficient was calculated assuming AER = 1.33 ac/d, these coefficients were calculated again now using AER = 0.12 ac/d. The results are nearly the same considering the uncertainty of the experiment. This means that the AER has no effect on the derivation of the moisture transfer coefficient, at least when evaluated over a daily time domain. Overall, we observed that with the newly found moisture content coefficients our model does replicate the experiment results with a significant level of accuracy.

Chapter 5 describes this sensitivity analysis. The following parameters were considered as independent.

The change in relative humidity outside of the display case

The temperature change

The air exchange rate

The time domain

The moisture transfer coefficient

The dependent parameter was the change in relative humidity inside of the display case. The assessment of these results was divided in two parts: the evaluation of trends and the buffering effect. we could recognize four trends: trend a when the change in relative humidity inside shows to be insensitive to

the change in relative humidity outside, trend b when the behavior of the change in relative humidity inside is controlled by the change in relative humidity outside, trend c when the temperature change controls the behavior of the change in relative humidity inside, and finally trend d when the change in relative humidity inside shows to be insensitive to the temperature change. The combination of these trends was observed across all simulation results, and only three combinations were found present; The buffering factor is a measure of how much the change in relative humidity inside of the display case is reduced (below zero) or increased (above zero) when compared to another display case situation. We can see that some display case situations present no difference at all. On the other hand, we observe that certain parameters have a great influence in the buffering effect of the display case. Due to these results, we can observe that the buffering mechanism of the display case does not depend on one single parameter.

Assessment of the research questions

1. What are the mechanisms that allow hygroscopic materials to maintain a specific level of humidity, and how do they differ from other materials?

We saw in Chapter 3 that the main mechanisms that allow hygroscopic materials to maintain a specific level of humidity are surface and Knudsen diffusion. Due to its porous nature and great amount of surface area, these materials can withhold a significant amount of water. Take, for instance, ProSorb, whose moisture content is 174.18 kg/m^3 when it is at 50% and 20 °C. Air at the same conditions has a moisture content of 0.86 x 10-2 kg/m^3.

2. How does a passive conditioned display case work and what parameters for the internal and external environment are assumed in order to ensure their performance?

In Chapter 3, we saw how the display case works by means of the model structure. The hygroscopic material behaves as a dual porosity model while the interaction with the space voids in the packed bed is controlled by a moisture transfer coefficient. The transfer between the packed bed and the inside air is controlled by another moisture transfer coefficient. Finally, the interaction between the inside and the outside of the display case is controlled by the air exchange rate. We saw how important the moisture transfer coefficient and air exchange rate were. The performance of the display case relies significantly on these two parameters. However, it is the combination of the change in relative humidity outside of the display case, the temperature change, the air exchange rate, the time domain and the moisture transfer coefficient that define the performance of the display case as seen in Chapter 5.

3. What is the effect of the air exchange rate of the display case on the performance of the passive conditioned display case?

In Chapter 5, we can see the actual effect of the air exchange rate in the buffering performance of the display case. Within trends ***a*** and **c**, we see that there is no significant difference between an air exchange rate of 0.12 ac/d and no air exchange rate when there is no ProSorb in the daily and yearly time domain. Air exchange rate starts becoming significant when it is 1.33 ac/d in the daily time domain, as evidenced in trends **a**, **b** and **c**. However, air exchange rate becomes most significant in trends **b** and ***d*** in the yearly domain.

4. What is the effect of the exterior climate on the performance of the passive conditioned display case?

The effect of the exterior climate is very much related to the air exchange rate. It is by means of the air exchange rate that the exterior climate enters the display case. However, the effect of the change in temperature can have an effect on the display case when no air exchange is present. Nevertheless, the air exchange rate clearly has a more dramatic effect than the temperature induced effect.

5. Can the original design of the passive conditioned display case be optimized, and if so how?

Due to the parameters studied in Chapter 5, we discover that it is not only a matter of optimizing the display case, but of understanding the conditions of the space where it is located. We recognize that there are some scenarios where a lower air exchange rate would be desirable for providing a better conditioning, however, the display case in question could be in a situation that produces no major influence for the AER. The condition where these scenarios produce no difference is shown in Table 35. The scenarios that produce some buffering is shown in Table 36 , presented in the next section.

Final remarks

The work presented in this project is based on the development of a numerical model that simulates the performance of a display case. With this model we were able to develop a display case situation matrix were five parameters were studied independently. It is here were the value of this work can be appreciated. This display case situation matrix illustrate the relevance and potential of the developed numerical model. The idea that we can map the performance of a display case based on its most relevant parameters has multiple implications for the field of conservation of art. Take for instance, its use to aid during the decision process when choosing a display case for the display of an object of art as shown in the example presented in Chapter 5 in page 83. However, there are still some significant limitations found in this project. This limitations are explained in the following section as recommendations for further research.

Recommendations for further research

Some recommendations about the experiments and the model validation were mentioned in the previous sections. However, the main recommendation for further research is to evaluate the performance of the display case on the long term, that is, in a seasonal and annual time domain. We observed in Chapter 5 that the air exchange rate becomes the most significant parameter in an annual time domain. This is important because it is in this time domain that display cases usually fail to provide protection to the art objects, as shown by Martens (2012). Further investigation and validation of our model in this time domain is encouraged.

Additionally, in this work we evaluated three different ProSorb containing scenarios, as shown in Chapter 3 in the environment control experiments. These results could pave the way for optimization of the original design of the display case, however, we recognize that further investigation about the moisture transfer coefficient is required. We could conclude from this work that the exposed surface area is an influential parameter when defining the moisture transfer coefficient. Even by only modifying this parameter we could observe significant buffering as shown in Chapter 5.

References

Achenbach, E. (1995), 'Heat and Flow Characteristics of Packed Beds', Experimental Thermal and Fluid Science 10(17 - 27).

Adan, O. C. G. (1994), 'On the fungal defacement of interior finishes', PhD thesis, Technische Universiteit Eindhoven.

Andersson, A. C. (1985), 'Verification of calculation methods for moisture transport in porous building materials, Swedish Council for Building Research', Swedish Council for Building Research Report D6:1995. Retrieved from Hagentoft (2001).

Ankersmit, B. (2009), Klimaatwerk: Richtlijnen voor het museale Binnenklimaat, Amsterdam University Press. Retrieved from Martens, M. (2012).

ASHRAE Handbook (21.1 - 21.23) (2007), American Society of Heating, Refrigerating, and Air-Conditioning Engineers.

Beuchat, L. (1987), Food and Beverage Mycology, Springer. Retrieved from Martens, M. (2012).

British Patent 396.439 (1933),. Referred to by LW Burridge in Journal of the Institute of Heating and Ventilation Engineers, 1935, 132-134. Retrieved from Shiner, J. (2007).

Brown, J. & Rose, W. B. (1997), 'Development of humidity recommendations in museums and moisture control in buildings', .

Buttler, C. (2007), Conservation Matters in Wales: On Display: Showcases and Enclosures, in 'The History of the Showcase, a Conference on Museum Microclimates'. Retrieved from Shiner, J. (2007).

China Silica Gel Co. Ltd., 'Silica Gel Basics'.

Clark, M. D. T. (2006), 'Paints and pigments', .

Erhardt, D.; Tumosa, C. S. & Mecklenburg, M. F. (2007), Applying science to the question of museum climate, in 'Museum Microclimates', pp. 11–18.

Eqn.1: Silicon Dioxide, Audiopedia'.

GeeJay Chemicals Ltd., 'What is silica gel?', .

Hagentoft, C.E. (2001), 'HAMSTAD- WP 2 Modelling: Determination of liquid water transfer properties of porous building materials and development of numerical assesment methods', Chalmers University of Technology Report R-02:9.

International Silica Gel Co.Ltd, 'Silica gel blue (Color change from blue to pink)'.

Kozlowski (2007), 'Climate-Induced Damage of Wood: Numerical Modeling and Direct Tracing', The Getty Conservation Institute. Retrieved from Martens, M. (2012).

Kruckels, W. W. (1973), 'On Gradient Dependent Diffusivity', Chemical Engineering Science 28(1565 - 1576). Retrieved from Martens, M. (2012). Retrieved from Pesaran and Mills (1986)

Krus, M.; Kilian, R. & Sedlbauer, K. (2007), Mould growth prediction by computational simulation on historic buildings, in 'Museum Microclimates', pp. 185–189.

Lord, G. & Lord, B. (1999), The Manual of Museum Planning, Stationery Office. Retrieved from Martens, M. (2012).

Martens, M. (2012), 'Climate risk assessment in museums : degradation risks determined from temperature and relative humidity data', PhD thesis, Technische Universiteit Eindhoven.

Mathworks (), 'ode23tb: Algorithms', .

Mecklenburg, M. F. (2007), Micro Climates and Moisture Induced Damage to Paintings, in 'Museum Microclimates', pp. 19–25.

Michalski, S. (1993), Relative humidity: a discussion of correct/incorrect values, in 'ICOM Committee for Conservation tenth triennial meeting', pp. 624 - 629. Retrieved from Martens, M. (2012).

National Park Service, P. M. M. P. (2001), 'Cobalt Indicating Silica Gel Health and Safety Update', Conserve O Gram 12(2).

Pesaran, A.; Mills, A.; Institute, S. E. R. & of Energy, U. S. D. (1986), Moisture Transport in Silica Gel Packed Beds: Theoretical study. I, Solar Energy Research Institute.

Pesaran, A.; Mills, A.; Institute, S. E. R. & of Energy, U. S. D. (1986), Moisture Transport in Silica Gel Packed Beds: Experimental study. II, Solar Energy Research Institute.

Primary Information Services, 'Silica Gel'.

Richard, M. (2007), The benefits and disadvantages of adding silica gel to microclimate packages for panel paintings, in 'Museum Microclimates', pp. 237–243.

Saitzyk, S. (1987), 'Sizing Painting Surfaces: ART HARDWARE: The Definitive Guide to Artists' Materials', .

Sherwood, T.; Pigford, R. & Wilke, C. (1975), Mass transfer, McGraw-Hill.

Shiner, J. (2007), Trends in microclimate control of display cases, in 'Museum Microclimates', pp. 267–275.

Silica Gel Dessicants (2015), 'Orange indicating silica gel'.

Sladek, K. J.; Gilliland, E. R. & Baddour, R. F. (1974), 'Diffusion on Surfaces. II: Correlation of Diffusivities of Physically and Chemically Adsorbed Species,', Industrial & Engineering Chemistry Fundamentals 13(2), 100 - 105. Retrieved from Pesaran and Mills (1986)

Thickett, D.; Fletcher, P.; Calver, A. & Lambarth, S. (2007), The effect of air tightness on RH buffering and control, in 'Museum Microclimates', pp. 245–251.

Toledo, F. (2007), 'Museum Passive Buildings in Warm, Humid Climates', The Getty Conservation Institute.

Urbani, G.Price, N.; Talley, M. & Vaccaro, A., ed., (1981), Historical and Philosophical Issues in the Conservation of Cultural Heritage, Getty Conservation Institute, pp. 445-450.

Waller, C. (), 'Long Life for Art: ProSorb Humidity Stabilizer', .

Watts, S.; Crombie, D.; Jones, S. & Yates, S. A. (2007), Museum showcases: specification and reality, costs and benefits, in 'Museum Microclimates', pp. 253–260.

Westfield, M.; Ortega, R. I. & Conrad, E. A. (1996), 'What Made Lucy Rot? A Case Study of Cyclical Moisture Absorption', APT Bulletin 27(3), 31–36. Retrieved from Martens, M. (2012).

Young, B. (1938), 'Copies of his original notes courtesy of Will Jeffers, Boston Museum of Fine Arts, 2006.', Retrieved from Shiner, J. (2007).

Yu, D.; Klein, S. A. & Reindl, D. T. (2001), 'An Evaluation of Silica Gel for Humidity Control in Display Cases', Western Association for Art Conservation Newsletter 23(2).

List of figures

List of tables

Appendix 1 : The Matlab code

```
% model of air flow through a bed of hygroscopic material

clear all

start_time = 0;
end_time   = 2*365*86400;

load Pres_1995_double;

% tube geometry, conditions and material parameters
      R_v                     = 462;
      V_v                     = 0.000863376;
      l_bed                   = V_v/(n_bed*m_bed);
      V_case                  = 0.656*0.727*0.094;
      A_bed                   = m_bed*n_bed;
      R_sp                    = 0.001;
      d_sg                    = 1e-9;
      e_bed                   = 0.64;
      A_z                     = e_bed*A_bed;
      d_air                   = 2.4e-5;
      t_bed                   = e_bed^-0.4;
      beta_c_g                = 0.024;
      f_flow_gel              = 0;
      beta_out                = 0;
      loss_coef               = 1.33*V_case/86400;
      beta_in                 = 0.5;

% start moisture content in all free nodes air system
c1_sorp                        = 510;
c2_sorp                        = -81;
a_sorp                    = 0.0172/c1_sorp;
b_sorp                    = -0.0172/c1_sorp*c2_sorp;
W_init_a = 0.008606;
W_init_g = W_init_a/a_sorp-b_sorp/a_sorp;


% defining the nodes and control volumes

 % (free) nodes along the tube;
I=6;

% (free) nodes along the depth of the hygroscopic material (perpendicular to
tube), excluding air
J=4;

% number of bound nodes air system
nnb_a = 1;

% number of free nodes air system in bed (excludes node in display case)
nnf_a =  I;

% total number of  nodes air system
nnt_a = nnb_a + nnf_a + 1;

% number of bound nodes gel system
nnb_g = 0;

% number of free nodes gel system
nnf_g =  I*J;

% total number of  nodes gel system
nnt_g = nnb_g + nnf_g;

% distance between nodes inside the hygroscopic material
d_0 = (R_sp)/(J-1);

% distance between nodes inside the hygroscopic material (z-direction)
d_z = l_bed/(I);

% length of effective hygroscopic material facing its respective air node
(z-direction)
l_r = l_bed/(I);
```

```
% effective area of hygroscopic material facing its respective air node
A_r = 3*(1-e_bed)*A_bed*l_r/R_sp;

% nr of  beads in node
nr_beads = A_r/(4*pi*R_sp^2);

%definition of mass matrix
M_a=zeros(nnf_a+1);

%air nodes
for j=1:1
  for i=1:I
          x=i;
          y=i;
          M_a(x,y)=A_z*l_r;
  end
end
M_a(nnf_a+1,nnf_a+1) = V_case;

M_g=zeros(nnf_g);
%nodes in the hygroscopic material
for j=1:J
          for i=1:I
            x=I*(j-1)+i;
            y=I*(j-1)+i;

          if j==1
          M_g(x,y)= nr_beads*(4/3)*pi*(R_sp^3-(R_sp-(d_0/2))^3);

          elseif j==J
          M_g(x,y)= nr_beads*(4/3)*pi*((d_0/2)^3);

% input of vectors connecting air and gel system
L_a_a=zeros(nnf_a+1,nnf_a+1);
L_a_g=zeros(nnf_a+1,nnf_g);
L_a_c=zeros(nnf_a+1,1);

L_g_a=zeros(nnf_g,nnf_a+1);
L_g_g=zeros(nnf_g,nnf_g);
L_g_c=zeros(nnf_g,1);

      for i=1:nnf_a
          L_a_a(i,i)=beta_c_g*A_r;
          L_a_g(i,i)=-beta_c_g*A_r;
          L_a_c(i,1)=-beta_c_g*A_r;
          L_g_a(i,i)=beta_c_g*A_r;
          L_g_g(i,i)=-beta_c_g*A_r;
          L_g_c(i,1)=-beta_c_g*A_r;

      end

% pre-input for stiffness matrix
Y_a=zeros(nnt_a);
Y_a_c1=zeros(nnt_a);
Y_a_c2=zeros(nnt_a);


%transfer between air in bed and the environment
Y_a(I,nnf_a+1)= beta_in*A_z;
Y_a(1,nnf_a+2)= beta_out*A_z;

% loop for nodes in the air in the bed
      for i = 1:I-1;
      Y_a(i,i+1)  = ((d_air*e_bed*A_z)/(t_bed*d_z));
      end

%direct coupling due to diffusive losses between display case and outside
Y_a(nnf_a+1,nnf_a+2) = loss_coef;

Y_g=zeros(nnt_g);
for j=1:J-1
    for i=1:I
        node_nr1=I*(j-1)+i;
        node_nr2=I*j+i;
        Y_g(node_nr1,node_nr2)= nr_beads*(d_sg*4*pi*(R_sp-(d_0*(j)+d_0/2))^2)/d_0;
    end
end

% create empty initial stiffness matrix with nnt rows and columns
Si_a = zeros(nnt_a);
Si_a_c1 = zeros(nnt_a);
Si_a_c2 = zeros(nnt_a);
Si_a_c3 = zeros(nnt_a);
Si_a_c4 = zeros(nnt_a);
Si_g = zeros(nnt_g);

for i=1:nnt_a-1
```

```
   for j=i+1:nnt_a
      if Y_a(i,j) ~= 0
          Si_a=fillS(Si_a,Y_a,i,j);  %subroutine is in fillS.m
      end
   end
end

S_a = Si_a(1:nnf_a+1,1:nnf_a+1);
S_a_bound = Si_a(1:nnf_a+1,nnf_a+1+1:nnt_a);

for i=1:nnt_g-1
   for j=i+1:nnt_g
      if Y_g(i,j) ~= 0
          Si_g=fillS(Si_g,Y_g,i,j);  %subroutine is in fillS.m
      end
   end
end

S_g = Si_g(1:nnf_g,1:nnf_g);

%constant part of stifness matrix, advection in air phase packed bed from outside
to display case
Y_a_c1(1,nnf_a+2) = -1*1i;
 for i = 1:I-1;
        Y_a_c1(i,i+1)  = 1*1i;
 end
Y_a_c1(I,nnf_a+1)= 1*1i;

%constant part of stifness matrix, advection in air phase packed be from display
case to outside
Y_a_c2(1,nnf_a+2) = 1*1i;
 for i = 1:I-1;
        Y_a_c2(i,i+1)  = -1*1i;
 end
Y_a_c2(I,nnf_a+1)= -1*1i;

% fill initial stiffness matrix for part 1 with values
% constants in the variable part of the stiffness matrix
for i=1:nnt_a-1
   for j=i+1:nnt_a
      if Y_a_c1(i,j) ~= 0
         Si_a_c1=fillS(Si_a_c1,Y_a_c1,i,j);  %subroutine in fillS.m
      end
   end
end

% definition of stiffness matrix for part 1, to be used in the Simulink model
S_a_c1 = Si_a_c1(1:nnt_a-nnb_a,:);

%correction, for flow into the case, there is no loss of moisture from the case,
S_a_c1(nnf_a+1,nnf_a+1) = 0;

% fill initial stiffness matrix for part 2 with values
% constants in the variable part of the stiffness matrix
for i=1:nnt_a-1
   for j=i+1:nnt_a
      if Y_a_c2(i,j) ~= 0
        Si_a_c2=fillS(Si_a_c2,Y_a_c2,i,j);  %subroutine in fillS.m
      end
   end
end

% definition of stiffness matrix for part 1, to be used in the Simulink model
S_a_c2 = Si_a_c2(1:nnt_a-nnb_a,:);


%correction, for flow out the case, there is loss of moisture from the case, so:
S_a_c2(nnf_a+1,nnf_a+1) = 1;

%constant part of stifness matrix, flow from outside directly to display case
Y_a_c3(nnf_a+1,nnf_a+2)= -1*1i;

%constant part of stifness matrix, flow from display case directly to outsidee
Y_a_c4(nnf_a+1,nnf_a+2)= 1*1i;

% fill initial stiffness matrix for part 3 with values
% constants in the variable part of the stiffness matrix
for i=1:nnt_a-1
   for j=i+1:nnt_a
      if Y_a_c3(i,j) ~= 0
         Si_a_c3=fillS(Si_a_c3,Y_a_c3,i,j);  %subroutine in fillS.m
      end
   end
end

% definition of stiffness matrix for part 3, to be used in the Simulink model
S_a_c3 = Si_a_c3(1:nnt_a-nnb_a,:);
```

```
%correction, for flow into the case, there is no loss of moisture from the case,
so:
S_a_c3(nnf_a+1,nnf_a+1) = 0;



% fill initial stiffness matrix for part 4 with values
% constants in the variable part of the stiffness matrix
for i=1:nnt_a-1
   for j=i+1:nnt_a
      if Y_a_c4(i,j) ~= 0
        Si_a_c4=fillS(Si_a_c4,Y_a_c4,i,j);  %subroutine in fillS.m
      end
   end
end

% definition of stiffness matrix for part 1, to be used in the Simulink model
S_a_c4 = Si_a_c4(1:nnt_a-nnb_a,:);

%correction, for flow out the case, there is loss of moisture from the case, so:
S_a_c4(nnf_a+1,nnf_a+1) = 1;
```

Appendix 2: The Equipment

The data logger

The RX250AL, Figure 93, Receiver/logger from Eltek was used for the environment control experiments. It was selected because it can be used with wireless sensors/transmitters; this is particularly useful since any alteration made to the display case (such as holes for cables) would modify the air exchange rate. The main function of this logger is to store and receive data from the transmitters. It has a built in battery to ensure reliability, and has one megabyte for digital storage. In order to access the logger system the Darca software was used. This software allowed the the logger to be configured from an external computer; furthermore, this software was used to access and download the logged data. Find in the next page, Table 37, the specifications of the RX250AL:

Figure 93: RX250AL Logger

Table 37: Specifications of the RX250AL Logger

Number of channels:	Up to 250
Number of transmitters:	Up to 125
Ambient temperature:	-10 to +55°C
Humidity:	Up to 95% (non condensing)
Power supply:	12V DC at 500mA powered using type MP12U, (input 100-250V AC)
Built-in batteries:	6 x AA Ni Mh battery
Backup battery life:	Typically 24 hours

Memory:	247,000 readings expandable to 2,000,000
Clock accuracy:	1 second/day at 20°C
Dimensions:	D 60mm x W 180mm x H 120mm
Weight:	1Kg inc. batteries
Case material:	Scratch resistant Nextel coated ABS
PC/modem interface:	RS232C up to 38.4K Baud
Receiver:	Crystal controlled
Sensitivity:	UHF: -117dBm
Antenna connector:	SMA 50 ohm female
Antenna:	Quarter wave standard, lightweight dipole optional
Communication options:	USB, GSM and Ethernet
Alarm:	RX250AL: SMS + 1 contact closure, RX250ALD: SMS + 2 contact closures

The sensors

GC10

The GC10 sensor, Figure 94, was used for the environment control experiments. This is particularly helpful since the sensor is built into the transmitter, which allows for this single piece of equipment to be used for both collecting the data and transmitting it to the RX250AL logger. The specifications, Table 38, and accuracy, Table 39, of the GC10 can be found below:

Figure 94: GC10 sensor

Table 38: Specifications of the GC10 sensor

RF specification:	EN300-220
RF power:	10mW
Environment specification	
Compliant to EN300-220:	-10 to +55°C
Actual:	-30 to +65°C
Humidity:	100% non condensing
Environmental rating:	IP40
Dimensions (footprint):	78 x 41mm

Battery endurance:	up to 5 years (interval set to 5 minutes) (less for GL-70 and GS40 series)
Transmission interval range:	1 sec to 4 hours
Indicator (red LED):	transmit active/on/off
Control switch (concealed):	test mode / hibernate
Antenna socket:	SMA

Table 39: Accuracy of the GC10 sensor

Model	Sensors	Range	Resolution	Accuracy
GC10	built-in temperature	-30 to 65°C	0.1°C	±0.4°C (+5 to +40°C) ±1.0°C (-20 to +80°C)
	built-in RH	0-100%	0.10%	±2% (10 to 90%RH) ±4% (0 to 100%RH)

HOBO – U12-012

The HOBO U12-012 sensor, Figure 95, was used for the AER experiments. This sensor has a built-in logger which is particularly helpful since there are no cables going in-out of the display case that may affect the AER measurements. However , different from the RX250-GC10 for the HOBO – U12-012, the data cannot be accessed until the experiment has been performed and disassembled since there are no data transmitters. The specifications, Table 40, of the HOBO U12-012 can be found below:

Figure 95: Accuracy of the GC10 sensor

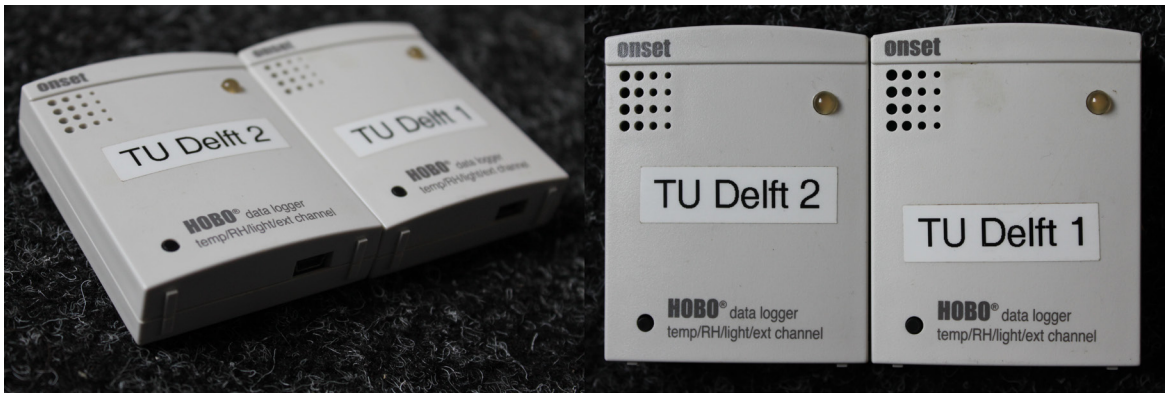

Table 40: Specifications of the HOBO U12-012 sensor

Measurement range:	Temperature:	-20° to 70°C (-4° to 158°F)
	RH:	5% to 95% RH
	Light intensity:	1 to 3000 footcandles (lumens/ft2) typical; maximum value varies from 1500 to 4500 footcandles (lumens/ft2)
	Analog channels:	0 to 2.5 Vdc (w/CABLE-2.5-STEREO); 0 to 5 Vdc (w/ CABLE-ADAP5); 0 to 10 Vdc (w/ CABLE-ADAP10); 4-20 mA (w/CABLE-4-20MA)

Accuracy:	Temperature:	± 0.35°C from 0° to 50°C (± 0.63°F from 32° to 122°F)
	RH:	±2.5% from 10% to 90% RH (typical), to a maximum of ±3.5%
	Light intensity:	Designed for indoor measurement of relative light levels
	External input channel (see sensor manual):	± 2 mV ± 2.5% of absolute reading
Resolution:	Temperature:	0.03°C at 25°C (0.05°F at 77°F)
	RH:	0.03% RH
Sample Rate:	1 second to 18 hours, user selectable	
Drift:	Temperature:	0.1°C/year (0.2°F/year)
	RH:	<1% per year typical; RH hysteresis 1%
Response time in airflow of 1 m/s (2.2 mph):	Temperature:	6 minutes, typical to 90%
	RH:	1 minute, typical to 90%
Time accuracy:	± 1 minute per month at 25°C (77°F)	
Operating temperature:	Logging:	-20° to 70°C (-4° to 158°F); 0 to 95% RH (non-condensing)
	Launch/readout:	0° to 50°C (32° to 122°F), per USB specification
Battery life:	1 year typical use	
Memory:	64K bytes (43,000 12-bit measurements)	
Weight:	46 g (1.6 oz)	
Dimensions:	58 x 74 x 22 mm (2.3 x 2.9 x 0.9 inches)	

Display case drawings

printdatum: 03.05.2013

GLASCOM MUSEUM
GLASSOLUTIONS
SAINT-GOBAIN

ordernummer: 130330

werk: Stedelijk museum Amsterdam

deel: Mondriaan vitrine

Opdrachtgever:

Saint Gobain Glass Solutions
Glascom Museum Presentations
Postbus 1521, 3800 GG Amersfoort
Lindenboomseweg 53, 3825 AL Amersfoort
tel: 033-4502 890
fax: 033-4502 899
E-mail: gmp@saint-gobain.com
www.glascom.eu

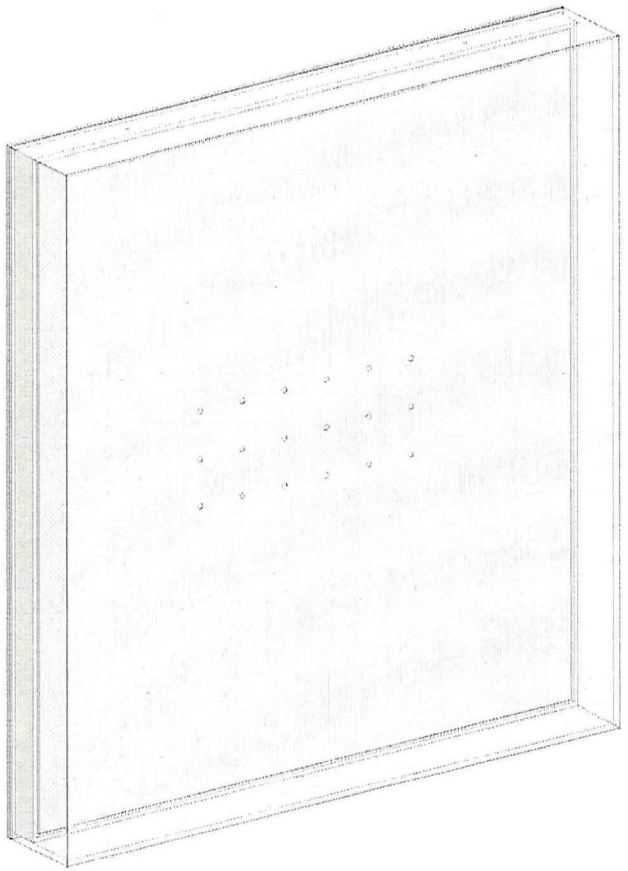

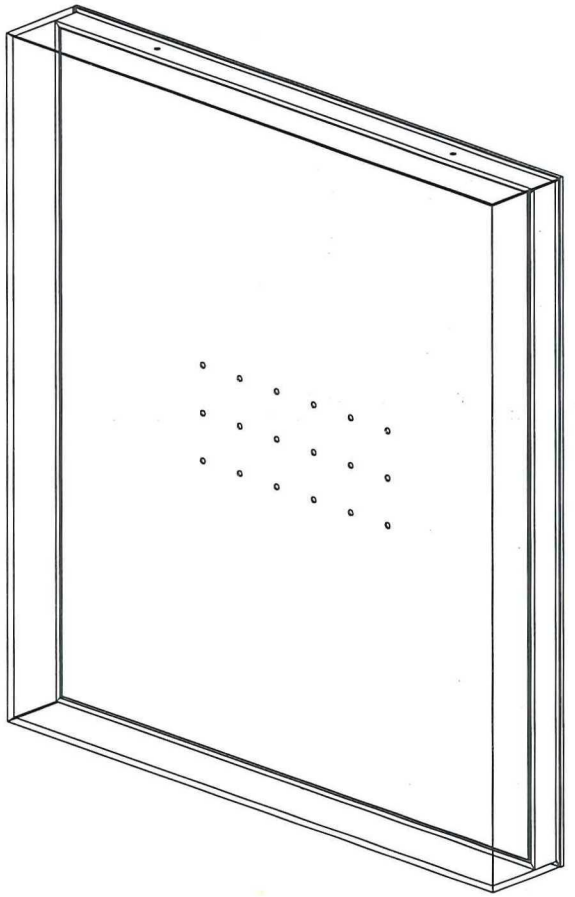

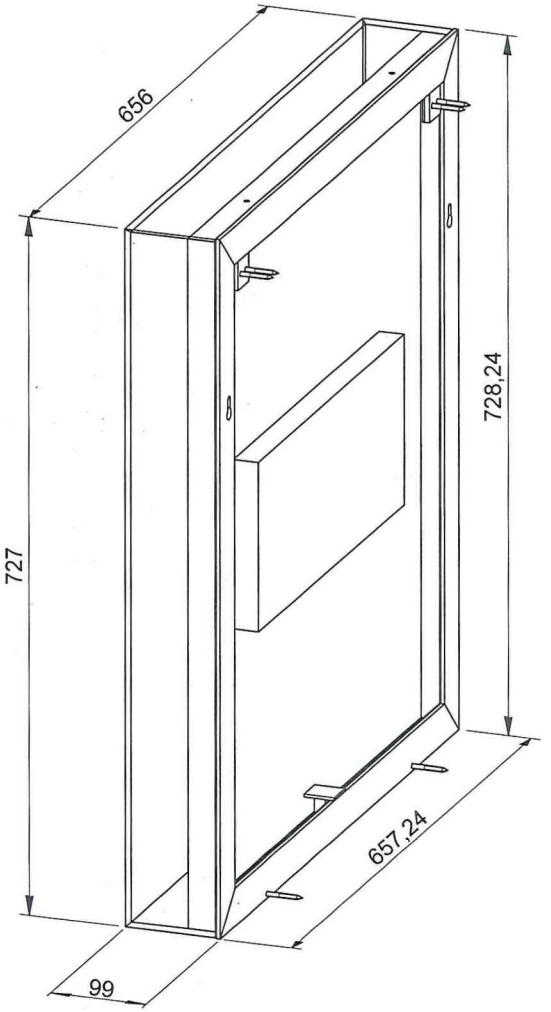

omschrijving:

Glas: clear lite 22.1
Stalen omranding kleur: RAL 9010 90% mat
stalen achterpaneel kleur: RAL 9010 90% mat
Absorptiemateriaal: ArtSorb cassette

isometrische aanzichten

werk: Stedelijk Museum te Amsterdam onderdeel: Mondriaanvitrine aanzicht en doorsneden	SCHAAL : 1 : 5 DATUM : 27-03-2013 GEW. : 03-05-2013 GEW. : GEW. : ORDERNR.: 130303 BLADNR. : 01-A AUTEURSRECHTEN VOORBEHOUDEN	GLASCOM MUSEUM GLASSOLUTIONS SAINT-GOBAIN Lindeboomseweg 53 3825 AL AMERSFOORT Postbus 1521 3800 GG AMERSFOORT Tel.: +31(0) 33 4502 830 Fax.: +31(0) 33 4502 859

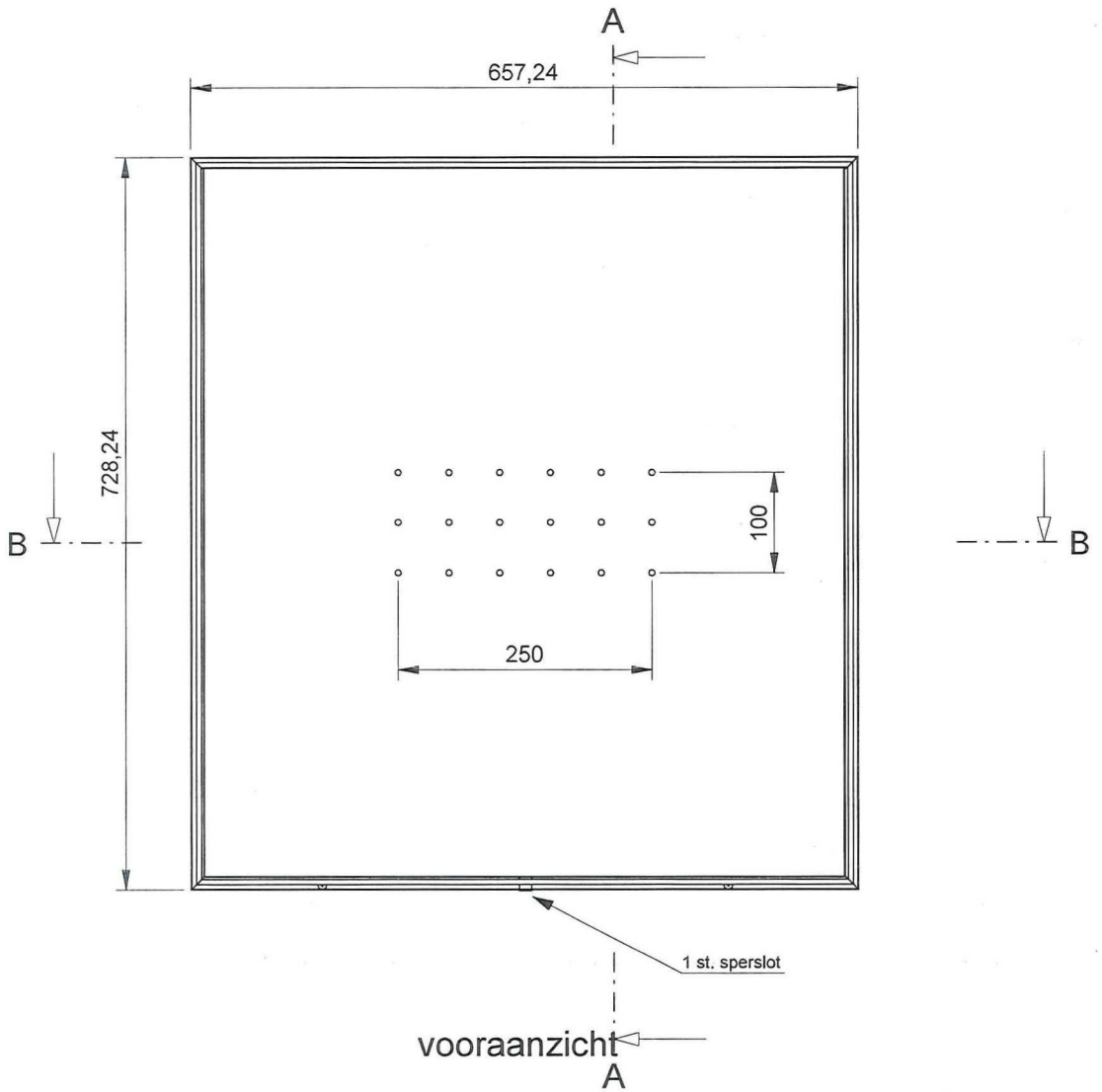

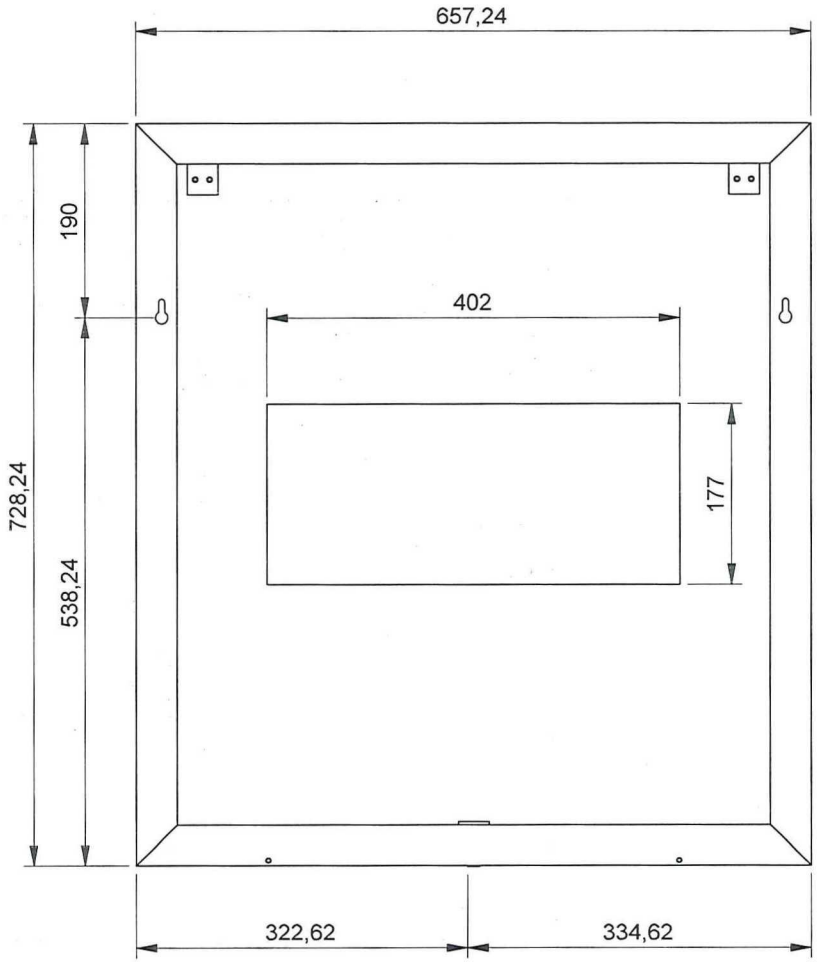

achteraanzicht

werk: Stedelijk Museum te Amsterdam onderdeel: Mondriaanvitrine aanzicht en doorsneden	SCHAAL : 1 : 5 DATUM : 27-03-2013 GEW. : 03-05-2013 GEW. : GEW. : ORDERNR.: 130303 BLADNR. : 01-B AUTEURSRECHTEN VOORBEHOUDEN	GLASCOM MUSEUM GLASSOLUTIONS SAINT-GOBAIN Lindeboomseweg 53 3825 AL AMERSFOORT Postbus 1521 3800 GG AMERSFOORT Tel.: +31(0) 33 4502 830 Fax.: +31(0) 33 4502 859

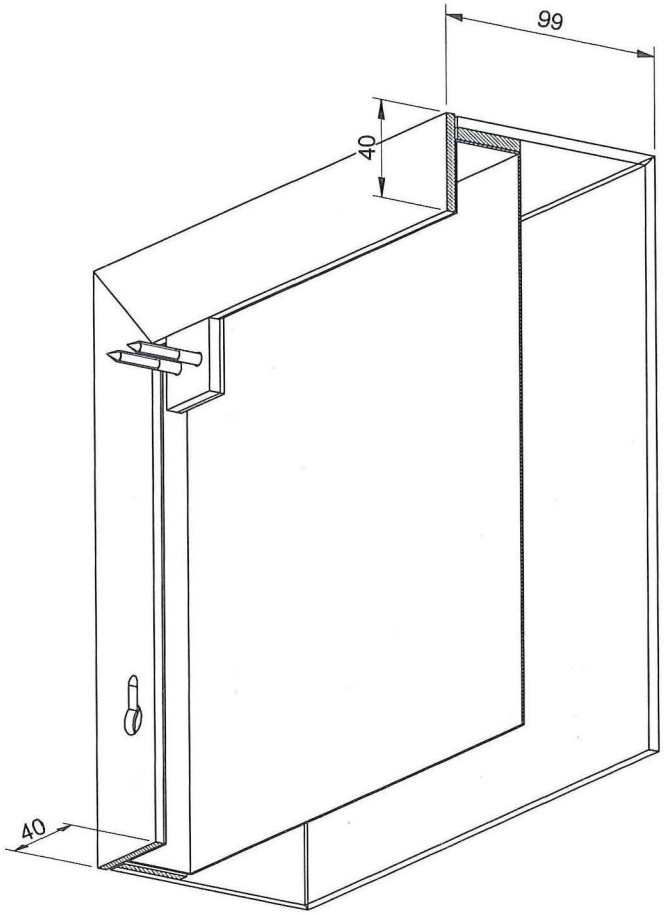

hoekdetail boven

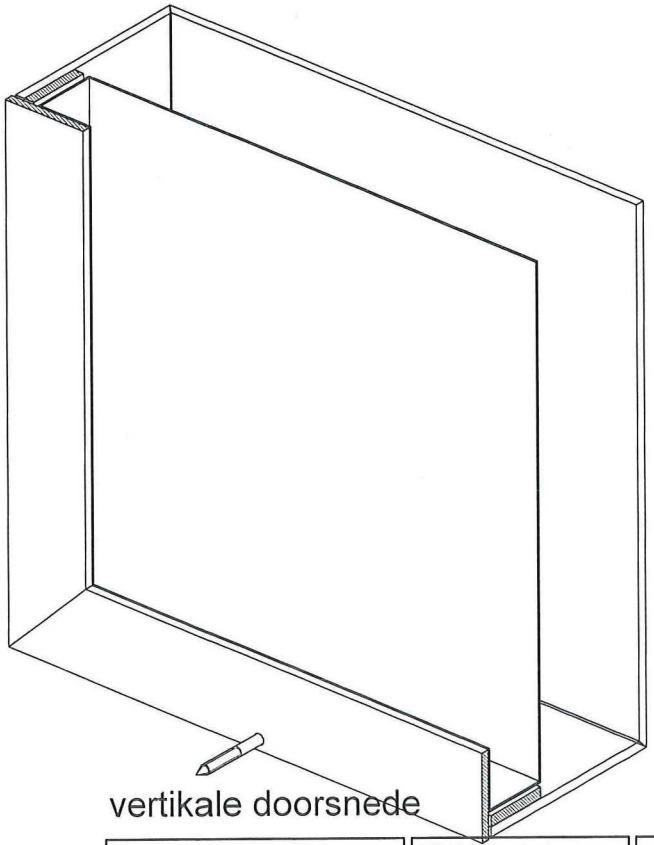

hoekdetail onder

vertikale doorsnede

werk: Stedelijk Museum te Amsterdam onderdeel: Mondriaanvitrine aanzicht en doorsneden	SCHAAL : 1 : 1 DATUM : 27-03-2013 GEW. : 03-05-2013 GEW. : GEW. : ORDERNR.: 130303 BLADNR. : 01-C AUTEURSRECHTEN VOORBEHOUDEN	GLASCOM MUSEUM GLASSOLUTIONS SAINT-GOBAIN Lindeboomseweg 53 3825 AL AMERSFOORT Postbus 1521 3800 GG AMERSFOORT Tel.: +31(0) 33 4502 830 Fax.: +31(0) 33 4502 859

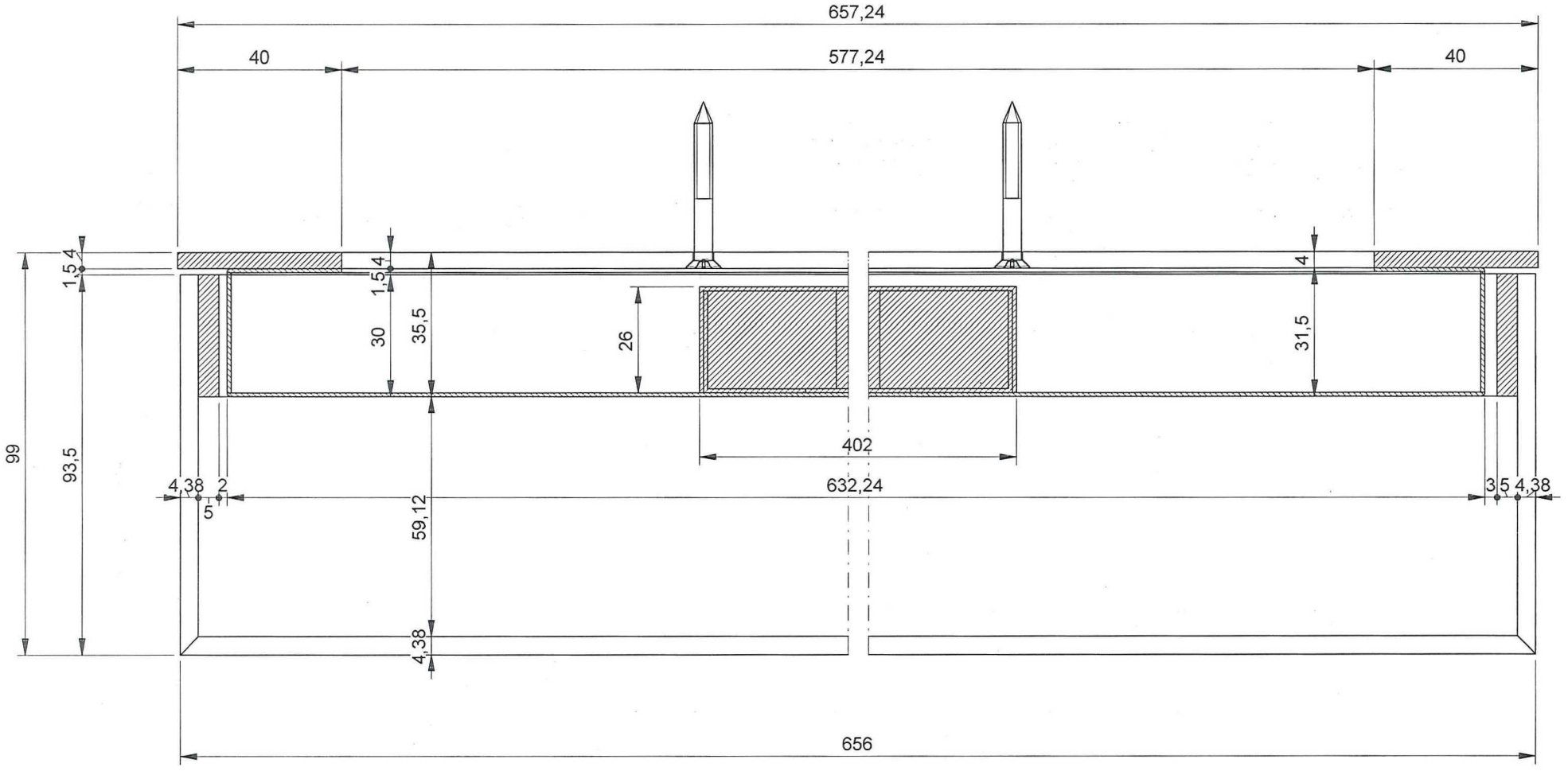

horizontale doorsnede

werk: Stedelijk Museum te Amsterdam	SCHAAL : 1 : 1 DATUM : 03-05-2013 GEW. : GEW. : GEW. :	GLASCOM MUSEUM GLASSOLUTIONS SAINT-GOBAIN
onderdeel: Mondriaanvitrine	ORDERNR.: 130303 BLADNR. : 01-D	
aanzicht en doorsneden	AUTEURSRECHTEN VOORBEHOUDEN	

Lindeboomseweg 53 3825 AL AMERSFOORT
Postbus 1521 3800 GG AMERSFOORT
Tel.: +31(0) 33 4502 830 Fax.: +31(0) 33 4502 859

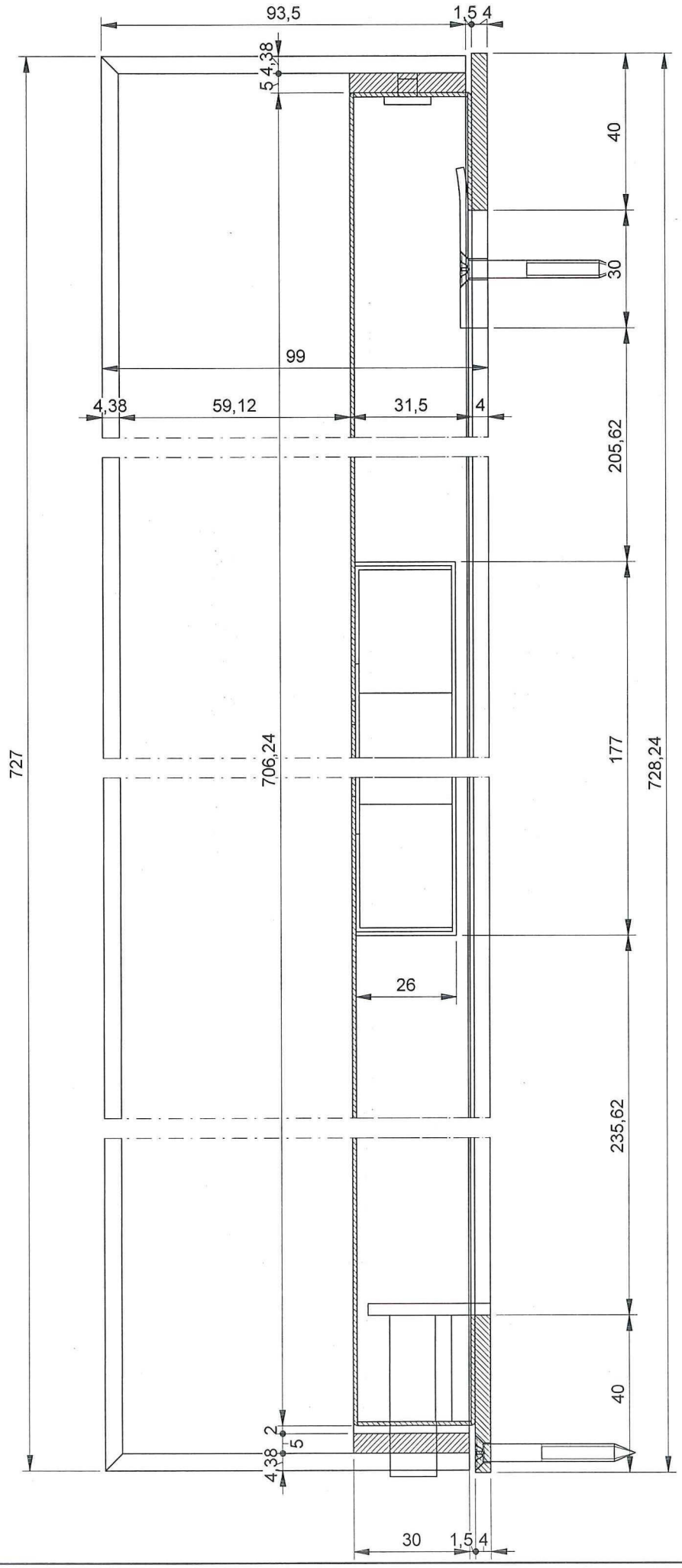

vertikale doorsnede

SCHAAL : 1 : 1
DATUM : 03-05-2013
GEW. :
GEW. :
GEW. :

ORDERNR.: 130303
BLADNR. : 01-E

AUTEURSRECHTEN VOORBEHOUDEN

werk: Stedelijk Museum
te Amsterdam

onderdeel: Mondriaanvitrine

aanzicht en doorsneden

GLASCOM MUSEUM
GLASSOLUTIONS
SAINT-GOBAIN

Lindeboomseweg 53 3825 AL AMERSFOORT
Postbus 1521 3800 GG AMERSFOORT
Tel.: +31(0) 33 4502 830 Fax.: +31(0) 33 4502 859

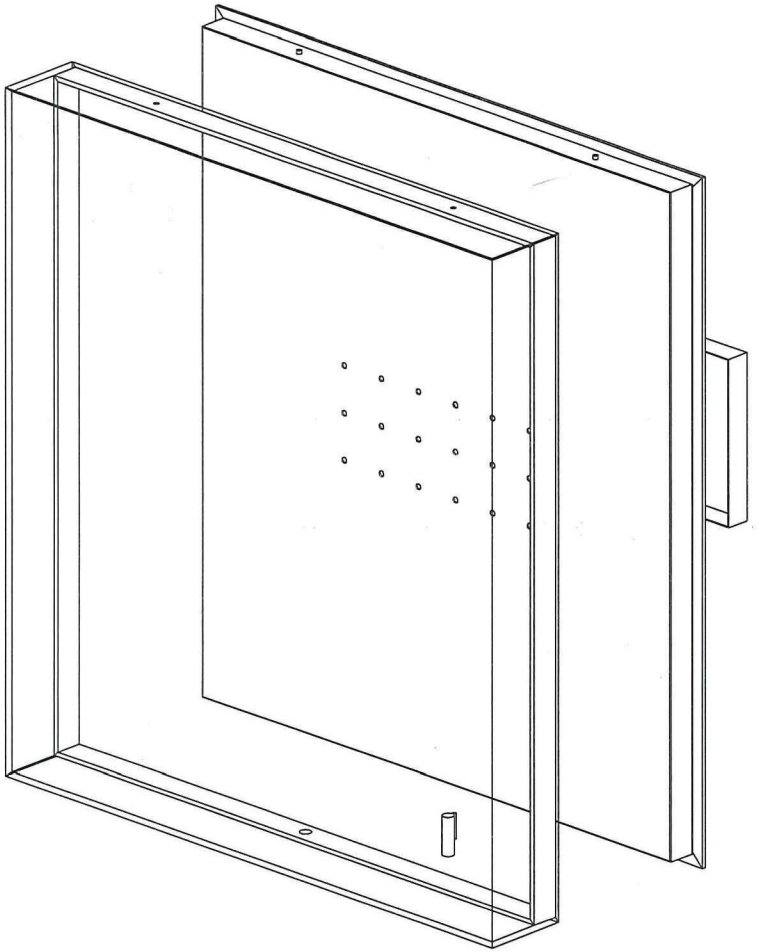

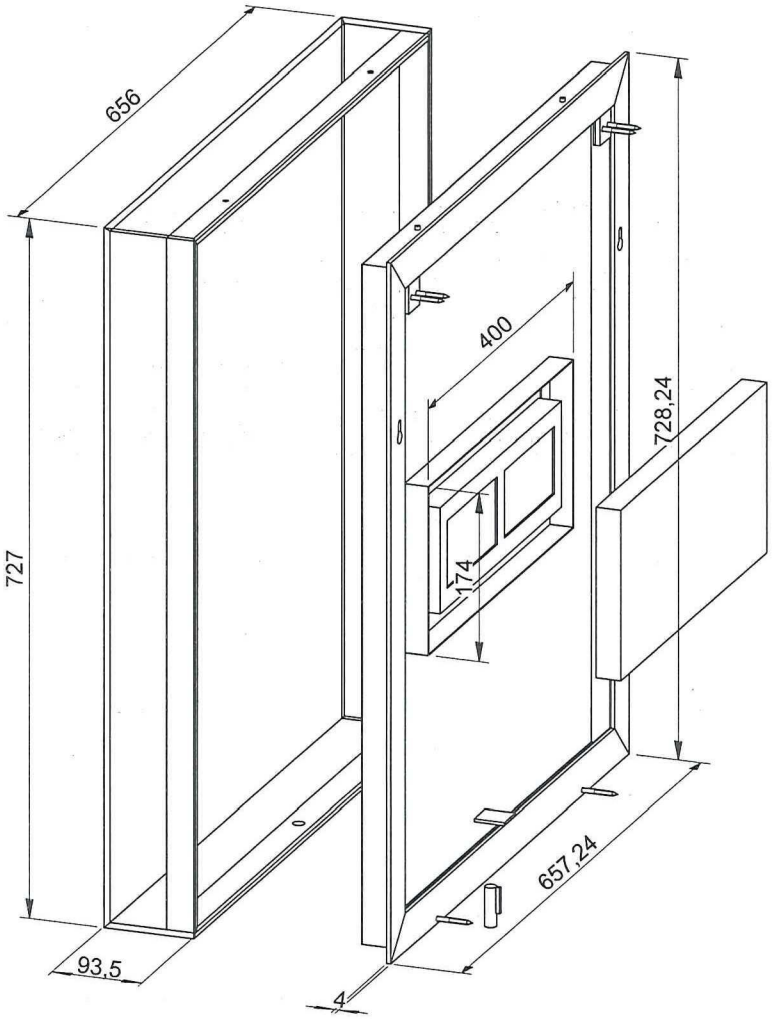

omschrijving:

Glas: clear lite 22.1
Stalen omranding kleur: RAL 9010 90% mat
stalen achterpaneel kleur: RAL 9010 90% mat
Absorptiemateriaal: ArtSorb cassette

isometrische aanzichten

werk: Stedelijk Museum te Amsterdam onderdeel: Mondriaanvitrine aanzicht en doorsneden	SCHAAL : 1 : 5 DATUM : 03-05-2013 GEW. : GEW. : GEW. : ORDERNR.: 130303 BLADNR. : 02 AUTEURSRECHTEN VOORBEHOUDEN	GLASCOM MUSEUM GLASSOLUTIONS SAINT-GOBAIN Lindeboomseweg 53 3825 AL AMERSFOORT Postbus 1521 3800 GG AMERSFOORT Tel.: +31(0) 33 4502 830 Fax.: +31(0) 33 4502 859

Appendix 3: AER experiments results

Sensor inside of the display case

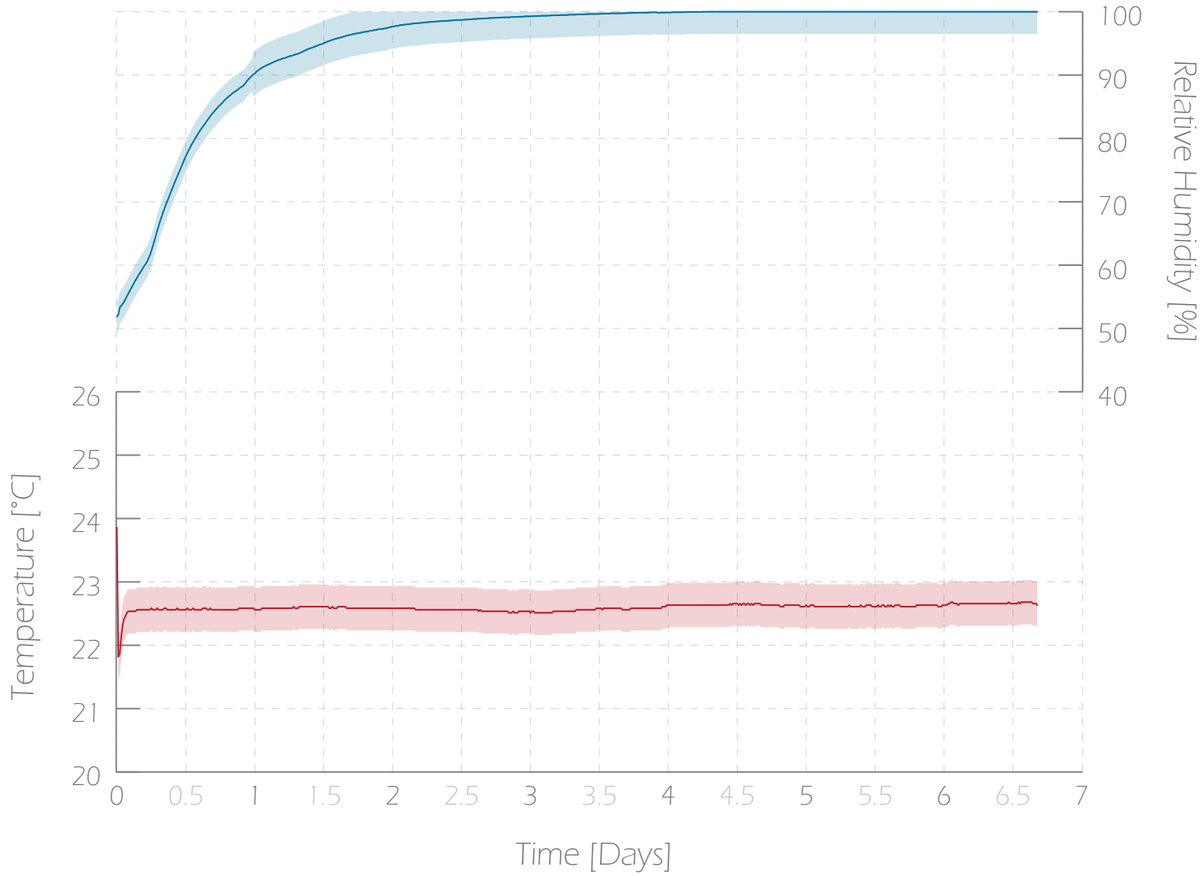

Sensor outside of the display case

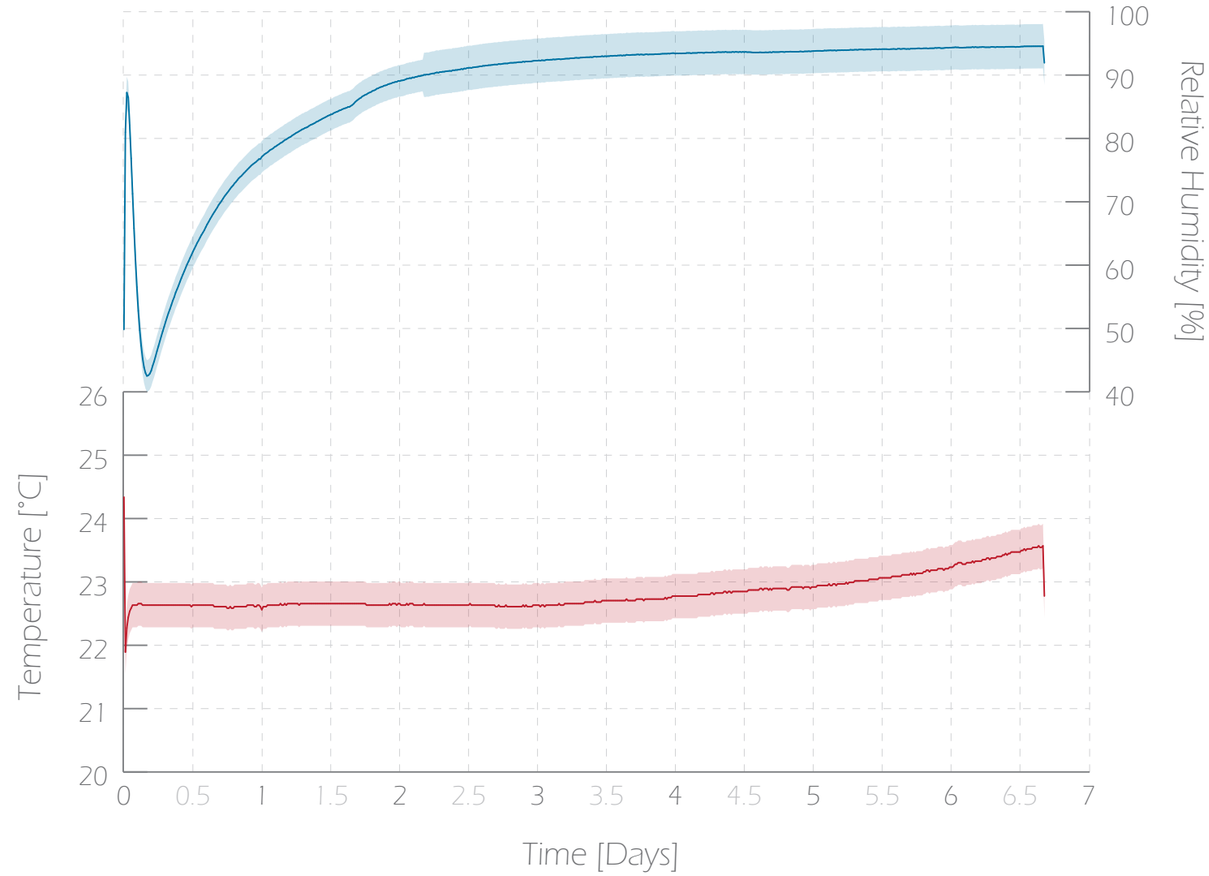

Calculation of the AER per unit day

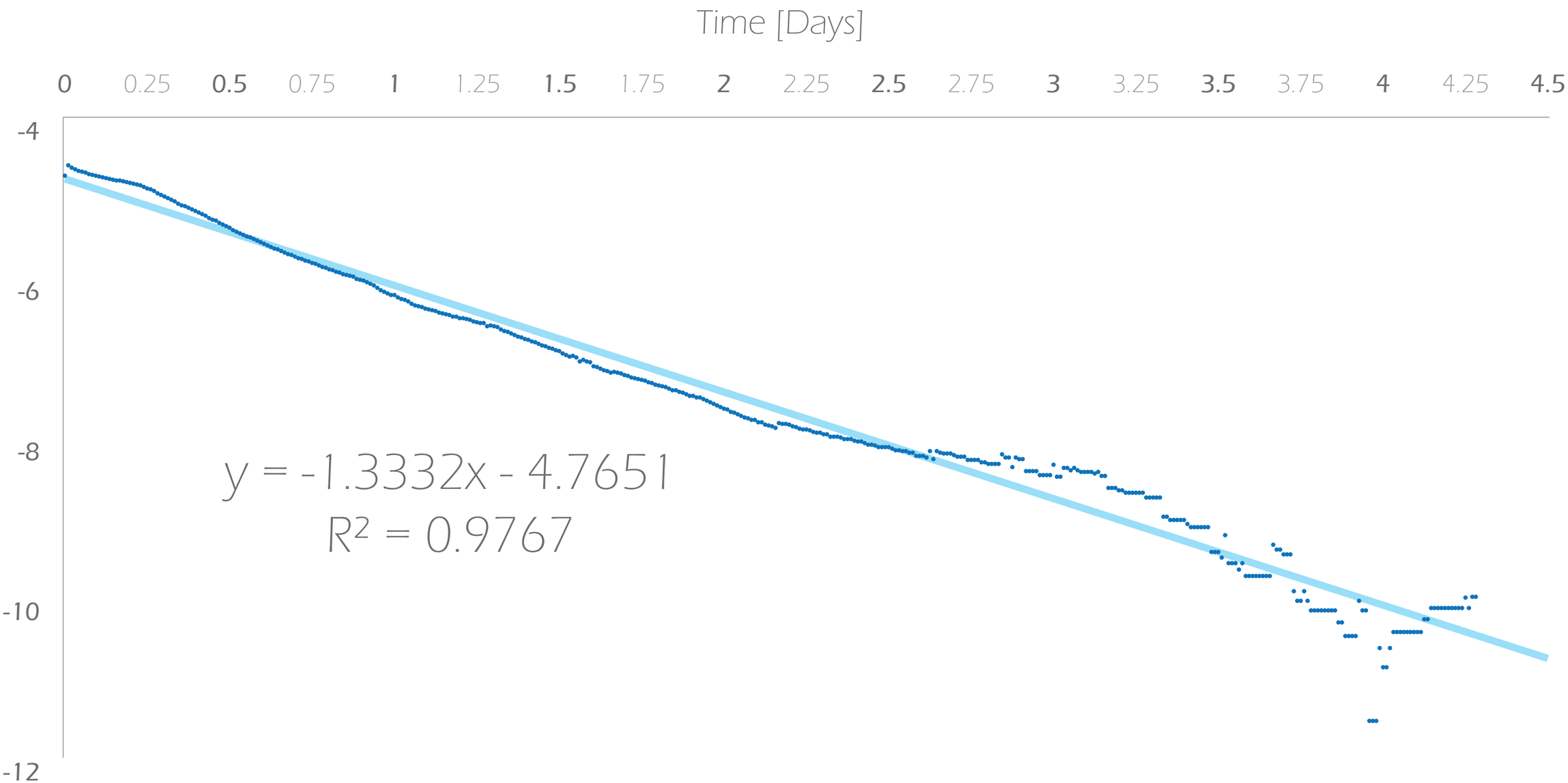

Appendix 4: Environment control experiment results

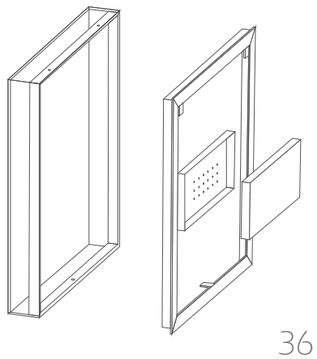

Scenario a No ProSorb

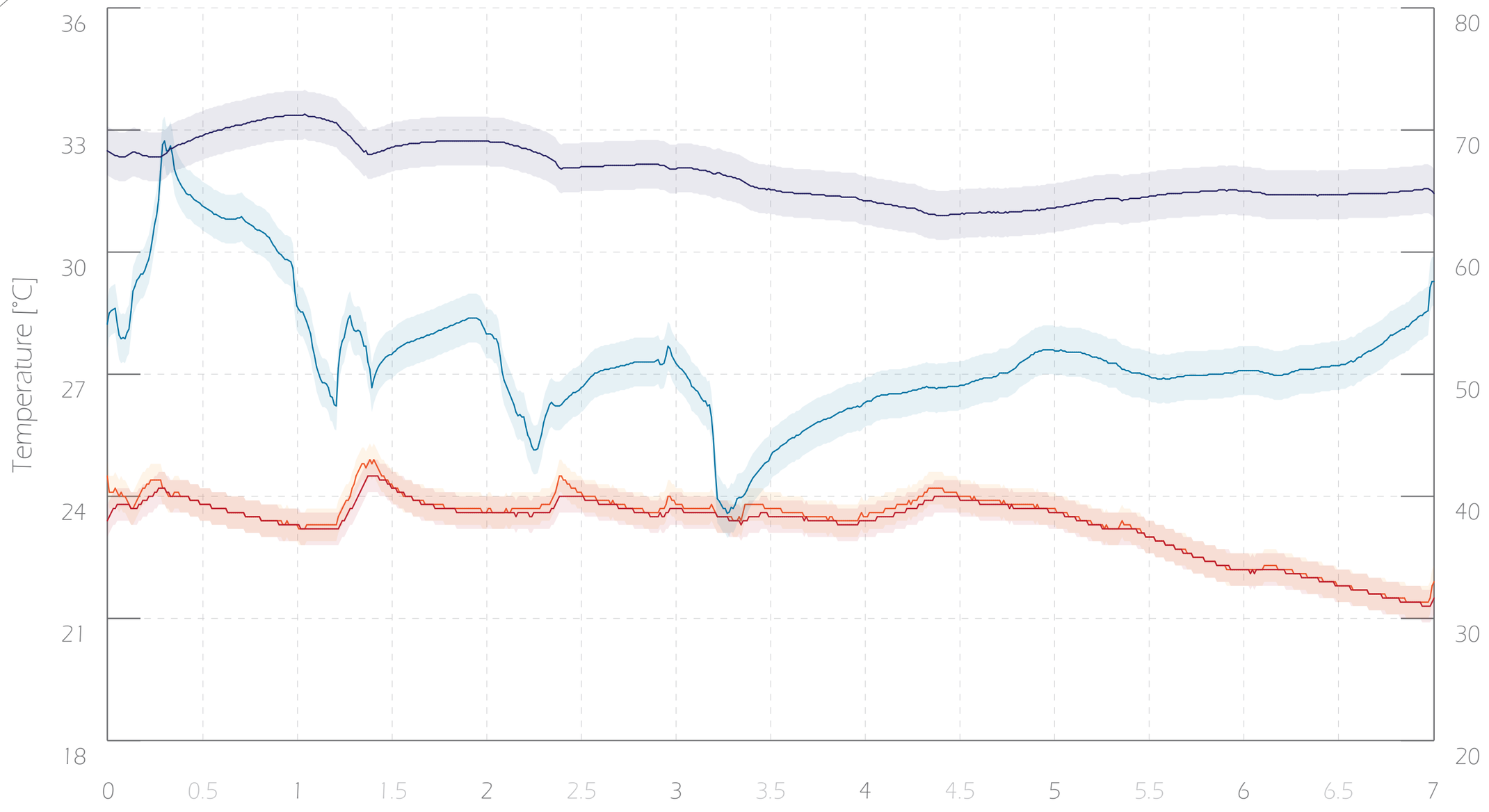

2015/07/20_10:38
at Time = 0

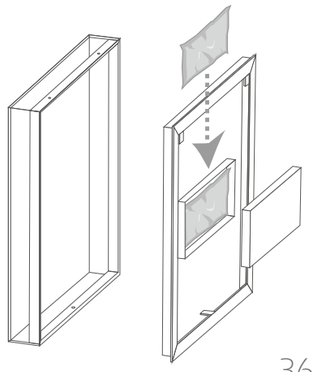

0.0444 m²

Scenario b ProSorb in drawer

661g → 662g

0.01222 kg/m³ Initial MC

0.01070 kg/m³ Final MC

0.068 g

0.01174 kg/m³ Max MC

0.01005 kg/m³ Min MC

0.076 g

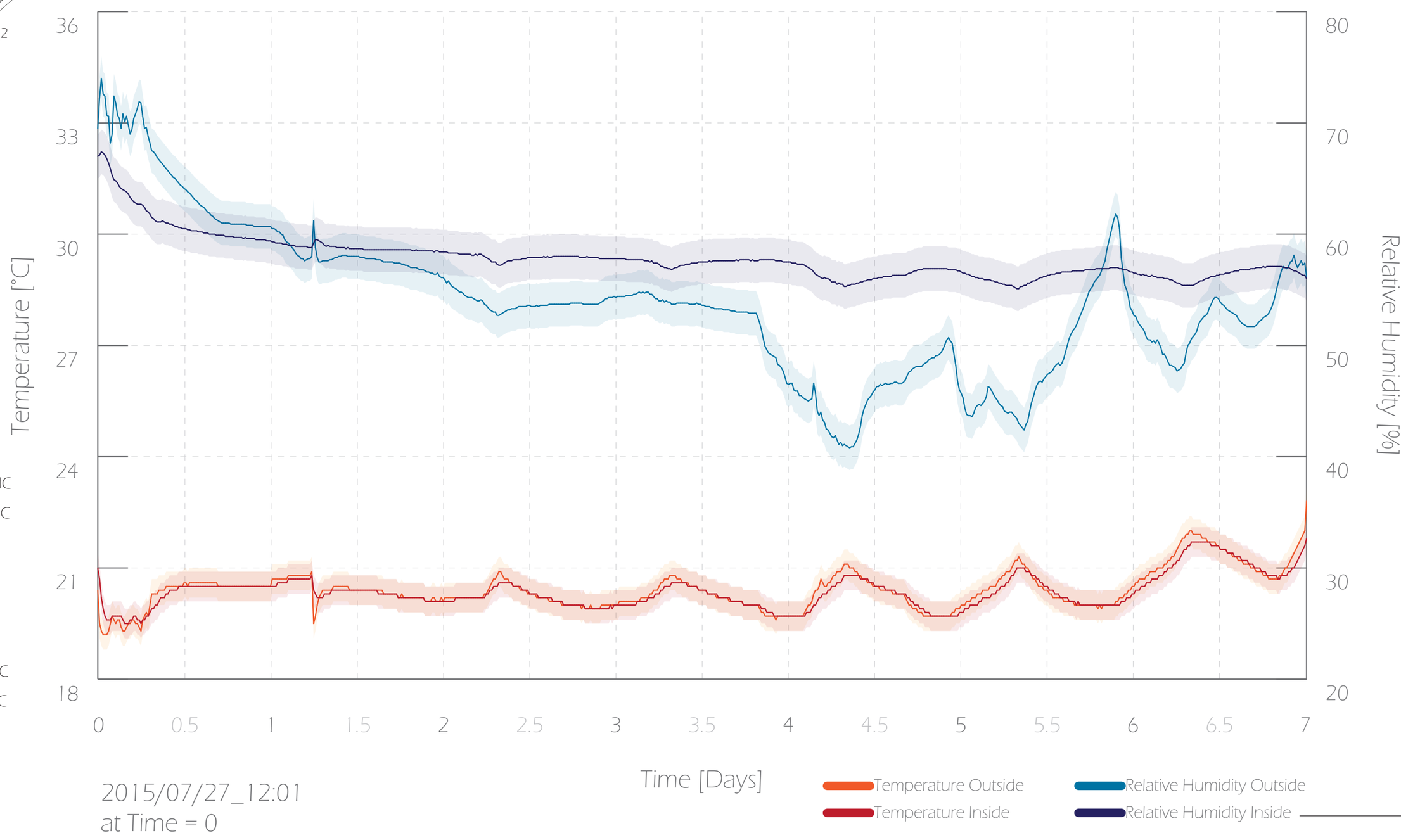

2015/07/27_12:01
at Time = 0

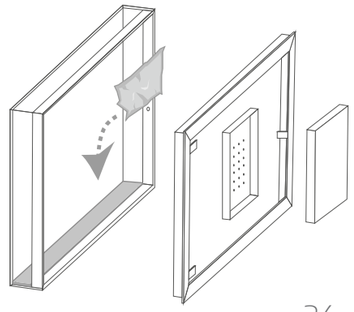

0.0432 m²

Scenario c ProSorb spread inside

651g → 652g

0.01205 kg/m³ Initial MC

0.01139 kg/m³ Final MC

0.030 g

0.01247 kg/m³ Max MC

0.01121 kg/m³ Min MC

0.056 g

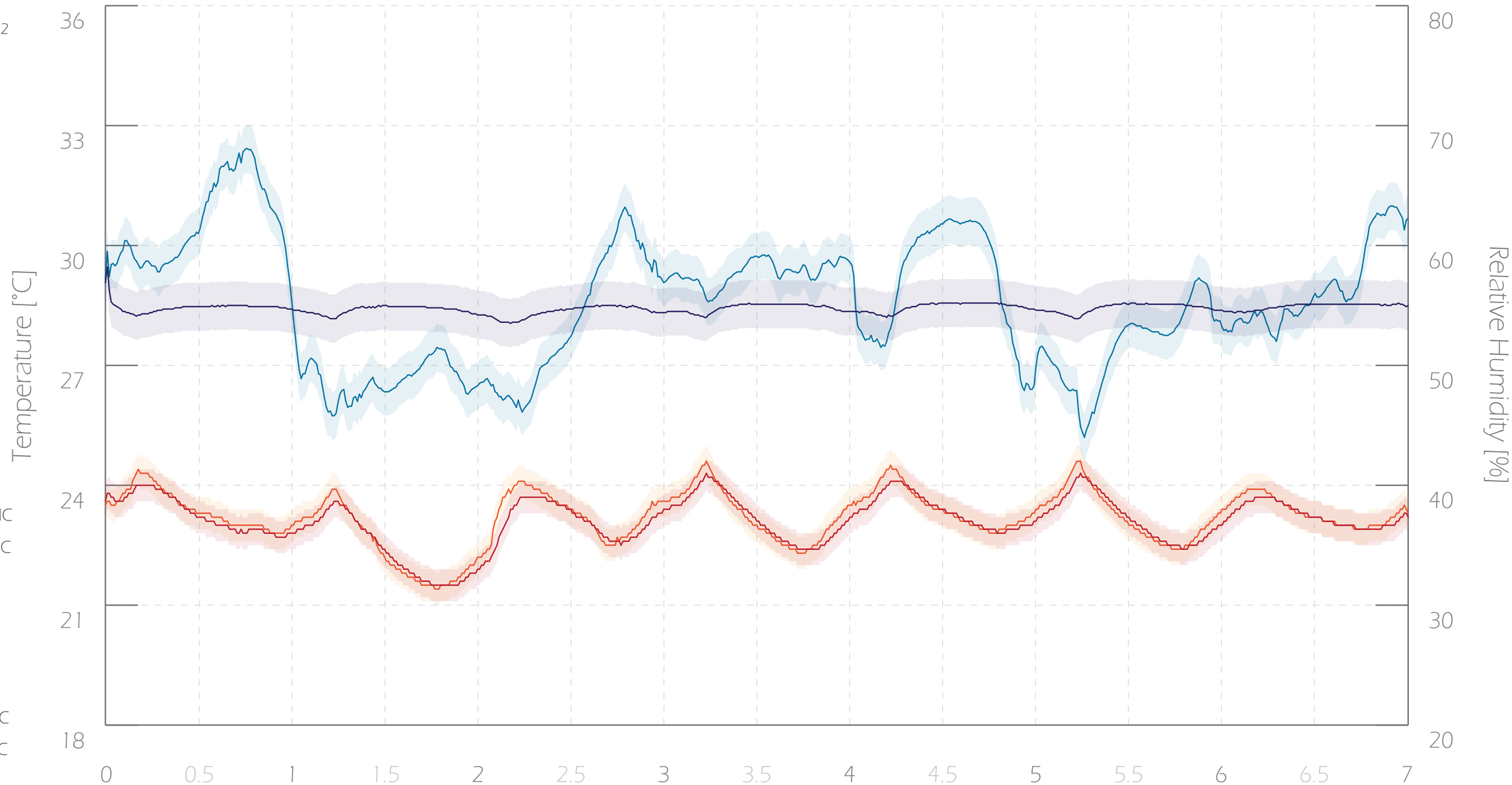

2015/08/03_14:06
at Time = 0

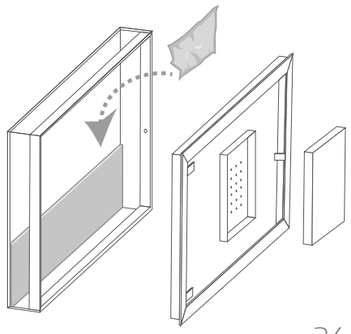

0.1079 m²

Scenario d ProSorb spread inside

652g → 653g

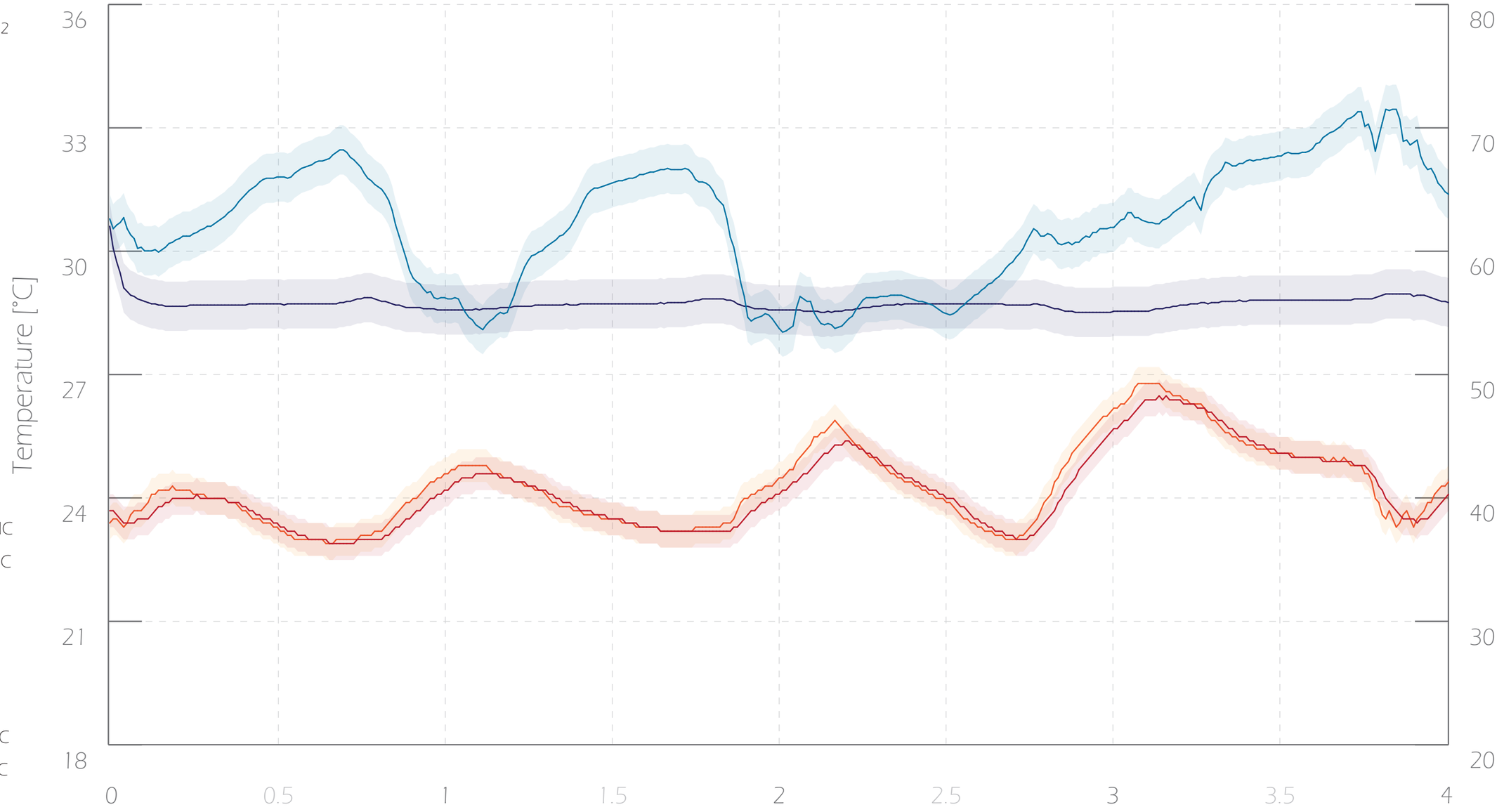

0.01323 kg/m³ Initial MC

0.01218 kg/m³ Final MC

0.047 g

0.01323 kg/m³ Max MC

0.01263 kg/m³ Min MC

0.027 g

2015/08/10_15:25
at Time = 0

Appendix 5: Environment control experiment fit analysis

Scenario a

No ProSorb

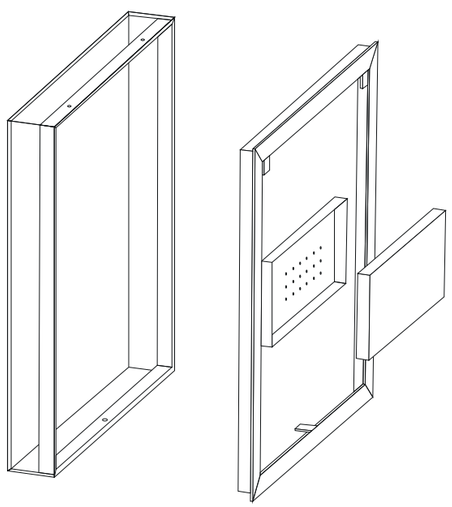

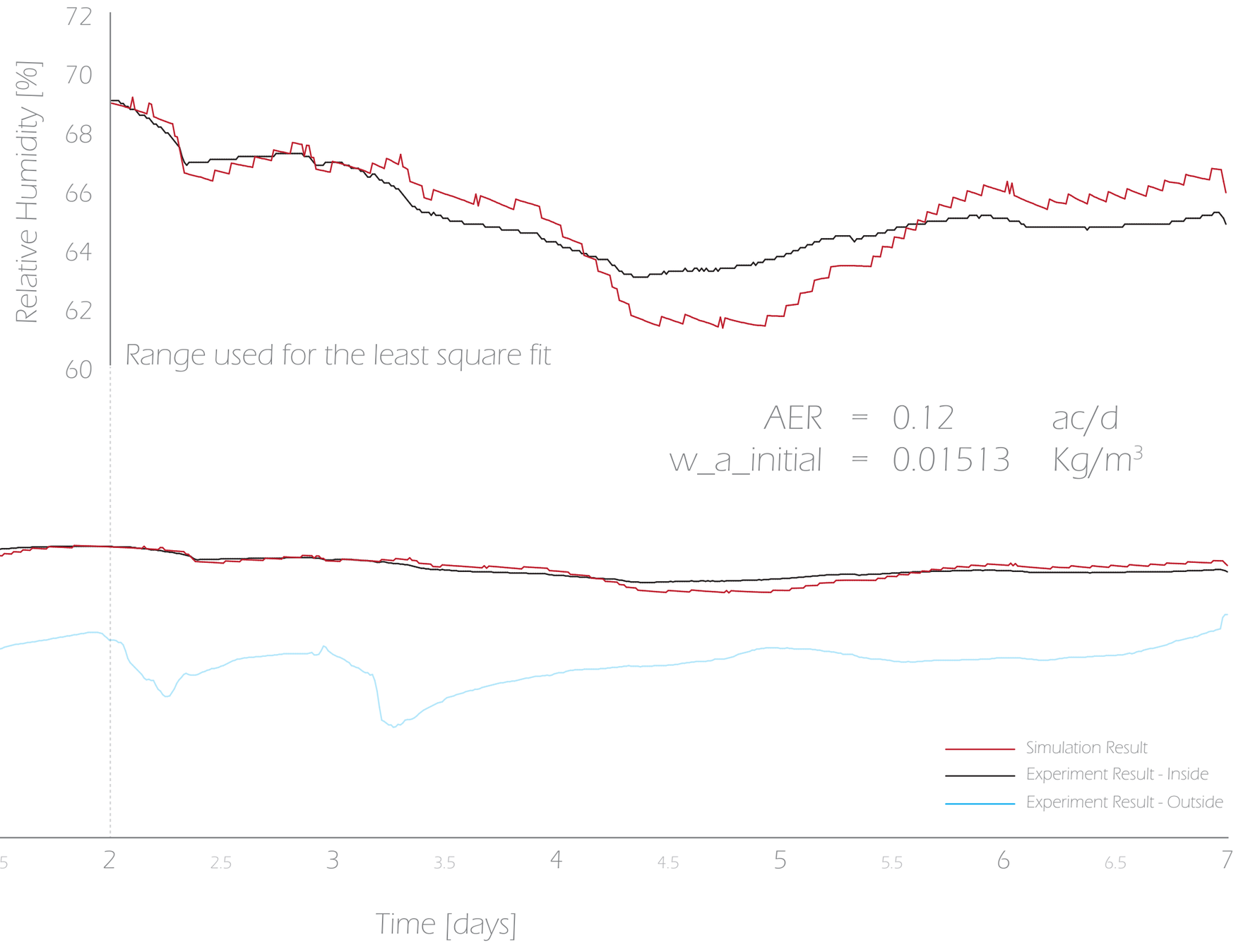

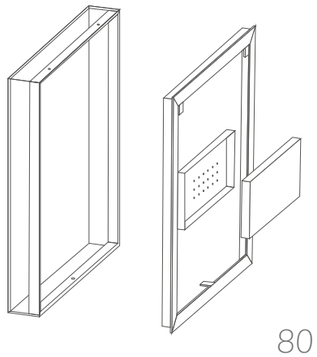

Scenario a No ProSorb

AER = 1.33 ac/d

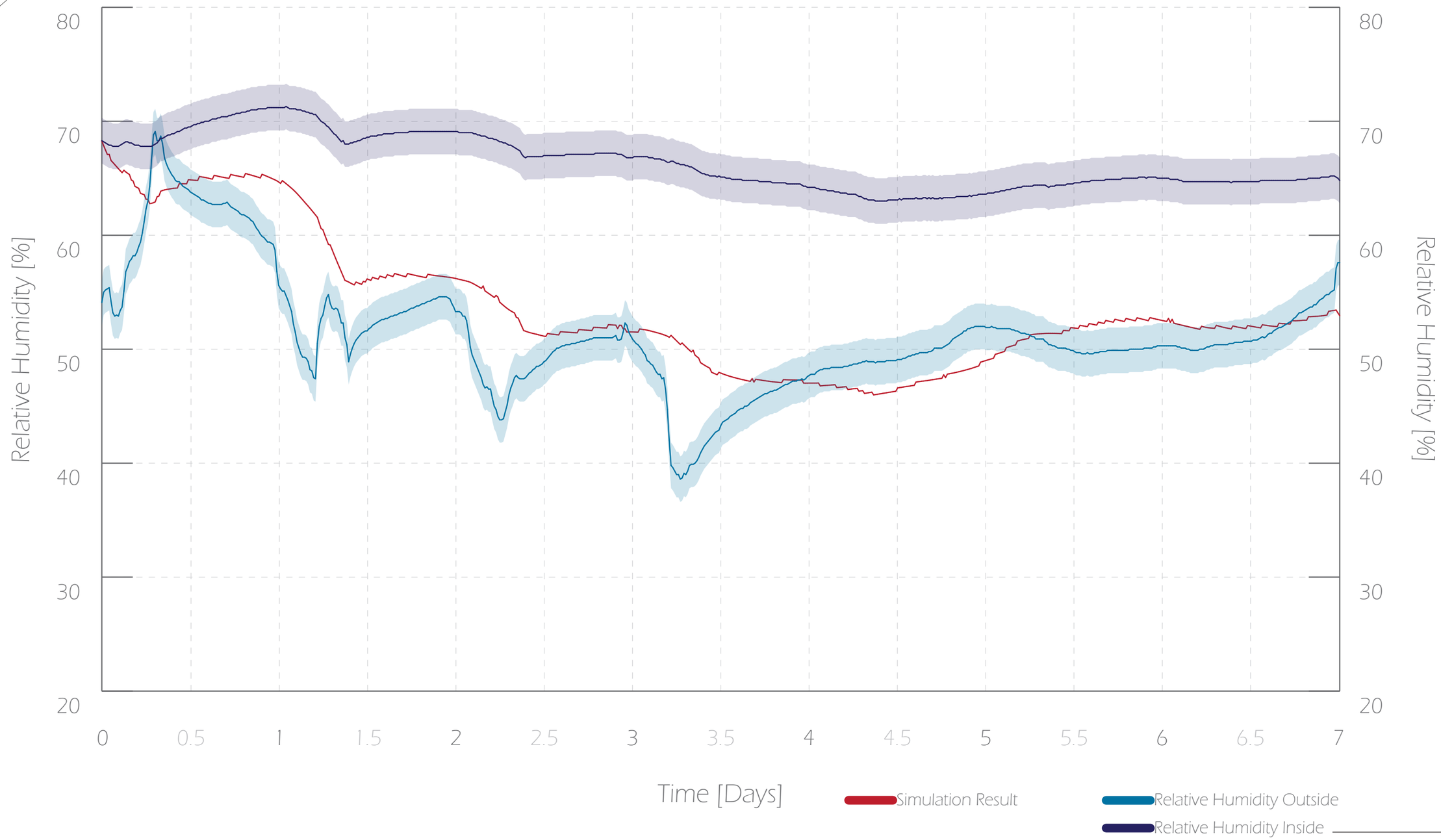

AER = 0.12 ac/d

Scenario b

ProSorb in drawer

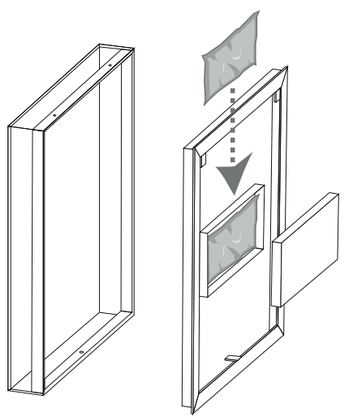

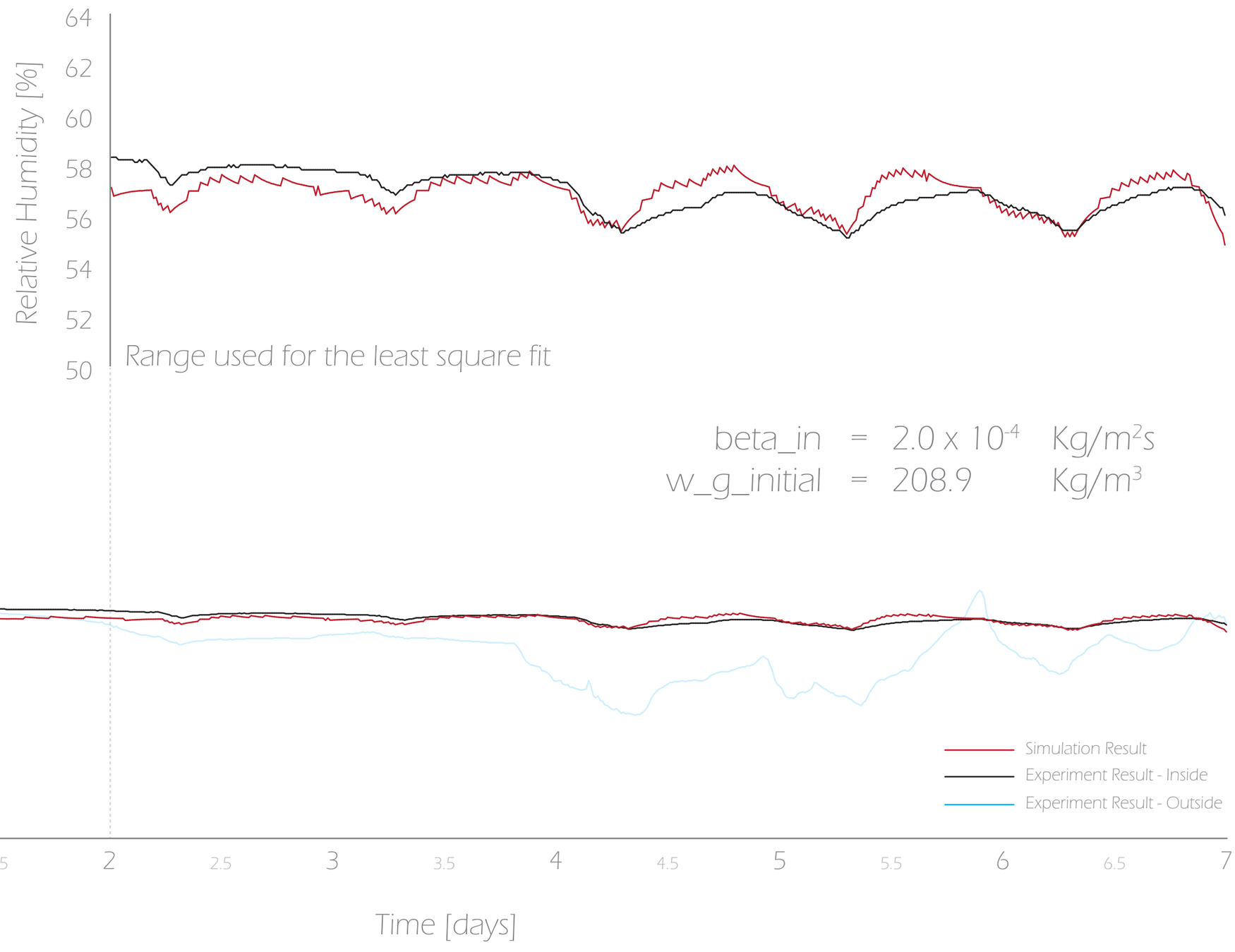

AER = 1.33 ac/d

Scenario b

ProSorb in drawer

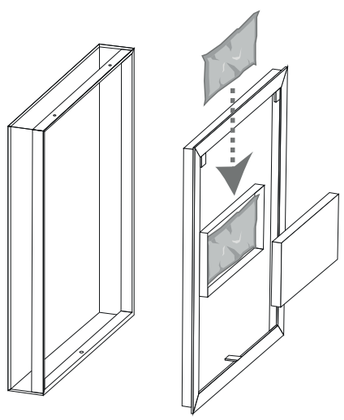

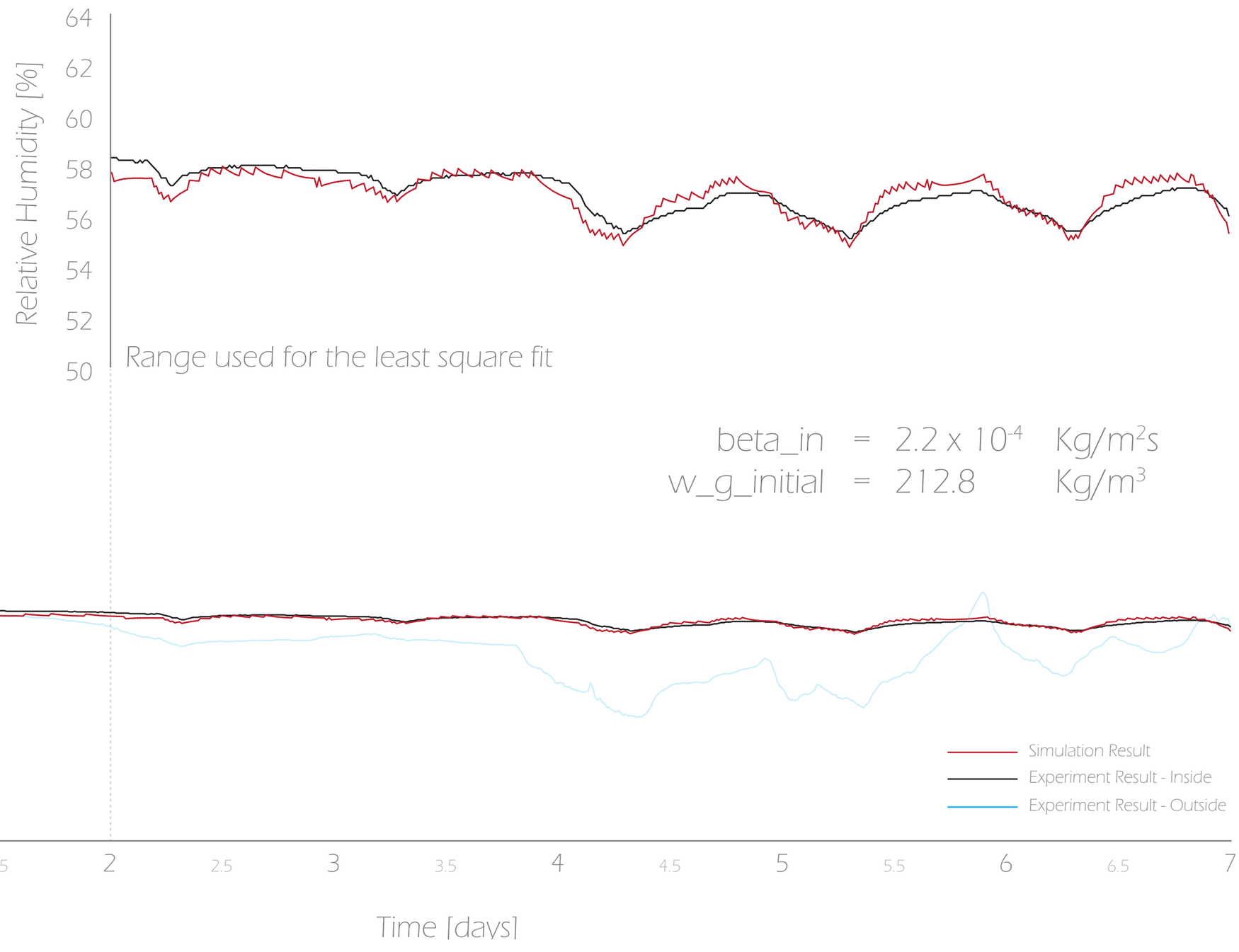

AER = 0.12 ac/d

Scenario c

ProSorb spread inside

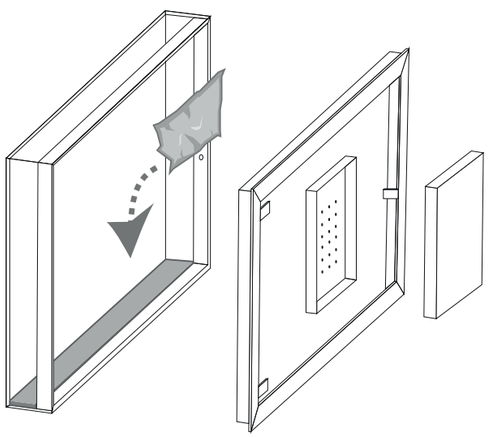

ProSorb area of exposure = 0.0432 m^3

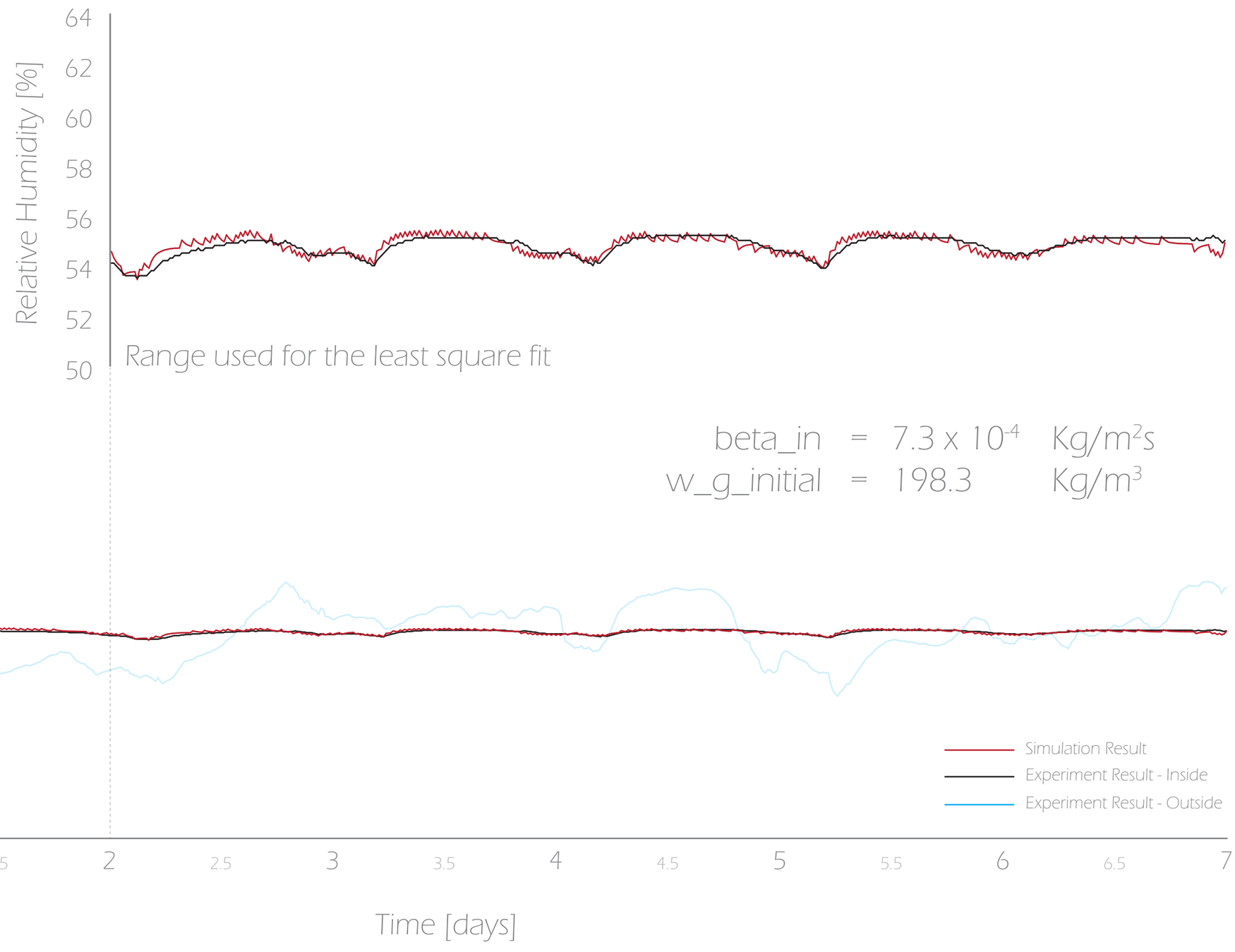

AER = 1.33 ac/d

Scenario c

ProSorb spread inside

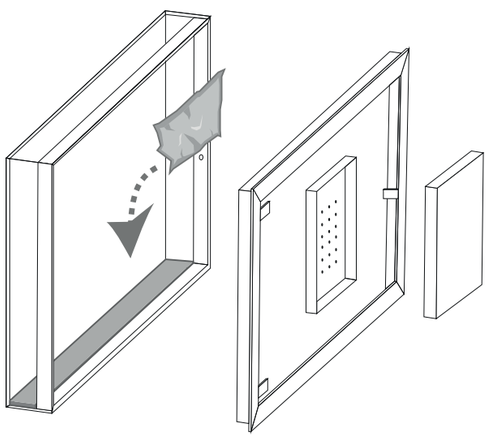

ProSorb area of exposure = 0.0432 m^3

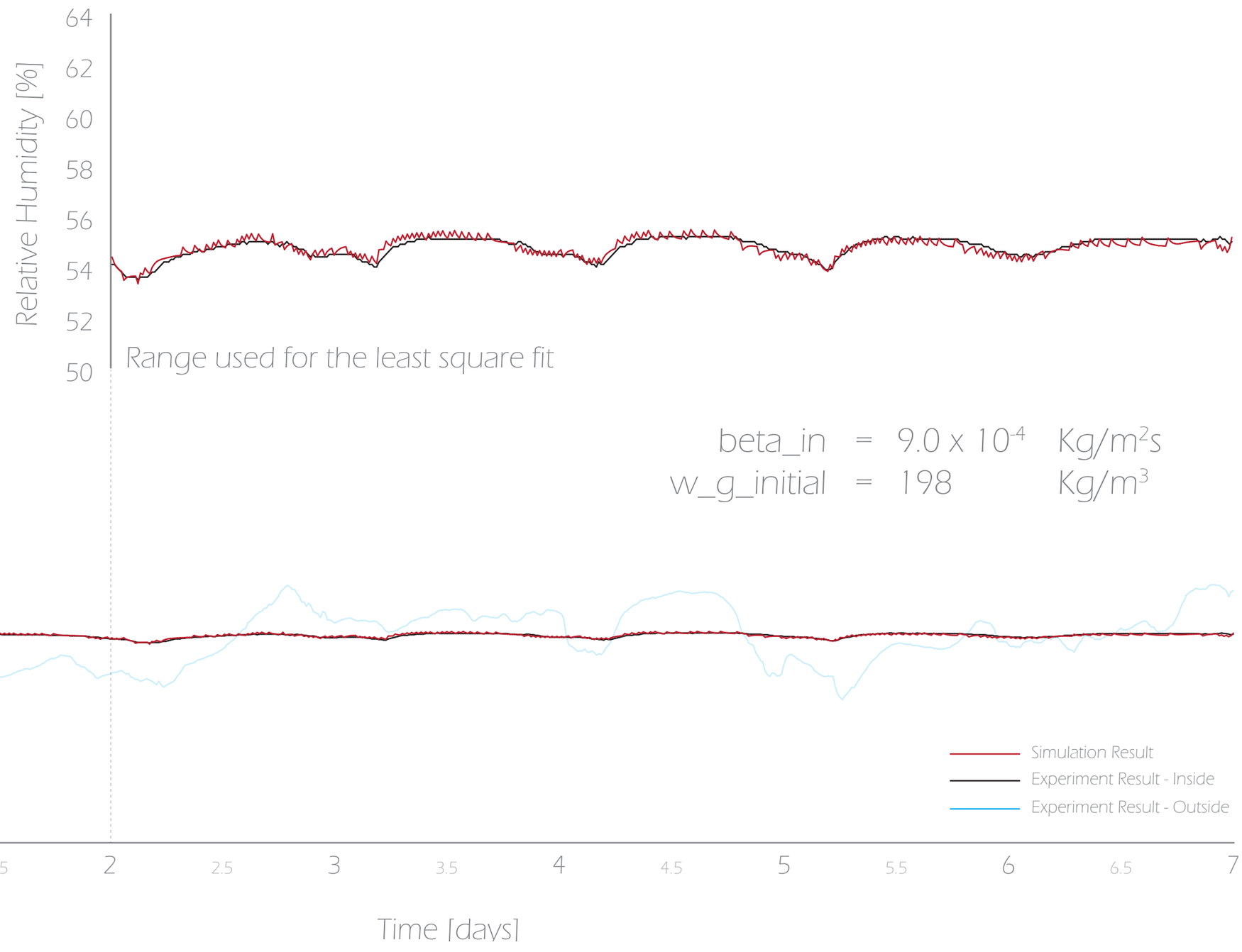

AER = 0.12 ac/d

Scenario d

ProSorb spread inside

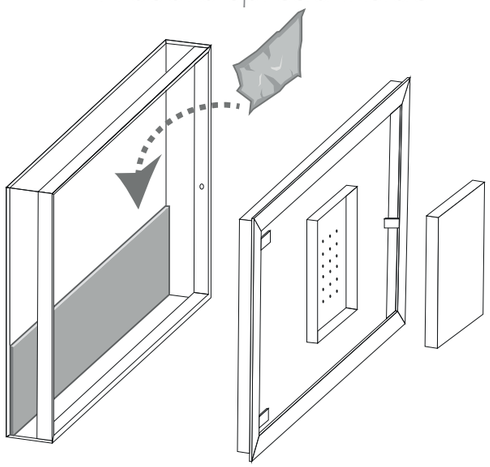

ProSorb area of exposure = 0.1080 m^3

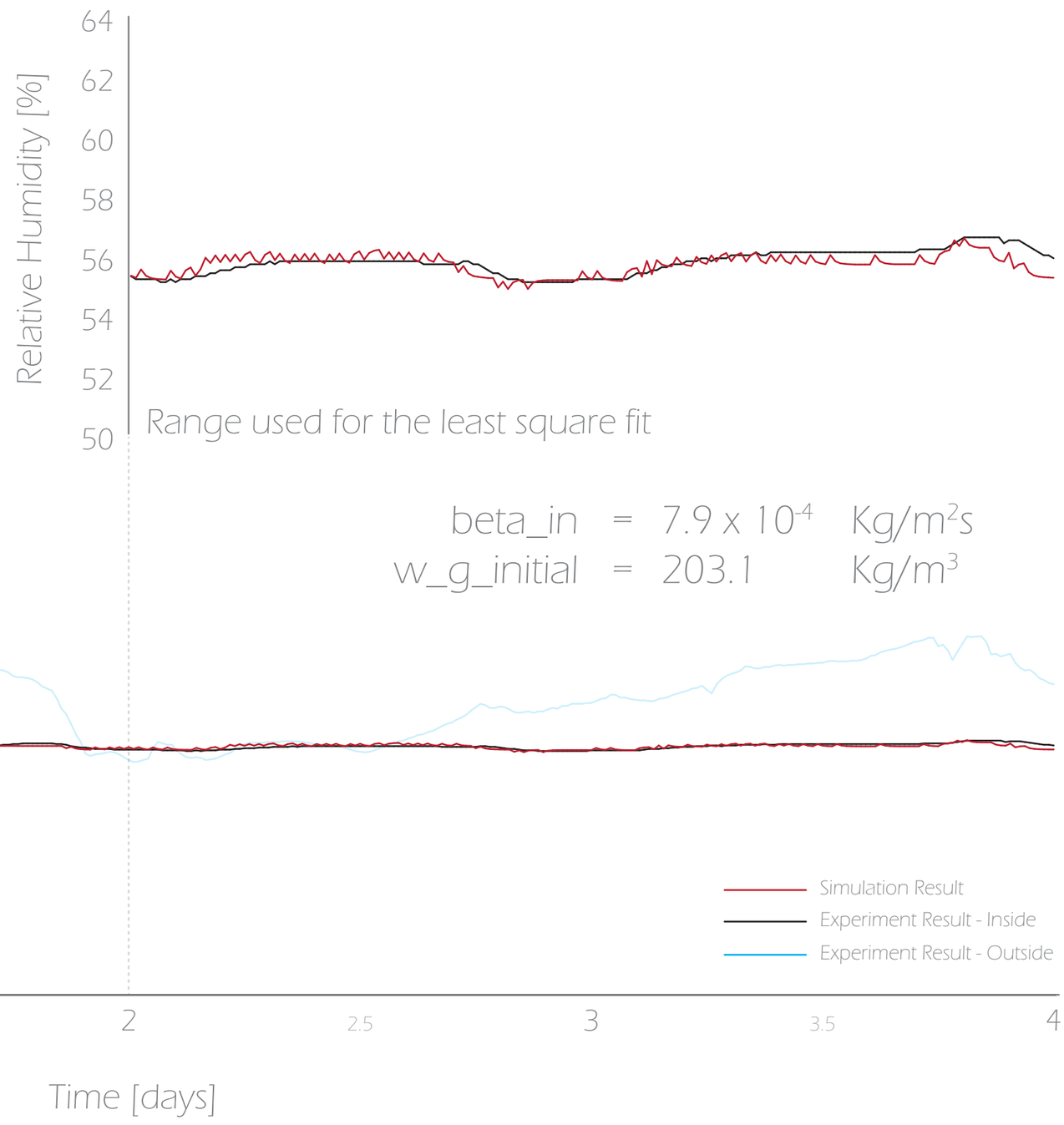

AER = 1.33 ac/d

Scenario d

ProSorb spread inside

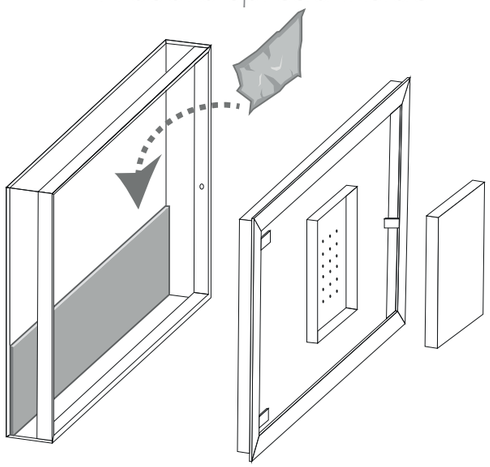

ProSorb area of exposure = 0.1080 m^3

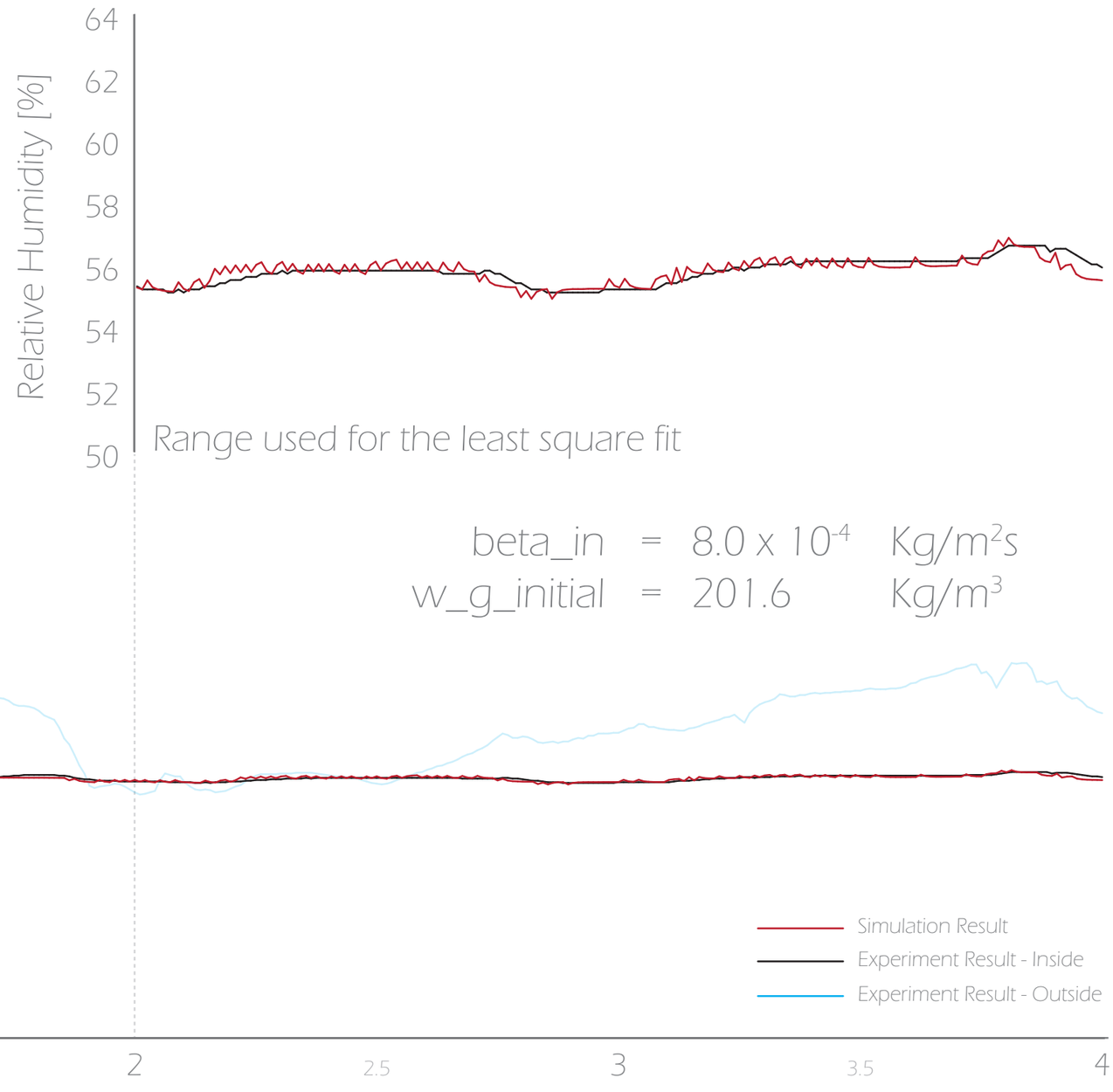

Appendix 6: Sensitivity analysis results

Sensitivity analysis results

Find in the following tables and figures the results from the sensitivity analysis :

Table 41: ΔRH_{in} when AER = 0.00, Time domain = daily, and no ProSorb is present

ΔRH_{out} [%] \ ΔT [°C]	0	1	2	3
0	0.00	2.93	5.87	8.84
5	0.00	2.93	5.87	8.84
10	0.00	2.93	5.87	8.84
20	0.00	2.93	5.87	8.84

Figure 96: ΔRH_{in} when AER = 0.00, Time domain = daily, and no ProSorb is present

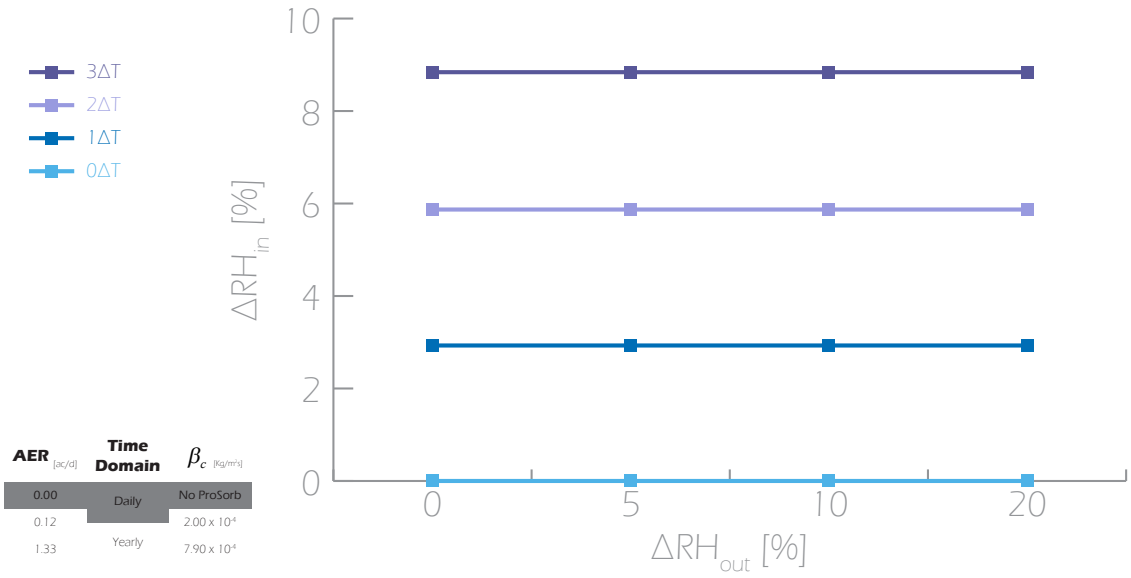

Table 42: ΔRH_{in} when AER = 0.12, Time domain = daily, and no ProSorb is present

ΔRH_{out} [%] \ ΔT [°C]	0	1	2	3
0	0.00	3.10	6.22	9.40
5	0.09	3.09	6.19	9.33
10	0.19	3.08	6.16	9.27
20	0.37	3.07	6.11	9.15

Figure 97: ΔRH_{in} when AER = 0.12, Time domain = daily, and no ProSorb is present

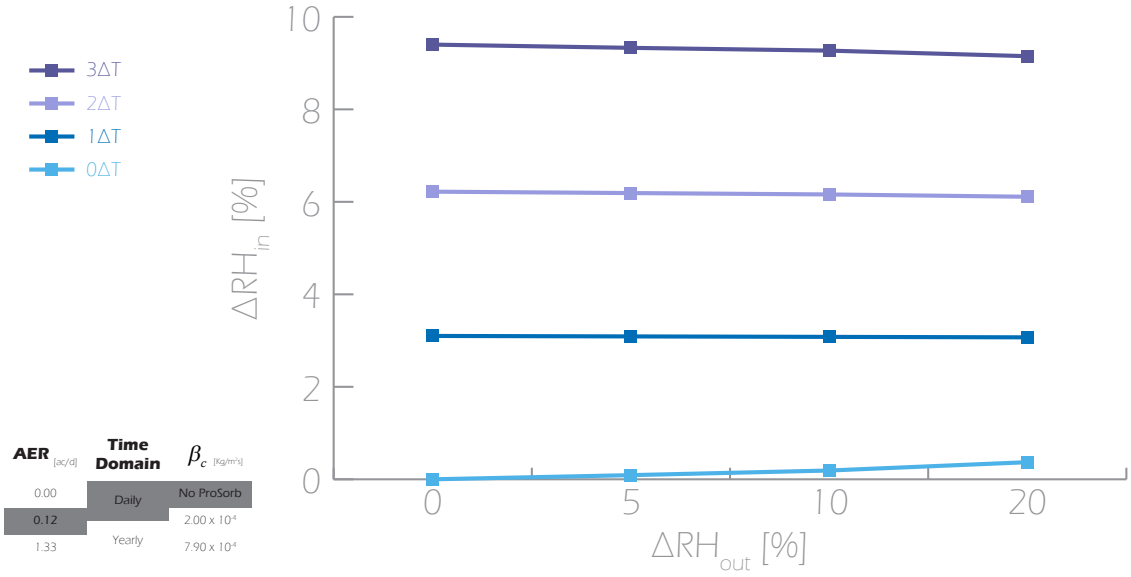

Table 43: ΔRH_{in} when AER = 1.33, Time domain = daily, and no ProSorb is present

ΔRH_{out} [%] \ ΔT [°C]	0	1	2	3
0	0.00	3.03	6.09	9.20
5	1.02	3.15	6.10	9.15
10	2.05	3.58	6.29	9.21
20	4.09	4.99	7.11	9.66

Figure 98: ΔRH_{in} when AER = 1.33, Time domain = daily, and no ProSorb is present

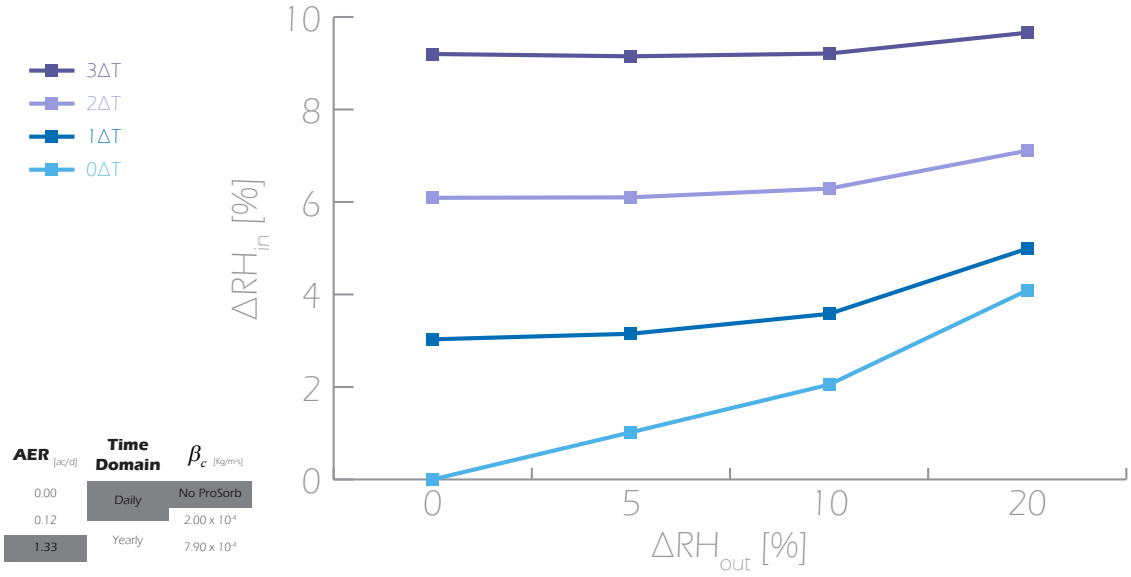

Table 44: ΔRH_{in} when AER = 0.00, Time domain = yearly, and no ProSorb is present

ΔRH_{out} [%] \ **ΔT** [°C]	0	1	2	3
0	0.00	2.93	5.87	8.84
5	0.00	2.93	5.87	8.84
10	0.00	2.93	5.87	8.84
20	0.00	2.93	5.87	8.84

Figure 99: ΔRH_{in} when AER = 0.00, Time domain = yearly, and no ProSorb is present

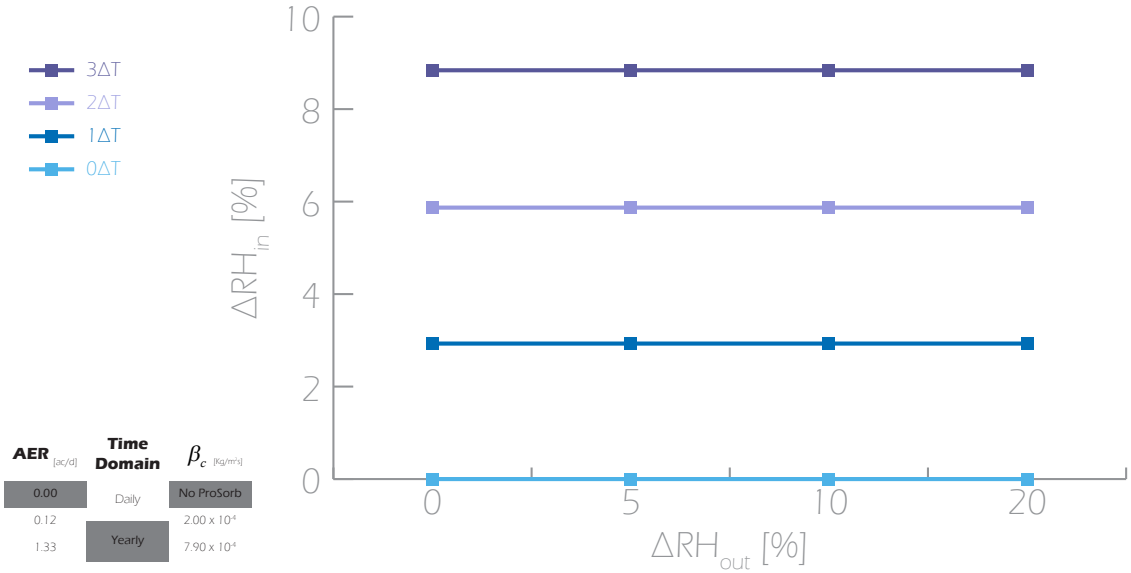

Table 45: ΔRH_{in} when AER = 0.12, Time domain = yearly, and no ProSorb is present

ΔRH$_{out}$ [%] \ **ΔT** [°C]	0	1	2	3
0	0.00	0.42	0.84	1.26
5	4.95	5.14	5.37	5.62
10	9.90	10.09	10.29	10.51
20	19.79	19.98	20.18	20.38

Figure 100: ΔRH_{in} when AER = 0.12, Time domain = yearly, and no ProSorb is present

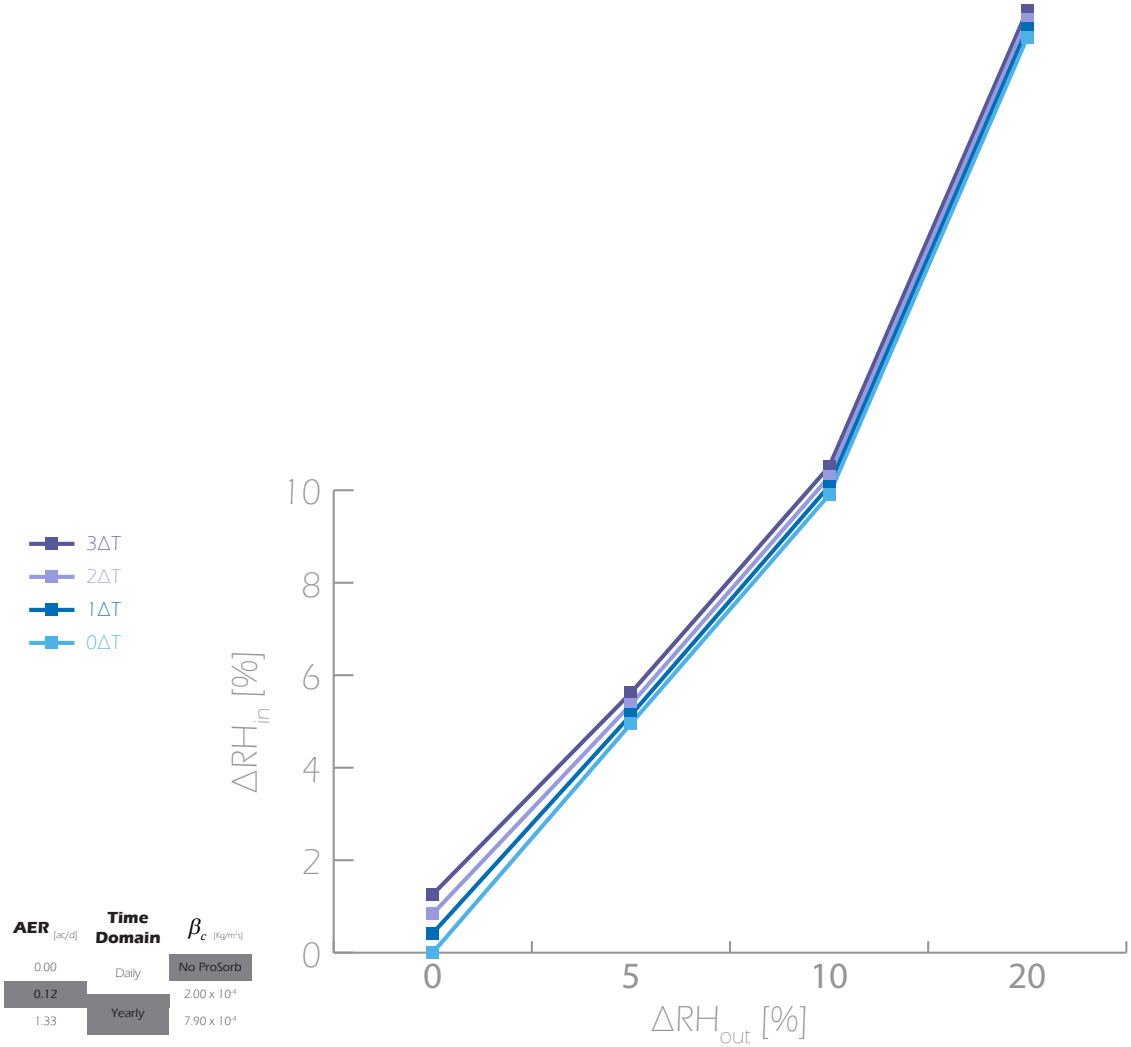

Table 46: ΔRH_{in} when AER = 1.33, Time domain = yearly, and no ProSorb is present

ΔRH_{out} [%] \ **ΔT** [°C]	0	1	2	3
0	0.00	0.04	0.08	0.12
5	5.00	5.02	5.03	5.05
10	10.00	10.02	10.03	10.05
20	20.00	20.02	20.03	20.05

Figure 101: ΔRH_{in} when AER = 1.33, Time domain = yearly, and no ProSorb is present

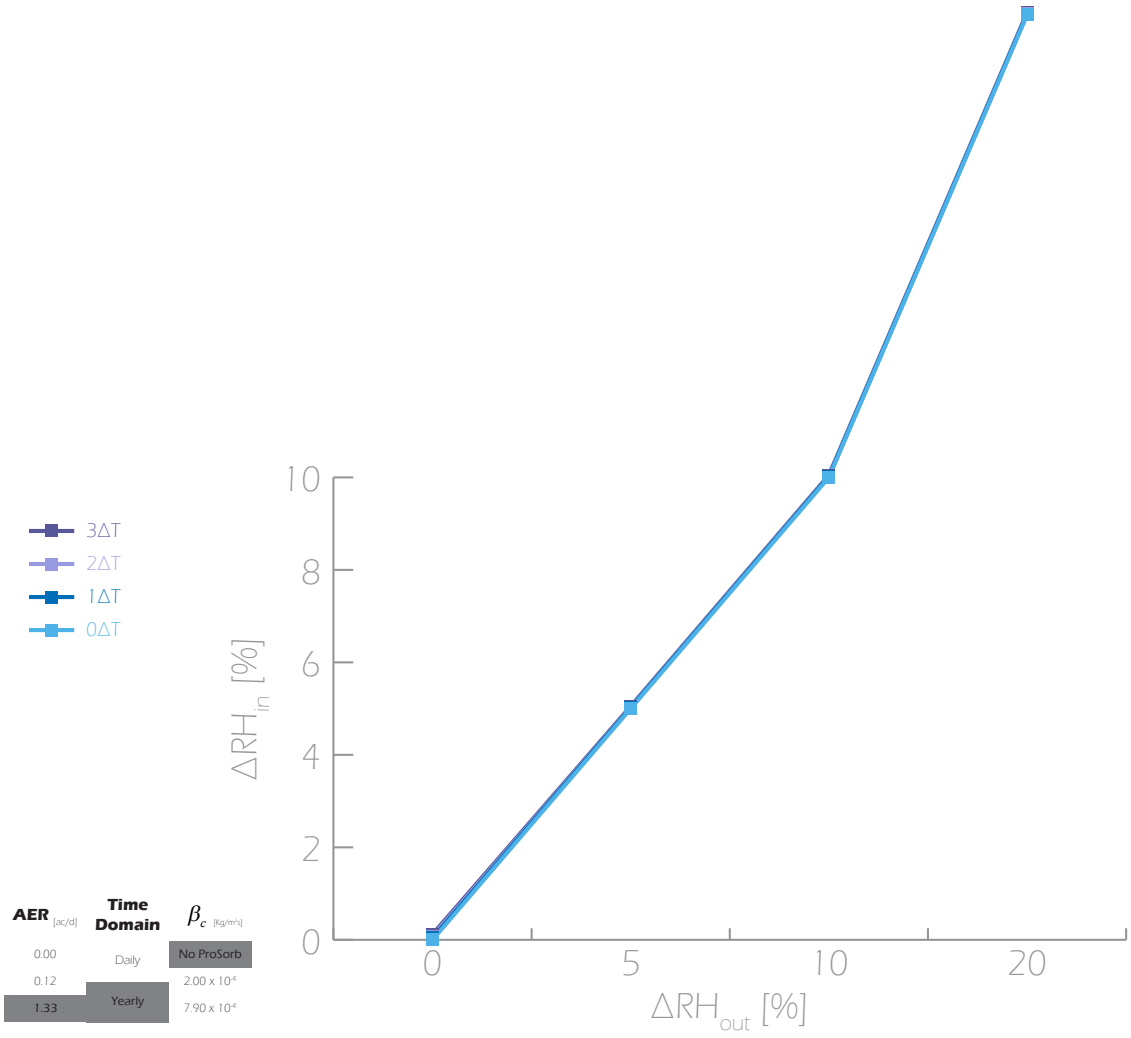

Table 47: ΔRH_{in} when AER = 0.00, Time domain = daily, and β_c = 2.00 x 10^{-4} Kg/m^2s

ΔRH_{out} [%] \ **ΔT** [°C]	0	1	2	3
0	0.00	1.46	2.92	4.40
5	0.00	1.46	2.92	4.40
10	0.00	1.46	2.92	4.40
20	0.00	1.46	2.92	4.40

Figure 102: ΔRH_{in} when AER = 0.00, Time domain = daily, and β_c = 2.00 x 10^{-4} Kg/m^2s

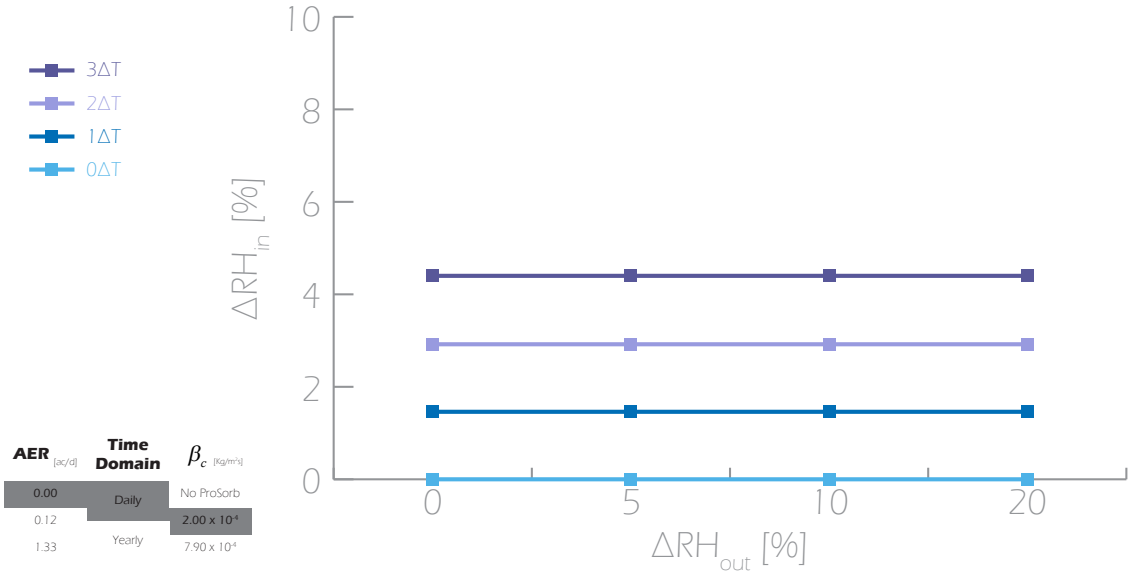

Table 48: ΔRH_{in} when AER = 0.12, Time domain = daily, and β_c = 2.00 x 10^{-4} Kg/m^2s

ΔRH_{out} [%] \ **ΔT** [°C]	0	1	2	3
0	0.00	1.53	3.06	4.60
5	0.05	1.53	3.06	4.60
10	0.09	1.53	3.06	4.60
20	0.19	1.54	3.06	4.60

Figure 103: ΔRH_{in} when AER = 0.12, Time domain = daily, and β_c = 2.00 x 10^{-4} Kg/m^2s

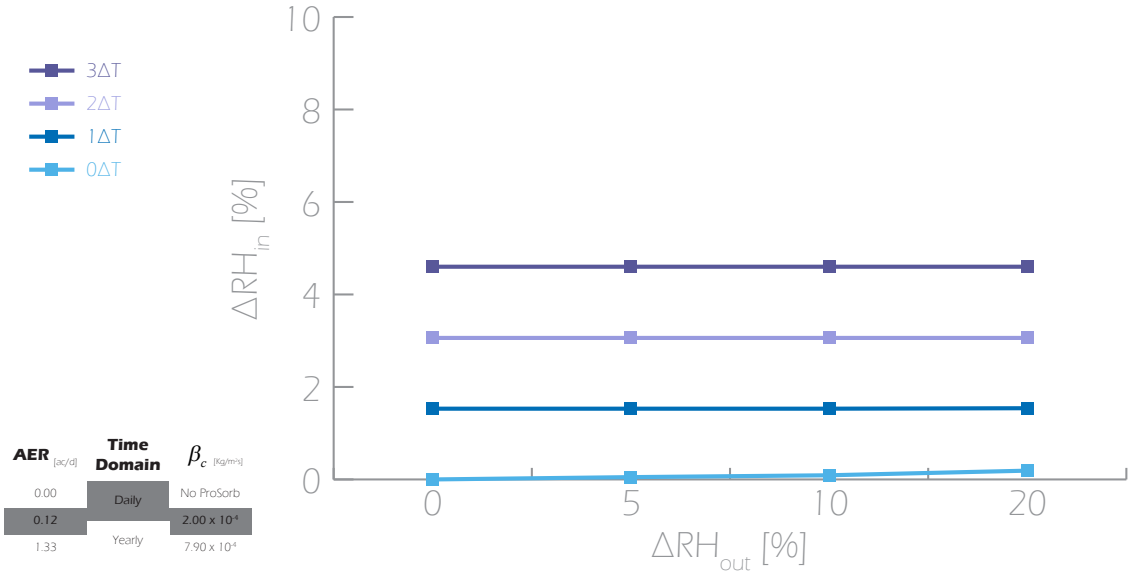

Table 49: ΔRH_{in} when AER = 1.33, Time domain = daily, and β_c = 2.00 x 10^{-4} Kg/m²s

ΔRH$_{out}$ [%] \ ΔT [°C]	0	1	2	3
0	0.00	1.41	2.83	4.25
5	0.48	1.48	2.85	4.26
10	0.97	1.68	2.96	4.32
20	1.93	2.35	3.37	4.60

Figure 104: ΔRH_{in} when AER = 1.33, Time domain = daily, and β_c = 2.00 x 10^{-4} Kg/m²s

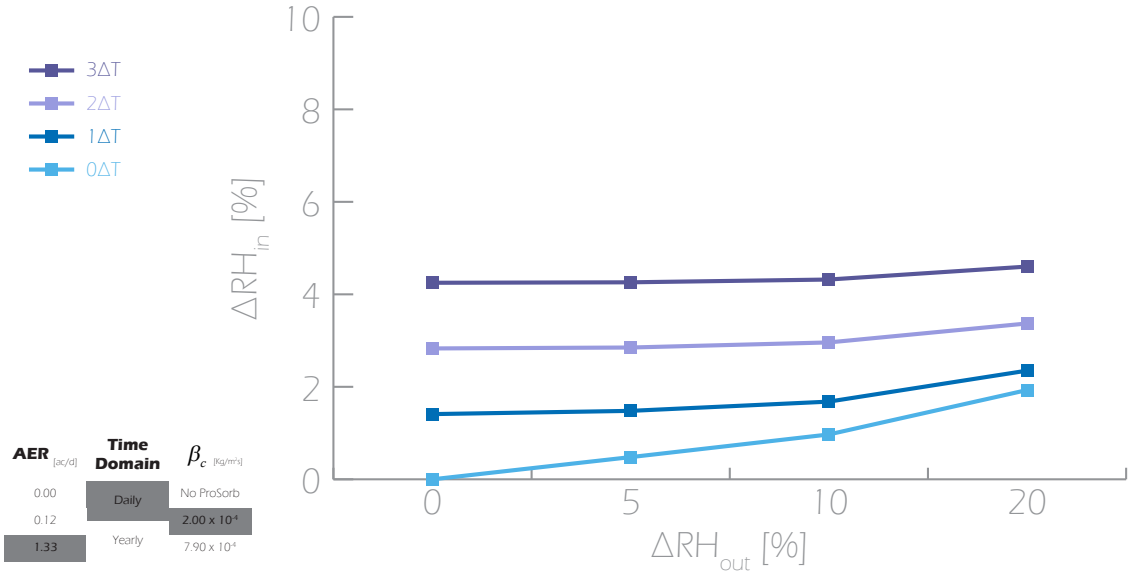

Table 50: ΔRH_{in} when AER = 0.00, Time domain = yearly, and β_c = 2.00 x 10^{-4} Kg/m²s

ΔRH$_{out}$ [%] \ ΔT [°C]	0	1	2	3
0	0.00	0.03	0.05	0.08
5	0.00	0.03	0.05	0.08
10	0.00	0.03	0.05	0.08
20	0.00	0.03	0.05	0.08

Figure 105: ΔRH_{in} when AER = 0.00, Time domain = yearly, and β_c = 2.00 x 10^{-4} Kg/m²s

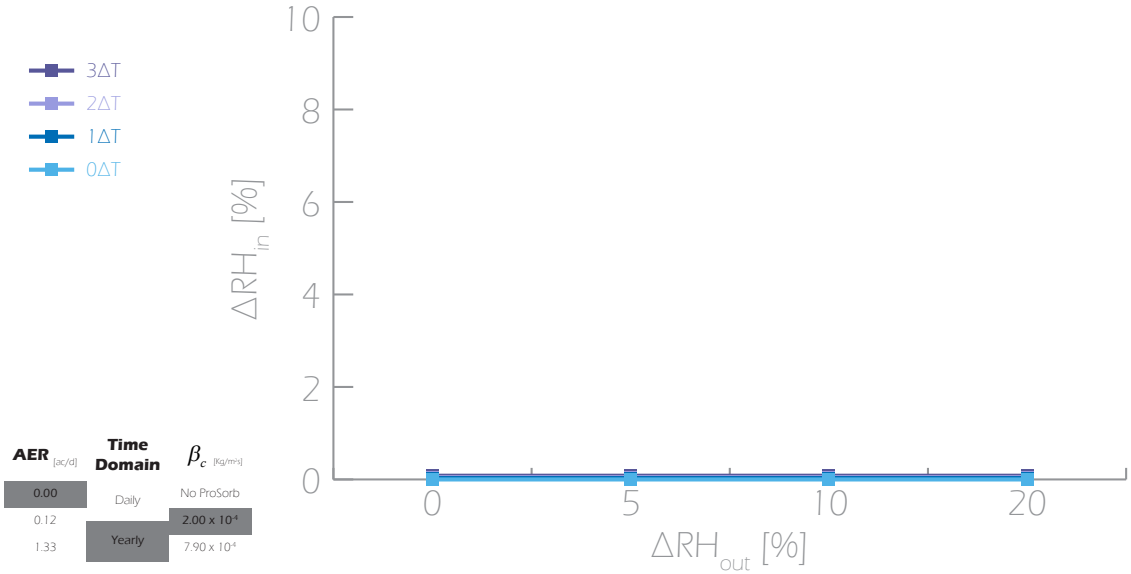

Table 51: ΔRH_{in} when AER = 0.12, Time domain = yearly, and β_c = 2.00 x 10^{-4} Kg/m²s

ΔRH_{out} [%] \ **ΔT** [°C]	0	1	2	3
0	0.00	0.03	0.05	0.08
5	0.32	0.33	0.33	0.34
10	0.63	0.64	0.63	0.64
20	1.27	1.26	1.24	1.23

Figure 106: ΔRH_{in} when AER = 0.12, Time domain = yearly, and β_c = 2.00 x 10^{-4} Kg/m²s

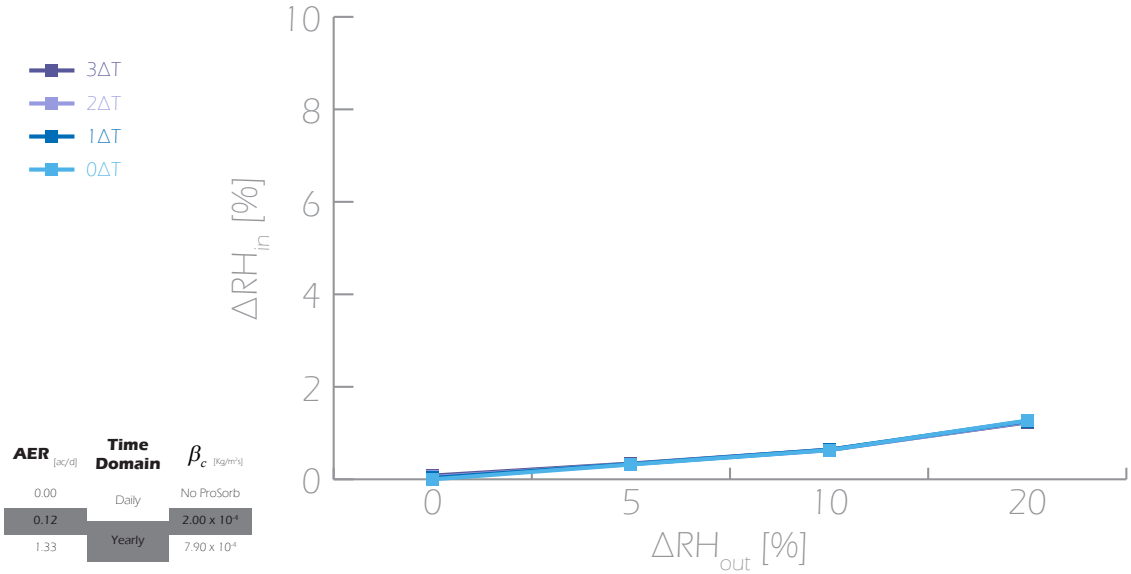

Table 52: ΔRH_{in} when AER = 1.33, Time domain = yearly, and β_c = 2.00 x 10^{-4} Kg/m²s

ΔRH_{out} [%] \ **ΔT** [°C]	0	1	2	3
0	0.00	0.02	0.04	0.06
5	2.61	2.62	2.62	2.63
10	5.21	5.22	5.23	5.23
20	10.43	10.43	10.44	10.44

Figure 107: ΔRH_{in} when AER = 1.33, Time domain = yearly, and β_c = 2.00 x 10^{-4} Kg/m²s

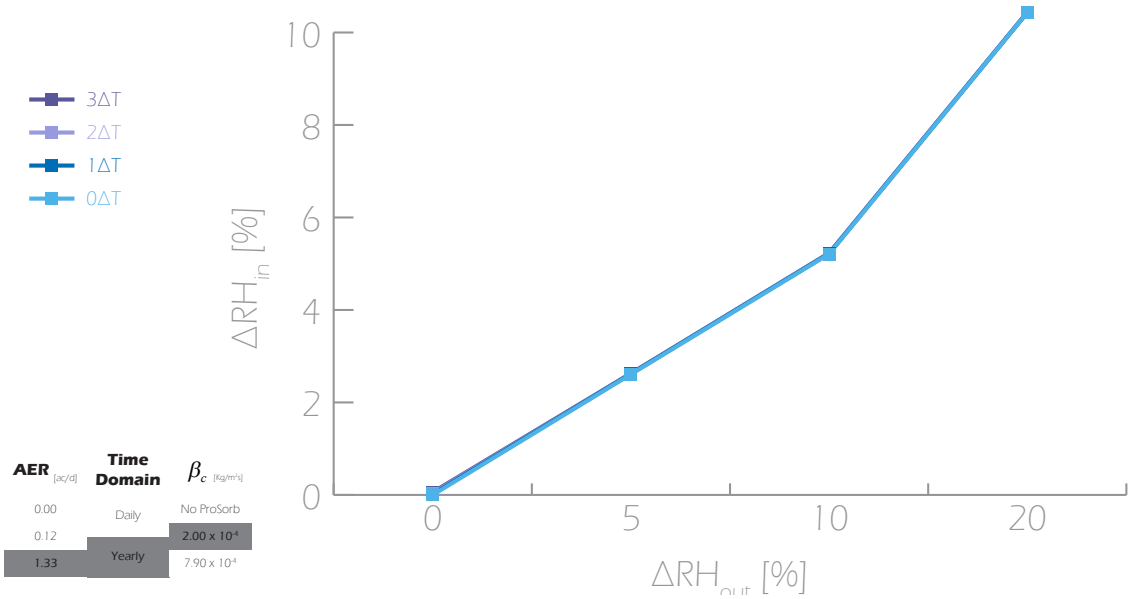

Table 53: ΔRH_{in} when AER = 0.00, Time domain = daily, and β_c = 7.90 x 10^{-4} Kg/m^{2}s

ΔRH$_{out}$ [%] \ ΔT [°C]	0	1	2	3
0	0.00	0.20	0.39	0.59
5	0.00	0.20	0.39	0.59
10	0.00	0.20	0.39	0.59
20	0.00	0.20	0.39	0.59

Figure 108: ΔRH_{in} when AER = 0.00, Time domain = daily, and β_c = 7.90 x 10^{-4} Kg/m^{2}s

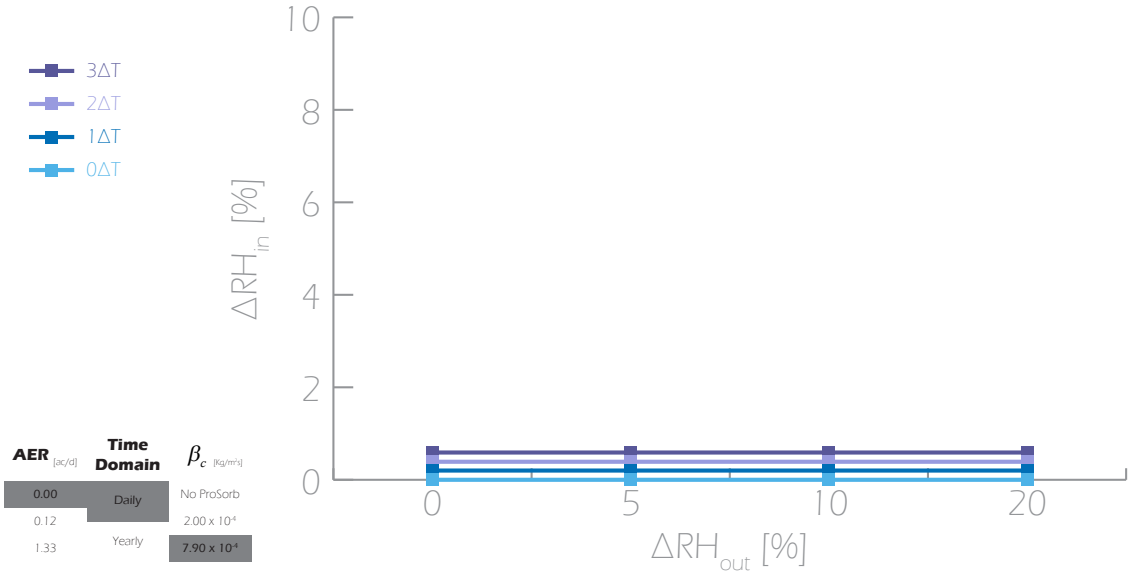

Table 54: ΔRH_{in} when AER = 0.12, Time domain = daily, and β_c = 7.90x 10^{-4} Kg/m^{2}s

ΔRH$_{out}$ [%] \ ΔT [°C]	0	1	2	3
0	0.00	0.21	0.41	0.62
5	0.01	0.21	0.41	0.62
10	0.01	0.21	0.41	0.62
20	0.02	0.21	0.41	0.62

Figure 109: ΔRH_{in} when AER = 0.12, Time domain = daily, and β_c = 7.90x 10^{-4} Kg/m^{2}s

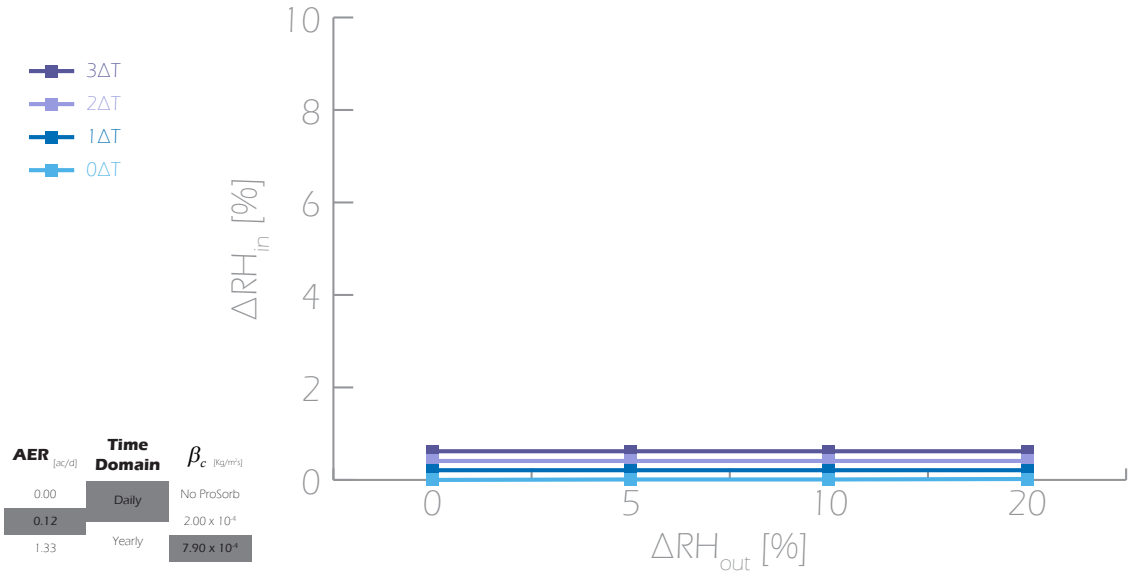

Table 55: ΔRH_{in} when AER = 1.33, Time domain = daily, and β_c = 7.90 x 10^{-4} Kg/m²s

ΔRH_{out} [%] \ **ΔT** [°C]	0	1	2	3
0	0.00	0.20	0.41	0.61
5	0.07	0.21	0.41	0.61
10	0.14	0.24	0.42	0.62
20	0.28	0.34	0.48	0.66

Figure 110: ΔRH_{in} when AER = 1.33, Time domain = daily, and β_c = 7.90 x 10^{-4} Kg/m²s

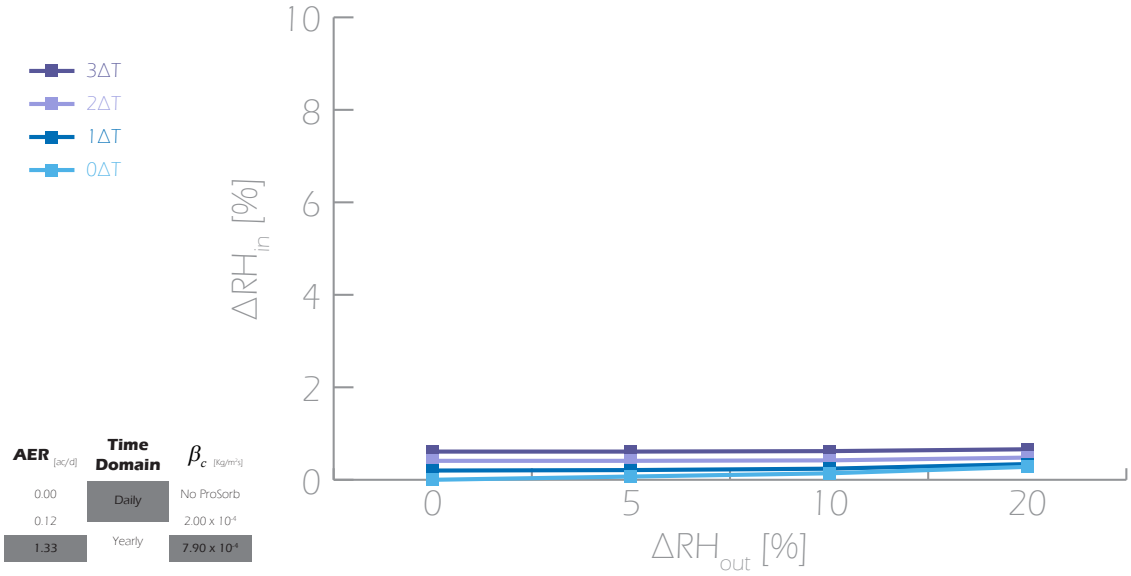

Table 56: ΔRH_{in} when AER = 0.00, Time domain = yearly, and β_c = 7.90 x 10^{-4} Kg/m²s

ΔRH_{out} [%] \ **ΔT** [°C]	0	1	2	3
0	0.00	0.03	0.05	0.08
5	0.00	0.03	0.05	0.08
10	0.00	0.03	0.05	0.08
20	0.00	0.03	0.05	0.08

Figure 111: ΔRH_{in} when AER = 0.00, Time domain = yearly, and β_c = 7.90 x 10^{-4} Kg/m²s

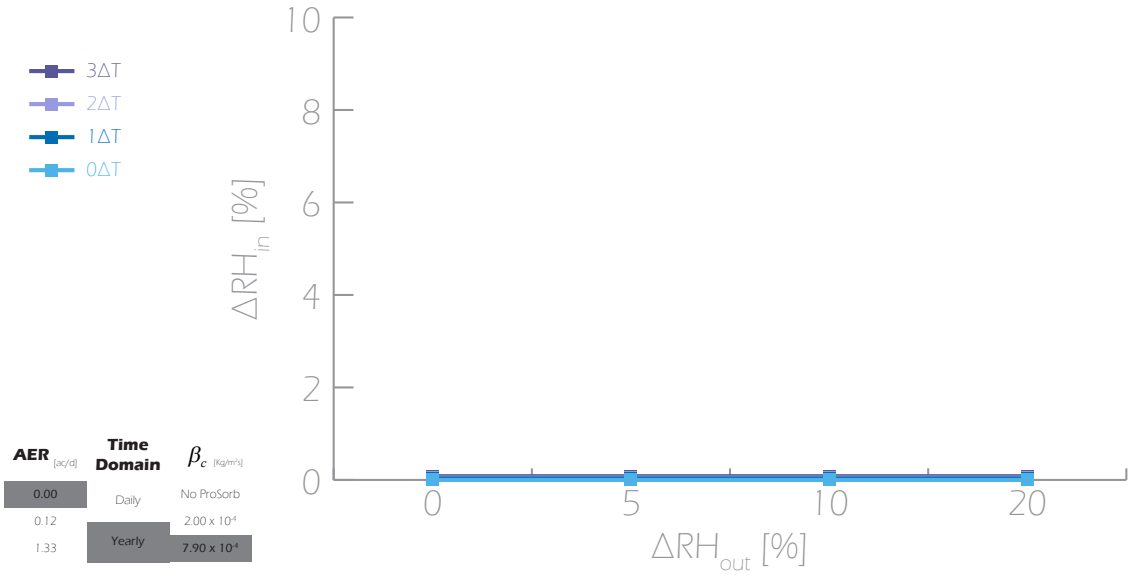

Table 57: ΔRH_{in} when AER = 0.12, Time domain = yearly, and β_c = 7.90 x 10^{-4} Kg/m²s

ΔRH_{out} [%] \ **ΔT** [°C]	0	1	2	3
0	0.00	0.03	0.05	0.08
5	0.31	0.32	0.32	0.34
10	0.63	0.63	0.63	0.63
20	1.26	1.25	1.23	1.22

Figure 112: ΔRH_{in} when AER = 0.12, Time domain = yearly, and β_c = 7.90 x 10^{-4} Kg/m²s

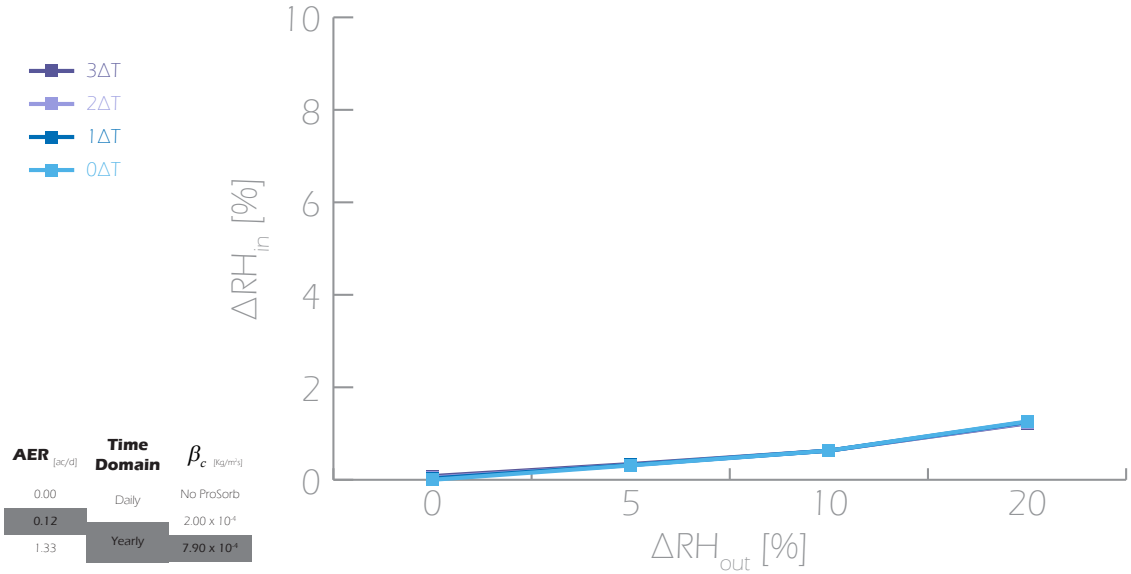

Table 58: ΔRH_{in} when AER = 1.33, Time domain = yearly, and β_c = 7.90 x 10^{-4} Kg/m²s

ΔRH_{out} [%] \ **ΔT** [°C]	0	1	2	3
0	0.00	0.02	0.04	0.07
5	2.76	2.77	2.78	2.79
10	5.53	5.53	5.54	5.55
20	11.05	11.06	11.06	11.06

Figure 113: ΔRH_{in} when AER = 1.33, Time domain = yearly, and β_c = 7.90 x 10^{-4} Kg/m²s

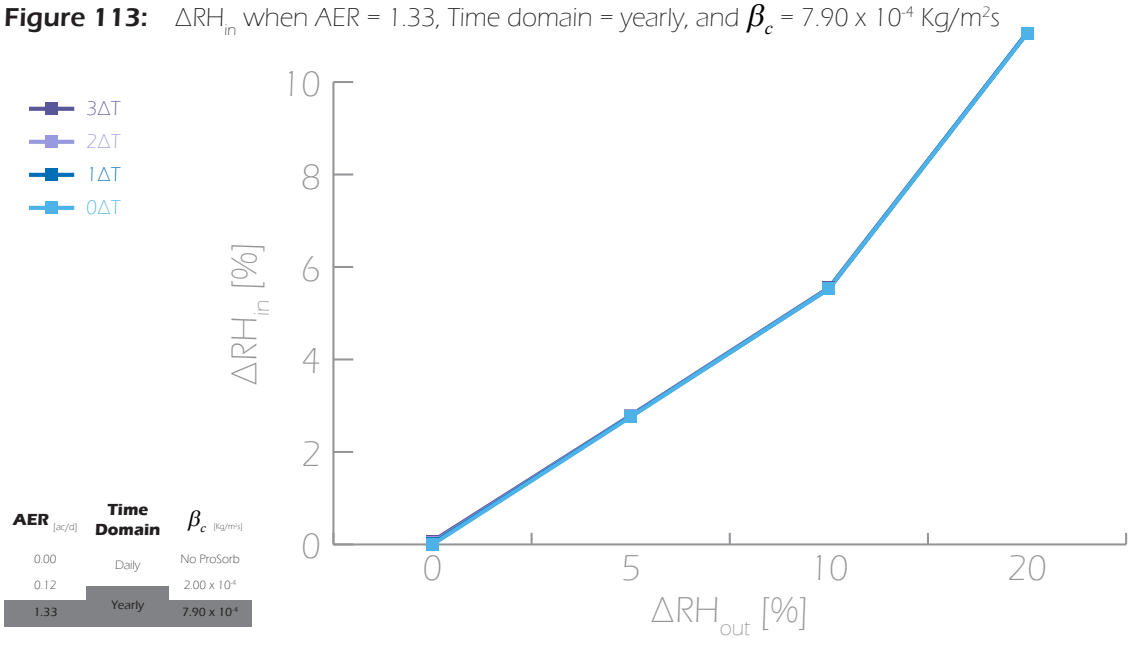

ΔT-ΔRH_{OUT}-ΔRH_{IN} TREND GROUP RESULTS

Table 59: Trend a and c: Group 1 ΔRH_{in} average

ΔRH$_{out}$ [%] \ **ΔT** [°C]	0	1	2	3
0	0.00 ±0.00	2.98 ±0.10	5.99 ±0.20	9.03 ±0.32
5	0.03 ±0.05	2.98 ±0.09	5.98 ±0.19	9.00 ±0.29
10	0.06 ±0.11	2.98 ±0.09	5.97 ±0.17	8.98 ±0.25
20	0.12 ±0.21	2.98 ±0.08	5.95 ±0.14	8.94 ±0.18

Table 60: Trend a and c: Group 2 ΔRH_{in} average

ΔRH$_{out}$ [%] \ **ΔT** [°C]	0	1	2	3
0	0.00 ±0.00	1.49 ±0.05	2.99 ±0.10	4.50 ±0.14
5	0.02 ±0.03	1.49 ±0.05	2.99 ±0.10	4.50 ±0.14
10	0.05 ±0.07	1.49 ±0.05	2.99 ±0.10	4.50 ±0.14
20	0.09 ±0.13	1.50 ±0.05	2.99 ±0.10	4.50 ±0.14

Table 61: Trend a and c: Group 3 ΔRH_{in} average

ΔRH$_{out}$ [%] \ **ΔT** [°C]	0	1	2	3
0	0.00 ±0.00	0.03 ±0.00	0.05 ±0.00	0.08 ±0.00
5	0.00 ±0.00	0.03 ±0.00	0.05 ±0.00	0.08 ±0.00
10	0.00 ±0.00	0.03 ±0.00	0.05 ±0.00	0.08 ±0.00
20	0.00 ±0.00	0.03 ±0.00	0.05 ±0.00	0.08 ±0.00

Table 62: Trend a and c: Group 4 ΔRH_{in} average

ΔRH$_{out}$ [%] \ **ΔT** [°C]	0	1	2	3
0	0.00 ±0.00	0.20 ±0.01	0.40 ±0.02	0.60 ±0.02
5	0.00 ±0.00	0.20 ±0.01	0.40 ±0.02	0.60 ±0.02
10	0.01 ±0.01	0.20 ±0.01	0.40 ±0.02	0.60 ±0.02
20	0.01 ±0.02	0.20 ±0.01	0.40 ±0.02	0.60 ±0.02

Table 63: Trend a, b and c: Group 5 ΔRH_{in} average

ΔRH$_{out}$ [%] \ **ΔT** [°C]	0	1	2	3
0	0.00 ±0.00	3.03 ±0.00	6.09 ±0.00	9.20 ±0.00
5	1.02 ±0.00	3.15 ±0.00	6.10 ±0.00	9.15 ±0.00
10	2.05 ±0.00	3.58 ±0.00	6.29 ±0.00	9.21 ±0.00
20	4.09 ±0.00	4.99 ±0.00	7.11 ±0.00	9.66 ±0.00

Table 64: Trend a, b and c: Group 6 ΔRH_{in} average

ΔRH_{out} [%] \ ΔT [°C]	0	1	2	3
0	0.00 ±0.00	1.41 ±0.00	2.83 ±0.00	4.25 ±0.00
5	0.48 ±0.00	1.48 ±0.00	2.85 ±0.00	4.26 ±0.00
10	0.97 ±0.00	1.68 ±0.00	2.96 ±0.00	4.32 ±0.00
20	1.93 ±0.00	2.35 ±0.00	3.37 ±0.00	4.60 ±0.00

Table 65: Trend a, b and c: Group 7 ΔRH_{in} average

ΔRH_{out} [%] \ ΔT [°C]	0	1	2	3
0	0.00 ±0.00	0.20 ±0.00	0.41 ±0.00	0.61 ±0.00
5	0.07 ±0.00	0.21 ±0.00	0.41 ±0.00	0.61 ±0.00
10	0.14 ±0.00	0.24 ±0.00	0.42 ±0.00	0.62 ±0.00
20	0.28 ±0.00	0.34 ±0.00	0.48 ±0.00	0.66 ±0.00

Table 66: Trend b and d: Group 8 ΔRH_{in} average

ΔRH_{out} [%] \ ΔT [°C]	0	1	2	3
0	0.00 ±0.00	0.23 ±0.27	0.46 ±0.54	0.69 ±0.81
5	4.97 ±0.04	5.08 ±0.09	5.20 ±0.24	5.33 ±0.40
10	9.95 ±0.07	10.05 ±0.05	10.16 ±0.18	10.28 ±0.33
20	19.90 ±0.15	20.00 ±0.03	20.10 ±0.10	20.22 ±0.24

Table 67: Trend b and d: Group 9 ΔRH_{in} average

ΔRH_{out} [%] \ ΔT [°C]	0	1	2	3
0	0.00 ±0.00	0.03 ±0.00	0.05 ±0.00	0.08 ±0.00
5	0.31 ±0.00	0.32 ±0.00	0.32 ±0.00	0.34 ±0.00
10	0.63 ±0.00	0.63 ±0.01	0.63 ±0.00	0.63 ±0.00
20	1.26 ±0.01	1.25 ±0.01	1.24 ±0.01	1.23 ±0.01

Table 68: Trend b and d: Group 10 ΔRH_{in} average

ΔRH_{out} [%] \ ΔT [°C]	0	1	2	3
0	0.00 ±0.00	0.02 ±0.00	0.04 ±0.00	0.07 ±0.00
5	2.68 ±0.11	2.69 ±0.11	2.70 ±0.11	2.71 ±0.11
10	5.37 ±0.22	5.38 ±0.22	5.38 ±0.22	5.39 ±0.22
20	10.74 ±0.44	10.75 ±0.44	10.75 ±0.44	10.75 ±0.44

Appendix 7 : The display case situation matrix

	daily	yearly	daily	yearly	daily	yearly
0.00 [ac/d]	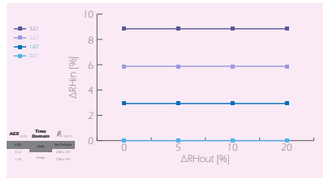	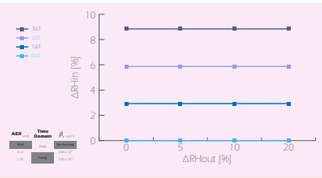	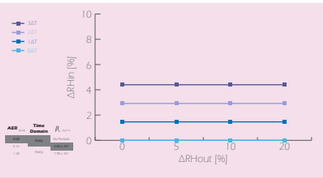	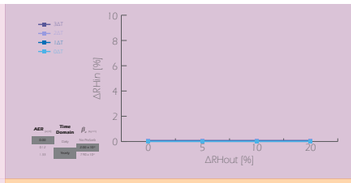	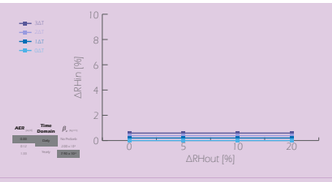	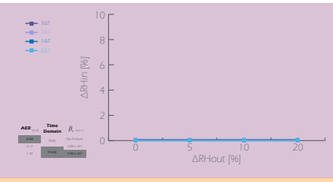
0.12 [ac/d]	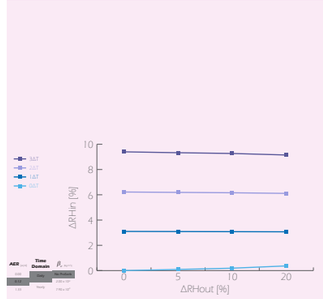	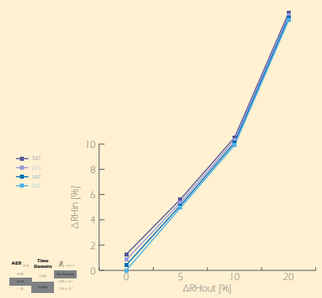	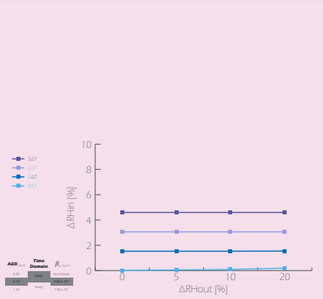	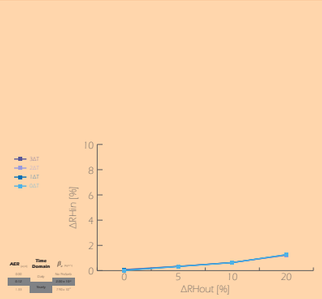	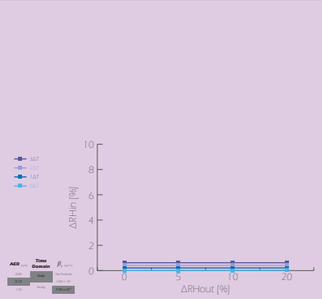	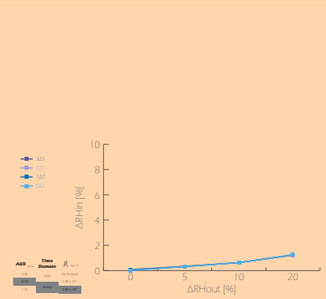
1.33 [ac/d]	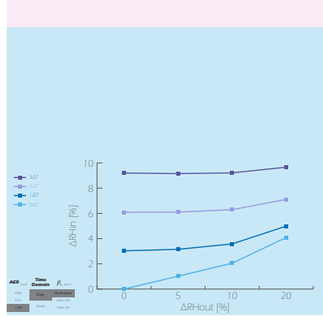	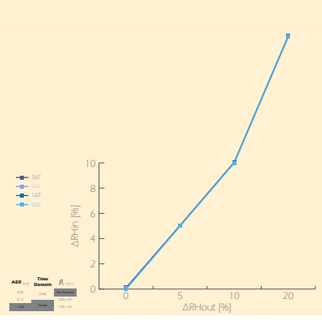	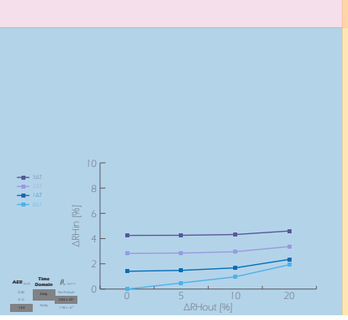	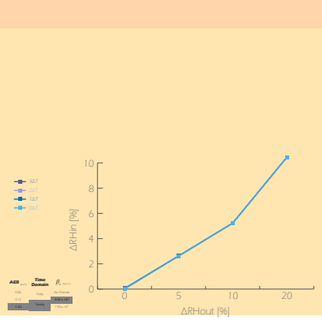	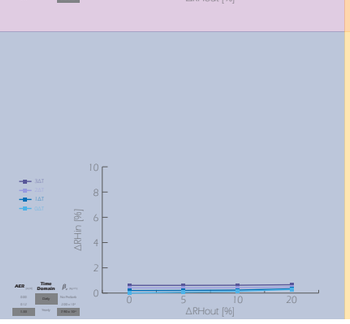	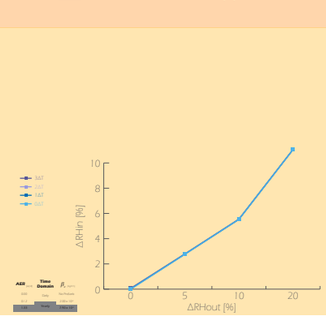

No ProSorb

β_c = 2.00 [x 10^{-4} Kg/m^2s]

β_c = 7.90 [x 10^{-4} Kg/m^2s]

Group 1
Group 2

Group 3
Group 4

Trend a and c

Group 5
Group 6
Group 7

Trend a, b and c

Group 8
Group 9
Group 10

Trend b and d


TUDelft